

Expulsion of Leaving Groups from Zwitterionic Intermediates Generated via Photochemical Electrocyclic Ring Closure Reactions and an Investigation on TPE Oligomers

Tasnuva Shahrin

Marquette University, tasnuva.shahrin@marquette.edu

Recommended Citation

Shahrin, Tasnuva, "Expulsion of Leaving Groups from Zwitterionic Intermediates Generated via Photochemical Electrocyclic Ring Closure Reactions and an Investigation on TPE Oligomers" (2013). *Dissertations (2009 -)*. Paper 246.
http://epublications.marquette.edu/dissertations_mu/246

EXPULSION OF LEAVING GROUPS FROM ZWITTERIONIC INTERMEDIATES
GENERATED via PHOTOCHEMICAL ELECTROCYCLIC RING CLOSURE
REACTIONS AND AN INVESTIGATION ON TPE OLIGOMERS.

by

Tasnuva Shahrin

A Dissertation submitted to the Faculty of the Graduate School,
Marquette University,
in Partial Fulfillment of the Requirements
for the Degree of Doctor of Philosophy

Milwaukee, Wisconsin

May 2013

ABSTRACT

EXPULSION OF LEAVING GROUPS FROM ZWITTERIONIC INTERMEDIATES GENERATED via PHOTOCHEMICAL ELECTROCYCLIC RING CLOSURE REACTIONS AND AN INVESTIGATION ON TPE OLIGOMERS.

Tasnuva Shahrin

Marquette University, May 2013

Photochemical cleavage reactions have been found widespread use in biological applications that require intracellular photochemical release of biologically active substrates such as peptides, proteins, neurotransmitters, or nucleotide phosphates. The research is to devise photoremovable protecting groups (cage compounds) that can be used to deprotect those biological substrates by irradiation. A number of photocleavage reactions have been developed in recent years which release chlorides, hydroxides, carboxylates, thiolates, and phenolates leaving groups for use in such applications. Nevertheless, photochemical elimination reactions that expel such leaving group anions remain quite uncommon. The cleavage of cage compounds via photolysis requires heterolysis of a bond to the substrate or leaving group. Heterolysis of a C-Cl, C-O or C-S σ -bonds in a zwitterionic intermediate is proposed. The study also involves benzothiophene carboxanilides. The photolysis wavelength can be 365 nm by introducing a benzoyl group into the para position of the carboxanilide. The electrocyclization appears to be a triplet excited state reaction, according to the quenching studies. Heavy atom effect has been investigated for this system by introducing Br-atom at C-6 position of benzothiophene ring and also leading to a very efficient reaction. Chloride, hydroxyl, carboxylate, thiolate and phenolate leaving groups can be released photolytically. The proposed mechanism involves excited state electrocyclization to produce a ground state zwitterionic intermediate which eliminates the leaving group. We found quantum yields for leaving group expulsion decrease with the increased basicity of leaving groups, consistent with elimination of the leaving group directly from the zwitterionic intermediate. The zwitterion also likely undergoes competing ring opening to regenerate the photoreactant. Moreover, the inclusion of a carboxylate group at the C-6 position of the benzothiophene ring improves solubility in aqueous media.

In addition, the ionic behavior of di-phenyl substituted poly(phenylene vinylene) as well as well-defined tetraphenyl ethylene (TPE) oligomers have been investigated as in another part of my research.

ACKNOWLEDGMENTS

Tasnuva Shahrin

First, I wish to express my sincere gratitude to my research advisor Professor **Rajendra Rathore** for his enthusiastic support, sagacious advice and patience during working in his laboratory. It has been a pleasure being associated with him.

Second. I would also like to take the opportunity to express my gratitude to my dissertation committee members Professor **Mark G. Steinmetz**, Professor **William A. Donaldson**, Professor **Daniel S. Sem** and Professor **Scott Reid** for their evaluation and critique and also their advice and time throughout the project work.

My special sincerity to my lab mates Dr. Majher Sarker, Khushabu Thakur, Anitha Boddedda, Mosharraf Hossain for their selfless help and many useful suggestions and also thanks to other lab mates Dr. Marat Talipov, Joe Kearney and Marek Piechowicz. My special thanks to Dr. Sheng Cai in NMR spectroscopy and MALDI and Dr. Sergey Lindeman in Crystallography and other help associated with this research. My special gratitude to Mr. Vaughn Ausman, Dr. Sandra Lukaszewski-Rose, Dr. Ruchi Shukla, Mr. Paul Dion and Ms. Linda Davis for their nice assistance.

Finally my very special thanks are due to my parents and husband whose love, sacrifice and inspiration always cheered me up which led this dissertation in its final form.

TABLE OF CONTENTS

ACKNOWLEDGMENTS	i
CHAPTER 1. INTRODUCTION	1
CHAPTER 2. EXPULSION OF LEAVING GROUPS FROM ZWITTERIONIC INTERMEDIATES GENERATED VIA PHOTOCHEMICAL ELECTROCYCLIC RING CLOSURE REACTIONS.	
2.1. Introduction.....	16
2.2. Results.....	22
2.2.1. Photochemical reactant, 43	22
2.2.2. UV- Spectra of Compound 43 ($\text{LG}^- = \text{Cl}^-$).....	23
2.2.3. Preparative Direct Photolysis of 43	24
2.2.4. Quantum Yield, 43	25
2.2.5. Photochemical Reactant, 20 ($\text{LG}^- = \text{OH}^-$).....	25
2.2.6. Crystal structure of 20 ($\text{LG}^- = \text{OH}^-$).....	26
2.2.7. Preparative Direct Photolysis 20	28
2.2.8. Crystal Structure of Photoproduct 23	29
2.2.9. Quantum Yield, 20	31
2.2.10. Synthesis of Compound 44	32
2.2.11. Crystal Structure of the Photoreactant 44	32
2.2.12. UV- Spectra of Compound 44	34
2.2.13. Preparative Direct Photolysis, 44	35
2.2.14. Quantum Yield, 44	35
2.2.15. Quenching Studies, 44	37
2.2.16. Synthesis of Compound 46 ($\text{LG}^- = \text{Cl}^-$).....	38

2.2.17. Crystal structure of the Photoreactant 46	38
2.2.18. UV Spectra of Compound 46	40
2.2.19. Preparative Direct Photolysis, 46	41
2.2.20. Quantum Yield, 46	41
2.2.21. Synthesis of Photoreactant 38	43
2.2.22. Preparative Direct Photolysis of 37	44
2.2.23. Quantum Yield, 37	45
2.2.24. Preparative Direct Photolysis of 38	46
2.2.25. Quantum Yield, 38	46
2.3. Discussion.....	50
2.4. Experimental.....	60
2.5. Supporting Information.....	83
 CHAPTER 3. AN INVESTIGATION ON TPE OLIGOMERS.	
3.1. Introduction	84
3.2. Results and Discussion	86
3.3. Electrochemistry	95
3.4. Experimental Section	99
 Bibliography.....	 105
Appendix I, NMR and MALDI Spectra.....	111

LIST OF TABLES

Table 1: Aromatic stabilization energy difference	10
Table 2: Quantum yields of the reaction of eq. 7.....	36
Table 3: Quenching studies of the reaction of eq. 7.....	37
Table 4: Quantum yields of the reaction of eq. 8.....	42
Table 5: Quantum yields of the reaction of eq. 10.....	47
Table 6: Ox. Potentials of the oligomeric models 82 – 86 and 78 (DP-PPV)....	95

LIST OF FIGURES

Fig, 2.1: Absorption Spectra of 43 (LG ⁻ = Cl ⁻).....	23
Fig, 2.2: ORTEP representation of molecular structure of photoreactant 20 (LG ⁻ = OH ⁻)	27
Fig, 2.3: ORTEP representation of molecular structure of photoproduct 23 ...	30
Fig, 2.4: ORTEP representation of molecular structure of photoreactant 44 ...	33
Fig, 2.5: Absorption Spectra of 44	34
Fig, 2.6: ORTEP representation of molecular structure of photoreactant 46	39
Fig, 2.7: Absorption Spectra of 46	40
Fig, 2.8: Absorption Spectra of 44 and 46	40
Fig, 3.1: MALDI spectrum of the reaction mixture of eq. 20.1.....	89
Fig, 3.2: MALDI spectrum of the reaction mixture of eq. 20.2.....	90
Fig, 3.3: MALDI spectrum of the reaction mixture of eq. 20.3.....	90
Fig, 3.4: MALDI spectrum of the reaction mixture of eq. 20.4.....	91
Fig, 3.5: MALDI spectrum of the mixture of oligomers, n = 4, 5 and 6.....	92
Fig, 3.6: MALDI spectrum of the mixture of oligomers, n = 5 and 6.....	92
Fig, 3.7: MALDI spectrum of the mixture of oligomers, n = 5 and 6.....	93
Fig, 3.8: MALDI spectrum of the mixture of oligomers, n = 5, 6 and 7.....	93
Fig, 3.9: MALDI spectrum of the mixture of oligomers, n = 6 and 7.....	94
Fig, 3.10: Cyclic- and SW voltammogram of 82	96
Fig, 3.11: Cyclic- and SW voltammogram of 83	97
Fig, 3.12: Cyclic- and SW voltammogram of 84	97
Fig, 3.13: Cyclic- and SW voltammogram of 85 , 86 and DP-PPV.....	98

LIST OF SCHEMES

Scheme 1.....	7
Scheme 2.....	8
Scheme 3.....	10
Scheme 4.....	10
Scheme 5.....	10
Scheme 6.....	11
Scheme 7.....	13
Scheme 8.....	16
Scheme 9.....	21
Scheme 10.....	22
Scheme 11.....	26
Scheme 12.....	32
Scheme 13.....	38
Scheme 14.....	44
Scheme 15.....	49
Scheme 16.....	51
Scheme 17.....	52
Scheme 18.....	58
Scheme 19.....	59

LIST OF EQUATIONS

Equation, 1.....	9
Equation, 2.....	14
Equation, 3.....	15
Equation, 4.....	17
Equation, 5.....	24
Equation, 6.....	28
Equation, 7.....	35
Equation, 8.....	41
Equation, 9.....	45
Equation, 10.....	46
Equation, 11.....	56
Equation, 12.....	57
Equation, 13.....	57
Equation, 14.....	57
Equation, 15.....	58
Equation, 16.....	87
Equation, 17.....	87
Equation, 18.....	87
Equation, 19.....	87
Equation, 20.1.....	88
Equation, 20.2.....	89
Equation, 20.3.....	89
Equation, 20.4.....	89

LIST OF NMR SPECTRA AND MALDI FOR APPENDIX I

^1H NMR spectrum of 50	112
^1H NMR spectrum of 51	113
^1H NMR spectrum of 43 ($\text{LG}^- = \text{Cl}^-$)	114
^{13}C NMR spectrum of 43 ($\text{LG}^- = \text{Cl}^-$)	115
^1H NMR spectrum of 53	116
^{13}C NMR spectrum of 53	117
^1H NMR spectrum of 20 ($\text{LG}^- = \text{OH}^-$).....	118
^{13}C NMR spectrum of 20 ($\text{LG}^- = \text{OH}^-$).....	119
^1H NMR spectrum of 23	120
^{13}C NMR spectrum of 23	121
^1H NMR spectrum of 44 ($\text{LG}^- = \text{Cl}^-$)	122
^{13}C NMR spectrum of 44 ($\text{LG}^- = \text{Cl}^-$)	123
^1H NMR spectrum of 58	124
^{13}C NMR spectrum of 58	125
^1H NMR spectrum of 46 ($\text{LG}^- = \text{Cl}^-$)	126
^{13}C NMR spectrum of 46 ($\text{LG}^- = \text{Cl}^-$)	127
^1H NMR spectrum of 62	128
^{13}C NMR spectrum of 62	129
^1H NMR spectrum of 37 ($\text{LG}^- = \text{Cl}^-$)	130
^{13}C NMR spectrum of 37 ($\text{LG}^- = \text{Cl}^-$)	131
^1H NMR spectrum of 66	132
^{13}C NMR spectrum of 66	133
^1H NMR spectrum of 38 ($\text{LG}^- = \text{Cl}^-$)	134

¹³ C NMR spectrum of 38 (LG ⁻ = Cl ⁻)	135
¹ H NMR spectrum 67	136
¹³ C NMR spectrum 67	137
¹ H NMR spectrum of 68	138
¹³ C NMR spectrum of 68	139
¹ H NMR spectrum of 69	140
¹ H NMR spectrum of 70	141
¹³ C NMR spectrum of 70	142
¹ H NMR spectrum of 71	143
¹³ C NMR spectrum of 71	144
¹ H NMR spectrum of 80	145
¹ H NMR spectrum of 81	146
¹³ C NMR spectrum of 81	147
¹ H NMR spectrum of 82	148
¹³ C NMR spectrum of 82	149
MALDI spectrum of 83	150
¹ H NMR spectrum of 83	151
¹³ C NMR spectrum of 83	152
MALDI spectrum of 84	153
¹ H NMR spectrum of 84	154
¹³ C NMR spectrum of 84	155
MALDI spectrum of 85	156
¹ H NMR spectrum of 85	157
¹³ C NMR spectrum of 85	158
MALDI spectrum of 86	159
¹ H NMR spectrum of 86	160

^{13}C NMR spectrum of 86	161
---	-----

CHAPTER 1: INTRODUCTION

Photoremovable protecting groups are enjoying a resurgence of interest since their introduction by Kaplan^{1a} and Engels^{1b} in the late 1970s. In general, photolysis reactions present a noteworthy and often ideal alternative to all other methods for introducing reagents or substrates into reactions or biological media. The ability to control the spatial, temporal, and concentration variables by using light to photochemically release a substrate provides the researcher with the ability to design more precisely the experimental applications in synthesis, physiology, and molecular biology. Among the many possible examples is the recently reported inhibition–reactivation of protein kinase A by photolysis of the dormant enzyme.^{2–4} In this demonstration, it is necessary that the deprotection process be initiated by photolysis of the dominant chromophore of the protecting group. Covalent blocking of the functional groups at the active site of an enzyme essentially suspends its mode of action and virtually shuts down the catalytic cycle. It is this feature that has attracted biochemists to the use of protecting groups for the investigation of biological mechanisms.

Cage compounds or photoremovable protecting groups (PRPGs) are broadly used in biochemical applications, in cellular biology and physiology, because they allow light-controlled release of bioeffectors with microscopic spatial resolution.⁵ Cage compounds can also be used for thermoelectric applications. A number of such compounds are now available; but there is no universal photocleavable protecting group that is satisfactory for all applications. Therefore there is still the need for the development of new

photoremovable protecting groups which could be used for some specific application.

Many cage compounds have drawbacks:

1. The photolytic release step often requires use of UV-light which can cause cell damage and unintended side reactions of biological molecules.⁶ Few cage compounds are available that release bioeffectors upon exposure to visible light wavelengths.⁷

2. Another problem is that the bioeffector may be released prematurely in the dark under physiological conditions,⁶ because many cage compounds are not stable with respect to solvolysis at high ionic strengths under aqueous conditions which are encountered in biological systems.

Neurotransmitter receptors are transiently inactivated (desensitized) during prolonged (milliseconds) exposure to neurotransmitter. Dark hydrolysis would lead to liberation of the neurotransmitter and, therefore, to transient inactivation of the receptor before the reaction can be investigated.

3. Moreover, the released molecules usually are weak bases such as carboxylate or phosphate, while many of the functional groups that need to be released are much stronger bases, such as thiolate or phenolate.

Therefore an important goal of our research is to release these stronger bases. For those molecules that are less basic, the goal is to design a PRPG that is more stable and not released prematurely. Finally, the PRPG is designed to be removed by photolysis at longer wavelengths with high chemical and quantum yields to minimize photolysis of intracellular components such as proteins, DNA, RNA etc. which would damage or kill

cells. And to be useful in biological applications, they and their photochemical byproducts must possess sufficient stability and must not interfere biologically. Studies of rapid biological processes also require substrate release on the microsecond or shorter timescale, thus avoiding any long-lived intermediates prior to substrate release. Moreover, the photoproduct must not absorb at the same wavelength as the activating radiation for cage compounds which can block the light absorbance by the cage compounds.

Our research mainly focused on developing photochemically removable groups that would absorb light beyond 300 nm or 350 nm (for biological purpose) and would be capable of releasing a very wide range of leaving groups. A list of common criteria⁸ should be assigned for a suitable cage compound as follows:

1. Synthesis: Easy and inexpensive to prepare with high yield.
2. Chromophore: The chromophore should have a reasonable absorptivity to capture the incident light efficiently.
3. Wavelength: Excitation wavelengths should be longer than 300 nm that extend into the visible region for biological application and must not be absorbed by the media.
4. Capability: Ability to release more basic leaving group anions than carboxylate or phosphate.
5. Solubility: The cage compounds should have good aqueous solubility for biological studies. For synthetic applications, this requirement is relaxed.

6. Stability: All photoproducts should be stable to the photolysis environment. The caged compounds should be inert or at least benign with respect to the media or other reagents.

7. Efficiency: The photochemical release must be efficient and the reaction should be clean.

Neurons in human brain communicate primarily by the release of small quantities of chemical messengers commonly called neurotransmitters. These chemicals alter the electrical activity of neurons after they interact with receptors on cell surfaces. Photochemically removable protecting group (PRPG) can be covalently attached to a functional group of a molecule in order to make a cage compound which is inert to some particular set of reaction conditions. The PRPG is then removed by photolysis to release the molecule. If the released molecule is a biological agent, its photochemical deprotection can be conducted intracellularly or in tissue to trigger some desired biological responses. Usually the release step involves photolysis by a pulse of light. The release then can be nearly instantaneous, depending on the time period of the light pulse and the rate of the deprotection reaction. The time period can be, for example, minutes (caged protein kinase A)⁶, seconds (caged tyrosine Ca/calmodulin inhibitory peptide)⁶, milliseconds (caged ATP)⁶, and microseconds (caged neurotransmitters)^{6,9}. In addition, the site of the release can be controlled on a microscopic level by use of this technique.

The research and development of releaseable bioeffectors from photocleavable groups additionally would provide opportunities for collaboration with investigators in diverse fields of biochemistry, biology, physiology, and medicine. Based on above, the

photoreleased bioeffector leaving groups may be small molecules, or they may be polypeptides, proteins, oligonucleotides, RNA, and DNA. There are numerous examples to illustrate the utility of photocleavable groups in fields outside of chemistry:

- To identify specific receptors in neuronal circuits with the use of high microscopic spatial resolution.
- To investigate the kinetics and distribution of synaptic processes through bindings of neurotransmitters GABA (γ -aminobutyrate) and L-glu (glutamate) at the squid giant synapse, for mapping connections between different regions of the brain.
- A well known example is caged DNA microarrays prepared by photolithography with free 3'-ends (DNA chips) which is removed photolytically in quantitative yields to ensure high purity of synthesized probes.
- Photolabile Ca^{+2} -caged compounds, to explore the Ca-dynamics of variety biological systems by two photon excitation techniques.
- Another application is the use of photocleavable linkers to anchor bio-oligomers to a resin, especially in solid phase peptide synthesis.
- The study of cAMP-dependent protein kinase A (PKA) in cell signaling by blocking and unblocking of a phosphorylated thr-197 of the catalytic subunit (C) using the caging group like 4-hydroxyphenacyl.⁶
- The use of caged peptides as with caged tyrosine residue of the Ca/calmodulin inhibitory peptide RS-20 to probe the role of specific proteins in cell function, where the photoreleased peptide inhibits calmodulin or myosin light chain kinase (MLCK)

activity, which in turn blocks cell locomotion involving myosin II as the motor protein.⁶

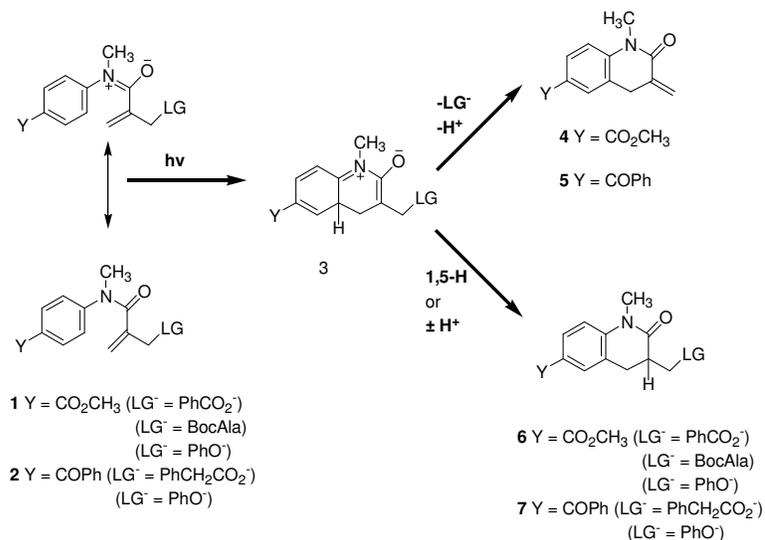
- Well-known caged neurotransmitters in investigations of the mechanisms of neurotransmitter-mediated reactions on cell surfaces.¹⁰
- The photorelease of caged aspartate to study chemotaxis of *Escherichia coli*.¹¹
- The study of GTP-Ras complex in cell signaling pathways plays an important role in controlling cell proliferation, differentiation, and metabolism by releasing GTP from 4-hydroxyphenacyl and ortho-nitrophenylethyl caging groups.¹²
- Caged ATP is required in the study of Na⁺/K⁺-ATPase pump for ion transport across the cell membrane and planar lipid membrane both and for muscle contraction of the biological process.¹³
- Additionally, caged cAMP and other caged cNMP are also utilized to investigate the mechanism of olfactory transduction in cilia of the olfactory cell.¹⁴ Caged cAMP also plays a role to investigate the mechanism of cAMP-dependent inhibition of Ca²⁺ mobilization in tissue cells.¹⁵

Photolithographic applications have emerged in which photocleavable protecting groups have been used to implement a combinatorial synthesis strategy to fabricate arrays of oligonucleotides on chips. Such arrays have been of interest for use as sensors for complementary sequences of DNA. The methodology has also been applied to combinatorial synthesis of peptides. A very early applications in conventional photolithography incorporated caged carboxylic acids into methyl

methacrylate/methacrylic acid copolymer photoresist material. When the polymer thin films were irradiated through a mask, the photoreleased acid rendered the material in exposed regions more soluble to aqueous alkali developer.

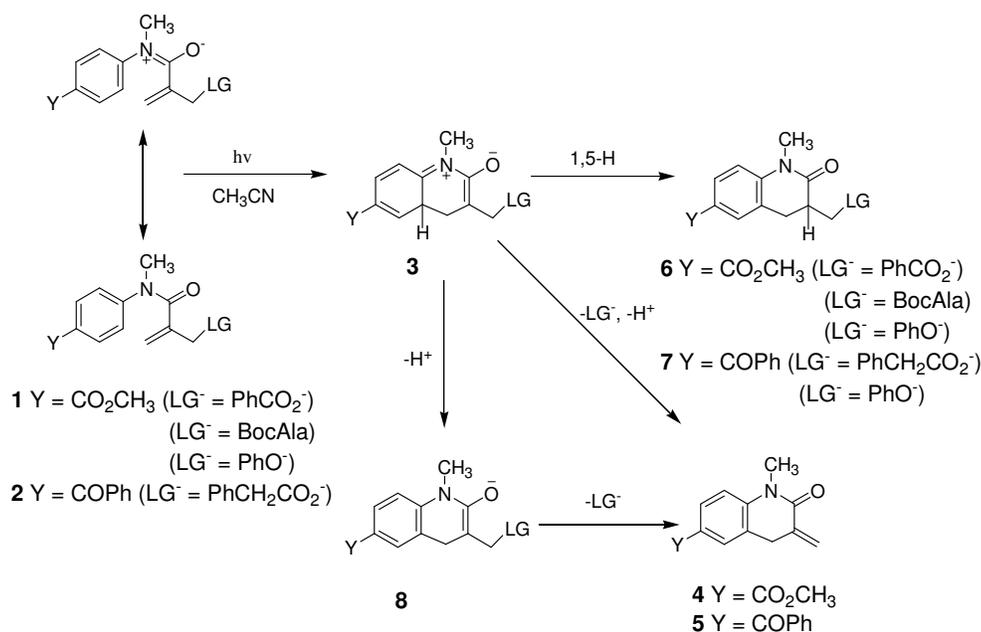
Photochemical electrocyclic ring closure has been previously used in this laboratory to generate zwitterionic intermediates that, in principle, would be capable of expelling leaving groups such as carboxylates and phenolates, which are functionally present in many biologically important molecules. The study used a photochemical electrocyclic ring closure to generate zwitterionic intermediates from acrylic anilides (Scheme 1).¹⁶ The photochemical reaction likely proceeds via an electrocyclic ring closure to give an intermediate that has zwitterionic character.^{17,18} The zwitterionic intermediate is converted to a lactam photoproduct via either intramolecular 1,5-H rearrangement or a series of proton transfers, depending on the solvent and the substituents attached to the amide nitrogen.^{17,19,20a}

Scheme 1 (acrylic anilides)



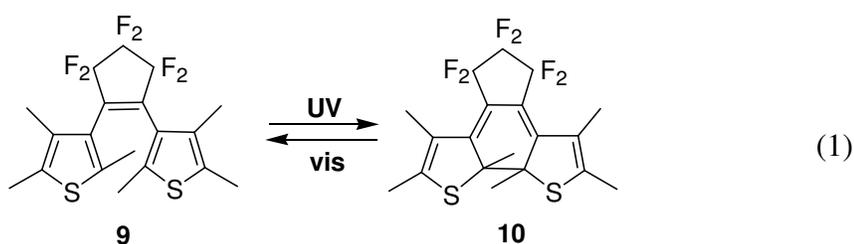
The photochemical electrocyclicization was 8-10% efficient with respect to light utilization. However, the leaving groups were evidently not expelled directly from the putative zwitterionic intermediate, unlike Scheme 1, but instead were eliminated from an enolate formed upon deprotonation of the zwitterion.¹⁶ This deprotonation step had to compete with a 1,5-H shift in the zwitterionic intermediate that gave a product which retained the leaving group, and thus, leaving group expulsion did not represent 100% of the reaction. Furthermore, the quantum yields for leaving group release appeared to be controlled by the competition between deprotonation and 1,5-H shift and were largely independent on leaving group basicity (Scheme 2) which we proved afterwards.^{20b,c}

Scheme 2



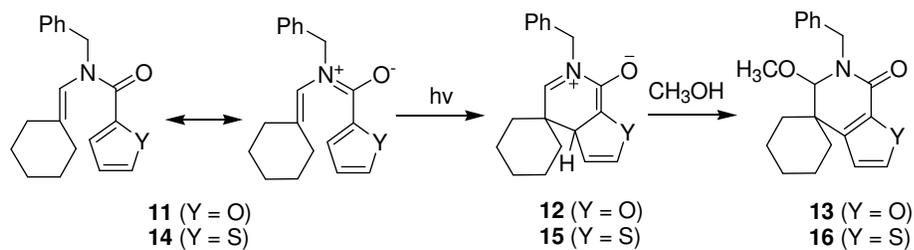
Given the previous results, efforts then focused upon improving the efficiency of the electrocyclic ring closure reaction. In addition, it was desirable to attempt to make the elimination of the leaving group from the zwitterionic intermediate more favorable by replacing the acrylanilide group by an aromatic group which had the leaving group in an ortho position so that it would restore aromaticity after the electrocyclization had been effected. In other words, in place of acrylic group (Scheme 1), there would be an aromatic ring. The choice of aromatic ring in such place (Scheme 1) is critical. For example, quantum yields are low for the electrocyclization if the aromatic ring is phenyl. Ultimately, the best choice appeared to be either a furanyl ring or a thienyl ring, based on the following considerations.

The energetics for electrocyclization can be made more favorable by cyclizing onto *N*-furyl and *N*-thienyl groups. This principle has been exploited in photochromic 1,2-diarylethenes (eq. 1), for which excited state electrocyclization occurs rapidly on the order of 10 ps.²⁰

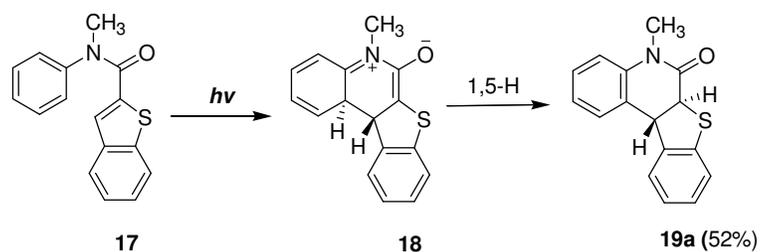


Some examples of photochemical electrocyclization of furyl and thienyl groups to form zwitterionic intermediates are already known (Schemes 3²¹ and 4²²), but no quantum yields have been reported.

Scheme 3



Scheme 4



Irie has noted for the analogous conversions of **A** to **B** (Scheme 5) that the loss of aromatic stabilization energy substantially decreases when the aromatic group in structure **A** is changed from phenyl to pyrrolyl to furyl to thienyl (Table 1).^{23a,b}

Scheme 5

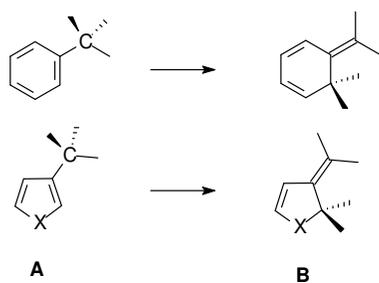


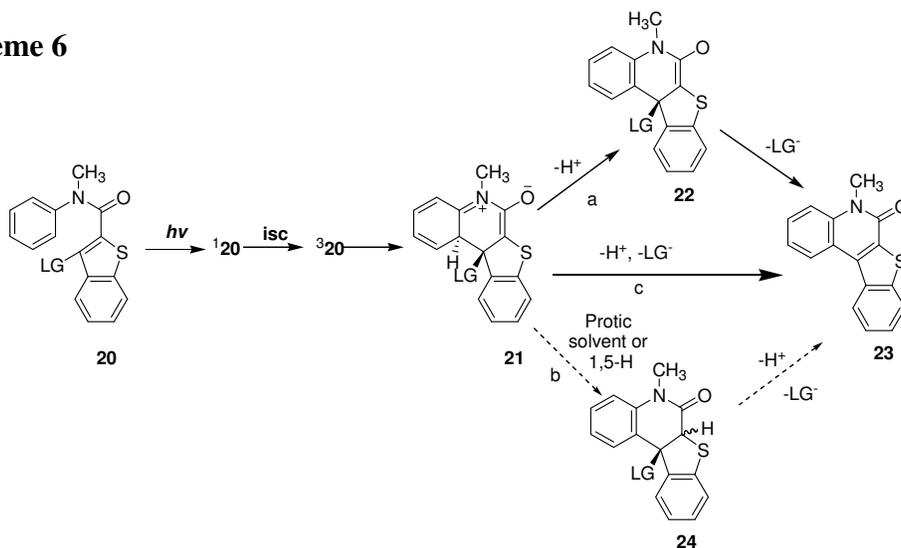
Table 1. Aromatic stabilization energy difference (**A**→**B**)

group	energy (kcal mol ⁻¹)
phenyl	27.7
pyrrolyl	13.8
furyl	9.1
thienyl	4.7

Structures **A** and **B** are quite analogous to the structures for reactant and zwitterionic intermediate in the photocyclization of methacrylanilides (Scheme 2). Although quantum yields were not reported, the chemical yields for **17** (Scheme 4) suggested that the benzothiophene carboxanilide system might be efficient in undergoing electrocyclic ring closure. The paper²² also reported that the reaction could be quenched, which suggested that the electrocyclization might be a triplet excited state reaction.

Initial studies with **17** focused upon placing various leaving groups at the C-3 position of the benzothiophene ring system. We conducted a preliminary study of the photochemistry of **20** ($\text{LG}^- = \text{Cl}^-, \text{PhCH}_2\text{CO}_2^-, \text{PhCH}_2\text{S}^-, \text{PhO}^-, \text{OH}^-$) in deaerated aq CH_3CN and with phosphate buffer at pH 7 (Scheme 6).^{23c} Upon direct photolysis, complete disappearance of **20** was observed with formation of **23** as the sole photoproduct after very short photolysis times. For $\text{LG}^- = \text{Cl}^-$, $\Phi = 0.22$ in deaerated solvent, while $\Phi = 0.076$ in the presence of air, consistent with triplet excited state photoreactivity. For $\text{LG}^- = \text{PhCH}_2\text{CO}_2^-$, $\Phi = 0.16$ and for $\text{LG}^- = \text{PhCH}_2\text{S}^-$, $\Phi = 0.076$; $\text{LG}^- = \text{PhO}^-$, $\Phi = 0.074$; $\text{LG}^- = \text{PhS}^-$, $\Phi = 0.10$; $\text{LG}^- = \text{OH}^-$, $\Phi = 0.007$.

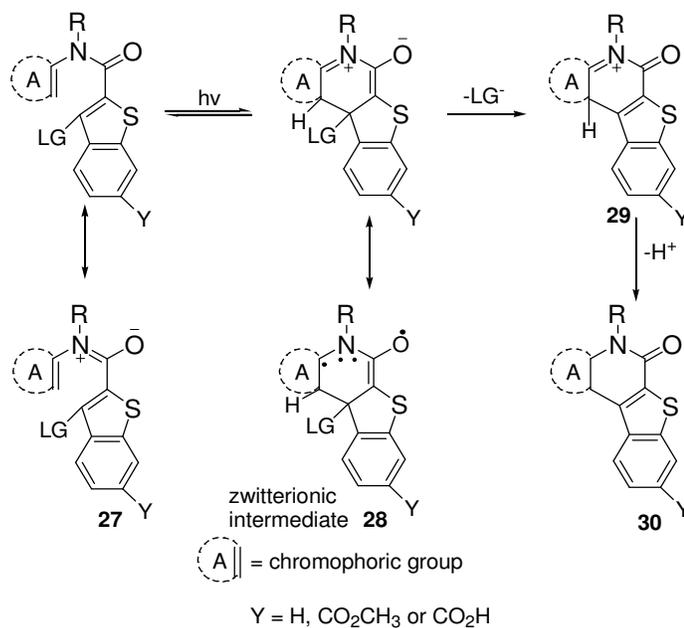
Scheme 6



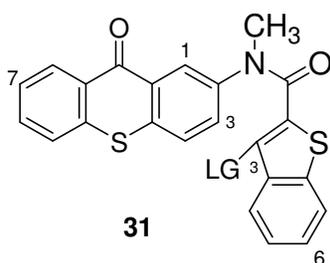
The mechanism shown in Scheme **6** is based on Schemes **2** and **4**. The above Φ , which decrease with increasing basicity of LG^- indicates path c is the most likely mechanism. Paths a or b or any combination would mean that Φ would be constant as LG^- basicity increases.

Our next attempt was to develop a real bioapplicable cage compounds. To do so, we needed to synthesize cage compounds which contain a chromophore that absorbs light at longer wavelengths that extend into visible region. We know that the cage compounds typically used have certain drawbacks, which may not always be obvious. In particular, UV light is most often used to photochemical release of the biologically active molecule, but may cause cellular damage and mortality. Cage compounds may undergo premature hydrolytic or even enzymatic release of the bioeffector in living cells. Our research attempted to address the above problems by expelling the bioeffector leaving groups via intermediates that have zwitterionic character. Intermediates **28** are generated upon photochemical electrocyclic ring closure reaction of derivatives of benzothiophene carboxanilides **27** (Scheme 7). Ring A subunit represents a chromophore that absorbs light at long wavelengths that extend into the visible region.

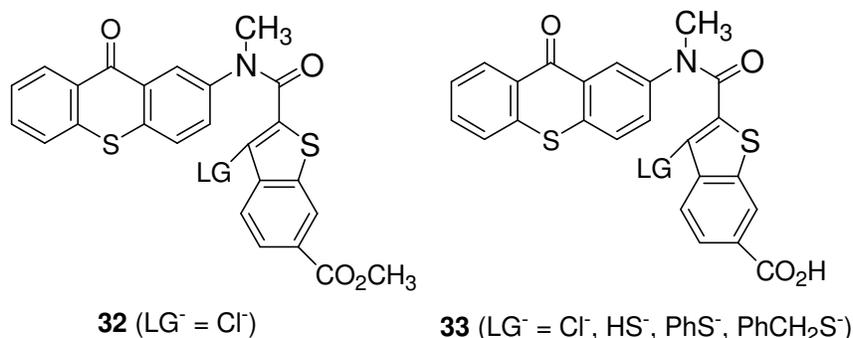
Scheme 7



The approach of using Scheme 7 to photochemically expel leaving groups from the C-3 position of the benzothioanthrone ring system was initially tested, experimentally by placing phenyl-group in position A, at short wavelengths in the UV like 310 nm but in here we extended the absorption of the chromophoric groups to 385 nm by use of thioanthrone chromophore as ring A.

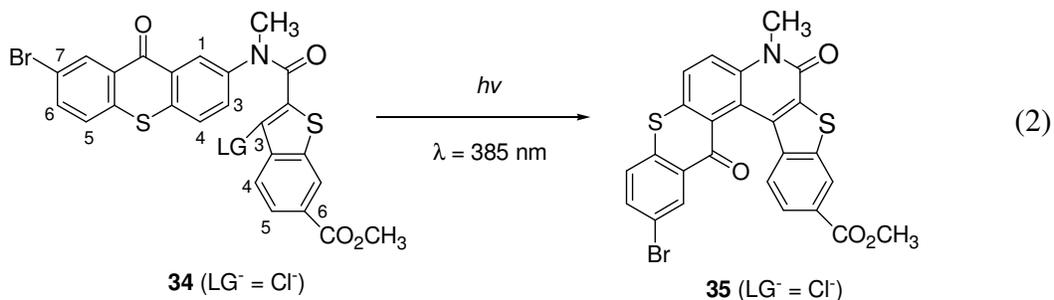


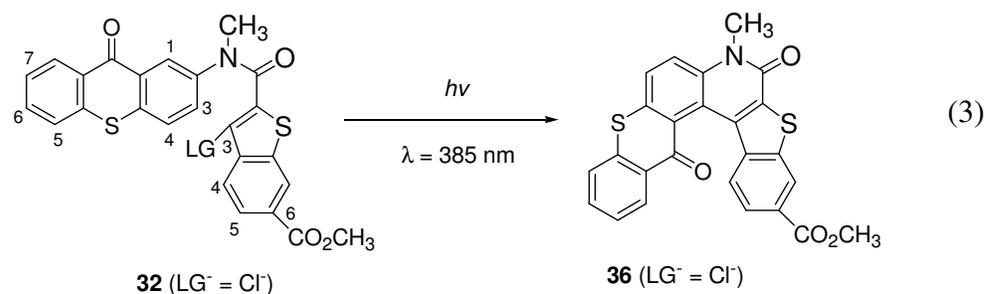
Additionally, solubility in aqueous buffered media were greatly improved by attaching a C-6 carboxylate group ($\text{Y} = \text{CO}_2\text{H}$) to the benzothioanthrone ring system (Scheme 7).



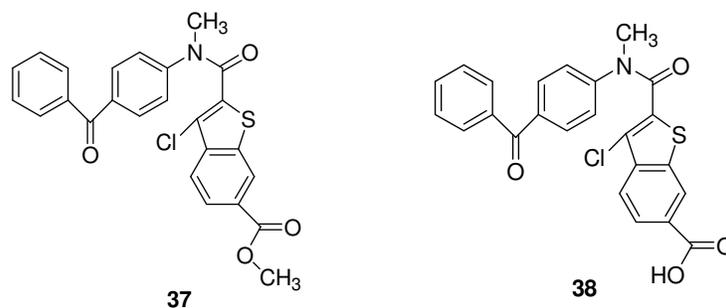
We reported **33** to release various leaving groups LG^- ($\text{LG}^- = \text{Cl}^-$, PhCH_2S^- , PhS^- , HS^-) where quantum yields decreased with increasing basicity of the LG^- released over the range $\Phi = 0.01$ – 0.03 . Secondly, releasing of S-containing LG^- anticipates of developing a photoremovable protecting group incorporated with cysteine or glutathione bioeffectors in C-3 position of benzothiophene ring.

To determine whether a “heavy atom effect” promoted intersystem crossing of the singlet excited state to the triplet excited state, work focused upon the C-7 bromide of thioxanthone ester **34** ($\text{LG}^- = \text{Cl}^-$). Quantum yield determinations gave $\Phi = 0.053 \pm 0.002$ for formation of **35**, which is 38% higher than $\Phi = 0.039 \pm 0.002$ found for ester without C-7 bromide of thioxanthone. These works have been recently published.^{23d}





As the quantum yields for these compounds of thioanthrone chromophore were found to be very low ($\Phi = 0.02 - 0.07$), the research was moved by changing the chromophore to benzophenone which absorbs light at maximum of 330 nm wavelength, the triplet yield is 1.0 and triplet lifetime is 50 μ s. We studied on this molecule introducing carboxylate substituent at C-6 position of benzothiophene ring system.



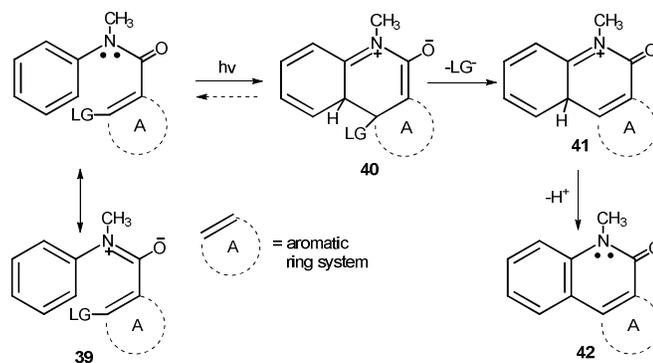
In our next phase of research, we focused to synthesize tetraphenyl ethylene (TPE) oligomers in an efficient way. The oligomers from the mixture with monomer starts from 1 to 5 were successfully separated and their physical and electrochemical properties have been investigated.

CHAPTER 2: Expulsion of Leaving Groups from Zwitterionic Intermediates Generated via Photochemical Electrocyclic Ring Closure Reactions.

2.1 Introduction

The purpose of the project is to utilize photochemical electrocyclic ring closure reactions of aromatic anilides to generate zwitterionic intermediates, which could expel leaving group anions (Scheme 8). The compounds which use this approach for the expulsion of leaving groups would represent a new type of cage compound for use in biological and biochemical applications.

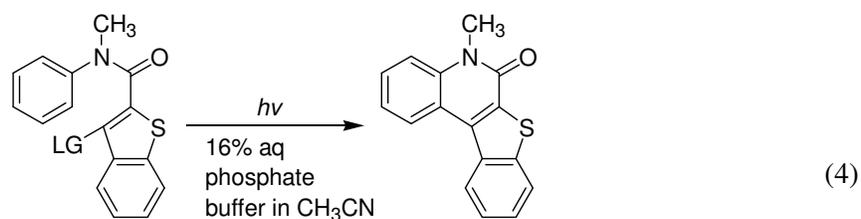
Scheme 8.



With modifications of the proposed compounds (*vide infra*), could be used as cage compounds for biological applications. As the cage compounds' criteria noted previously are, firstly, the photoreaction should be clean and occur with high chemical and quantum yield. Secondly, absorption should be as high as wavelengths above 350

nm. Third, they should possess sufficient stability and their byproducts should be biologically inert. They should also be stable with respect to premature release. Studies of rapid biological processes also require substrate release on the microsecond or shorter timescale. The release rate of the bioeffectors must be faster than that of the response found. The requirement of the release rate will depend on the biological system to be studied. Previously we have found that relatively nonbasic leaving groups like neurotransmitter carboxylates are released directly from zwitterionic intermediates produced by photolysis of α -keto amides on the microsecond timescale.²⁴

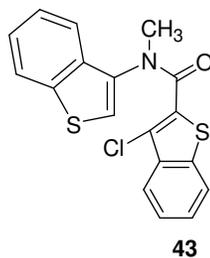
In organic synthesis, the proposed cage compounds may be important to be used as protecting groups as well as in array synthesis, under deaerated conditions.²⁵ 100% conversion of the protecting group without formation of byproducts may be completely removable, as noted from the preliminary results for **20** ($\text{LG}^- = \text{Cl}^-, \text{PhCH}_2\text{CO}_2^-, \text{PhCH}_2\text{S}^-, \text{PhO}^-, \text{OH}^-$) (Scheme 6). Since the resistancy of aromatic amide functionality in our few proposed protecting groups to a wide variety of chemical reagents, it is certain that they should be used as a protecting group in organic synthesis. High quantum yields under deaerated conditions will surely require short photolysis times for cleavage which may also require numerous light exposure steps to be important for array syntheses. This work constitutes our *Org. Lett.* communication.^{23c}



20 ($\text{LG}^- = \text{Cl}^-, \text{PhCH}_2\text{CO}_2^-, \text{PhCH}_2\text{S}^-, \text{PhO}^-, \text{PhS}^-, \text{HO}^-$) **23**

However, this report extends that work by exploring ways for improving (1) the efficiency for the electrocyclic ring closure reaction, and (2) the solubilities under aqueous conditions when the anilide phenyl group is replaced by other chromophores, such as benzophenone which absorbs light at 330 nm (λ_{max}) wavelength, has triplet lifetime 50 μs and triplet yield 1.0.

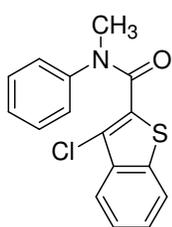
Our investigation of replacing an acrylamide group as A (Scheme 8) with benzothiophene results in a large increase in the quantum yield for electrocyclic ring closure, which has been reported in the communication. With a single benzothiophene ring, as in the case of **39**, the reaction was relatively efficient ($\Phi = 0.22$). So it was expected that by replacing the phenyl group of the anilide with a second benzothiophene ring, the quantum yield for electrocyclization would show a further increase. Thus, an important goal of this project became to synthesize benzothiophene carboxamide **43** as shown below.



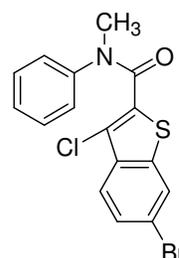
It is possible that the increase in quantum yield in case of one benzothiophene ring as A is due to a change in multiplicity from singlet to triplet. It also seems possible that it could reflect a decrease in aromatic stabilization energy in going from phenyl to

benzothiophene, as suggested in Table 1. Perhaps by replacing the anilide phenyl group with a second benzothiophene ring involves the electrocyclization of two less strongly aromatic benzothiophene rings and the formation of the pentacyclic product containing two five-membered rings is thermodynamically unfavorable.

So the second purpose of the project was to determine whether efficiencies would improve by promoting intersystem crossing by use of the heavy atom effect. Thus, the phenyl group instead of benzothiophene was retained and the 6-bromo derivative **30** was synthesized and studied. The results with this compound were incorporated into the communication.

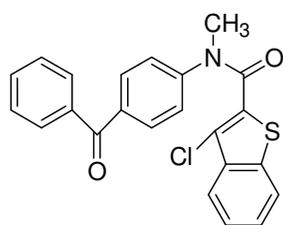


20 (LG = Cl⁻)

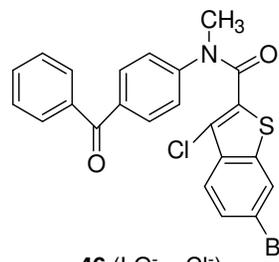


44 (LG = Cl⁻)

A third goal of the project was to incorporate a benzophenone chromophore in place of the anilide phenyl to improve absorption of light at wavelengths above 310 nm, which is where compound **17** absorbs light. A 6-bromo substituent was incorporated to provide a heavy atom effect.

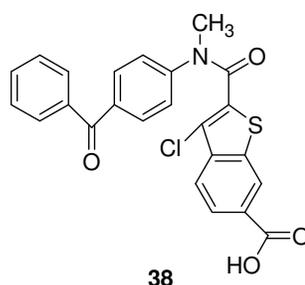


45 (LG⁻ = Cl⁻)

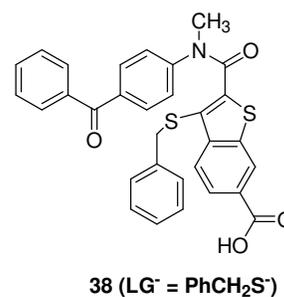
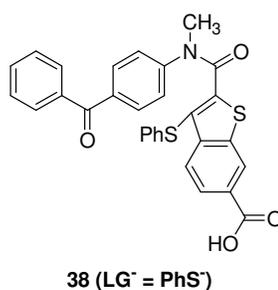
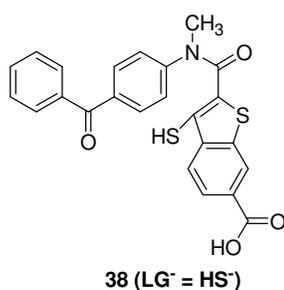


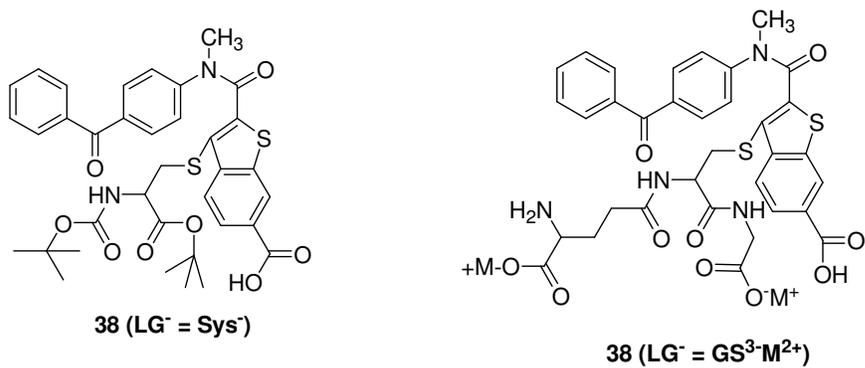
46 (LG⁻ = Cl⁻)

Finally, the results of the above work led to a reformulation of the basic strategy for the design of a cage compound based on **17**. Chromophores would be introduced in place of the phenyl group of the anilide. The benzothiophene aromatic ring would serve as a platform for placing the leaving group. It was also needed to be modified to improve solubility in aqueous media. To improve solubility, a major effort was launched to introduce a 6-carboxylate group into the benzothiophene ring system, as shown with **38**.



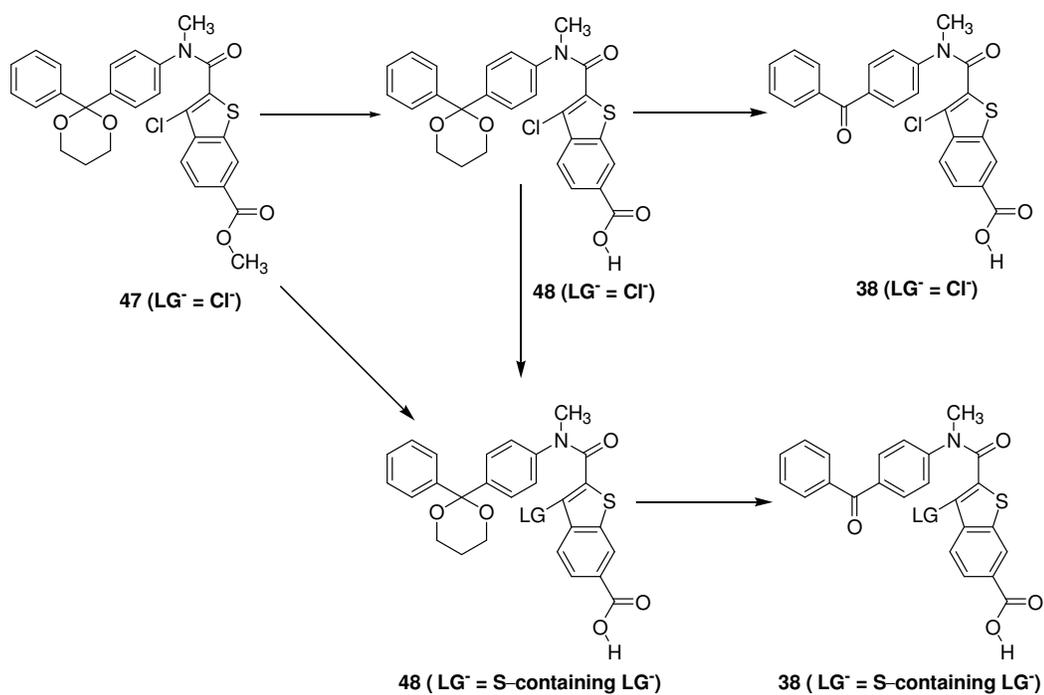
We successfully overcame the solubility problem with the benzophenone chromophore by introducing C-6 carboxylate group into the benzothiophene system. But incorporating S-containing LG⁻ in place of Cl⁻ in compound **38** generated another major problem due to the instability of amide bond. So the plan of the project was changed by protecting benzophenone carbonyl group to obtain the target molecules like:





So, Cl^- LG^- can be replaced by S-containing LG^- at compound **47** or **48**.

Scheme 9

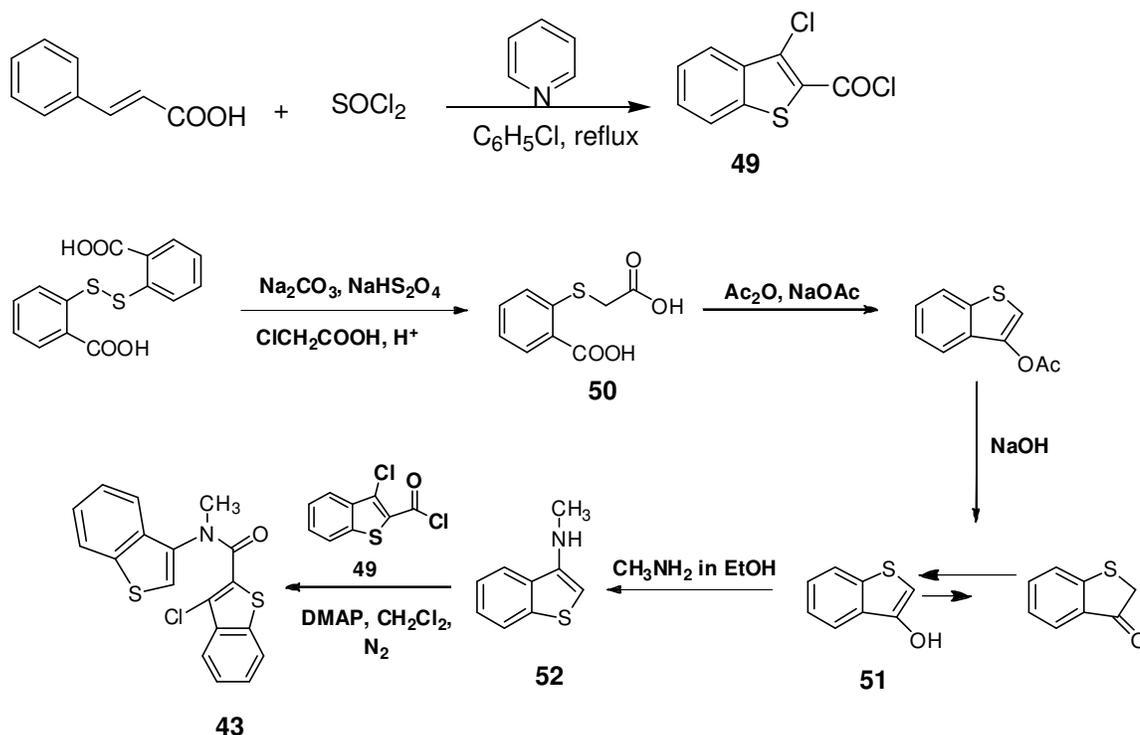


2.2 Results.

2.2.1 Photochemical Reactant.

The synthesis of amide **43** ($LG^- = Cl^-$) involved acylation of 3-methylaminothiophene (**52**) with 3-Chlorobenzo[b]thiophene-2-carbonyl chloride (**49**), which was initially prepared from the reaction of *trans*-cinnamic acid and thionyl chloride. 3-methylaminothiophene (**52**) was prepared from keto-enol tautomers (**51**) which was produced by a two steps process starting from 2,2'-dithiosalicylic acid (see Experimental).

Scheme 10



2.2.2 UV- Spectra of Compound **43** ($\text{LG}^- = \text{Cl}^-$).

The ultraviolet spectra of the starting material was taken at different concentrations in 20% 100 mM phosphate buffer in CH_3CN at pH 7.0 to observe the absorption characteristics. At lower concentrations, the compound shows an absorption maximum below 300 nm which tailed out into the 300-320 nm region. Compound **43** was photolyzed without a filter to obtain the photoproduct.

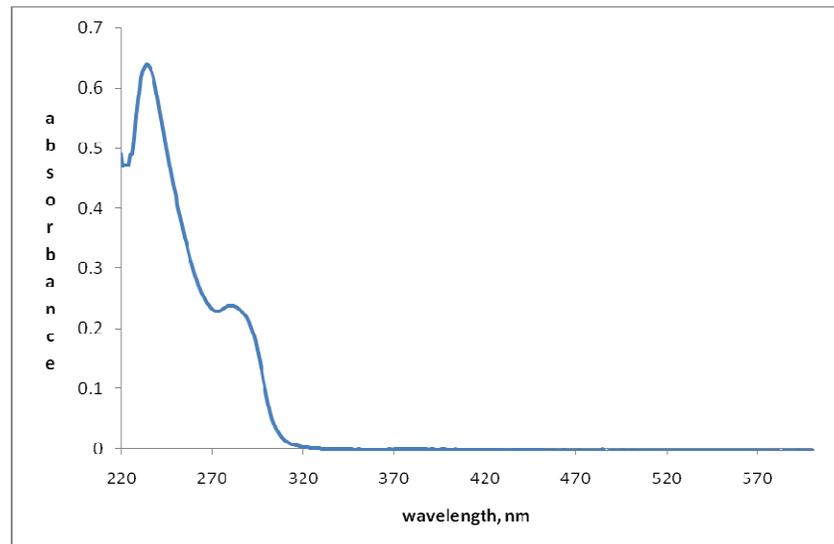
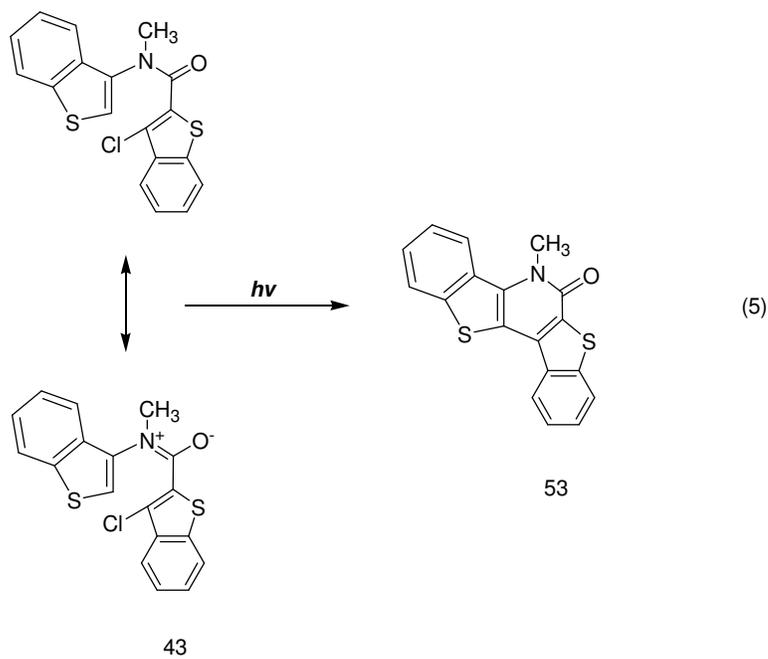


Figure 2.1 Absorption Spectrum of **43** ($\text{LG}^- = \text{Cl}^-$) at 5.7×10^{-5} M, in 20% 100 mM phosphate buffer in CH_3CN at pH 7.0.

2.2.3 Preparative Direct Photolysis.

Preparative direct photolysis of 0.021 M **43** ($\text{LG}^- = \text{Cl}^-$) with unfiltered light from a medium pressure mercury lamp in N_2 saturated 20% 100 mM phosphate buffer in CH_3CN at pH 7.0 for 3h resulted in the release of HCl to give **53** as the only photoproduct (eq. 5). The photoproduct (100% conversion by ^1H NMR) was isolated by extraction with ethyl acetate and purified by recrystallization from 1:3 ethyl acetate in hexane. The product was identified and distinguished from photoreactant by ^1H NMR as N-methyl peak shifted downfield from δ 3.55 to 4.36 ppm, and also aromatic region counts for 8 protons instead of 9 protons which were counted for photoreactant. Melting point also indicates the photoproduct as it is different by a large extent, mp found 244-245 $^\circ\text{C}$, where the photoreactant mp was found 132-133 $^\circ\text{C}$.

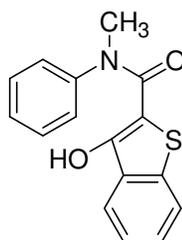


2.2.4 Quantum Yield.

The quantum yield for the electrocyclic ring closure reaction of amide **43** ($\text{LG}^- = \text{Cl}^-$) was determined at 310 nm in N_2 saturated 20% phosphate buffer at pH 7.0 in CH_3CN . The light output for the photochemical reaction was 0.027 mE/h. After 16 h photolysis the quantum yields of the reaction were found to be: $\Phi = 0.006 \pm 0.002$ and 0.008 ± 0.002 .

The quantum yield determinations involved quantifying the photoproduct formed by use of ^1H NMR spectroscopy with DMSO as an internal standard.

As found, this particular photoreaction is inefficient, so the project shifted to other benzothiophene carboxanilides with the focus on functionalizing the efficient benzothiophene ring A.



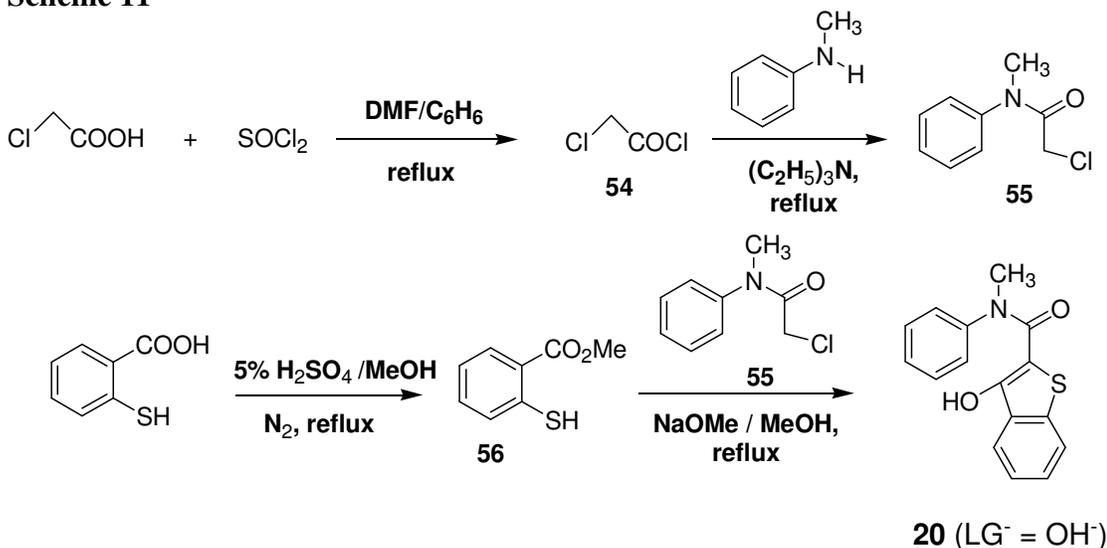
20 ($\text{LG}^- = \text{OH}^-$)

2.2.5 Photochemical Reactant.

The synthesis of anilide **20** ($\text{LG}^- = \text{OH}^-$) involved the reaction of ester **56** with amide **55** in excess of sodiummethoxide. Thiosalicylate **56** was produced from

thiosalicylic acid in presence of 5% H_2SO_4 in methanol. Synthesis of amide **55** involved acylation of N-methylaniline with chloroacetylchloride **54** which was initially prepared by the reaction of chloroacetic acid with thionylchloride.

Scheme 11



2.2.6 Crystal structure of the Photoreactant **20** ($\text{LG}^- = \text{OH}^-$).

According to the X-ray crystallographic data, the compound **20** ($\text{LG}^- = \text{OH}^-$) exhibits triclinic structure having empirical formula $\text{C}_{16}\text{H}_{13}\text{NO}_2\text{S}$. The intra-molecular H-bond makes benzothiophene moiety and amide group co-planar. This result in a short distance between S atom and plane of Ph substituent (just about 3.0 \AA) that forces the Ph group to be rotated almost perpendicular to the amide moiety.

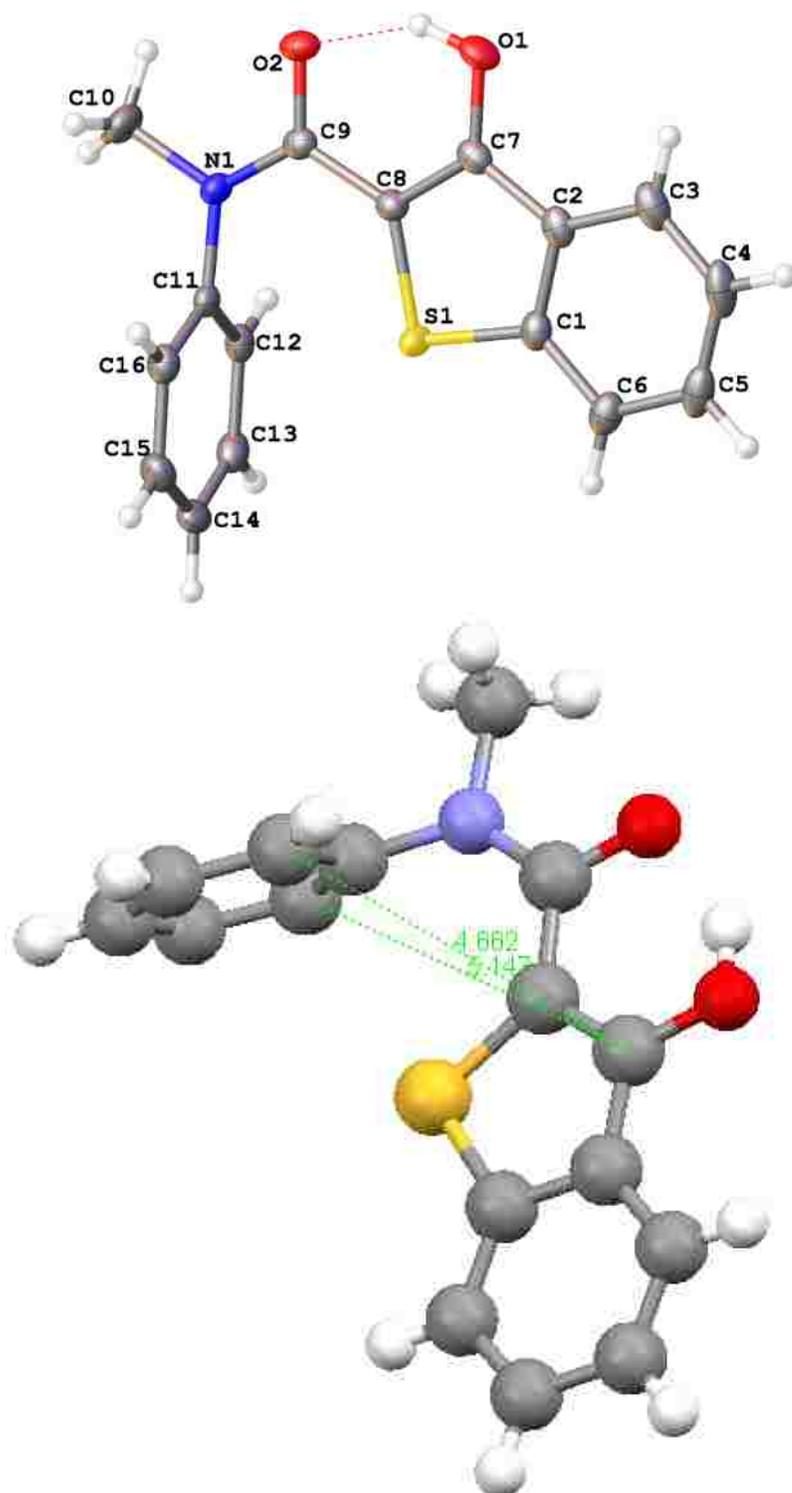
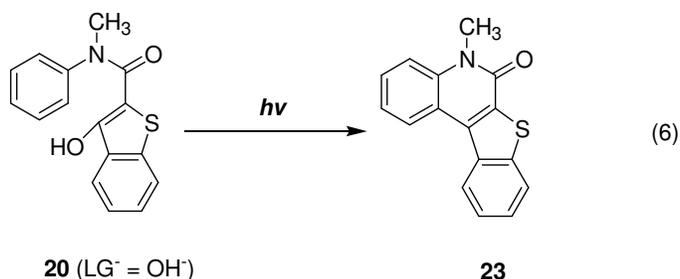


Figure 2.2 ORTEP representation of molecular structure of photoreactant **20**(LG⁻ = OH⁻).

Despite the unfavorable geometry of the crystalline material, in aqueous solution the compound cyclizes photochemically (*vide infra*). Two ortho-positions of the anilide ring are available in principle, for the cyclization to give the six-membered lactam. The distance from the carbon occupied by the hydroxyl leaving group to the two ortho-positions of the anilide ring are 4.662 and 5.147 Å.

2.2.7 Preparative Direct Photolysis.

Preparative direct photolysis of 0.021 M **20** ($\text{LG}^- = \text{OH}^-$) with unfiltered light from a medium pressure mercury lamp in N_2 saturated 30% 100 mM phosphate buffer in CH_3CN at pH 7 for 3h resulted in the release of H_2O to give **23** as the only photoproduct (eq. 6). The photoproduct (100% conversion by ^1H NMR) was isolated by extraction with ethyl acetate and purified by recrystallization from 1:3 ethyl acetate in hexane. The product was identified and distinguished from photoreactant by ^1H NMR as N-methyl peak shifted downfield from δ 3.47 to 3.92 ppm, and also aromatic region counts for 8 protons instead of 9 protons which were counted for photoreactant. Melting point also indicates the photoproduct as it is different by a large extent, mp found 204-205°C, where the photoreactant mp was found 115-117°C. Crystal structure and elemental analysis also suggest the photoproduct.



2.2.8 Crystal Structure of Photoproduct **23**.

According to the X-ray crystallographic data, the photoproduct **23** exhibits monoclinic structure having empirical formula $C_{16}H_{11}NOS$. The new bond formed by photochemical cyclization has a bond distance of 1.452 Å.

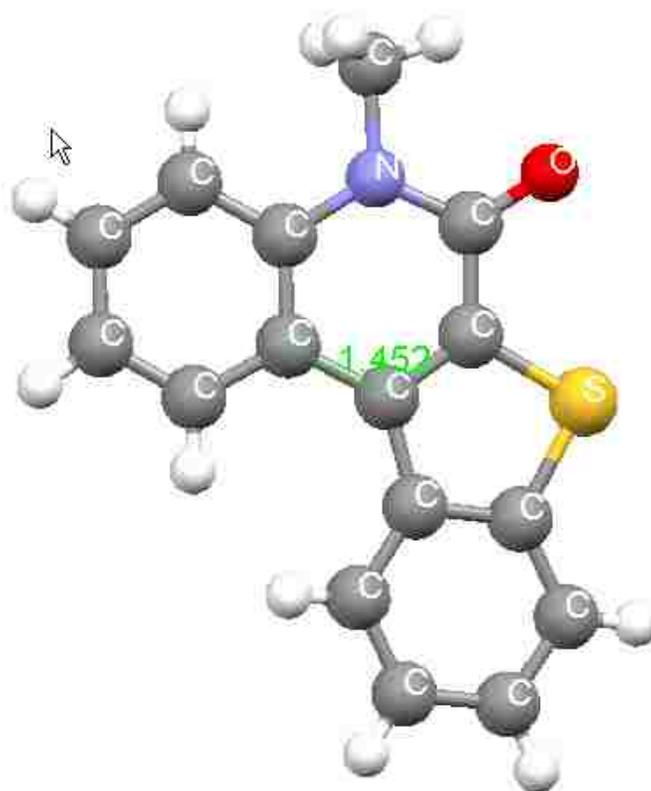
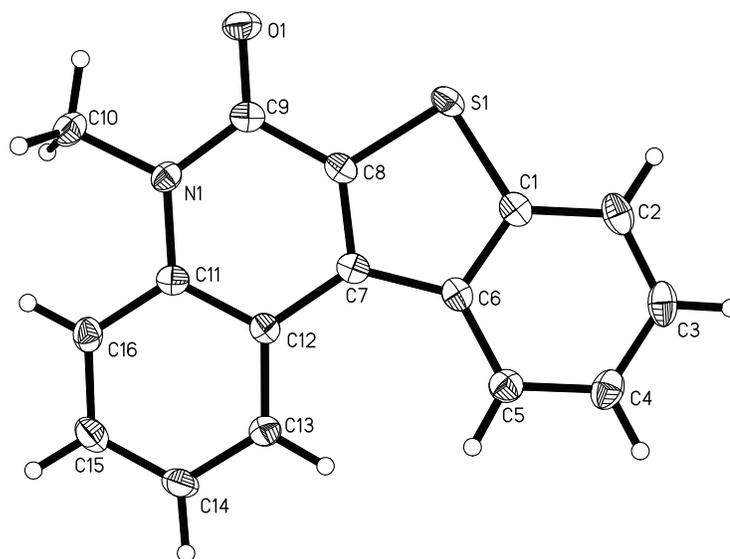


Figure. 2.3 ORTEP representation of molecular structure of photoproduct **23**.

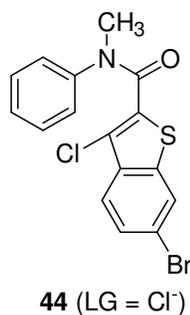
2.2.9 Quantum Yield.

The quantum yield for the electrocyclic ring closure reaction of anilide **20** ($\text{LG}^- = \text{OH}^-$) was determined at 310 nm in N_2 saturated 20% phosphate buffer at pH 7 in CH_3CN . The light output for the photochemical reaction was 0.027 mE/h. After 15.5 h photolysis the quantum yields of the reaction were found to be $\Phi = 0.008 \pm 0.002$ and 0.006 ± 0.002 .

The quantum yield determinations involved quantifying the photoproduct formed by use of ^1H NMR spectroscopy with DMSO as an internal standard. (Yields determined by ^1H NMR spectroscopy using DMSO as standard)

The result was consistent with our previous results observed with different leaving group having different basicity. Hydroxyl group is a very poor leaving group in compare to other leaving groups like chloride, carboxylate, phenolate or thiolate, the pK_a of the conjugate acid is the highest for hydroxy group. Only one photoproduct was observed. The mechanism may be like the one shown in scheme 1.

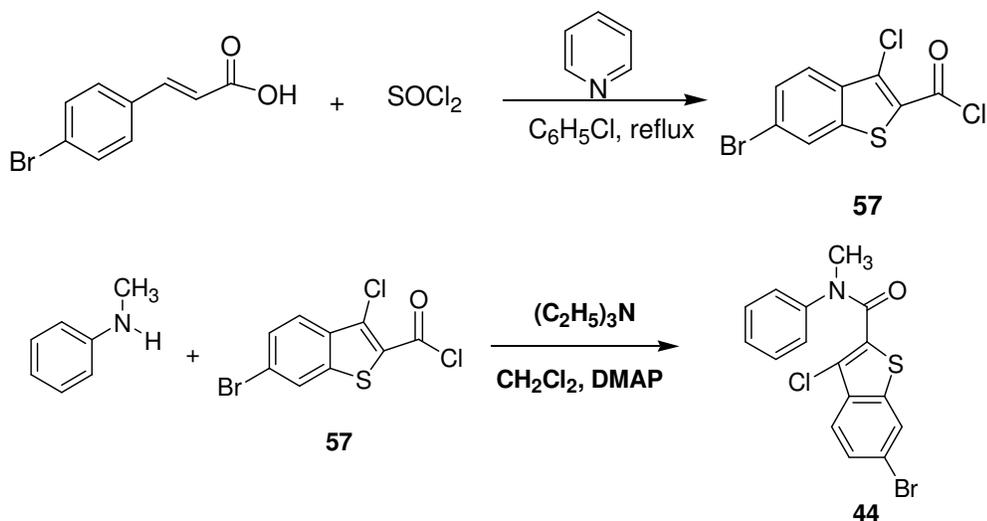
To observe the heavy atom effect of bromine on the quantum yield, the benzothiophene ring was modified by introducing a bromine atom at C-6. The compound **44** ($\text{LG}^- = \text{Cl}^-$) was synthesized.



2.2.10 Synthesis of Compound **44** ($\text{LG}^- = \text{Cl}^-$).

The synthesis of anilide **44** ($\text{LG}^- = \text{Cl}^-$) involved acylation of N-methylaniline with 6-bromo-3-chlorobenzothiophene carbonylchloride **57** (Scheme 12), which was initially prepared from the reaction of 4-bromocinnamic acid with thionyl chloride in the presence of a catalytic amount of pyridine.

Scheme 12



2.2.11 Crystal Structure of the Photoreactant **44** ($\text{LG}^- = \text{Cl}^-$).

According to the X-ray crystallographic data, the compound **44** ($\text{LG}^- = \text{Cl}^-$) exhibits monoclinic structure having empirical formula $\text{C}_{16}\text{H}_{11}\text{BrClNOS}$. The molecules form centrosymmetric anti-parallel pairs separated by $d = 3.51\text{\AA}$ (basically a Vander-Waals separation), possibly because of dipole-dipole interactions. There are somewhat shortened $\text{Br}\cdots\text{S-C}$ contacts (3.76\AA) that may correspond to a weak $\text{p}-\sigma^*$ interaction.

The bond distance from the carbon occupied by the chloride leaving group to two ortho-positions of the anilide ring are 4.194 and 5.247 Å.

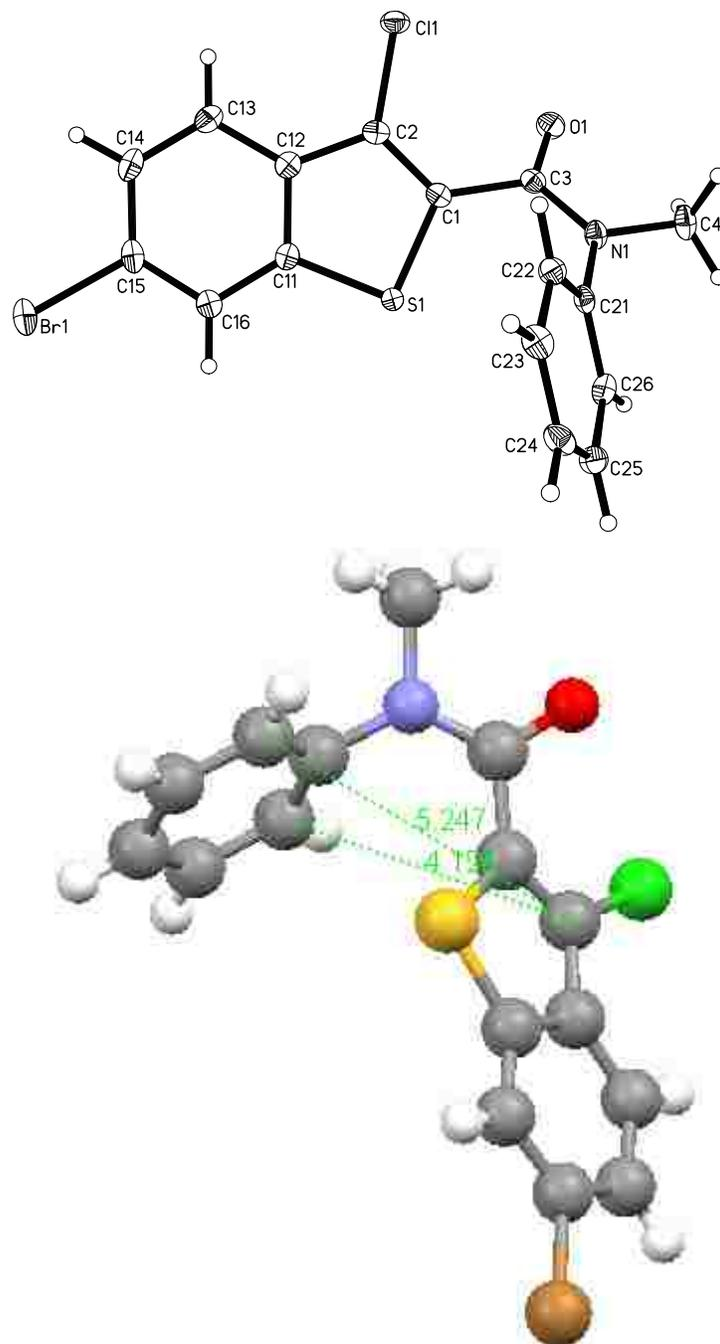


Figure 2.4 ORTEP representation of molecular structure of photoreactant **44** ($\text{LG}^- = \text{Cl}^-$).

2.2.12 UV- Spectra of Compound 44 ($\text{LG}^- = \text{Cl}^-$).

The ultraviolet spectra of the starting material was taken at different concentrations in 20% 100 mM phosphate buffer in CH_3CN to observe the absorption characteristics. At lower concentrations, the compound shows an absorption maximum below 300 nm which tailed out into the 300-350 nm region. Compound **44** was photolyzed without a filter to obtain the photoproduct.

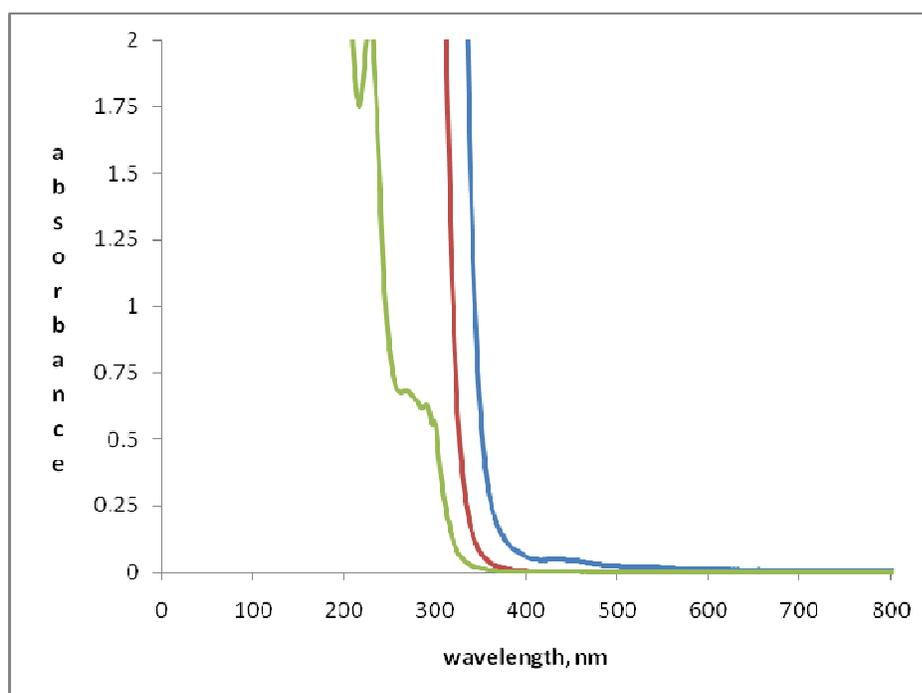
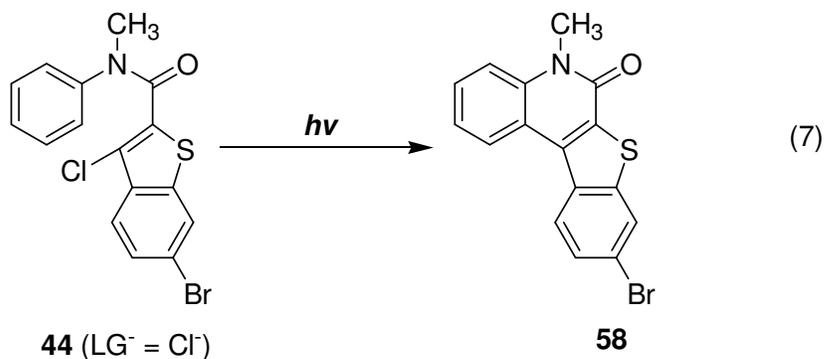


Figure. 2.5 Absorption Spectra of **44** ($\text{LG}^- = \text{Cl}^-$) at 3.0×10^{-3} M, 3.0×10^{-4} M, 3.0×10^{-5} M, in 20% 100 mM phosphate buffer in CH_3CN .

2.2.13 Preparative Direct Photolysis.

A 0.02 M solution of **44** ($\text{LG}^- = \text{Cl}^-$) in N_2 saturated 30% 100 mM phosphate buffer in dioxane at pH 7 was irradiated with a 450 W Hanovia medium pressure mercury lamp for 1 h. The photoproduct **58** was obtained by crystallization from benzene. Crystalline **58** (eq. 7) gave mp 262-263°C. The product was identified and distinguished from photoreactant by ^1H NMR as N-methyl peak shifted downfield from δ 3.520 to 3.886 ppm, and also aromatic region counts for 7 protons instead of 8 protons which was counted for photoreactant. Melting point also indicates the photoproduct as it is different by a large extent where the photoreactant mp was found 131-132°C and elemental analysis also suggests the photoproduct.



2.2.14 Quantum Yield

The quantum yield for the electrocyclic ring closure reaction of anilide **44** ($\text{LG}^- = \text{Cl}^-$) was determined at 310 nm in N_2 saturated 20% phosphate buffer at pH 7 in dioxane and in air saturated solution. The light output for the photochemical reaction was 0.027

mE/h. After 3 h photolysis the quantum yields of the reaction in various solvents and with without air present are summarized in **Table 2**.

Table 2: Quantum yields of the reaction of eq. 7

Solutions	Quantum Yield
CH ₃ CN (N ₂ saturated)	0.040±0.002
Dioxane (N ₂ saturated)	0.315±0.002
Dioxane (Air saturated)	0.161±0.002

The results in two different solvents varied strongly. The variation was due to solubility problems. The photoproduct **58** was not soluble in CH₃CN, so it crystallized on the front face of the sample cell, blocking the light. The solubility problem was solved by using dioxane, because the photoproduct **58** was soluble in it. The quantum yield was higher in N₂ saturated solution, likely because exclusion of air presented quenching of the triplet excited state by oxygen. In addition, the heavy atom effect of C-6 bromine likely caused the quantum yield to increase from 0.22 (observed in without bromine group) to 0.32.

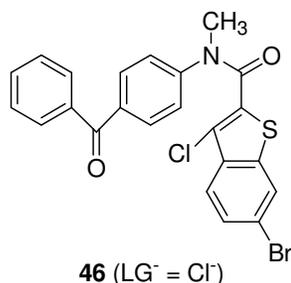
2.2.15 Quenching Studies.

To obtain more information on the multiplicity of the excited state involved in the reaction, quenching studies were performed using 1,3-pentadiene as a triplet quencher. The results indicated that the triplet-excited state likely was quenched in the presence of 1,3-pentadiene triplet quencher. The results are summarized in **Table 3**.

Table 3: Quenching studies of the reaction of eq. 7

Solution	Conc. of Quencher (1,3-pentadiene)	Quantum Yield
Dioxane (N ₂ Saturated)	0.01 M	0.029±0.002
Dioxane (N ₂ Saturated)	0.001 M	0.054±0.002
Dioxane (N ₂ Saturated)	0.0005 M	0.173±0.002

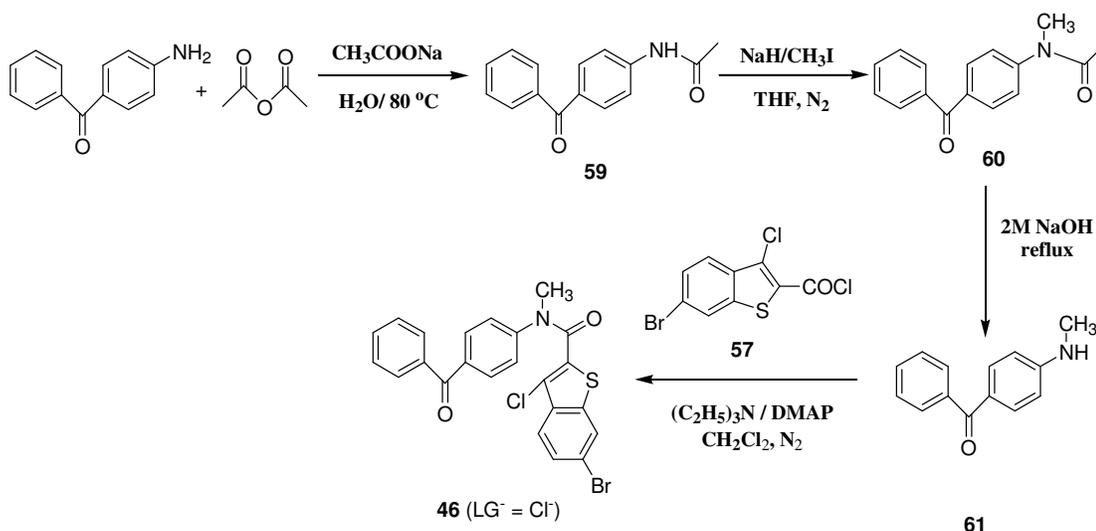
The next stage in the project was to shift the light absorption to longer wavelength so that compounds that are derivatives of **58** might have use for biological applications. Compound **46** (LG⁻ = Cl⁻) with a para benzoyl group was thus synthesized.



2.2.16 Synthesis of Compound **46** ($\text{LG}^- = \text{Cl}^-$).

The synthesis of anilide **46** ($\text{LG}^- = \text{Cl}^-$) involved acylation of 4-methylamino-benzophenone **61** with 6-bromo-3-chlorobenzothiophene-2-carbonyl chloride **57**. The compound **61** was initially prepared by a three step process starting from commercially available 4-aminobenzophenone (see Experimental).

Scheme 13



2.2.17 Crystal structure of the Photoreactant **46** ($\text{LG}^- = \text{Cl}^-$).

According to the X-ray crystallographic data, the compound **46** ($\text{LG}^- = \text{Cl}^-$), exhibits triclinic structure having empirical formula $\text{C}_{23}\text{H}_{15}\text{ClBrNO}_2\text{S}$. The amide group is planar with the Me-group trans-oriented relative to benzothiophene. Benzophenone

moiety is somewhat twisted. The bond distance from the carbon occupied by the chloride leaving group to two ortho-positions of the aniline ring are 4.073 and 3.302 Å.

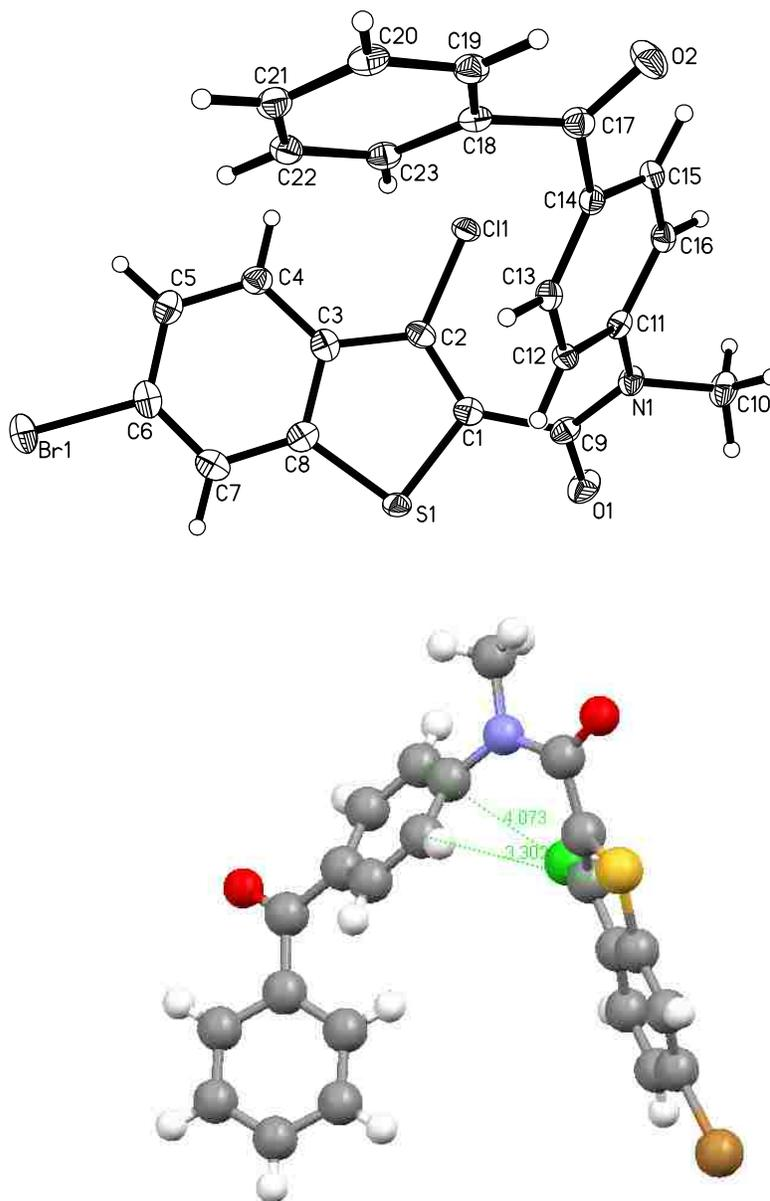


Figure 2.6 ORTEP representation of molecular structure of photoreactant **46** (LG⁻ = Cl⁻).

2.2.18 UV Spectra of Compound 46 (LG⁻ = Cl⁻)

The ultraviolet spectra of the starting material was taken at different concentrations in 15% 100 mM phosphate buffer in CH₃CN at pH 7.0 to observe the absorption characteristics. At lower concentrations, the compound shows an absorption maximum below 350 nm which tailed out into the 350-380 nm region. The compound was photolyzed without a filter to obtain the photoproduct.

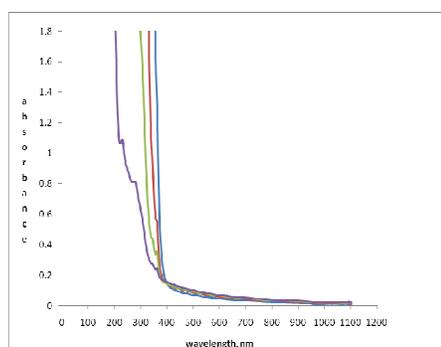


Figure 2.7 Absorption Spectra of **46** (LG⁻ = Cl⁻) at 3.0×10^{-3} M, 5.0×10^{-4} M, 1.0×10^{-4} M, 3.0×10^{-5} in 20% 100 mM phosphate buffer in CH₃CN at pH 7.0.

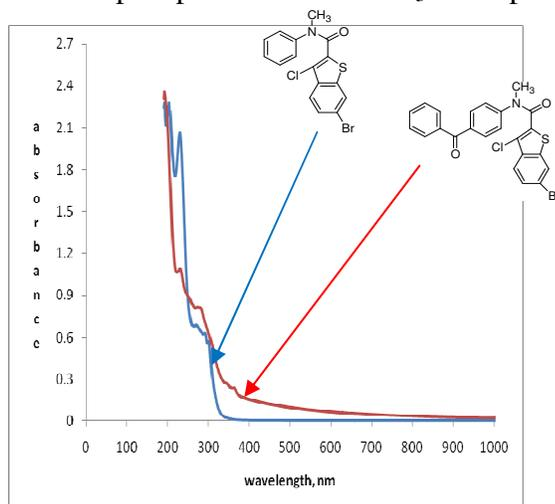
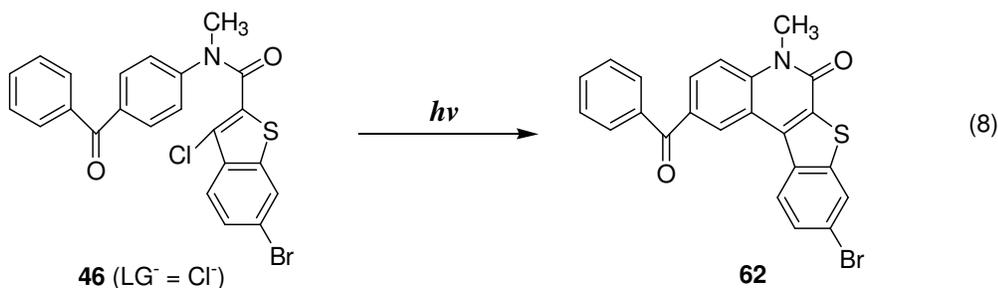


Figure 2.8 Absorption spectra of 3.0×10^{-5} M **44** (LG⁻ = Cl⁻) and 3.0×10^{-4} M **46** (LG⁻ = Cl⁻) 30% 100 mM phosphate buffer in CH₃CN at pH 7.0.

2.2.19 Preparative Direct Photolysis.

Preparative direct photolysis of 0.015 M **46** ($\text{LG}^- = \text{Cl}^-$) with unfiltered light from a medium pressure mercury lamp in N_2 saturated 30% 100 mM phosphate buffer in dioxane at pH 7.0 for 50 mins resulted in the release of hydrochloric acid to give **62** as the only photoproduct (equation 8). The photoproduct (100 % conversion by ^1H NMR) was isolated as a colorless powder, mp 264-265°C. The product was identified and distinguished from photoreactant by ^1H NMR as N-methyl peak shifted downfield from δ 3.578 to 3.952 ppm, and also aromatic region counts for 11 protons instead of 12 protons which were counted for photoreactant. Melting point also indicates the photoproduct as it is different by a large extent, where the photoreactant mp was found 113-114°C.



2.2.20 Quantum Yield.

The quantum yield for the electrocyclic ring closure reaction of compound **46** ($\text{LG}^- = \text{Cl}^-$) was determined separately at 365 nm in N_2 saturated 20% phosphate buffer at pH 7 in dioxane at variable irradiation times. The light output for the photochemical

reaction was 0.097 mE/h. The results of the quantum yields of the reaction are summarized in **Table 4**.

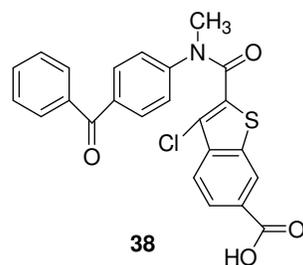
Table 4: Quantum yields of the reaction of eq. 8

Solutions	Irradiation time (h)	Quantum Yield
Buffer in Dioxane (N ₂ saturated)	3	0.179±0.002
Buffer in Dioxane (air saturated)	11.5	0.074±0.002

The calculated quantum yields varied with irradiation time, even in the same solvent. This was found to be due to solubility problem of photoproduct in dioxane. When the photolysis was conducted for longer than 3 h, more product was produced which resulted in the deposition of the photoproducts onto the front face of the sample cell, thus blocking the light during further photolysis and resulted in incorrect Φ . Again the reaction was quenched by oxygen, which indicates triplet excited state photoreaction. However the quantum yield was not as much higher from compound **45** (LG⁻ = Cl⁻) than observed in case of compounds from **20** (LG⁻ = Cl⁻) to **44** (LG⁻ = Cl⁻).

The solubility problems encountered with **46** and **62** required a change in strategy for the project. Thus, the plan became to enhance water solubility by introducing a carboxylic acid group onto the C-6 position of the benzothiophene ring system. This C-6 carboxylic acid group would mean that the bromine would need to be placed in the chromophoric group attached to the amide nitrogen. Further work on exploiting the

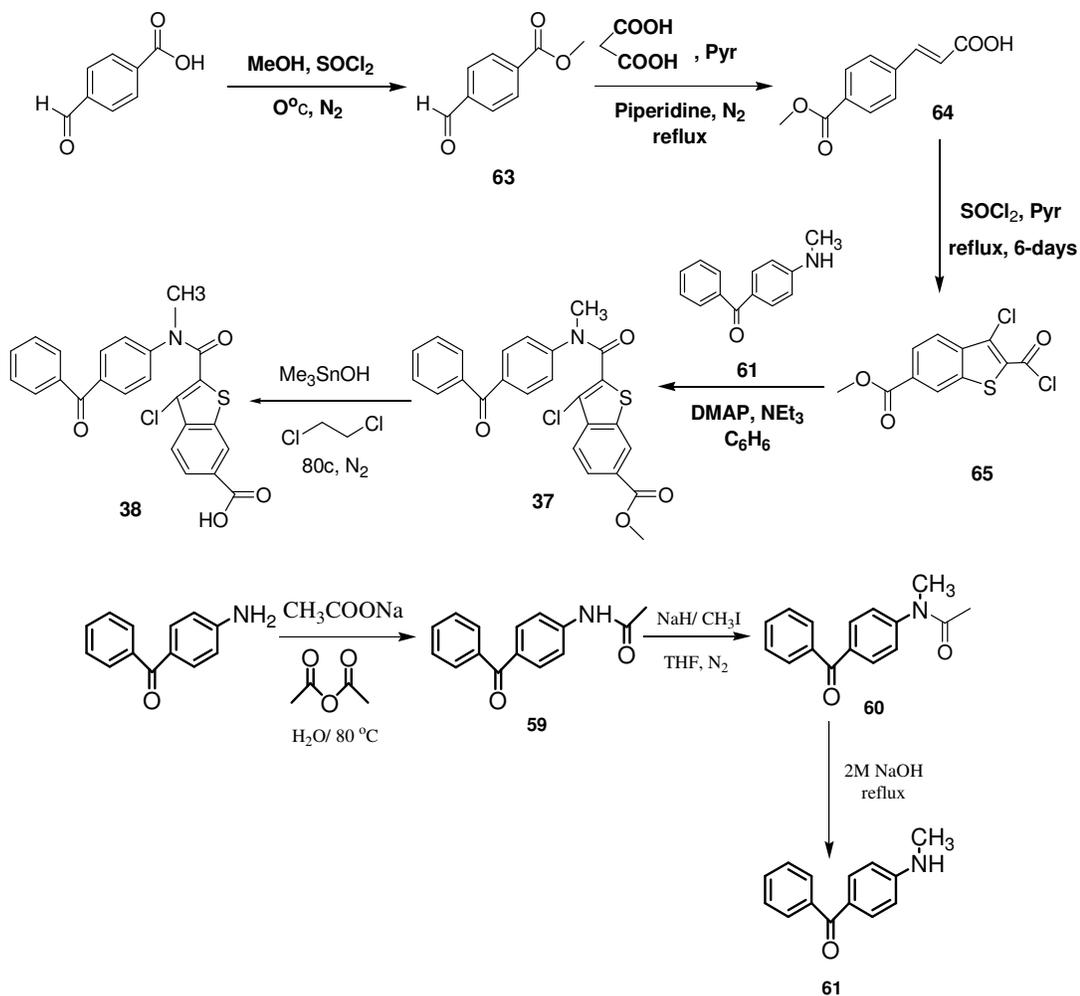
heavy atom effect to increase quantum yield thus was postponed. We already have been successful in synthesizing the compound **38** following the path described in Scheme 14.



2.2.21 Synthesis of Photoreactant **38**.

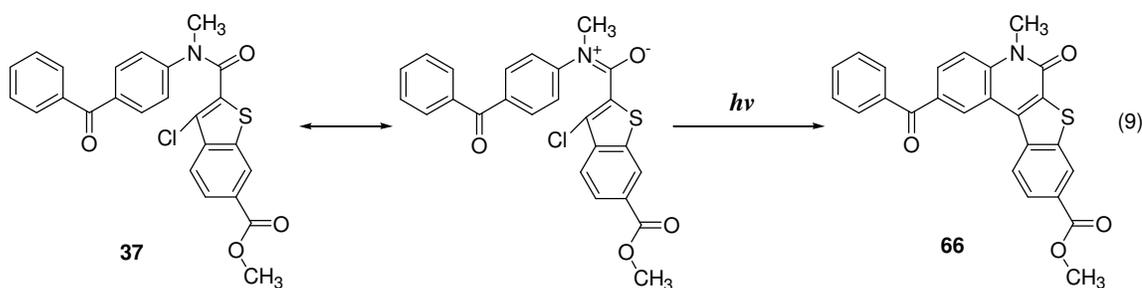
The synthesis of anilide **38** (LG⁻ = Cl⁻) involved hydrolysis of ester (**37**), which was initially prepared by acylation of 4-methylaminobenzophenone (**61**) with compound (**65**). The compound (**65**) was prepared by refluxing methyl ester of *trans*-cinnamic acid (**64**) with thionyl chloride for 6 days. Acid (**64**) was produced by a two steps process starting from 4-formylbenzoic acid (see Experimental).

Scheme 14

2.2.22 Preparative Direct Photolysis of **37** (LG = Cl).

Preparative direct photolysis of 0.02 M **37** (LG⁻ = Cl⁻) with unfiltered light from a medium pressure mercury lamp in N₂ saturated 15% 100 mM phosphate buffer in dioxane at pH 7 for 40 mins resulted in the release of hydrochloric acid to give **66** as the only photoproduct (equation 9). The photoproduct (100 % conversion characterized by ¹H NMR) was isolated as a brown solid, mp 284-285°C. The product was identified and

distinguished from photoreactant by ^1H NMR as N-methyl and O-methyl peaks shifted downfield from δ 3.58 and 3.93 to 3.89 and 3.99 ppm respectively, and also aromatic region counts for 11 protons instead of 12 protons which was counted for photoreactant. Melting point also indicates the photoproduct as it is different by a large extent, where the photoreactant mp was found 213-214 $^\circ\text{C}$.

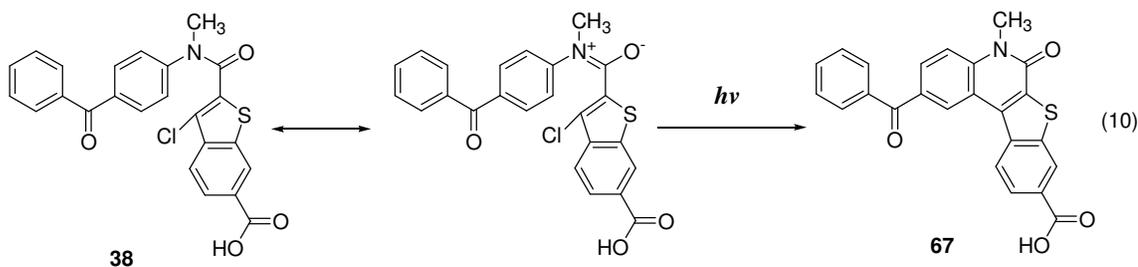


2.2.23 Quantum Yield.

The quantum yield for the electrocyclic ring closure reaction of compound **37** ($\text{LG}^- = \text{Cl}^-$) was determined separately at 365 nm in N_2 saturated 14.5% phosphate buffer at pH 7 in CH_3CN at variable irradiation time. The reaction was highly efficient and longer time irradiation resulted starting material conversion to photoproduct higher than 20%. After irradiation for 22 minutes the quantum yield was found 0.133 with 98.9% of material balance and 6.5% of starting material conversion to photoproduct. The total light output for the photochemical reaction was 0.104 mE/h. However the quantum yield was as similar as observed in case of compound **45** ($\text{LG}^- = \text{Cl}^-$).

2.2.24 Preparative Direct Photolysis of **38** (LG = Cl).

A 0.015 M solution of **38** in N₂ saturated 25% 100 mM phosphate buffer in dioxane at pH 7.0 was irradiated with an unfiltered light from 450 W Hanovia medium pressure mercury lamp for 1 h. The reaction mixture was acidified with dilute HCl to get solid precipitation. The off white powder was obtained from filtration of the mixture as the only photoproduct **67** (equation 10) and 100% conversion characterized by ¹H NMR, mp 300₊°C. The product was identified and distinguished from photoreactant by ¹H NMR as N-methyl peak shifted downfield from δ 3.60 to 3.82 and also aromatic region counts for 11 protons instead of 12 protons which was counted for photoreactant. Melting point also indicates the photoproduct as it is different by a very large extent, where the photoreactant mp was found 75 - 77°C.



2.2.25 Quantum Yield.

The quantum yield for the electrocyclic ring closure reaction of compound **38** (LG⁻ = Cl⁻) was determined separately at 365 nm in N₂ saturated phosphate buffer at pH 7 in different solvent at variable irradiation times. The reaction was highly efficient and

longer time irradiation resulted in starting material conversion to photoproduct higher than 20%. The light output for the photochemical reaction was 0.104 mE/h. The results of the quantum yields of the reaction are summarized in Table 5.

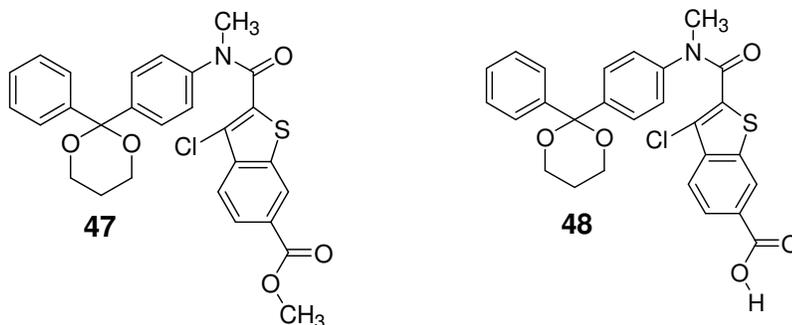
Table 5: Quantum yields of the reaction of eq. 10

Solution	Irradiation time	Product conversion, %	Quantum Yield
74.55% aq. Buffer in N ₂ saturated CH ₃ CN	3 h	18	0.019±0.002
65.45% aq. Buffer in N ₂ saturated Dioxane	40 min	13	0.147±0.002
25.45% aq. Buffer in N ₂ saturated Dioxane	30 min	12	0.137±0.002

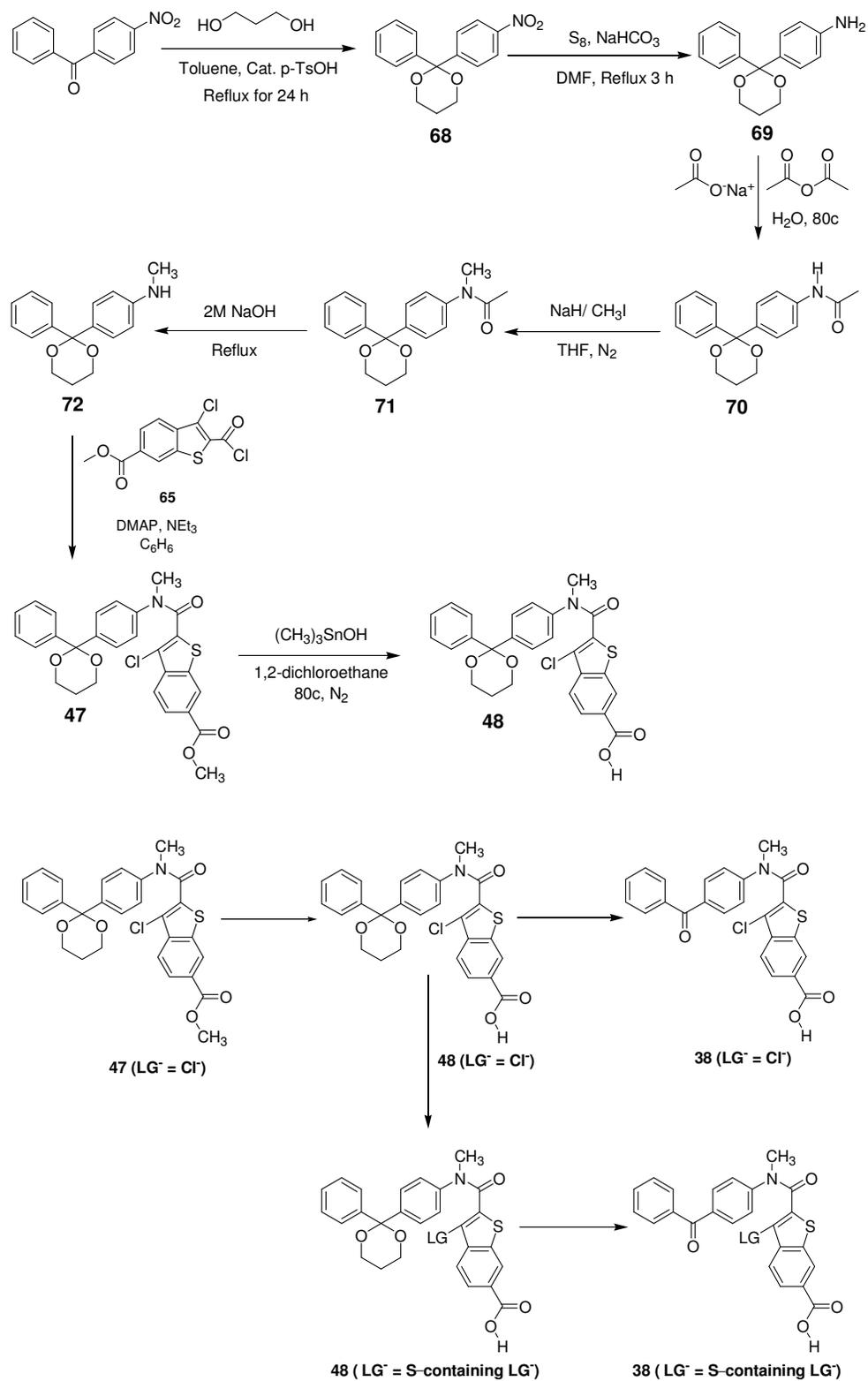
The quantum yields varied with different solvents even in same solvent with variable concentration of buffer. This was found to be due to solubility problems. The photoproduct **67** was not soluble in CH₃CN which results the deposition of the photoproducts onto the front face of the sample cell, thus blocking the light during further photolysis resulted in incorrect Φ . Thus the poor solubility of the photoproduct in CH₃CN was solved using dioxane. But even in dioxane, the quantum yields were found higher in higher concentration of buffer than the same in lower. It seems possible that buffer

facilitates the higher production of photoproduct. However the quantum yield was as much higher as observed in case of compound **45** ($\text{LG}^- = \text{Cl}^-$).

But in case of incorporating S-containing LG in place of Cl^- had been encountered a lot difficulties with compound **38**, required another change in strategy for the project. Thus, the plan became to protect the carbonyl group of the benzophenone chromophore to obtain our biologically important target molecules. We already have been successful in synthesizing the compound **71** following the path described in Scheme 15. However, we could not reach our target point due to the shortage of time. But even though it is conceivable to reach the goal by following the reaction pathways showed in Scheme 15 with additional steps from using **71**.



Scheme 15



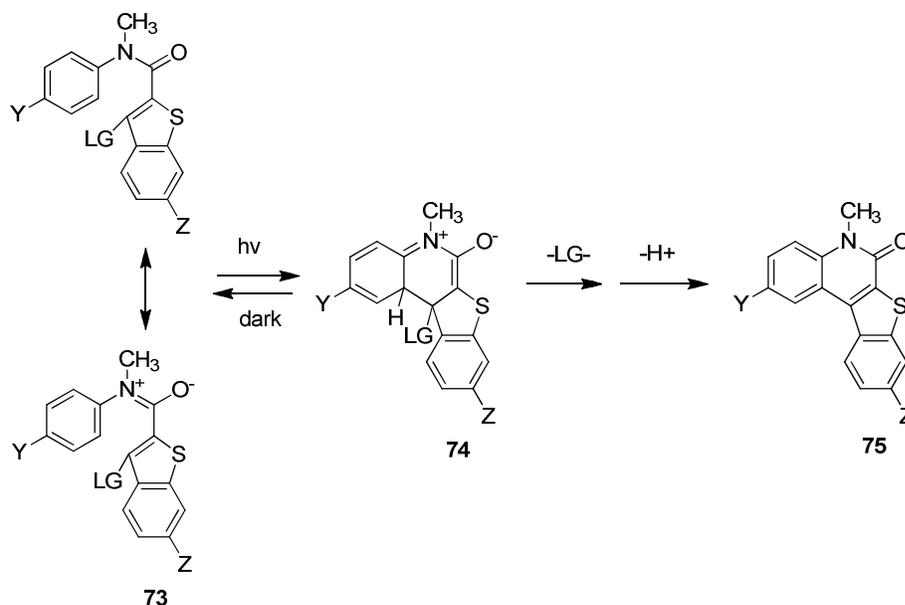
2.3 Discussion

As stated in the Introduction, the goal of the project is to develop a practically useful photochemically removable protecting group that is based upon a photochemical electrocyclic ring closure reaction to generate a zwitterionic intermediate. The zwitterionic intermediate would be capable of expelling a variety of leaving group anions, which are expected to range in basicity from carboxylate anions to phenolate anions. Scheme 8 describes the general mechanism envisioned for the photoreactivity of such “cage” compounds.

This project specifically exploits the benzothiophene ring system to control the regioselectivity for the photochemical ring closure (Scheme 16). Only a single pathway is available for the cyclization that generates the key zwitterionic intermediate. Thus, there would be only a single photoproduct formed, compound **75**, after the zwitterionic intermediate expels the leaving group, LG^- . Note that Scheme 16 corresponds to pathway c in Scheme 6, and thus simplifies the mechanism considerably. Omission of paths a and b is justified by preliminary results obtained prior to the study. The key from that study was that quantum yields for photoproduct **23** decreased with increasing leaving group basicity and showed an approximate linear dependence on the pK_a of LG-H . On the other hand, if paths a and b governed the photochemistry of **73**, the quantum yields would remain approximately constant as a function of LG^- basicity. For example, expulsion of LG^- occurs subsequent to loss of a proton via path a. The quantum yield for photoproduct **75** would then depend on the competition between paths a and b, which

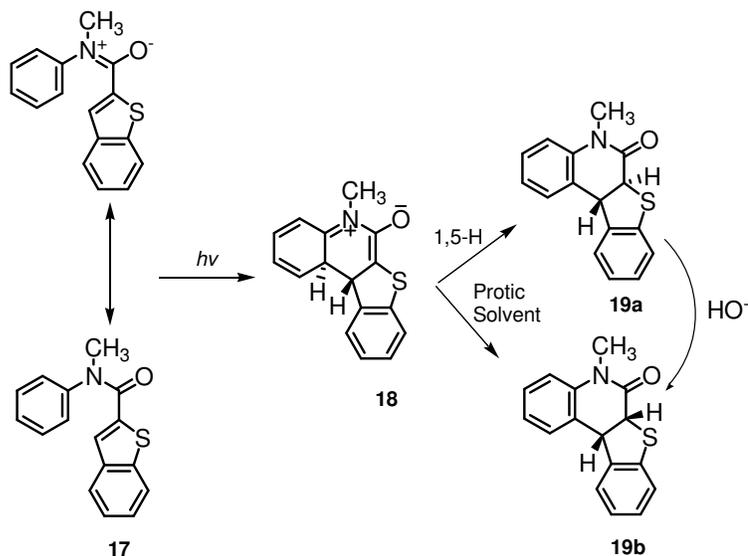
would not be subject to LG^- basicity. Nearly constant Φ as the LG^- is varied was observed previously for acrylanilides bearing a variety of LG^- .

Scheme 16



At the onset of the study little was known about the photochemistry of benzothiophene carboxanilides. The mechanism was previously studied to determine the stereochemistry of the photochemical ring closure, which was found to be conrotatory. Since no LG^- was present, the conrotatory cyclization produced a putative zwitterion, analogous to **74**, and in aprotic solvent, a 1,5-H shift took place to afford a product with *trans* stereochemistry at the newly-formed ring junction. This constituted good evidence for a conrotatory ring closure. In protic solvent the more stable *cis* isomer was also observed due to competing protonation of the enolate and tautomerization of the resulting enol.

Scheme 17



However, no quantum yields had been determined, and the multiplicity of the photoreaction was uncertain by this previous study. The quantum yield for **73** ($\text{LG}^- = \text{Cl}^-$) was determined, experimentally, by a coworker, early in the present project. The benzothioamide **73** with $\text{LG}^- = \text{Cl}^-$, photolyzed with $\Phi = 0.22$, to give **75** under buffered aqueous conditions. In addition, it appeared that the Φ for photocyclization to **75** was lower in air-saturated solvents, suggestive of triplet multiplicity for the photoreaction because O_2 is a well-known triplet quencher and it quenches the triplet multiplicity of the photoreactant by gaining energy from it. The project initially focused on two aspects: (1) work was initiated to obtain a more efficient benzothioamide system, and (2) studies were performed to obtain additional evidence for triplet multiplicity by exploiting the heavy atom effect of bromine substituent.

Based on the studies of photochromism by Irie, the thiophene and benzothiophene ring systems would be expected to undergo efficient photochemical electrocyclic ring closure reactions. The findings of Irie are summarized in the introduction. With a single benzothiophene ring, as in the case of **73**, the reaction was relatively efficient ($\Phi = 0.22$). It was expected that by replacing the phenyl group of the anilide with a second benzothiophene ring, the quantum yield for electrocyclization would show a further increase. The benzothiophene carboxamide **43** was thus synthesized by a convergent, six-step route (Scheme 10, Results).

Photolysis of **43** in aqueous buffer afforded the cyclized product **53** in essentially quantitative yield, and thus, the photochemistry appeared to be promising. However, quantum yield determinations gave $\Phi = 0.006 \pm 0.002 - 0.008 \pm 0.002$. The photochemical electrocyclic ring closure was surprisingly inefficient. The reason for the inefficient photocyclization of **43** is a matter of speculation. It is possible that the increase in quantum yield in case of one benzothiophene ring as **A** is due to a change in multiplicity from singlet to triplet. It also seems possible that the increase in Φ could reflect a decrease in aromatic stabilization energy in going from phenyl to benzothiophene, as suggested in Table 1. Perhaps by replacing the anilide phenyl group with a second benzothiophene ring involves the electrocyclization of two less strongly aromatic benzothiophene rings and the formation of the pentacyclic product containing two five-membered rings is thermodynamically unfavorable.

Attention was next turned to obtaining additional evidence for the triplet multiplicity of the photocyclization of benzothiophene carboxamides by use of the heavy

atom effect. This led to the synthesis of the C-6 bromide, compound **44**. An excursion was made from this goal to help a coworker devise a synthesis of the C-3 hydroxy-substituted benzothiophene carboxamide **20**, which was essential for introducing carboxylate groups into the C-3 position of the benzothiophene ring. This excursion expedited the synthesis of **20**, and eventually **73** ($\text{LG}^- = \text{PhCH}_2\text{CO}_2^-$, which was a subject of our published communication.^{23c} The excursion provided the necessary experience for constructing the benzothiophene ring system by the Claisen condensation route.

Photolysis of the C-6 bromide **44** in aqueous buffer ($\text{pH} = 7$) produced photoproduct **58** in essentially quantitative yield. The quantum yield was found to be 0.315, which is substantially higher than $\Phi = 0.22$ for compound **20** (without the C-6 bromide and Cl^- LG^- in C-3 position of benzothiophene ring). For **44** in air-saturated solvent $\Phi = 0.161$, consistent with quenching of a triplet excited state in the presence of dissolved oxygen. Addition of 1,3-pentadiene also resulted in decreased quantum yields, likely as a consequence of quenching of the triplet excited state. Such quenching became more pronounced with increasing concentrations of the 1,3-diene. This result was incorporated in the communication.^{23c}

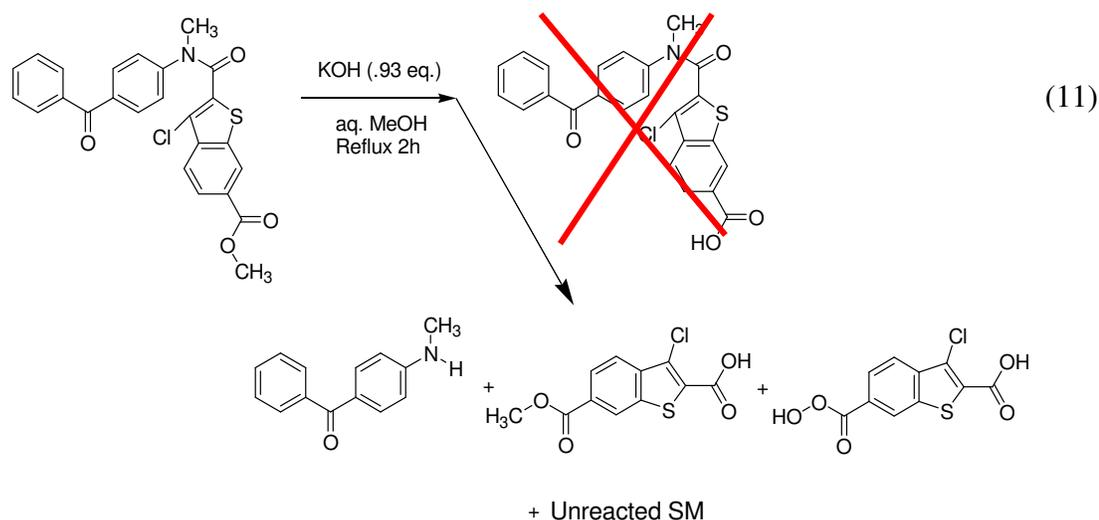
The original plan was to incorporate various long-wavelength chromophores in place of the phenyl substituent attached to the amide nitrogen. As a test case, a para benzoyl substituent was introduced at the phenyl group of **44**. The heavy atom bromide was retained to determine if further increases in quantum efficiency could be achieved. Compound **46** was thus synthesized via acylation of a *p*-methylaminobenzophenone **61** by C-6 substituted benzothiophene carbonyl chloride **57**. The UV spectrum of **46** (Figure

2.7) suggested that the photolysis wavelength could then be shifted to 365 nm from 310 nm, which had been used for **44** and **20**. When a preparative photolysis was conducted in aqueous CH₃CN containing buffer, the photoproduct **62** was formed in essentially quantitative yield at 100% conversion, and **62** precipitated out of the solution. The poor solubility of **62** in aqueous CH₃CN seriously hampered the quantum yield determinations, even when the quantum yield runs were conducted in aqueous dioxane, for which the solubility was improved. The quantum yields were lowered by deposition of **62** onto the front face of the photolytic cell, which blocked further transmission of light through the cell.

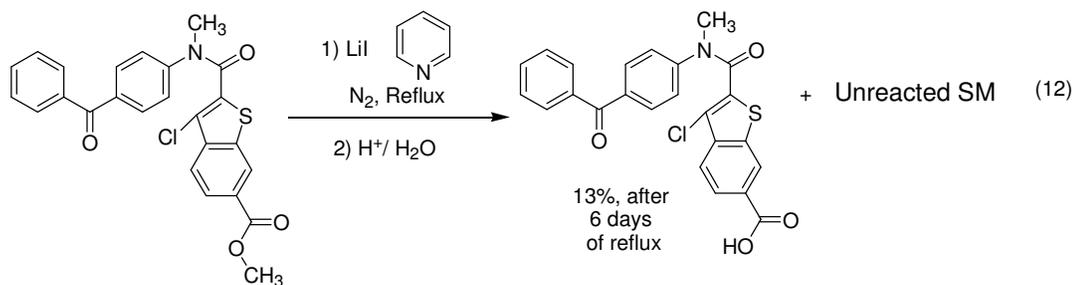
The aforementioned solubility problems encountered during photolyses of **44** required that the original research plan to be modified. The *N*-phenyl group of **1** would be exchanged for long wavelength chromophores. The C-6 position of the benzothiophene ring would be reserved for a substituent which would improve water solubility. Any heavy atom would be placed directly onto the chromophoric group, if needed.

In conformance with the revised plan, benzophenone derivative **38** was synthesized. Compound **38** has a solubilizing carboxylate group at the C-6 position. The eight step synthesis proved to be somewhat nontrivial, due to difficulties isolating good yields of **37**. The original literature procedure adopted used chlorobenzene as the solvent for the conversion of **64** to **65**, using thionyl chloride as the reagent. This solvent allowed the reaction to be performed at higher temperatures, which shortened the reaction times. However, the acid chloride **65** proved difficult to isolate from chlorobenzene. Thus, a

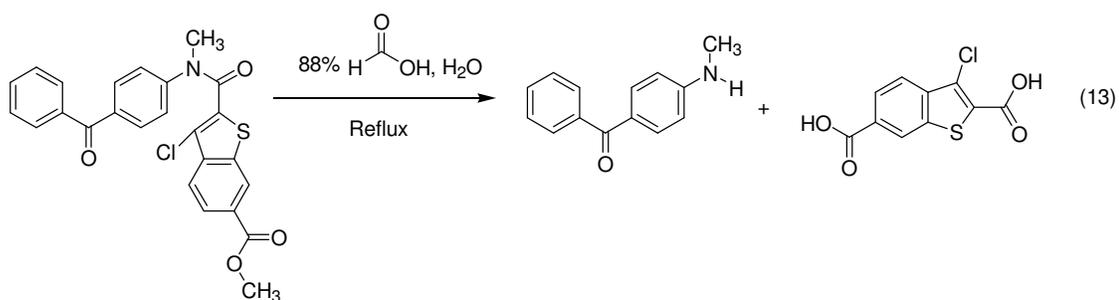
second procedure was adopted, which involved refluxing **64** with SOCl_2 , and this procedure made it possible to isolate **65** more easily, at the expense of long reaction times. Ultimately, however, the optimal procedure involved simply distilling the SOCl_2 and hydrolyzing the acid chloride to give the carboxylic acid, which was isolated. The acid was then converted to the acid chloride for the acylation of *p*-methylaminobenzophenone **61**. After acylation, the hydrolysis of amide product **37** proved to be difficult to isolate **38** in a reasonable yield. Several attempts were provided using different methods, but everytime the amide C-N bond were broken. The very first time following path of 0.93 eq. of KOH in aqueous MeOH was used in the ester and was refluxed for 2 h.



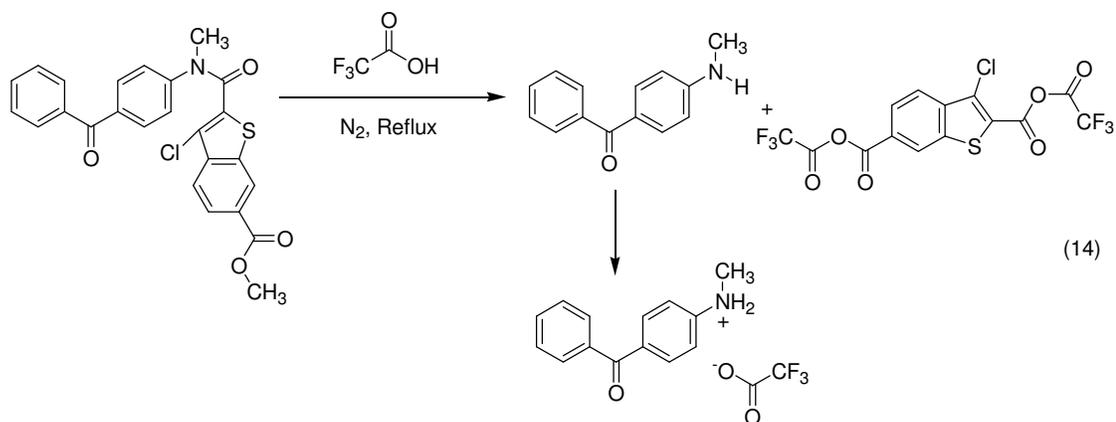
Secondly, the ester was refluxed with LiI in pyridine under N_2 environment and the reaction mixture was then acidified, but found only 13% of acid product after even 6 days of reflux.



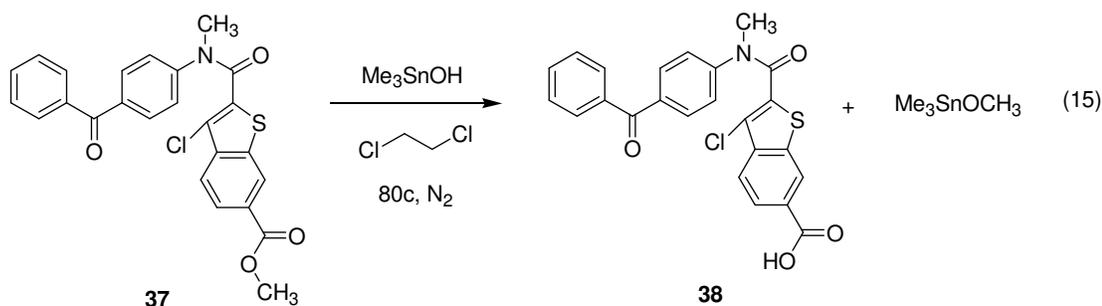
Another method of refluxing the ester with 88% formic acid in water was followed.



The next method was refluxing with trifluoroacetic acid but no fortune.

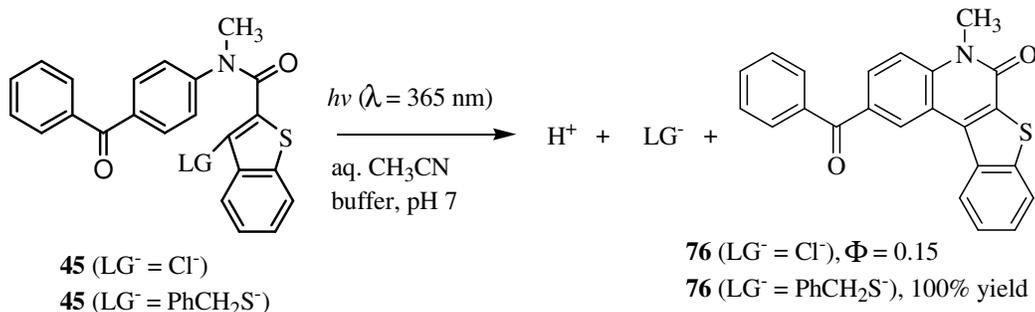


It could be possible that the carbonyl oxygen of the benzoyl group is relatively conjugated with amide N, so in case of hydrolysis, the amide C-N single bond breaks and the starting materials of the acylation step were isolated. Finally we successfully hydrolyzed the ester to acid in reasonable amount (>93%) following the procedure written in the literature by K. C. Nicolaou *et. al.*^{27b} Trimethyltin hydroxide was used as a mild hydrolyzing agent in the presence of dichloroethane in N₂-saturated reaction mixture at 80°C which required a longer reaction time.



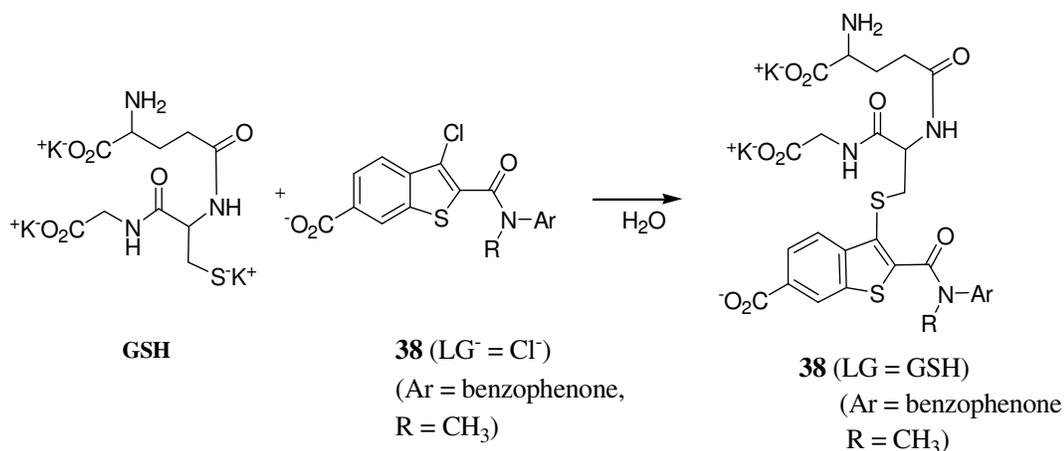
We conducted preparative photolysis of **38** and determined its quantum yield. The compound reacted similarly to **45** (LG⁻ = Cl⁻), whose efficiency has been measured previously as part of related research.

Scheme 18



As benzylthiolate was introduced successfully into **45** (Scheme 18), so it was expected that aqueous soluble carboxylate salt of **38** would also incorporate the other thiolate group like glutathione (GS⁻) following the same procedure under aqueous basic conditions (Scheme 19). However, such an attempt was beyond the scope at this part of our research.

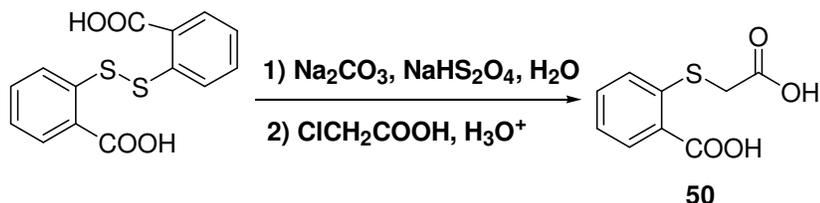
Scheme 19



Although a number of attempts were conducted to incorporate S-containing LG in place of Cl⁻ in **38**, but we had been unsuccessful using the similar method used previously in our laboratory.^{23c,d} At this point, a new approach was required to be implemented by protecting the carbonyl group of the benzophenone chromophore which could eliminate our problems to obtain our biologically important target molecules. I already have been successful in synthesizing the compound **71** (Scheme 15) and our target photoreactant was two steps away.

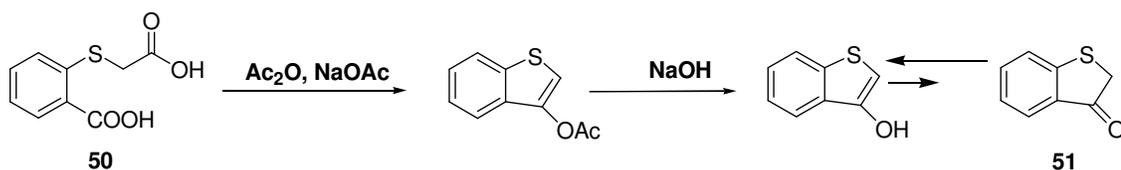
2.4 Experimental

Synthesis of *o*-carboxyphenylmercaptoacetic acid (**50**).



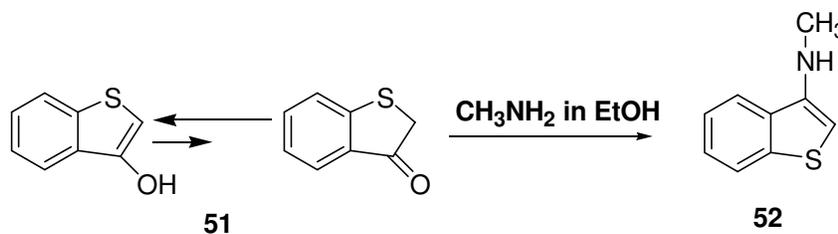
To commercially available 10 g (0.033 mol) of 2,2'-dithiosalicylic acid was added 20 g (0.19 mol) of anhydrous Na_2CO_3 dissolved in 150 mL of water followed by 15 g of NaHS_2O_4 . The reaction mixture was heated to reflux for 2 h. After reflux, was extracted by ethyl acetate, washed with aq. saturated NaHCO_3 , then with brine solution, dried over Na_2SO_4 and concentrated in vacuo. Which was then added in a mixture of 15 g of chloroacetic acid dissolved in water followed by 2M Na_2CO_3 to make pH = 7. The total water was used 200 mL. The mixture was then refluxed for 4 h followed by cooling down, then acidified to congo red using conc. H_2SO_4 , filtered, recrystallized from water to give 13.45 g (100% yield) of a greenish powder **50**, mp 217-218°C. The spectral data were as follows: $^1\text{H NMR}$ ($\text{C}_2\text{D}_6\text{CO}$) δ 3.83 (s, 2H), 7.26 (t, $J = 7.4$ Hz, 1H), 7.49 – 7.58 (m, 2H), 8.03 (d, $J = 7.7$ Hz, 1H).

Synthesis of benzothiophene-3(2H)-one (**51**).



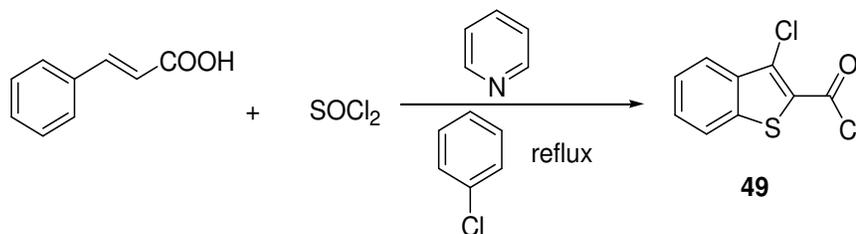
To 13.5 g (0.06 mol) of **50** was added 30 mL of acetic anhydride followed by 8.0 g (0.10 mol) of sodium acetate, placed over sand bath with stirring slowly to increase the temperature from 80° to 140° C for evolution of CO₂. The reaction mixture was heated to reflux for 1 h, then cooled to room temperature, added >30 g of NaOH dissolved in water to make pH = 8. A clear purple solution was obtained after refluxing the mixture for 2 h. It was then acidified by diluted aq. H₂SO₄, filtered to remove tar. The product **51** as a yellow powder was isolated by steam distillation. This product is air sensitive and used for the next step immediately. The spectral data were as follows: ¹H NMR (CDCl₃) δ 3.79 (s, 2H), 7.22 (t, *J* = 7.5 Hz, 1H), 7.43 (d, *J* = 7.8 Hz, 1H), 7.55 (t, *J* = 7.5 Hz, 1H), 7.78 (d, *J* = 7.7 Hz, 1H).

Synthesis of Compound 3-(N-methyl)benzothiophene (**52**).



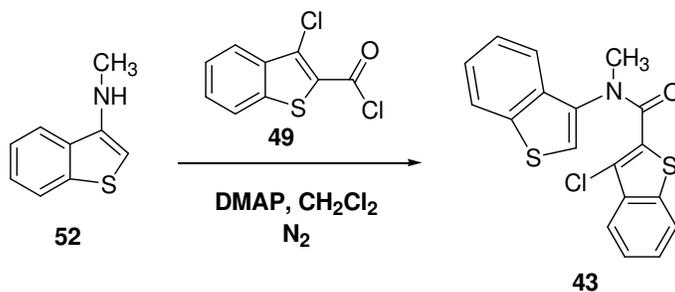
To 9.1 g (0.06 mol) **51** was added dropwise 60 mL (0.48 mol) of methylamine in ethanol and stirred for 4 h under N₂ environment. Then the mixture was extracted by ether, washed with brine solution, dried over Na₂SO₄ and concentrated in vacuo. It was then gravity chromatographed by 50-50 ethyl acetate and hexane. The product **52** was collected and concentrated in vacuo to obtain a dark brown viscous liquid. This product is air sensitive and used for the next step immediately without further purification.

Synthesis of 3-Chlorobenzo[b]thiophene-2-carbonyl chloride (49).



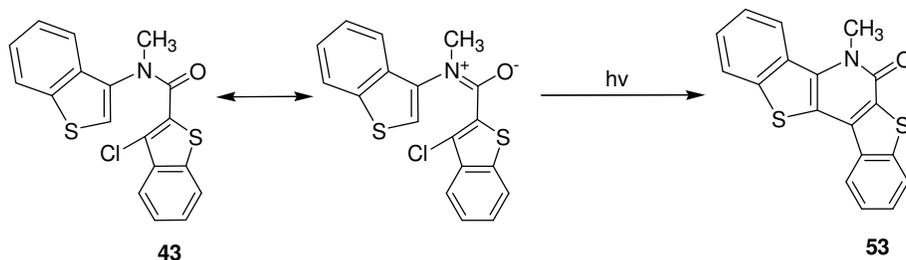
To commercially available 29.6 g (0.20 mol) of *trans* cinnamic acid in 150 mL chlorobenzene was added 119 g (1.00 mol) of thionyl chloride followed by dropwise addition of 1.6 mL of pyridine. The reaction mixture was heated at reflux for 72 h. To remove color particles the mixture was refluxed with norit for 2 h followed by vacuum filtration through celite. The filtrate was concentrated in vacuo and then suspended in 500 mL of hot hexane followed by immediate vacuum filtration. The filtrate was left overnight to be crystallized. The crystals were filtered, washed with cold hexane and dried to give 24.1 g (52.1 % yield) as brown needles, mp 112-114°C. The spectral data were as follows: ¹H NMR (CDCl₃) δ 7.55 (t, *J* = 7.7 Hz, 1H), 7.63 (t, *J* = 7.7 Hz, 1H), 7.86 (d, *J* = 8.4 Hz, 1H), 8.02 (d, *J* = 8.4 Hz, 1H).

Synthesis of benzothiothiophene-3-chloro-2-(benzothiothiophene-3-N-methyl)carboxamide (43).



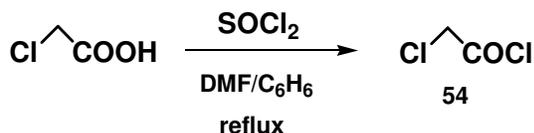
To 2.6 g (0.016 mol) of **52** in 20 mL anhydrous dichloromethane was added 15 mL triethylamine followed by 4.6 g (0.020 mol) of **49** dissolved in 30 mL anhydrous dichloromethane at 5-8°C. The reaction mixture was warmed to room temperature and stirred overnight. It was then filtered to remove triethylamine-hydrochloride salt, the filtrate was concentrated in vacuo, and the residue was dissolved in benzene. To remove color particles, the mixture was heated at reflux with norit (activated C) for 2 h followed by vacuum filtration through celite. The benzene solution was washed with aq. saturated NaHCO₃, with brine, dried over Na₂SO₄, and concentrated in vacuo to get dark red oil containing amide **43** (LG⁻ = Cl⁻). The oil was chromatographed on silica gel, eluting with 50% ethyl acetate in hexane to isolate the product 3.90 g (0.011 mol, 68% yield) as a yellow powder, mp 132 - 133°C. The spectral data were as follows; ¹H NMR (CDCl₃) δ 3.55 (s, 3H), 7.12-7.47 (m, 7H), 7.59-7.79 (m, 2H); ¹³C NMR (CDCl₃) δ 38.24, 120.60, 122.50, 122.56, 125.17, 126.49, 126.62, 127.48, 128.91, 129.17, 129.47, 130.84, 135.49, 137.69, 142.95, 162.81.

Synthesis of Compound **53** by Preparative Direct Photolysis of compound **43**.



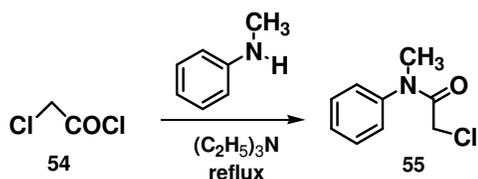
Preparative direct photolysis of 0.021 M **43** ($\text{LG}^- = \text{Cl}^-$) with unfiltered light from a medium pressure mercury lamp in N_2 saturated 20% 100 mM phosphate buffer in CH_3CN at pH 7 for 3h resulted in the release of HCl to give **53** as the only photoproduct (eq. 3). The product (100% conversion characterized by ^1H NMR) was isolated by extraction with ethyl acetate and purified by recrystallization from 1:3 ethyl acetate in hexane to give **53** as a pale yellow powder, m.p. 244.4 – 245.1 °C. ^1H NMR (CDCl_3) δ 4.24 (s, 3H), 7.41-7.55 (m, 4H), 7.85-7.93 (m, 2H), 8.25-8.33 (m, 2H); ^{13}C NMR (CDCl_3) δ 33.50, 114.48, 123.70, 123.75, 123.87, 124.70, 125.12, 125.35, 126.20, 127.96, 128.91, 129.73, 130.22, 134.68, 135.26, 138.98, 142.72, 159.06.

Synthesis of 2-chloroacetyl chloride (**54**).⁶



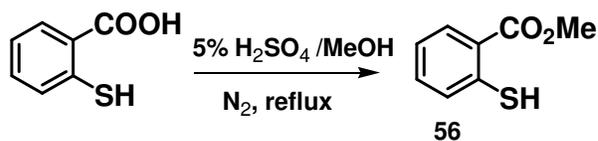
To a stirred solution of 10.0 g (105 mmol) of 2-chloroacetic acid in 100 mL of benzene was added 1.0 mL of DMF followed by 12.5 g (105 mmol) of thionylchloride. The mixture was heated at reflux overnight. Upon cooling the entire reaction mixture was used for the next step.

Synthesis of 2-chloro-N-methylacetanilide (**55**).



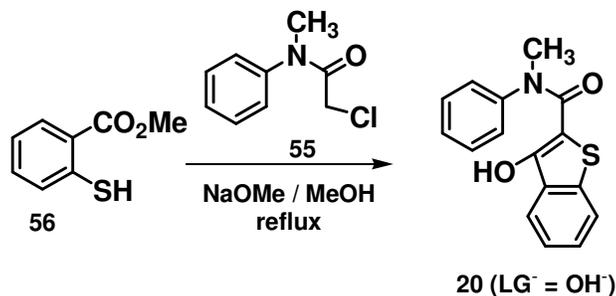
To a stirred solution of 8.41 g (78.6 mmol) of N-methylaniline in 15 mL triethylamine was added 11.87 g (105 mmol) of 2-chloroacetyl chloride **54** (33% excess) at 5-8°C. The reaction mixture was heated at reflux overnight. Upon cooling, the triethylamine hydrochloride salt was removed by filtration and the filtrate was washed with aq. saturated NaHCO₃, with brine, dried over Na₂SO₄, and concentrated in vacuo to give 11.5 g (80% yield) dark black solid of amide **55**. This compound was used for the next step without further purification. The spectral data were as follows: ¹H NMR (CDCl₃) δ 3.32 (s, 3H), 3.86 (s, 2H), 7.24 (d, *J* = 6.4 Hz, 2H), 7.33-7.57 (m, 3H).

Synthesis of thio-methylsalicylate (**56**).



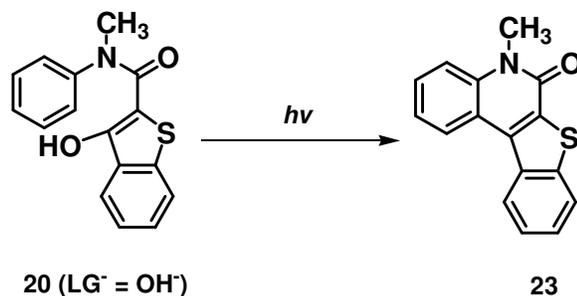
To a stirred solution of 31.4 g (0.2 mol) of thiosalicylic acid, was added 500 mL of 5% H₂SO₄ in methanol. The mixture was refluxed for 36 h in N₂ atmosphere. The reaction mixture was concentrated in vacuo. To the mixture was added a large amount of H₂O. The solution was made basic with solid NaHCO₃, extracted two times with benzene, washed with brine, dried over Na₂SO₄ and concentrated in vacuo to give 28.6 g (85 % yield) of ester **56** as a yellow liquid. The spectral data were as follows: ¹H NMR (CDCl₃) δ 3.91 (s, 3H), 4.69 (s, 2H), 7.09-7.18 (br, 1H), 7.24-7.36 (m, 2H), 7.99 (d, *J* = 7.8 Hz, 1H).

Synthesis of 3-hydroxybenzo[b]thiophene-2-(N-methyl-N-phenyl) carboxamide **20 (LG⁻ = OH⁻).**



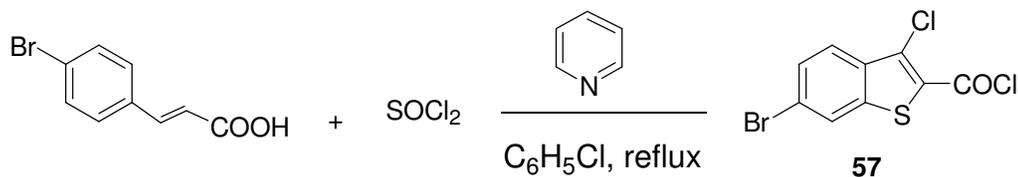
To a stirred solution of 3.5 g (0.02 mol) of thiomethylsalicylate **56** in 50 mL methanol was added 1.1 g (0.02 mol) of sodium methoxide. After stirring the mixture for 10 min was added 3.8 g (0.02 mol) of amide **55**, followed by addition of 2.3 g (0.04 mol) of sodium methoxide. The reaction mixture was heated at reflux for 24 h. Upon cooling the solution was acidified with 10% HCl (pH = 3), and extracted with ethyl acetate. The extract was washed with H₂O, brine, dried over Na₂SO₄, and concentrated in vacuo. The oil was chromatographed on silica gel, eluting with 50% ethyl acetate in hexane. The isolated product was purified by crystallization from 1:10 ethyl acetate in hexane to obtain 1.70 g (30 % yield) of pure crystal of compound **20**, mp 115-117°C. The spectral data were as follows: ¹H NMR (CDCl₃) δ 3.47 (s, 3H), 7.23-7.61 (m, 8H), 7.92 (d, *J* = 7.5 Hz, 1H); ¹³C NMR (CDCl₃) δ 38.64, 101.59, 122.08, 122.66, 124.00, 128.25, 129.42, 129.47, 129.98, 130.04, 138.99, 141.66, 161.82, 167.72. Anal. Calcd for C₁₆H₁₃NO₂S : C 67.82%, H 4.59%, N 4.95%; found 67.94.10%, 4.68%, 4.88%.

Synthesis of 5-methyl-[1]benzothiopheno[2,3-c]quinolin-6-one (23) by photolysis of 20 (LG = OH⁻).



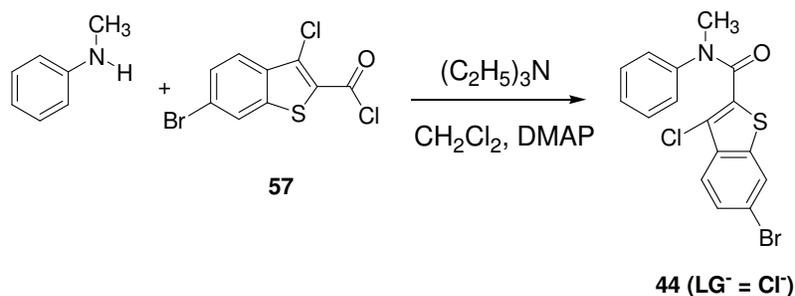
A 0.019 M solution of **20** (LG⁻ = OH⁻) in N₂ saturated 30% 100 mM phosphate buffer in CH₃CN at pH 7 was irradiated with a 450 W Hanovia medium pressure mercury lamp for 30 min. The product was isolated by extraction with ethyl acetate and purified by recrystallization from 1:3 ethyl acetate in hexane to give **23** as a solid white crystal, mp 204-205°C. The spectral data were as follows: ¹H NMR (CDCl₃) δ 3.92 (s, 3H), 7.46 (t, *J* = 8.1, 1H), 7.55-7.67 (m, 4H), 8.05 (d, *J* = 8.1 Hz, 1H), 8.72 (d, *J* = 8.1 Hz, 2H); ¹³C NMR (CDCl₃) δ 29.83, 115.24, 119.24, 122.40, 123.67, 123.75, 125.19, 125.32, 126.83, 128.45, 132.62, 134.93, 135.70, 138.33, 142.44, 158.28. Anal. Calcd for C₁₆H₁₁NOS: C 72.45%, H 4.15%, N 5.28%; Found 72.10%, 4.31%, 5.31%.

Synthesis of 6-bromo-3-chlorobenzo[*b*]thiophene-2-carbonyl chloride (57).⁹



To commercially available 22.7 g (0.10 mol) of 4-bromocinnamic acid in 80 mL chlorobenzene was added 59.5 g (0.50 mol) of thionyl chloride followed by dropwise addition of 0.8 mL of pyridine. The reaction mixture was heated at reflux for 72 h. To remove color particles the mixture was heated to reflux with norit for 2 h followed by vacuum filtration through celite. The filtrate was concentrated in vacuo and then suspended in 250 mL of hot hexane followed by immediate vacuum filtration. The filtrate was left overnight to crystallize. The crystals were filtered, washed with cold hexane and dried to give 17.05 g (55 % yield) of yellow needles **57**, mp 107-109 °C. The spectral data were as follows: ¹H NMR (CDCl₃) δ 7.59 (d, J = 8.9 Hz, 1H), 7.80 (d, J = 8.9 Hz, 1H), 7.96 (s, 1H).

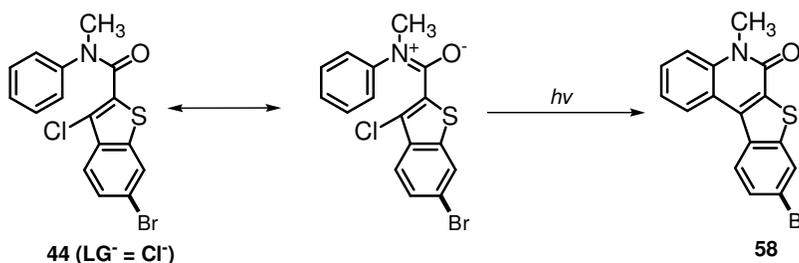
Synthesis of 6-bromo-3-chloro-benzo[b]thiophene-2(N-methyl-N-phenyl)carboxamide (44).



To a stirred solution of commercially available 1.345 g (12.57 mmol) of N-methylaniline and 15 mL of triethylamine in 20 mL of anhydrous dichloromethane was added 5.4 g (17.28 mmol) of 6-bromo-3-chlorobenzo[b]thiophene-2-carbonyl chloride (**57**) dissolved in 10 mL of anhydrous dichloromethane at 5-8°C in an ice bath under N₂.

A catalytic amount of DMAP was added. The reaction mixture was warmed to room temperature and stirred for 24 h. The reaction mixture was filtered to remove triethylamine hydrochloride salt and the filtrate was washed with aq. saturated NaHCO_3 , with H_2O , dried over Na_2SO_4 , and concentrated in vacuo to give 2.176 g (45.49% yield) of a brown solid (**44**). The crude product was chromatographed on silica gel, eluting with 50% ethyl acetate in hexane to obtain brown crystals, mp 130-131°C. The spectral data were as follows; ^1H NMR (CDCl_3) δ 3.52 (s, 3H), 7.12-7.31 (m, 5H), 7.48 (d, $J = 8.9$ Hz, 1H), 7.57 (d, $J = 8.9$ Hz, 1H), 7.81 (s, 1H); ^{13}C NMR (CDCl_3) δ 38.85, 120.78, 120.84, 123.99, 125.19, 126.86, 127.86, 128.94, 129.45, 131.45, 134.59, 139.21, 143.02, 162.49. Anal. Calcd for $\text{C}_{16}\text{H}_{11}\text{NOCIS}$: C 50.46%, H 2.89%, N 3.68%; Found 50.67%, 2.97%, 3.54%.

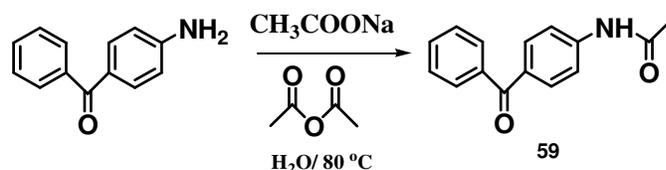
Synthesis of 5-methyl-1-[6-bromo-benzothiopheno]-[2,3-c]quinolin-6-one (58**) by photolysis of 6-bromo-3-chloro-benzo[b]thiophene-2(N-methyl-N-phenyl)carboxamide (**44**).**



A 0.02 M solution of **44** in N_2 saturated 30% 100 mM phosphate buffer in dioxane at pH 7 was irradiated with a 450 W Hanovia medium pressure mercury lamp for

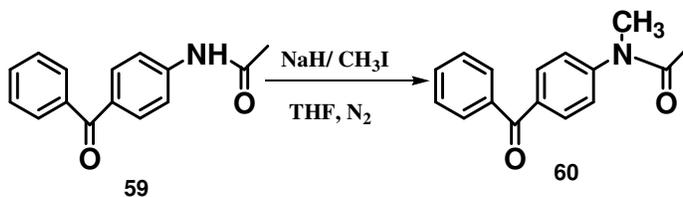
1 h. The product was purified by recrystallization from benzene to give compound **58** as a solid light orange crystal, mp 262-263°C. The spectral data were as follows: ^1H NMR (CDCl_3) δ 3.89 (s, 3H), 7.43 (t, $J = 7.7$, 1H), 7.52-7.74 (m, 3H), 8.17 (s, 1H), 8.53 (d, $J = 9.4$ Hz, 1H), 8.61 (d, $J = 8.5$ Hz, 1H); ^{13}C NMR (CDCl_3) δ 30.28, 67.31, 115.82, 119.31, 121.60, 122.93, 124.01, 126.60, 128.97, 129.21, 133.21, 134.85, 134.95, 138.86, 144.23, 158.43. Anal. Calcd for $\text{C}_{16}\text{H}_{10}\text{NOSBr}$: C 55.81%, H 2.91%, N 4.07%; Found 55.94%, 3.01%, 4.05% respectively.

Synthesis of 4-acetamidobenzophenone (**59**).



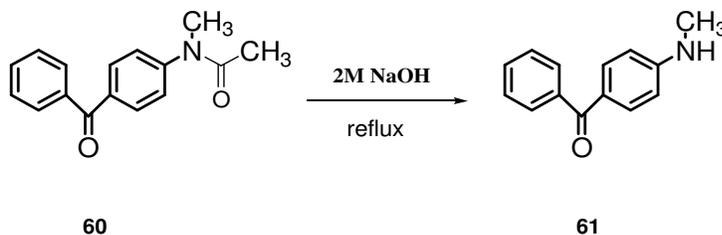
To commercially available 10.1 g (0.05 mol) of 4-aminobenzophenone was added 3.8 g (0.04 mol) of acetic anhydride followed by 100 mL of H_2O . The mixture was stirred for 10 min before adding 4.4 g (0.05 mol) of sodium acetate. The reaction mixture was heated to 80°C with stirring for overnight. Upon cooling the mixture was extracted with ethyl acetate, washed with H_2O , aq. saturated NaHCO_3 , with brine, dried over Na_2SO_4 and concentrated in vacuo to give 9.5 g (80% yield) of a yellow solid of compound **59**. The spectral data were as follows: ^1H NMR (CDCl_3) δ 2.21 (s, 3H), 4.08-4.25 (br, 1H), 6.58 (d, $J = 8.8$ Hz, 2H), 7.45 (t, $J = 7.4$ Hz, 2H), 7.52 (t, $J = 7.4$ Hz, 1H), 7.71 (d, $J = 7.8$ Hz, 2H), 7.76 (d, $J = 8.2$ Hz, 2H).

Synthesis of 4-(N-methylacetamido)benzophenone (**60**).



To a stirred solution of 8.0 g (0.03 mol) of 4-acetamidobenzophenone (**59**) in 50 mL of THF was added 1.7 g (0.04 mol) of NaH (60%) in N₂ atmosphere. The mixture was stirred for 15 min followed by the dropwise addition of 7.0 g (0.05 mol) of methyl iodide. The reaction mixture was stirred at room temperature overnight. The solution was concentrated in vacuo to obtain 6.50 g (80% yield) of compound **60**. The spectral data were as follows: ¹H NMR (CDCl₃) δ 1.84 (s, 3H), 3.74 (s, 3H), 6.58 (d, *J* = 8.8 Hz, 2H), 7.45 (t, *J* = 7.4 Hz, 2H), 7.52 (t, *J* = 7.4 Hz, 1H), 7.71 (d, *J* = 7.8 Hz, 2H), 7.76 (d, *J* = 8.2 Hz, 2H).

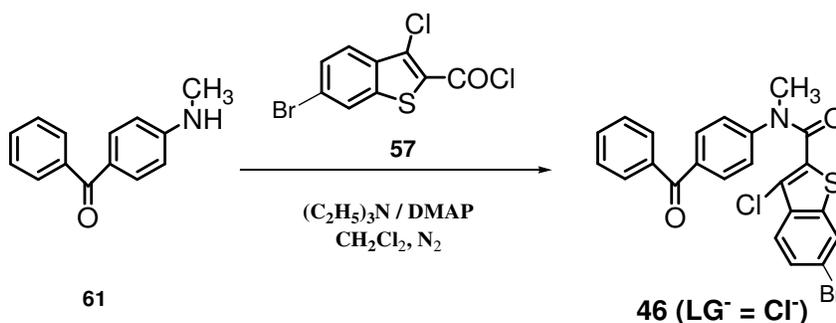
Synthesis of 4-(methylamino)benzophenone (**61**).



To 6.5 g (0.03 mol) of 4-(N-methylacetamido)benzophenone (**60**) was added 100 mL of aqueous 2 M NaOH. The mixture was heated to reflux for 12 h. Upon cooling the

reaction mixture was extracted with ether, washed with enough water for >3 times, washed over brine solution then Na₂SO₄ and concentrated in vacuo to give crude product which was then recrystallized from ethyl acetate and hexane mixture to obtain a pure orange solid 4.6 g (87% yield) of compound **61**. The spectral data were as follows; ¹H NMR (CDCl₃) δ 2.91 (s, 3H), 4.13-4.70 (broad, 1H), 6.58 (d, *J* = 8.8 Hz, 2H), 7.45 (t, *J* = 7.4 Hz, 2H), 7.52 (t, *J* = 7.4 Hz, 1H), 7.71 (d, *J* = 7.8 Hz, 2H), 7.76 (d, *J* = 8.2 Hz, 2H).

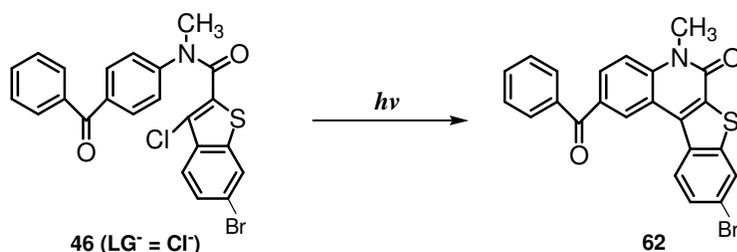
Synthesis of 6-bromo-3-chloro-benzo[b]thiophene-2(N-benzoylphenyl-N-methyl)carboxamide **46 (LG⁻ = Cl⁻).**



To a stirred solution of 2.3 g (11.06 mmol) of compound 4-methylaminobenzophenone (**61**) and 15 mL of triethylamine in 25 mL of anhydrous CH₂Cl₂ under N₂, was added catalytic amount of DMAP followed by 4.51 g (14.5 mmol) of 6-bromo-3-chlorobenzo[b]thiophene-2-carbonyl chloride **57** at 5-8 °C in an ice bath. The reaction mixture was warmed at room temperature and stirred for 24 h. The solution was filtered off to remove Et₃N-HCl salt, washed three times with aq saturated NaHCO₃ solution, then with brine, dried over Na₂SO₄, and concentrated in vacuo to give 3.8 g (7.9

mmol, 71% yield) of compound **46** ($\text{LG}^- = \text{Cl}^-$) as a viscous oil. The oil was chromatographed on silica gel, eluting with 20% ethyl acetate in hexane to obtain pure brown crystals, mp 113-114°C. The spectral data were as follows: ^1H NMR (CDCl_3) δ 3.58 (s, 3H), 7.29 (d, $J = 8.5$ Hz, 2H), 7.43 (t, $J = 7.8$ Hz, 2H), 7.50 (d, $J = 8.7$ Hz, 1H), 7.56 (t, $J = 8.5$ Hz, 2H), 7.68 (t, $J = 8.1$ Hz, 4H), 7.84 (s, 1H); ^{13}C NMR (CDCl_3) δ 38.18, 121.19, 121.24, 124.18, 125.35, 126.22, 126.48, 128.59, 129.24, 130.11, 131.29, 132.48, 132.86, 134.60, 136.21, 137.39, 139.25, 146.65, 162.50, 195.60.

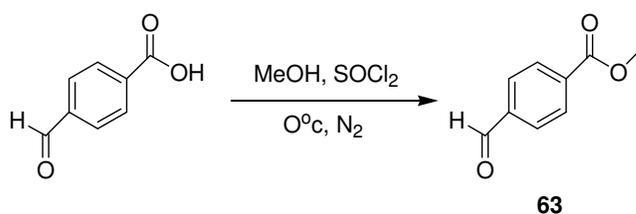
Synthesis of 5-benzoyl-9-methyl-1-(6-bromobenzothiopheno)-[2,3-c]quinolin-10-one (62) by photolysis of 6-bromo-3-chloro-benzo[b]thiophene-2(N-benzoylphenyl-N-methyl) carboxamide 46.



Preparative direct photolysis of 0.015 M **46** ($\text{LG}^- = \text{Cl}^-$) with unfiltered light from a 450 W Hanovia medium pressure mercury lamp in N_2 saturated 30% 100 mM phosphate buffer in dioxane at pH 7 for 50 min resulted in the release of hydrochloric acid to give **62** as the only photoproduct. The photoproduct (100 % conversion characterized by ^1H NMR) was isolated by filtration as a colorless powder, mp 264-265°C. The spectral data were as follows: ^1H NMR (CDCl_3) δ 3.94 (s, 3H), 7.57 (t, $J =$

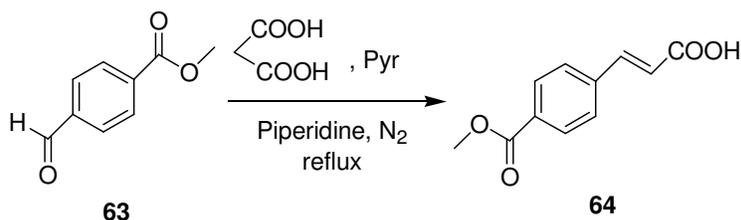
7.6 Hz, 2H), 7.66 (t, $J = 8.6$ Hz, 3H), 7.89 (d, $J = 7.5$ Hz, 2H), 8.09 (d, $J = 8.7$ Hz, 1H), 8.17 (s, 1H), 8.39 (d, $J = 8.7$ Hz, 1H), 9.13 (s, 1H); ^{13}C NMR (CDCl_3) δ 30.62, 115.54, 119.30, 124.19, 125.69, 126.0, 127.07, 127.64, 128.74, 130.26, 130.56, 131.58, 132.86, 133.64, 135.32, 135.82, 137.92, 141.62, 144.97, 158.62, 195.40.

Synthesis of Methyl 4-formylbenzoate (**63**).



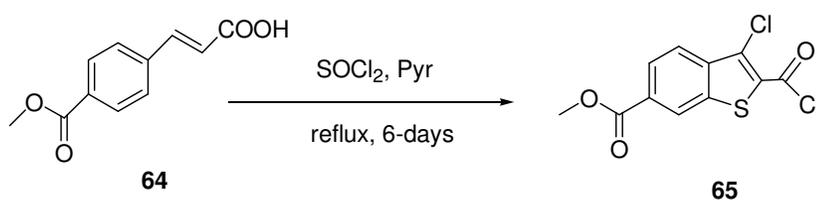
To commercially available 10 g (0.067 mol) of 4-formylbenzoic acid dissolved in 150 mL of anhydrous MeOH was added 10 mL (0.137 mol) of thionyl chloride dropwise at 0 °C under N_2 environment. The reaction mixture was slowly brought to room temperature and stirred for overnight. The solvent was removed in vacuo by co-evaporation with dichloromethane (3 X 100 mL) to remove the excess of thionyl chloride to give 98.2% conversion of **63** as a brown crystal. The m.p. of the compound **63** was found 51 - 52 °C. The spectral data were as follows: ^1H NMR (CDCl_3) δ 3.96 (s, 3H), 7.95 (d, $J = 6.7$ Hz, 2H), 8.20 (d, $J = 6.7$ Hz, 2H), 10.11 (s, 1H).

Synthesis of 4-Methoxycarbonylcinnamic acid (**64**).



To a solution of commercially available malonic acid (3.5 g, 0.03 mol) dissolved in 20 mL of anhydrous pyridine was added at room temperature 4.3 g (0.026 mol) of methyl-4-formylbenzoate **63** dissolved in another 20 mL anhydrous pyridine followed by 1 mL piperidine (cat. amount) dropwise under N₂ environment. The mixture was then placed over a sand bath and slowly stirred while the temperature was increased to 80° to 90° C for evolution of CO₂, then heated to reflux until the formation of CO₂ stopped. After cooling to room temperature, the reaction solution was poured onto iced-concd. HCl to begin forming acid precipitation. The acid **64** was filtered off, washed with water several times, dried to give pure **64** as a creamy white solid with 97% yield; m.p. 234.5 – 236.2 °C. The spectral data were as follows: ¹H NMR (CDCl₃) δ 3.84 (s, 3H), 6.63 (d, *J* = 7.9 Hz, 1H), 7.62 (d, *J* = 8.2 Hz, 1H), 7.80 (d, *J* = 8.3 Hz, 2H), 7.95 (d, *J* = 8.2 Hz, 2H), 12.59 (s, 1H).

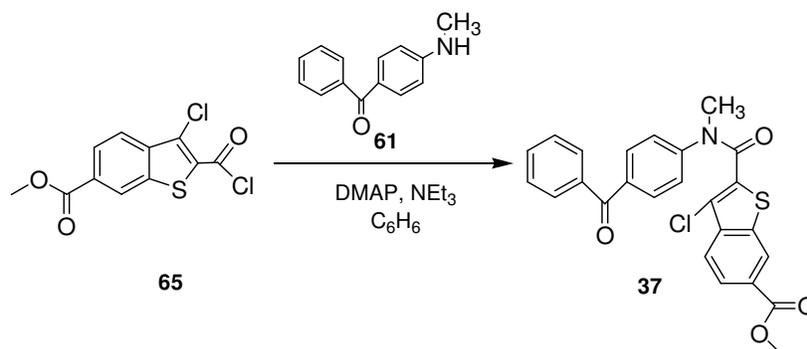
Synthesis of 6-Methoxycarbonyl-3-chlorobenzo[b]thiophene-2-carbonyl chloride (65).



To a stirred solution of 10.0 g (0.05 mol) of 4-methylester cinnamic acid **64** in 52.5 mL (0.72 mol, 15 x SM) of thionyl chloride, was added dropwise 0.8 mL of pyridine. The reaction mixture was heated at reflux for 6 d. The hot reaction mixture was filtered off to remove pyridine-hydrochloride salt. Enough water was added to the filtrate

to convert the dissolved acid chloride to carboxylic acid precipitation. Conc. HCl was added to make pH 2, filtered off and the residue was again refluxed with 3.5 mL (0.05 mol) thionyl chloride in 40 mL benzene with catalytic amount of DMF under N₂ to convert again acid to acid chloride **65** as off white solid which is air sensitive. The reaction mixture was then used for the next step without further purification, only after evaporating the solvent.

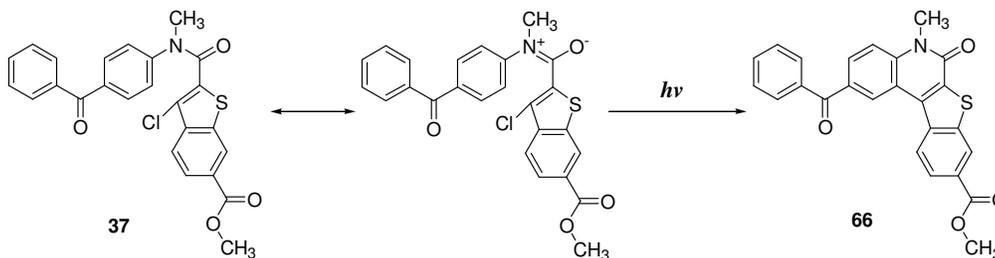
Synthesis of 6-Methoxycarbonyl-3-chloro-benzo[b]thiophene-2(N-benzoylphenyl-N-methyl) carboxamide **37 (LG⁻ = Cl⁻).**



To a stirred solution of 6.4 g (0.03 mol) of compound 4-(methylamino)benzophenone (**61**) and 15 mL of triethylamine in 50 mL of anhydrous C₆H₆ under N₂, was added a catalytic amount of DMAP followed by the reaction mixture of 6-methoxycarbonyl-3-chlorobenzo[b]thiophene-2-carbonyl chloride (**65**) at 5-8 °C in an ice bath. The reaction mixture was warmed to room temperature and stirred for 24 h, then filtered to remove Et₃N-HCl salt. The filtrate was diluted with ether, washed three times with aq. saturated Na₂CO₃, three times with 1 N HCl and then washed with water, brine and finally dried over Na₂SO₄, concentrated in vacuo to give 5.6 g (0.012 mol, 40%

yield) of compound **37** ($\text{LG}^- = \text{Cl}^-$) as a viscous oil. The oil was chromatographed on silica gel, eluting with 20% ethyl acetate in hexane to obtain a solid. This solid was recrystallized from benzene to get pure crystal, mp 213-214°C. The spectral data were as follows: ^1H NMR (CDCl_3) δ 3.58 (s, 3H), 3.93 (s, 3H), 7.31 (d, $J = 8.6$ Hz, 2H), 7.42 (t, $J = 7.8$ Hz, 2H), 7.55 (t, $J = 7.4$ Hz, 1H), 7.67 (d, $J = 8.2$ Hz, 2H), 7.70 (d, $J = 8.6$ Hz, 2H), 7.77 (d, $J = 9.0$ Hz, 1H), 8.06 (d, $J = 9.0$ Hz, 1H), 8.43 (s, 1H). ^{13}C NMR (DMSO-D_6) δ 38.20, 57.72, 121.05, 122.91, 125.00, 126.26, 126.38, 128.59, 128.78, 130.11, 131.33, 132.88, 134.31, 136.30, 137.35, 137.59, 138.83, 146.50, 162.46, 166.58, 195.61.

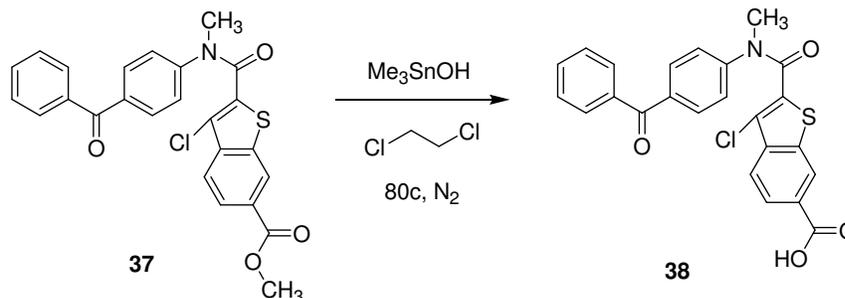
Synthesis of 5-Benzoyl-9-methyl-1-(benzothiopheno-6-methylcarboxylate)-[2,3-c]quinolin-10-one (66) by photolysis of 6-methoxycarbonyl-3-chloro-benzo[b]thiophene-2(N-benzoylphenyl-N-methyl) carboxamide 37 ($\text{LG}^- = \text{Cl}^-$).



Preparative direct photolysis of 0.02 M **37** ($\text{LG}^- = \text{Cl}^-$) with unfiltered light from a 450 W Hanovia medium pressure mercury lamp in N_2 saturated 15% 100 mM phosphate buffer in CH_3CN at pH 7 for 30 min resulted in the release of hydrochloric acid to give **66** as the only photoproduct (and 100 % conversion characterized by ^1H NMR). The photoproduct was isolated as a brown solid followed by extraction with CH_2Cl_2 , wash

with water (x 3), saturated brine wash, dry over NaSO₄, rotovap and concentrated in vacuo, mp 284-285°C. The spectral data were as follows: ¹H NMR (CDCl₃) δ: 3.89 (s, 3H), 3.99 (s, 3H), 7.54 (t, *J* = 8.2 Hz, 2H), 7.63 (t, *J* = 7.4 Hz, 2H), 7.88 (d, *J* = 7.9 Hz, 2H), 8.06 (d, *J* = 8.4 Hz, 1H), 8.14 (d, *J* = 8.4 Hz, 1H), 8.44 (d, *J* = 9.0 Hz, 1H), 8.61 (s, 1H), 9.05 (s, 1H); ¹³C NMR (CDCl₃) δ 30.38, 52.58, 115.32, 118.62, 125.08, 125.58, 126.25, 126.70, 128.53, 128.73, 129.96, 130.52, 131.41, 132.69, 134.40, 135.82, 137.50, 138.53, 141.28, 142.21, 158.22, 166.22, 195.03.

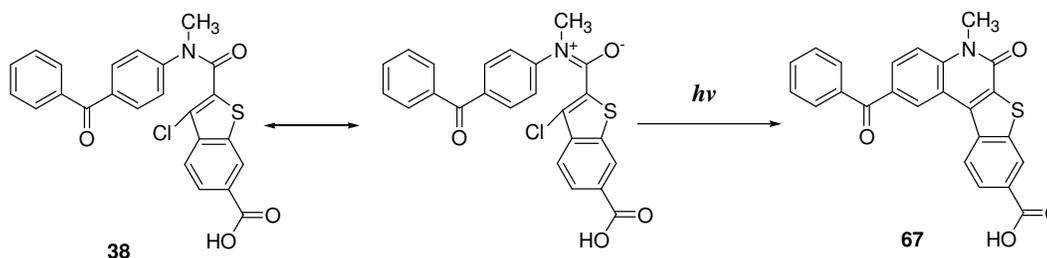
Synthesis of 3-Chloro-benzo[b]thiophene-2(N-benzoylphenyl-N-methylcarboxamide)-6-carboxylic acid (38).



To a stirred solution of 5.0 g (0.01 mol) methyl ester **37** in 30 mL dichloroethane at 80°C under N₂ environment was added 5.4 g (0.03 mol) of trimethyltinhydroxide and was heated to reflux until it was hydrolyzed off into carboxylic acid **38** by checking with ¹H NMR. After completion, the acid was separated out from the solid formation by filtration, the filtrate was then washed with water and extracted by dichloromethane to obtain pure acid as brown powder (>93% yield), mp: 75 – 77°C. ¹H NMR (CDCl₃):

δ 3.60 (s, 3H), 7.34 (d, $J = 8.3$ Hz, 2H), 7.43 (t, $J = 8.1$ Hz, 2H), 7.56 (t, $J = 7.5$ Hz, 1H), 7.68 (d, $J = 7.5$ Hz, 2H), 7.72 (d, $J = 8.7$ Hz, 2H), 7.80 (d, $J = 9.1$ Hz, 1H), 8.12 (d, $J = 9.1$ Hz, 1H), 8.51 (s, 1H), 11.94 (broad s, 1H); ^{13}C NMR(CDCl_3) δ 38.0, 120.9, 122.8, 125.5, 126.1, 126.5, 127.7, 128.4, 129.9, 131.2, 132.7, 134.6, 136.1, 137.1, 137.4, 139.2, 146.2, 162.3, 171.1, 195.5.

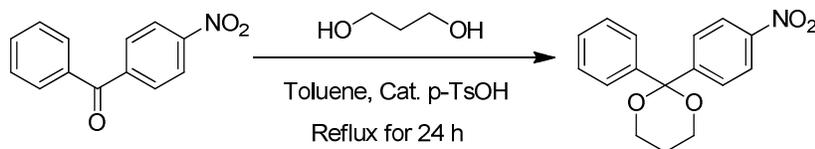
Synthesis of 5-benzoyl-9-methyl-1-(benzothiopheno-6-carboxylic acid)-[2,3-c]quinolin-10-one (67) by photolysis of 3-chloro-benzo[b]thiophene-2(N-benzoylphenyl-N-methyl carboxamide)6-carboxylic acid (38).



A 0.015 M solution of **38** in N_2 saturated 25% 100 mM phosphate buffer in dioxane at pH 7 was irradiated with an unfiltered light from 450 W Hanovia medium pressure mercury lamp for 1 h. The reaction mixture was acidified with dilute HCl to get solid precipitation. The off white powder was obtained from filtration of the mixture as the only photoproduct **67** and 100% conversion characterized by ^1H NMR, mp 300_+°C . The spectral data were as follows: ^1H NMR (DMSO- D_6) δ 3.82 (s, 3H), 7.62 (t, $J = 7.8$ Hz, 2H), 7.72 (t, $J = 7.8$ Hz, 1H), 7.81 (d, $J = 8.7$ Hz, 1H), 7.84 (d, $J = 7.8$ Hz, 2H), 8.00 (d, $J = 9.1$ Hz, 1H), 8.04 (d, $J = 8.7$ Hz, 1H), 8.37 (d, $J = 8.7$ Hz, 1H), 8.65 (s, 1H), 8.98

(s, 1H); ^{13}C NMR (DMSO- D_6) δ 30.56, 116.66, 118.26, 124.67, 125.55, 126.38, 127.05, 128.98, 129.82, 129.85, 130.30, 131.44, 132.83, 134.49, 138.06, 141.64, 141.94, 157.98, 194.73.

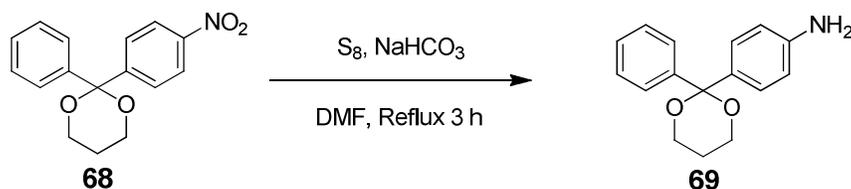
Synthesis of (68).



In a stirred solution of 10 g (44 mmol) 4-nitroacetophenone in 100 mL toluene was added 7.4 mL (102.6 mmol) of propane-1,3-diol and 85 mg (0.44 mmol) of 4-tosylic acid (p-TsOH). The reaction mixture was heated to reflux for 24 h. After reflux, the mixture was cooled to room temperature and kept for crystals growing. The pure product **68** was isolated from the mixture and recrystallized from benzene – ether solvent mixture as colorless crystals with 99.8% yield; mp: 117-118°C. ^1H NMR analysis (CDCl_3) δ : 1.70 (m, 1H), 1.97 (m, 1H), 4.05 (m, 1H), 7.29 (t, $J = 7.1$ Hz, 1H), 7.38 (t, $J = 7.9$ Hz, 2H), 7.53 (d, $J = 7.9$ Hz, 2H), 7.73 (d, $J = 8.8$ Hz, 2H), 8.17 (d, $J = 8.9$ Hz, 2H) and ^{13}C NMR analysis (CDCl_3) δ : 25.4, 61.8, 100.2, 123.7, 126.5, 127.0, 128.3, 128.9, 140.5, 150.3, 201.

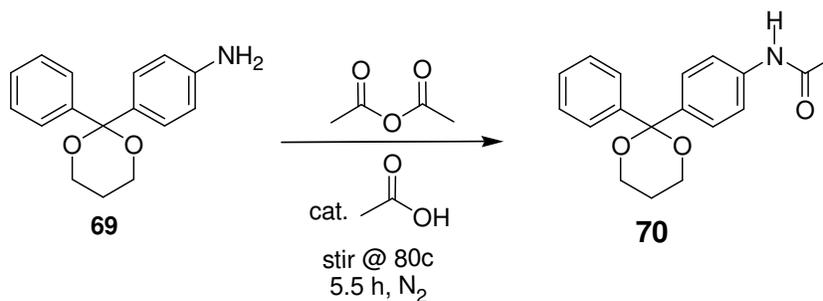
9.

Synthesis of (69).



In a stirred solution of 1.0 g (3.5 mmol) of **68** in 20 mL DMF was added 300 mg (9.4 mmol) of ^{32}S and 880 mg (10.5 mmol) of NaHCO_3 and the reaction mixture was heated to reflux for 18 h. After reflux, the mixture was diluted with CH_2Cl_2 and filtered to remove inorganics. The filtrate was then washed with water several times to remove DMF, then with saturated brine solution and finally dried over Na_2SO_4 and concentrated the CH_2Cl_2 layer in vacuo to obtain pure product **69** as a red viscous liquid with >94% yield. ^1H NMR analysis (CDCl_3) δ : 1.71 – 1.86 (m, 2H), 3.64 (broad s, 2H), 3.94 – 4.09 (m, 4H), 6.63 (d, $J = 8.7$ Hz, 2H), 7.22 (t, $J = 7.4$ Hz, 1H), 7.26 (d, $J = 8.4$ Hz, 2H), 7.32 (t, $J = 7.4$ Hz, 2H), 7.49 (d, $J = 8.7$ Hz, 2H).

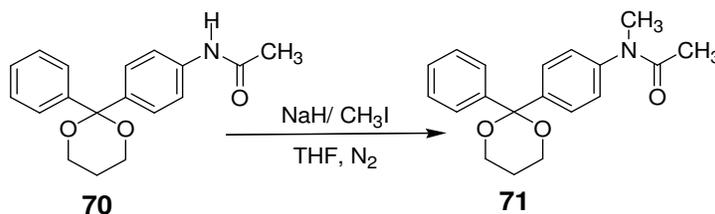
Synthesis of (70).



To a stirred solution of 1.0 g (3.9 mmol) of **69** in 8 mL acetic anhydride was added a catalytic amount of acetic acid (0.1 mL) and the reaction mixture was heated to 80°C for 5.5 h. After heating, excess of acetic anhydride was removed very carefully by simple distillation under reduced pressure and the residue was then diluted with CH_2Cl_2 and filtered to remove when any solid was appeared. The filtrate was then washed with water several times, then with saturated brine solution, dried over Na_2SO_4 and concentrated in vacuo respectively to obtain a crude mixture of product. The mixture was then purified through SiO_2 column chromatography and recrystallized from ethyl acetate-

hexane solvent mixtures to finally acquire **70** as nice colorless crystals. ^1H NMR (CDCl_3) δ : 1.75 – 1.86 (m, 2H), 2.12 (s, 3H), 4.02 (t, $J = 5.5$ Hz 4H), 7.14 (broad s, 1H), 7.23 (t, $J = 7.4$ Hz, 1H), 7.32 (t, $J = 7.9$ Hz, 2H), 7.42 – 7.54 (m, 6H); ^{13}C NMR (CDCl_3) δ : 24.8, 25.8, 61.9, 101.0, 120.1, 126.6, 127.5, 128.0, 128.7, 137.6, 138.5, 142.7, 168.7.

Synthesis of (71).



To a stirred solution of 1 g (3.37 mmol) of **70** in 10 mL of THF was added very carefully 175 mg (1.3 eq. of **70** = 4.38 mmol) of 60% NaH under N_2 gas flow. After stirring for 15 minutes to the mixture was added 0.3 mL (1.5 eq. of **70** = 5.06 mmol) of CH_3I and stirred the resulting mixture for overnight in N_2 environment. The pure product **71** was obtained by removing THF by simple distillation under reduced pressure followed by diluted the residue with CH_2Cl_2 and washed several times with water, then with saturated brine solution and dried over NaSO_4 , concentrated in vacuo respectively. ^1H NMR (CDCl_3) δ : 1.59 – 1.69 (m, 1H), 1.83 (s, 3H), 1.95 – 2.07 (m, 1H), 3.20 (s, 3H), 4.02 – 4.08 (m, 4H), 7.12 (d, $J = 8.4$ Hz, 2H), 7.30 (t, $J = 7.4$ Hz, 1H), 7.39 (t, $J = 7.6$ Hz, 2H), 7.55 (d, $J = 6.1$ Hz, 2H), 7.56 (d, $J = 6.7$ Hz, 2H); ^{13}C NMR (CDCl_3) δ : 22.51, 25.52, 29.74, 37.11, 61.73, 100.61, 126.83, 126.87, 127.43, 127.99, 128.74, 140.89, 143.11, 143.88, 170.57.

General Procedure for Product Quantum Yield Determinations. A semi-micro optical bench was used for quantum yield determinations, similar to the apparatus described by Zimmerman.^{26, 27} Light from a 200 W high-pressure mercury lamp was passed through an Oriel monochromator, which was set to 310 nm or 365 nm wavelengths. The light was collimated through a lens. A fraction of the light was diverted 90° by a beam splitter to a 10 x 3.6 cm side quartz cylindrical cell containing an actinometer. The photolysate was contained in a 10 x 1.8 cm quartz cylindrical cell of 25 mL volume. All quantum yields reported herein were the average of two or more independent runs. Behind the photolysate was mounted a quartz cylindrical cell containing 25 mL of actinometer. Light output was monitored by ferrioxalate actinometry using the splitting ratio technique. Products were analyzed by ¹H NMR spectroscopy using DMF or DMSO as the internal standard and the conversions were between 12 and 18%.

General Procedure for Quenching Studies. Solutions of ca. 0.005 M of investigated compound and various amounts of 1,3-pentadiene in N₂ saturated 15% phosphate buffer in CH₃CN at pH 7 were photolyzed at 310 nm for 2-5 h while performing actinometry, as in the quantum yield determinations. Yields were determined by ¹H NMR spectroscopy using DMSO as the internal standard.

2.5 Supporting Information: See Appendix I

CHAPTER 3: An Investigation on TPE Oligomers

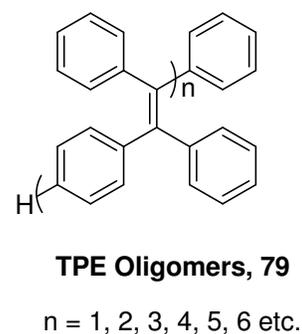
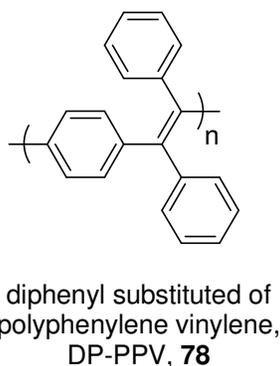
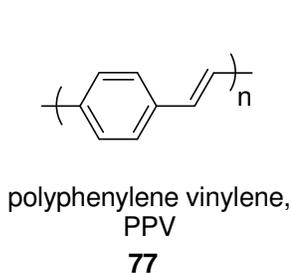
3.1 Introduction

In the field of chemistry, polymer consists of a nearly unlimited number of monomers where an oligomer in principle, is a molecule that consists of a relatively small and specifiable number of monomer units.²⁸ Dimers, trimers, tetramers etc. are oligomers. Oligomerization is a chemical process that converts monomers to a finite degree of polymerization. The actual figure is a matter of debate- often a value between 10 and 100.²⁹ Unlike a polymer, if one of the monomer is removed from an oligomer, its chemical properties are altered. Many oils are oligomeric such as liquid paraffin. Plasticizers are oligomeric esters widely used to soften the thermoplastics such as PVC. They could be made from monomers by linking them together or by separation from the higher fractions of crude oil. In biochemistry, the term oligonucleotide or normally "oligo" - is used for short, single-stranded nucleic acid fragments, such as DNA or RNA, or similar fragments of analogs of nucleic acids such as peptide nucleic acid or morpholinos. Such oligos are used in hybridization experiments, as probes for in situ hybridization or in antisense experiments such as gene knockdowns. It can also refer to a protein complex made of two or more subunits. In this case, a complex made of several different protein subunits is called a hetero-oligomer or heteromer where only one type of protein subunit used in a complex is homo-oligomer or homomer. A biomolecule formed of four same units such as ConcanavalinA (homotetramer) and different units such as hemoglobin (heterotetramer). Hemoglobin has four different sub-units while

immunoglobulins have 2 very different sub-units where each have their own activities or have a common biological property.

In the last few decades conjugated polymers such as polyacetylene (PA), poly(*p*-phenylene) (PPP), poly(*p*-phenylenevinylene) (PPV), polypyrrole (PPy), polythiophene (PTh) etc. have acquired a vast interest mainly because of their high conductivity in reduced or oxidized ionic states. Oxidation and reduction of conjugated polymers are combined with the phenomena of charge storage and electroluminescence. Moreover, the photo-induced ionization processes are known to be the origin of the photoconductivity and it is also connected with the nonlinear optical phenomena observed in transparent polymer films. This is how, electrochemical methods play an increasing role in the investigation of conjugated polymers. Thus, the development of the electrochemical techniques, especially cyclic voltammetry (CV), electrochemical potential spectroscopy (ECPS) and differential pulse polarography (DPP) have revealed more information in the understanding of the behavior of conjugated polymers.^{30, 31a,b}

My research focuses on to characterize the ionic behavior of tetraphenyl ethelene (TPE) oligomers and their verification in the corresponding di-phenyl substituted poly(phenylene vinylene) DP-PPV by conducting cyclic voltammetry (CV).



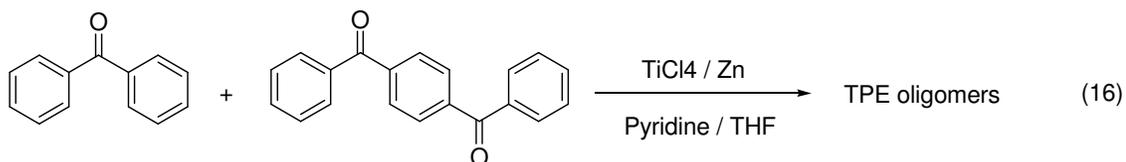
3.2 Results and Discussion

The reductive coupling of carbonyl compounds to produce olefins through low valent titanium in presence of zinc, known as the Cross McMurry Coupling,³² has achieved enormous interest in the field of organic synthesis which can be expressed by a number of reviews outlining the synthetic applications and mechanism.³³ The couplings are particularly prominent in preparation of (a) sterically hindered alkenes through homocouplings and (b) of cycloalkenes with ring sizes ranging from 3 to 72 via intramolecular couplings.³⁴ The utility of the reaction is highlighted as the key step in numerous syntheses of natural products.³⁵

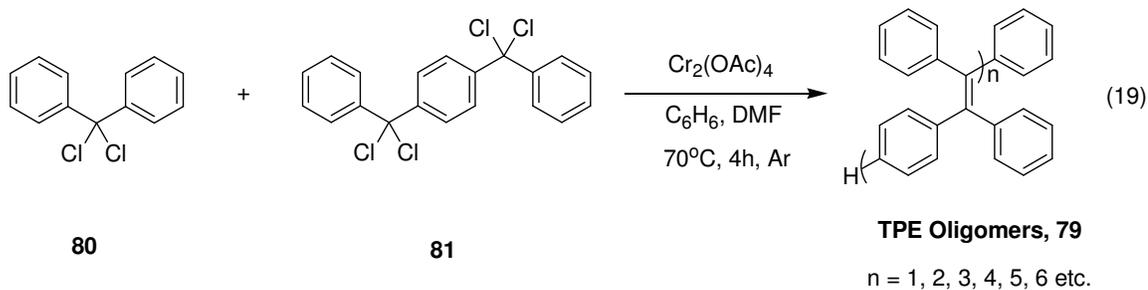
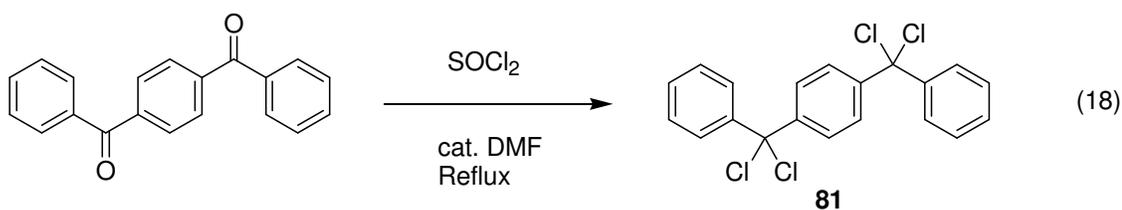
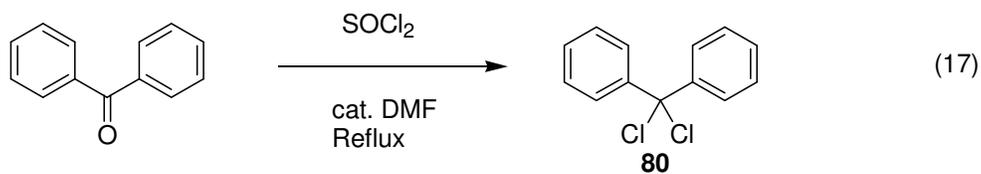
There are, however, remarkably few recorded examples of cross McMurry couplings between two different carbonyl compounds. It is generally believed that this kind of cross coupling will generate a roughly statistical mixture of the possible coupling products. For synthetic purposes, such mixed couplings are useful when conducted with one component in excess or when the products are easily separable.^{36,37}

Our purpose was to synthesize tetraphenylethelene oligomers with the use of benzophenone and 1,4-dibenzoylbenzene in the solutions of Pyridine and THF with Zn and TiCl₄ following this method found in the procedure of *J. Org. Chem.*³⁸

Cross McMurry Reaction



But the reaction was unsuccessful forming the oligomers led to change in strategy. So, the reaction pathways were changed and followed the procedure written in the literature *Makromol. Chem.*^{31a} They produced first the corresponding di- and tetra-chlorides of the ketones. Then the chlorides were used together to react with freshly prepared chromium acetate in benzene and DMF in 70°C under Ar –atmosphere where Cr provides e^- to the reaction mixture and the di- and tetra- chlorides reduces to form the alkenes of tetraphenylethelene oligomers.



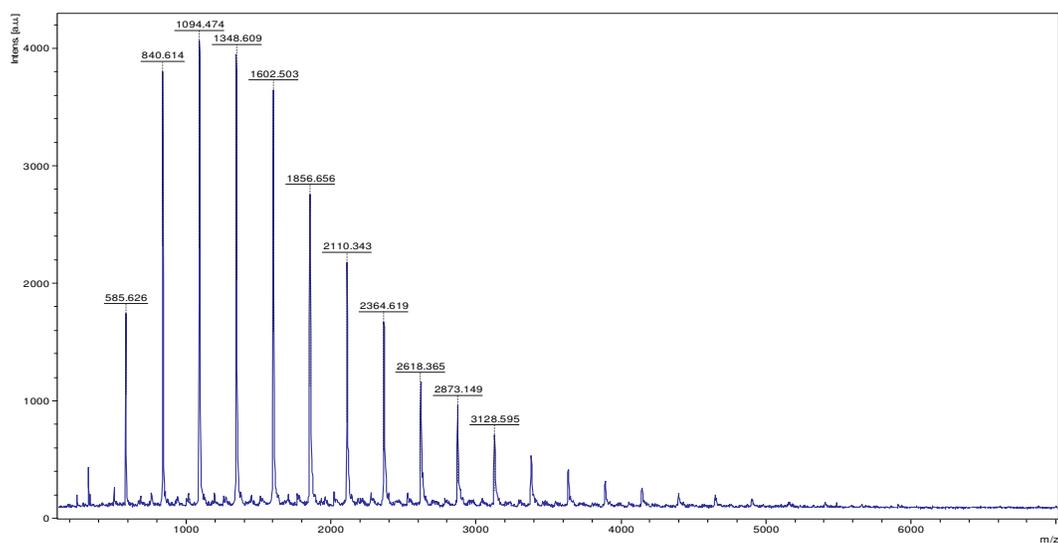


Figure 3.2: MALDI spectrum of the reaction mixture of equation 20.2 (ratio 2:1)

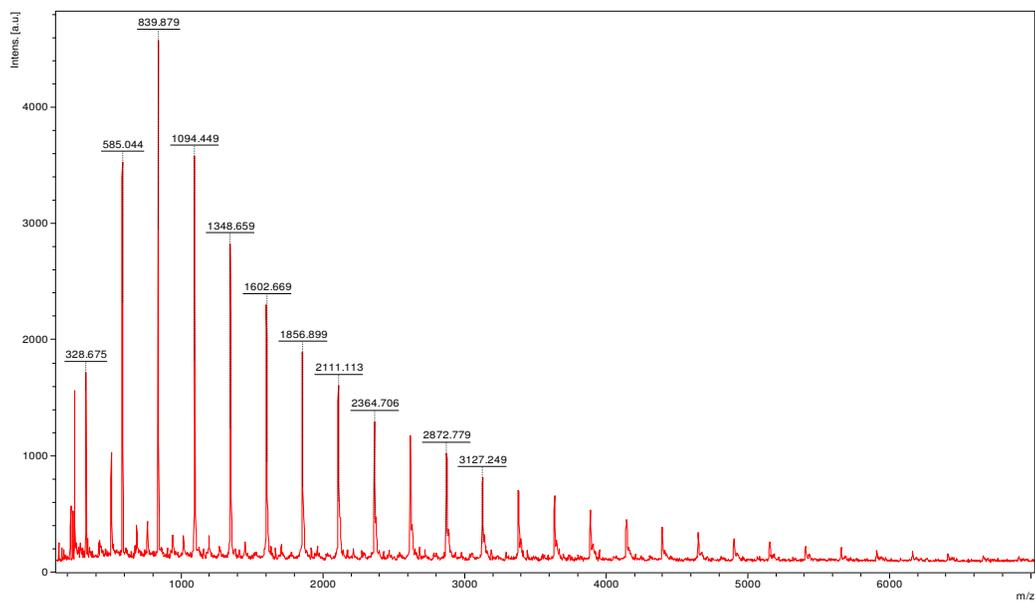


Figure 3.3: MALDI spectrum of the reaction mixture of equation 20.3 (ratio 1:2)

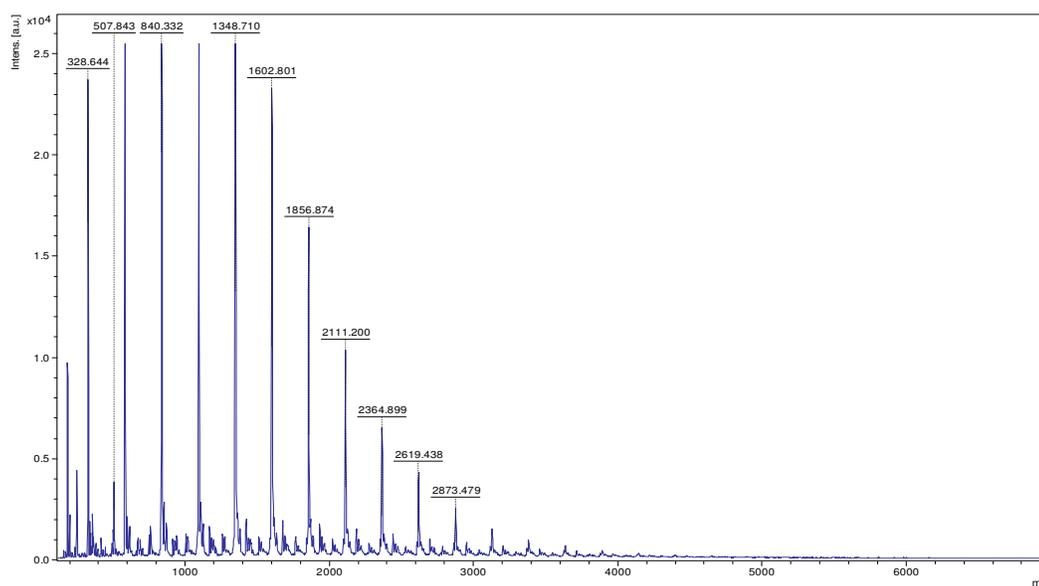


Figure 3.4: MALDI spectrum of the reaction mixture of equation 20.4 (ratio 4:1)

The intensities of the product mass from these spectra show that when the ratio of dichlorides are larger than the corresponding tetrachlorides, oligomers with less molecular weight form more than the higher ones. Similarly, when the ratio of dichlorides are lower than the corresponding tetrachlorides, oligomers with higher molecular weight form more than in previous case.

The obtained oligomeric mixtures were treated by column chromatography to separate the oligos where $n = 1, 2, 3, 4, 5$ and a mixture of other oligomers. All oligomers were yellow, strongly fluorescent solids except colors of model, $n = 1$ was colorless crystal, model, $n = 2$ was colorless crystal to white solid and model, $n = 3$ was light yellow solid. Although our goal was to separate more oligomers, it was quite difficult to

accomplish the job by using conventional method. The following MALDI spectra demonstrate the level of difficulties we faced to isolate the higher oligomers, even after carrying out flash column chromatography multiple times.

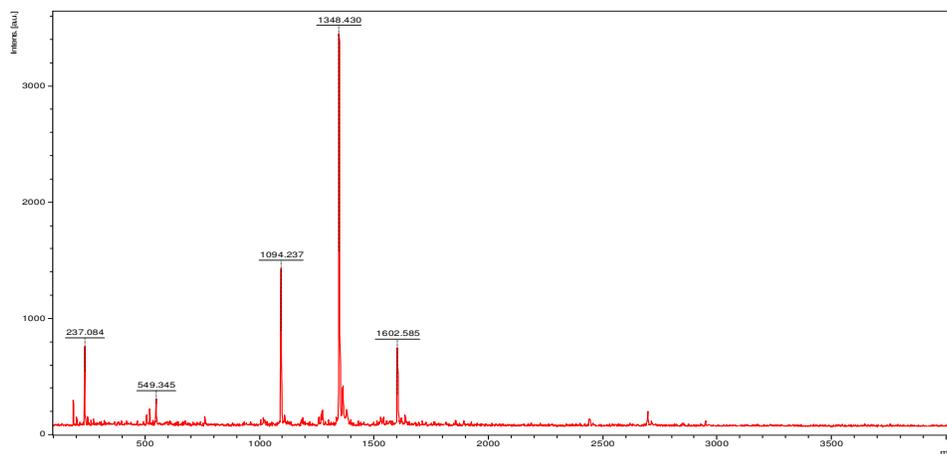


Figure 3.5: MALDI spectrum of the mixture of oligomers, $n = 4, 5$ and 6

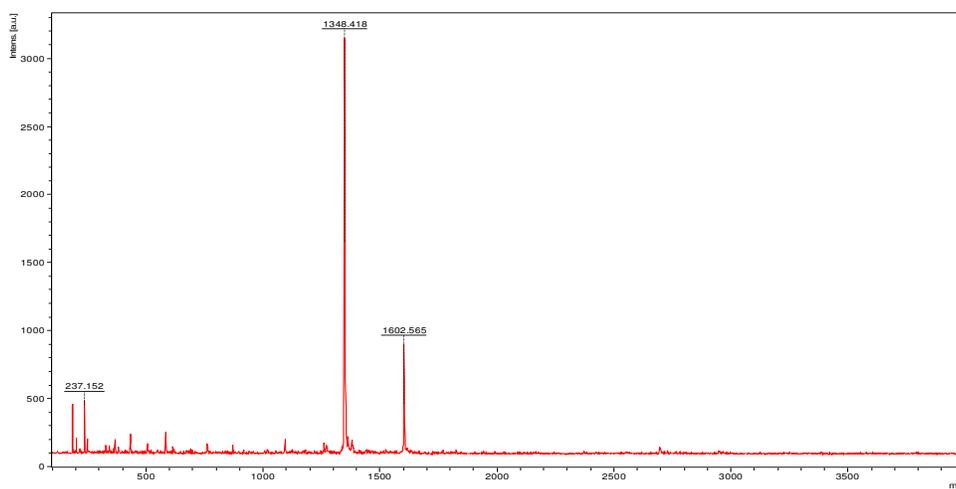


Figure 3.6: MALDI spectrum of the mixture of oligomers, $n = 5$ and 6

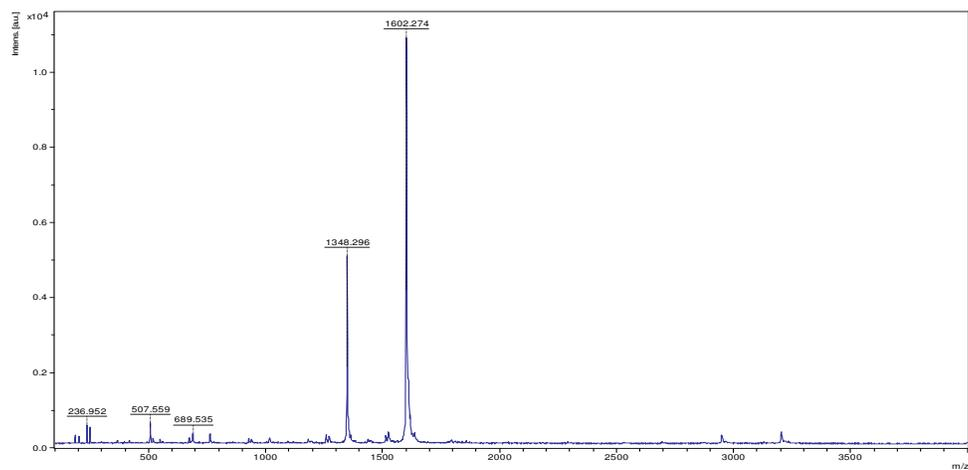


Figure 3.7: MALDI spectrum of the mixture of oligomers, $n = 5$ and 6

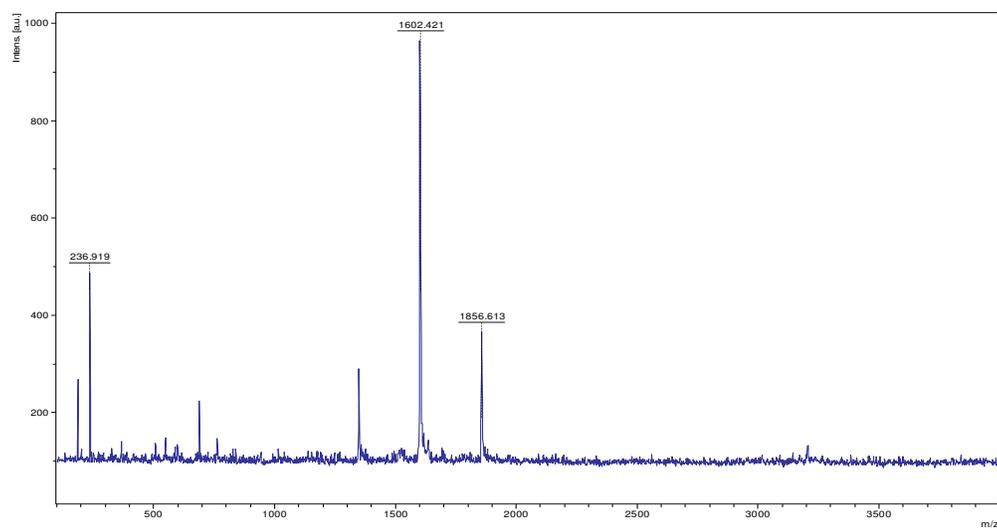


Figure 3.8: MALDI spectrum of the mixture of oligomers, $n = 5, 6$ and 7

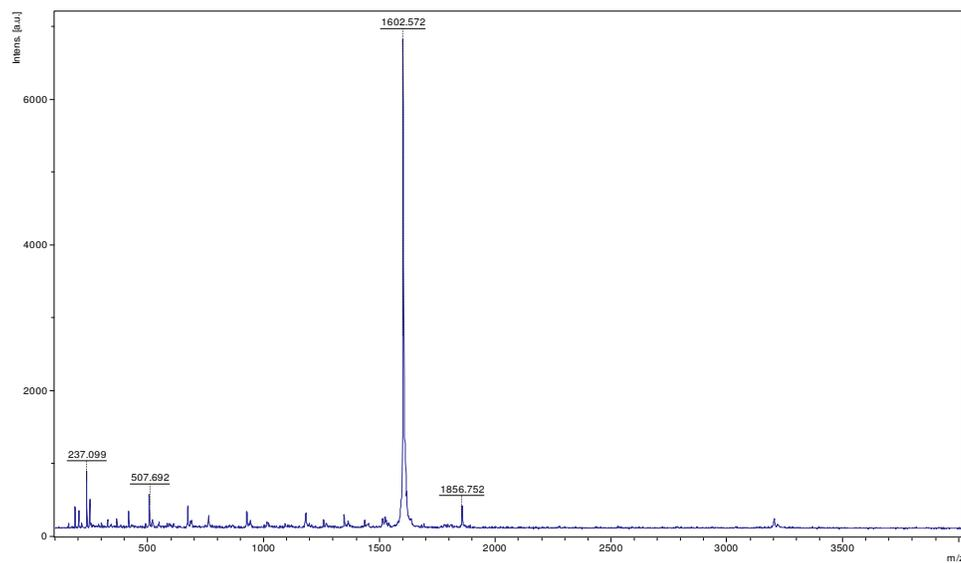


Figure 3.9: MALDI spectrum of the mixture of oligomers, $n = 6$ and 7

Isolation by using preparative HPLC could be investigated for a better result.

3.3 Electrochemistry:

Here are the Oxidation potentials for the Oligomers **82 - 86** ($n = 1, 2, 3, 4, 5$) conducted by CV and Square-wave Voltammetry described in Table 5.

Table 6: Oxidation potentials of the oligomeric models **82 – 86** and **78** (DP-PPV) (Electrolyte: 1.2×10^{-3} M tetra-*n*-butylammonium hexafluorophosphate, TBAPF₆ in CH₂Cl₂, Pt electrode)

Models	n	E_1	E_2	E_3	E_4	E_5
82	1	1.358	1.646			
83	2	1.215	1.387			
84	3	1.146	1.286	1.617		
85	4	1.129	1.234	1.430	1.557	
86	5	1.125	1.208	1.337	1.408	1.866
DP-PPV, 78		1.198	1.320	1.500	2.060	

In Table 5, the square-wave voltammetry peak potentials of both the oligomeric series **82 – 86** and the corresponding DP-PPV are listed. E_1 and E_2 represent the formation of radical cations and dication, respectively. With increasing n , these potentials decrease as well as their difference. At higher potentials and with increasing n

additional peaks were observed indicating the transfer of upto 5 electrons; the E_3 , E_4 and E_5 clearly represent the formation of tri-, tetra- and penta- radical cations as well. The oxidation potential values here are consistent with the results obtained by H. -H. Horhold et al. in an electrochemical study on the reduction of soluble PPV oligomers.³¹ From the figures 3.10 and 3.11 down, it is clear that for oligomers $n = 1$ and 2, 1st two oxidative electrons are chemically reversible but for the higher oligomers only one oxidative electrons show reversibility according to Cyclic Voltammogram.

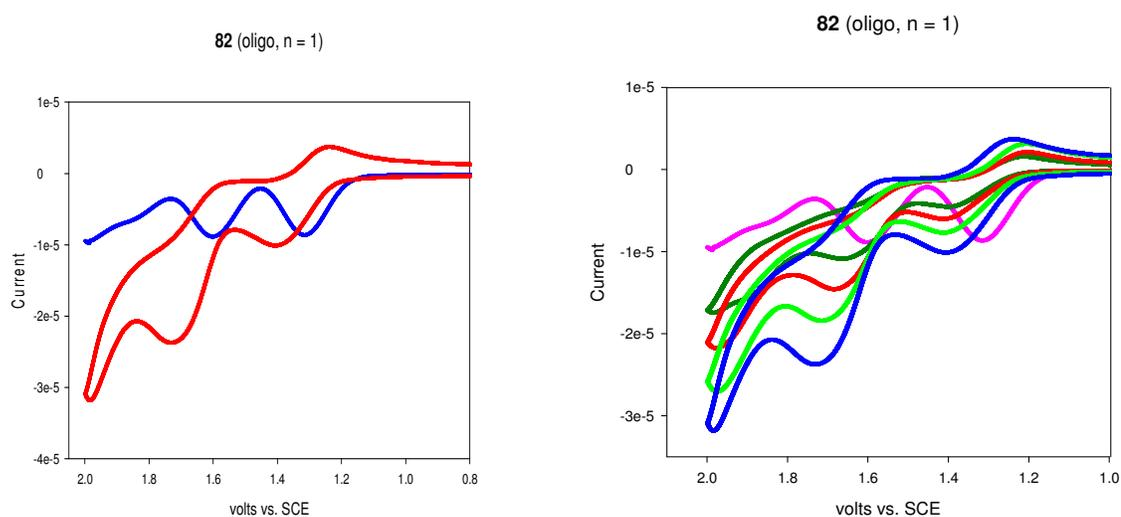


Figure 3.10: Cyclic- and SW voltammogram of **82** (Oligo, $n = 1$) as a 0.2 mM solution in CH_2Cl_2 containing 0.12 M TBAPF_6 as the supporting electrolyte at 22°C and scan rate of 200 mV s^{-1} for the left figure and 50, 100, 200 and 400 mV s^{-1} for the right figure.

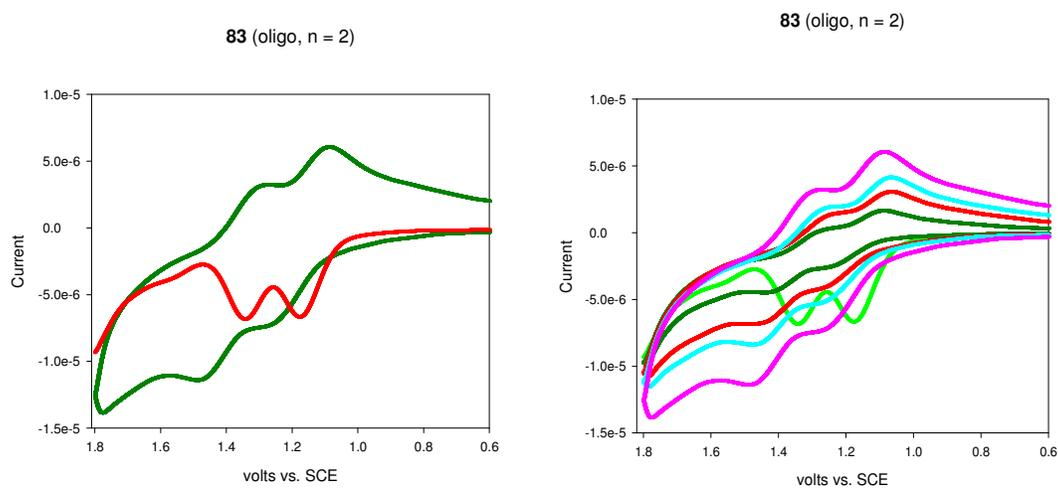


Figure 3.11: Cyclic- and SW voltammogram of **83** (Oligo, $n = 2$) as a 0.2 mM solution in CH_2Cl_2 containing 0.12 M TBAPF_6 as the supporting electrolyte at 22°C and scan rate of 400 mV s^{-1} for the left figure and 50, 100, 200 and 400 mV s^{-1} for the right figure.

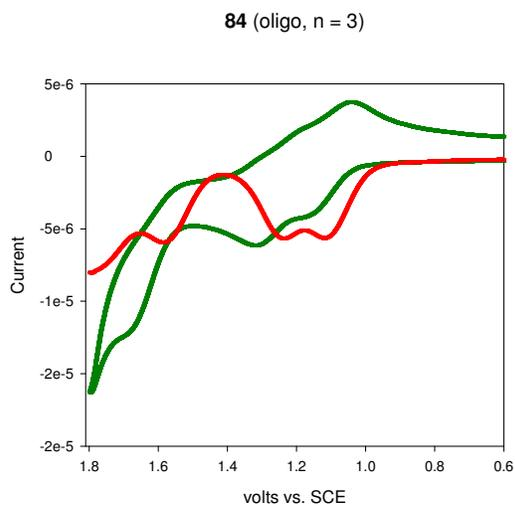


Figure 3.12: Cyclic- and SW voltammogram of **84** (Oligo, $n = 3$) as a 0.2 mM solution in CH_2Cl_2 containing 0.12 M TBAPF_6 as the supporting electrolyte at 22°C and scan rate of 200 mV s^{-1} .

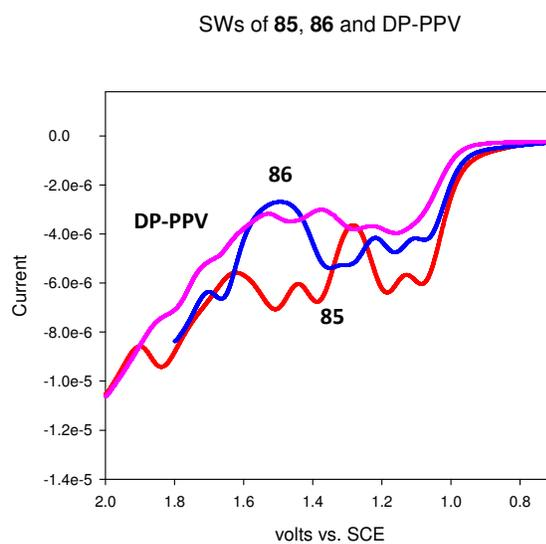


Figure 3.13: Square-Wave voltammogram of **85** (Oligo, $n = 4$), **86** (Oligo, $n = 5$) and DP-PPV as 0.2 mM solution in CH_2Cl_2 containing 0.12 M TBAPF_6 as the supporting electrolyte at 22°C .

3.4 Experimental Section

General Experimental Methods and Materials.

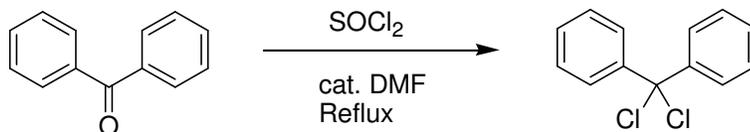
All reactions were performed under argon atmosphere using conventional vacuum-line techniques unless otherwise noted. All commercial reagents were used without further purification unless otherwise noted. Anhydrous tetrahydrofuran (THF) was prepared by refluxing the commercial tetrahydro-furan (Aldrich) over lithium aluminumhydried under an argon atmosphere for 24 hours followed by distillation. It was stored under an argon atmosphere in a Schlenk flask equipped with a Teflon valve fitted with Viton O-rings. Dichloromethane (Aldrich) was repeatedly stirred with fresh aliquots of conc. Sulfuric acid (~10% by volume) until the acid layer remained colorless. After separation it was washed successively with water, aqueous sodium bicarbonate, water, and saturated aqueous sodium chloride and dried over anhydrous calcium chloride by stirring the mixture for overnight. The dichloromethane was distilled twice from P₂O₅ under an argon atmosphere and stored in a Schlenk flask equipped with a Teflon valve fitted with Viton O-rings. Hexane and toluene were distilled from P₂O₅ under an argon atmosphere and then refluxed over calcium hydride (~12 hrs). After distillation from CaH₂, the solvents were stored in Schlenk flasks under argon atmosphere.

Cyclic Voltammetry (CV).

The CV cell was of an air-tight design with high vacuum Teflon valves and Viton O-ring seals to allow an inert atmosphere to be maintained without contamination by grease. The working electrode consisted of an adjustable platinum disk embedded in a glass seal to allow periodic polishing (with a fine emery cloth) without changing the surface area ($\sim 1 \text{ mm}^2$) significantly. The reference SCE electrode (saturated calomel electrode) and its salt bridge were separated from the catholyte by a sintered glass frit. The counter electrode consisted of a platinum gauze that was separated from the working electrode by $\sim 3 \text{ mm}$. The CV measurements were carried out in a solution of 0.1 to 0.2 M supporting electrolyte (tetra-*n*-butylammonium hexafluorophosphate, TBAPF₆) and the substrate $1\text{-}3 \times 10^{-3} \text{ M}$ in dry dichloromethane under an argon atmosphere. All the cyclic voltammograms were recorded at a sweep rate of 50 - 400 mV sec^{-1} , unless otherwise specified and were IR compensated.

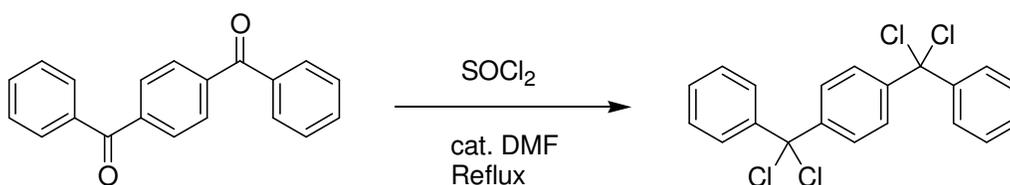
The oxidation potentials ($E_{1/2}$) were referenced to SCE, which was calibrated with added (equimolar) ferrocene ($E_{1/2} = 0.450 \text{ V vs. SCE}$). The $E_{1/2}$ values were calculated by taking the average of anodic and cathodic peak potentials in reversible cyclic voltammograms or directly from square-wave voltammograms in irreversible cyclic voltammograms.

Preparation of dichlorodiphenylmethane (**80**):



To a solution of benzophenone (10 g, 54.95 mmol) in DMF (5.5 mL, 71 mmol) under Ar flow, was added SOCl_2 (18 mL, 248 mmol) drop wise and heat the mixture to 90°C for 6 h. After completion of the reaction, simple vacuum distillation was performed promptly by adding hexane and distilling several times to remove excess of SOCl_2 as to prevent reversibility of the reaction. Overnight vacuum was used as well. After removing SOCl_2 , the mixture was washed with water several times by extracting with CH_2Cl_2 , dried over MgSO_4 and concentrated in vacuo. The sample was then diluted in hexane, filtered through celite and the filtrate was then kept in fridge to remove any dark brown precipitation (impurities) and finally obtained pure product **80** (12.46 g, 95.8% yield) as a colorless and odorless oil. ^1H NMR (CDCl_3 , 400 MHz): δ : 7.35 – 7.40 (m, 6H), 7.61 – 7.65 (m, 4H); ^{13}C NMR (CDCl_3 , 400 MHz): δ : 92.02, 127.46, 128.17, 129.1, 144.1.

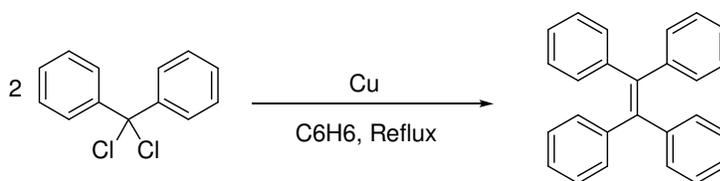
Preparation of 1,4-bis(1,1-dichlorobenzyl)benzene (**81**):



To a solution of 1,4-dibenzoylbenzene (10 g, 34.96 mmol) in DMF (7 mL, 90.4 mmol) under Ar flow, was added SOCl_2 (25 mL, 344.5 mmol) dropwise and heat the

mixture to 90°C for 5 h. After completion of the reaction, simple vacuum distillation was performed promptly by adding hexane and distilling several times to remove excess of SOCl₂ as to prevent reversibility of the reaction. Overnight vacuum was used as well which converts the mixture as brown solid. After removing SOCl₂, the solid was diluted in hexane, filtered through celite to remove any dark brown precipitation (impurities) and the filtrate was then kept in fridge to finally obtain pure product **81** (11.44 g, 82.9% yield) as stinky brown crystals; mp: 74 - 75°C; ¹H NMR (CDCl₃, 400 MHz): δ: 7.354 – 7.424 (m, 6H), 7.597 (s, 4H), 7.617 – 7.667 (m, 4H); ¹³C NMR (CDCl₃, 400 MHz): δ: 91.1, 127.22, 127.39, 128.27, 129.27, 143.34, 144.85.

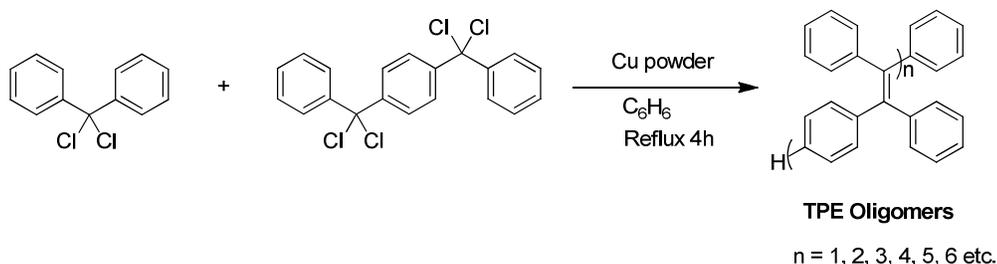
Preparation of tetra-phenylethelene (TPE) (82):



The TPE was produced following the reported procedure of Organic Syntheses, **1951**.³⁹ To a solution of dichlorodiphenylmethane (2.37 g, 10 mmol) dissolved in 10 mL anhydrous C₆H₆ under Ar was added Cu powder (1.5 g, 28 mmol) and the reaction mixture was heated to reflux for 3 h. After the completion of the reaction, the solution was hot filtered to remove inorganic solids out, wash the filtrate with water by extracting with CH₂Cl₂, dried the organic layer over MgSO₄, then keep in fridge to grow white crystals as pure product **82** (1.53 g, 92.2% yield), mp: 219°C. ¹H NMR analysis: δ

(CDCl₃, 400 MHz): 7.01 – 7.06 (m, 4H), 7.07 – 7.16 (m, 6H); ¹³C NMR (CDCl₃, 100 MHz): δ: 126.44, 127.68, 131.36, 140.96, 143.75.

Preparation of tetraphenylethelene (TPE) oligomers, 79:



To a mixture of Cu powder in anhydrous C₆H₆ under Ar flow, dichlorodiphenylmethane and 1,4-bis(1,1-dichlorobenzyl)benzene dissolved in anhydrous C₆H₆ under Ar was added dropwise and the reaction mixture was heated to reflux for 4 h. After the completion of the reaction, the solution was hot filtered to remove inorganic solids out, wash the filtrate with water by extracting with CH₂Cl₂, dried the organic layer over MgSO₄, then concentrated in vacuo. The obtained oligomeric mixture was treated by column chromatography to separate the models where n = 1, 2, 3, 4, 5 and a mixture of other oligomers. All oligomers were yellow, strongly fluorescent solids except colors of model, n = 1 was colorless crystal, model, n = 2 was colorless crystal to white solid and model, n = 3 was light yellow solid.

NMRs and mp data of,

model, n = 1 (82): mp : 219.0 - 219.6°C; ¹H NMR (CDCl₃, 400 MHz) : δ: 7.01 – 7.06 (m, 2H), 7.07 – 7.16 (m, 3H); ¹³C NMR (CDCl₃, 100 MHz) : δ: 126.44, 127.68, 131.36, 140.96, 143.75.

model, n = 2 (83): mp : 223.2 – 223.7°C; ¹H NMR (CDCl₃, 300 MHz) : δ: 6.75 (s, 2H), 6.93 – 7.04 (m, 6H), 7.04 – 7.16 (m, 9H); ¹³C NMR (CDCl₃, 75 MHz) : δ: 126.58, 126.67, 127.77, 127.84, 130.88, 131.57, 141.03, 142.1, 143.74, 143.96, 143.99.

model, n = 3 (84): mp : 254.5 – 255.3°C; ¹H NMR (CDCl₃, 400 MHz) : δ: 6.69 – 6.75 (m, 4H), 6.92 – 7.01 (m, 8H), 7.03 – 7.14 (m, 12H); ¹³C NMR (CDCl₃, 100 MHz) : δ: 126.36, 126.42, 126.44, 126.45, 127.53, 127.54, 127.61, 130.63, 130.66, 131.33, 131.39, 131.42, 140.68, 140.77, 140.81, 141.84, 141.91, 143.52, 143.57, 143.74, 143.76.

model, n = 4 (85): mp : 291.8 – 292.5°C; ¹H NMR (CDCl₃, 400 MHz) : δ: 6.71 (s, 2H), 6.72 - 6.75 (m, 4H), 6.91 – 7.04 (m, 10H), 7.04 – 7.18 (m, 15H); ¹³C NMR (CDCl₃, 100 MHz) : δ: 126.34, 126.39, 126.42, 127.42, 127.52, 127.59, 130.61, 130.64, 131.32, 131.37, 131.39, 140.63, 140.66, 140.75, 140.79, 141.81, 141.85, 141.89, 143.50, 143.54, 143.72, 143.74.

model, n = 5 (86): mp : 312.0 – 313.6°C; ¹H NMR (CDCl₃, 400 MHz) : δ: 6.69 (s, 4H), 6.69 – 6.75 (m, 4H), 6.90 – 7.01 (m, 12H), 7.02 – 7.14 (m, 18H); ¹³C NMR (CDCl₃, 100 MHz) : δ: 126.22 - 126.55 (multiple pks), 127.25 - 127.73 (multiple pks), 130.41 - 130.78 (multiple pks), 131.17 - 131.59 (multiple pks), 140.56 - 140.84 (multiple pks), 141.70 – 142.03 (multiple pks), 143.47 - 143.83 (multiple pks).

BIBLIOGRAPHY

1. (a) Kaplan, J. H., Forbush, B. I., and Hoffman, J. F., Rapid photolytic release of adenosine 5'-triphosphate from a protected analogue: utilization by the Na:K pump of human red blood cell ghosts, *Biochemistry*, **1978**, *17*, 1929–1935. (b) Engels, J. and chlaeger, E.-J., Synthesis, structure, and reactivity of adenosine cyclic 3',5'-phosphate benzyl triesters, *J. Med. Chem.*, **1977**, *20*, 907-911.
2. Zou, K., Miller, W. T., Givens, R. S., and Bayley, H., Caged thiophosphotryosine peptides, *Angew.Chem. Int. Ed. Engl.*, **2001**, *40*, 3049–3051.
3. Zou, K., Cheley, S., Givens, R. S., and Bayley, H., Catalytic subunit of protein kinase caged at the activating phosphothreonine, *J. Am. Chem. Soc.*, **2002**, *124*, 8220–8229.
4. Arabaci, G., Guo, X.-C., Beebe, K. D., Coggeshall, K. M., and Pei, D., α -Haloacetophenone derivatives as photoreversible covalent inhibitors of protein tyrosine phosphates, *J. Am. Chem. Soc.*, **1999**, *121*, 5085–5086.
5. (a) Pelliccioli, A.P.; Wirz, J. "Photoremovable Protecting Groups: Reaction Mechanisms and Applications", *Photochem. Photobiol. Sci.* **2002**, *1*, 441-458. (b) Mayer, G.; Heckel, A. "Biologically Active Molecules with a Light Switch", *Angew. Chem. Int. Ed.* **2006**, *45*, 4900-4921. (c) Zou, K.; Cheley, S.; Givens, R.S.; Bayley, H. "Catalytic Subunit of Protein Kinase A Caged at the Activating Phosphothreonine" *J. Am. Chem. Soc.* **2002**, *124*, 8220-8229. (d) Kaplan, J.H.; Forbush, B.; Hoffman, J.F. "Rapid Photolytic Release of Adenosine 5-Triphosphate from a Protected Analogue: Utilization by the Na:K Pump of Human Red Blood Cell Ghosts", *Biochemistry*, **1978**, *17*, 1929-1935.
6. (2) (a) Walker, J. W.; Gilbert, S.H.; Drummond, R.M.; Yamada, M.; Sreekumar, R.; Carraway, R.E.; Ikebe, M.; Fay, F.S. "Signaling Pathways Underlying Eosinophil Cell Motility Revealed By Using Caged Peptides", *Proc. Natl. Acad. Sci USA*, **1998**, *95*, 1568-1573. (b) Zou, K.; Cheley, S.; Givens, R.S.; Bayley, H. "Catalytic Subunit of Protein Kinase A Caged at the Activating Phosphothreonine", *J. Am. Chem. Soc.* **2002**, *124*, 8220-8229. (c) Kaplan, J.H.; Forbush, B. III; Hoffman, J.F. "Rapid Photolytic Release of Adenosine 5'-Triphosphate from a Protected Analogue: Utilization by the Na:K Pump of Human Red Blood Cell Ghosts", *Biochemistry*, **1978**, *17*, 1929-1935. (d) Canepari, M.; Nelson, L.; Papegeorgiou, G.; Corrie, J.E.T.; Ogden, D. "Photochemical and pharmacological evaluation of 7-nitroindoliny- and 4-methoxy-7-nitroindoliny-amino acids as novel, fast caged neurotransmitters", *J. Neurosci. Methods*, **2001**, *112*, 29-42.

7. (a) Banerjee, A.; Grewer, C.; Ramakrishnan, L.; Jager, J.; Ganeiro, A.; Breiting, H.-G.A.; Gee, K.R.; Carpenter, B.K.; Hess, G.P. "Toward the Development of New Photolabile Protecting Groups that Can Rapidly Release Bioactive Compounds upon Photolysis with Visible Light", *J. Org. Chem.* **2003**, *68*, 8361-8367. (b) Borak, J.B.; Lopez-Sola, S.; Falvey, D.E. "Photorelease of Carboxylic Acids Mediated by Visible-Light Absorbing Gold-Nanoparticles", *Org. Lett.* **2008**, *10*, 457-460. (c) Hagen, V.; Bendig, J.; Frings, S.; Eckardt, T.; Helm, S.; Reuter, D.; Kaupp, U.B. "Highly Efficient and Ultrafast Phototriggers for cAMP and cGMP by Using Long-Wavelength UV/Vis-Activation", *Angew. Chem. Int. Ed.* **2001**, *40*, 1046-1048. (d) Furuta, T.; Wang, S. S.-H.; Dantzker, J.L.; Dore, T.M.; Bybee, W.J.; Callaway, E.M.; Denk, W.; Tsien, R.Y. "Brominated 7-Hydroxycoumarin-4-ylmethyls: Photolabile Protecting Groups with Biologically Useful Cross Sections for Two Photon Photolysis", *Proc. Natl. Acad. Sci., U.S.A.* **1999**, *96*, 1193-1200. (e) Zhu, Y.; Pavlos, C.M.; Toscano, J.P.; Dore, T.M. "8-Bromo-7-hydroxyquinoline as a Photoremovable Protecting Group for Physiological Use: Mechanism and Scope", *J. Am. Chem. Soc.* **2006**, *128*, 4267-4276.
8. (a) Banerjee, A.; Grewer, C.; Ramakrishnan, L.; Jager, J.; Ganeiro, A.; Breiting, H.-G.A.; Gee, K.R.; Carpenter, B.K.; Hess, G.P. "Toward the Development of New Photolabile Protecting Groups that Can Rapidly Release Bioactive Compounds upon Photolysis with Visible Light", *J. Org. Chem.* **2003**, *68*, 8361-8367. (b) Corrie J.E.T., Trentham D.R. *J. Chem. Soc. Perkin Trans.* **1992**, 2409-17. (c) Givens R.S., Weber J.F.W., Jung A.H. Park C.H. *Methods in Enzymology*, **1998**, *291*, 1-29.
9. (a) Marriott, G., Ed., *Methods in Enzymology*; Academic Press: San Diego, 1998; Vol, 291. (b) Goeldner, M.; Givens, R. *Dynamic Studies in Biology*; Wiley-VCH: Weinheim, 2005. (c) Pelliccioli, A.P.; Wirz, J. "Photoremovable Protecting Groups: Reaction Mechanisms and Applications", *Photochem. Photobiol. Sci.* **2002**, *1*, 441-458. (d) Mayer, G.; Heckel, A. "Biologically Active Molecules with a Light Switch", *Angew. Chem. Int. Ed.* **2006**, *45*, 4900-4921.
10. Wang, L.; Corrie, J.E.T.; Wooton, J.F. "Photolabile Precursors of Cyclic Nucleotides with High Aqueous Solubility and Stability", *J. Org. Chem.* **2002**, *67*, 3474-3478.
11. Jasuja, R.; Keyoung, J.; Reid, G.P.; Trentham, D.R.; Khan, S. "Chemotactic Responses of *Escherichia coli* to Small Jumps of Photoreleased L-Aspartate," *Biophys. J.* **1999**, *76*, 1706-1719.
12. Du, X.; Frei, H.; Kim, S.-H. "The Mechanism of GTP Hydrolysis by Ras Probed by Fourier Transform Spectroscopy", *J. Biol. Chem.* **2000**, *275*, 8492-8500.
13. Pratap, P.R.; Dediu, O.; Nienhaus, G.U. "FTIR Study of ATP-Induced Changes in Na⁺/K⁺-ATPase from Duck Supraorbital Glands", *Biophys. J.* **2003**, *85*, 3707-3717.

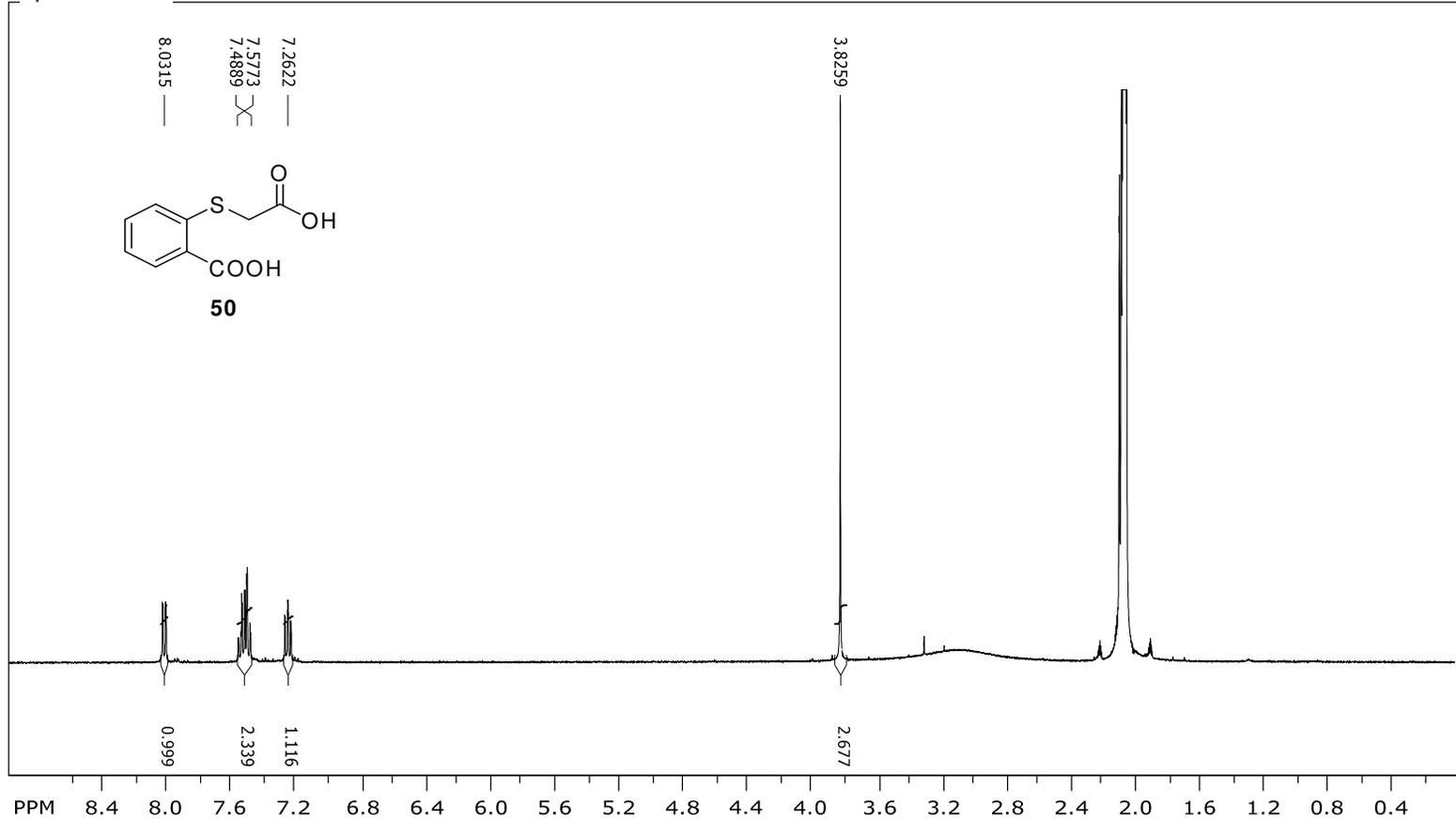
14. Takeuchi, H.; Kurahashi, T. "Photolysis of Caged Cyclic AMP in the Ciliary Cytoplasm of the Newt Olfactory Receptor Cell", *J. Physiol.* **2002**, *541*, 825-833.
15. Tertysnikova, S.; Fein, A. "Inhibition of Inositol 1,4,5-Triphosphate-Induced Ca^{2+} Release by cAMP-Dependent Protein Kinase in a Living Cell", *Proc. Natl. Acad. Sci. USA*, **1998**, *95*, 1613-1617.
16. (a) Ninomiya, I.; Naito, T. "Enamide Photocyclization and Its Application to the Synthesis of Heterocycles", *Heterocycles*, **1981**, *15*, 1433-1462. (b) Lenz, G.R. "The Ground and Excited State Reactions of Enamides", *Synthesis*, **1978**, 489-518. (c) Campbell, A.L.; Lenz, G.R. *Synthesis*, **1987**, 421-452.
17. Cleveland, P.G.; Chapman, O.L. *Chem. Commun.* **1967**, 1064-1065.
18. Ogata, Y.; Takagi, K.; Ishino, I. *J. Org. Chem.* **1971**, *36*, 3975-3979.
19. Ninomiya, I.; Yamauchi, S.; Kiguchi, T.; Shinohara, A.; Naito, T. *J. Chem. Soc., Perkin Trans. 1* **1974**, 1747-1751.
20. (a) Kanaoka, Y.; Itoh, K.; Hatanaka, Y.; Flippen, J.L.; Karle, I.; Witkop, B. *J. Org. Chem.* **1975**, 3001-3003. (b) Chen, Y.; Steinmetz, M.G. "Photochemical Cyclization with Release of Carboxylic Acids and Phenol from Pyrrolidino-Substituted 1,4-Benzoquinones Using Visible Light", *Org. Lett.* **2005**, *7*, 3729-3732. (c) Chen, Y.; Steinmetz, M.G. "Photoactivation of Amino-Substituted 1,4-Benzoquinones for Release of Carboxylate and Phenolate Leaving Groups Using Visible Light", *J. Org. Chem.* **2006**, *71*, 6053-6060.
21. Jasuja, R.; Keyoung, J.; Reid, G.P.; Trentham, D.R.; Khan, S. "Chemotactic Responses of *Escherichia coli* to Small Jumps of Photoreleased L-Aspartate," *Biophys. J.* **1999**, *76*, 1706-1719.
22. Du, X.; Frei, H.; Kim, S.-H. "The Mechanism of GTP Hydrolysis by Ras Probed by Fourier Transform Spectroscopy", *J. Biol. Chem.* **2000**, *275*, 8492-8500.
23. (a) Morrison, J.; Wan, P.; Corrie, J.E.T.; Papageorgiou, G. "Mechanisms of Photorelease of Carboxylic Acids from 1-Acyl-7-nitroindolines in Solutions of Varying Water Content", *Photochem. Photobiol. Sci.* **2002**, *1*, 960-969. (b) Papageorgiou, G.; Lukeman, M.; Wan, P.; Corrie, J.E.T. "An Antenna Triplet Sensitizer for 1-Acyl-7-nitroindolines Improves the Efficiency of Carboxylic Acid Photorelease" *Photochem. Photobiol. Sci.* **2004**, *3*, 366-373. (c) Sarker, M.; Shahrin, T.; Steinmetz, M.G.; "Photochemical Eliminations Involving Zwitterionic

- Intermediates Generated via Electrocyclic Ring Closure of Benzothiophene Carboxanilides”, *Org. Lett.*, **2011**, *13* (5), 872–875; (d) Sarker, M.; Shahrin, T.; Steinmetz, M.G.; Timerghazin, Q.; “Photochemical Electrocyclic Ring Closure and Leaving group expulsion from *N*-(9-oxohiozanthenyl)-benzothiophene carboxamidest”, *Photochem. Photobiol. Sci.*, **2013**, *12*, 309–322.
24. (a) Ma, C.; Steinmetz, M.G.; Cheng, Q.; Jayaraman, V. "Photochemical Cleavage and Release of Carboxylic Acids from α -Keto Amides", *Org. Lett.* **2003**, *5*, 71-74. (b) Ma, C.; Steinmetz, M.G.; Kopatz, E.J.; Rathore, R. "Time-resolved pH Jump Study of Photochemical Cleavage and Release of Carboxylic Acids from α -Keto Amides", *Tetrahedron Lett.* **2005**, *46*, 1045-1048. (c) Ma, C.; Steinmetz, M.G.; Kopatz, E.J.; Rathore, R. "Photochemical Cleavage and Release of Carboxylic Acids from α -Keto Amides", *J. Org. Chem.* **2005**, *70*, 4431-4442.
25. (a) Greenberg, M.M.; Venkatesan, H. “Improved Utility of Photolabile Solid Phase Synthesis Supports for the Synthesis of Oligonucleotides Containing 3'-Hydroxyl Termini”, *J. Org. Chem.* **1996**, *61*, 525-529. (b) Greenberg, M.M.; Gilmore, J.L. “Cleavage of Oligonucleotides from Solid-Phase Supports Using *o*-Nitrobenzyl Photochemistry”, *J. Org. Chem.* **1994**, *59*, 746-753. (c) Pirrung, M.C.; Bradley, J.-C. “Comparison of Methods for Photochemical Phosphoramidite-Based DNA Synthesis”, *J. Org. Chem.* **1995**, *60*, 6270-6276. (d) McGall, G.H.; Barone, A.D.; Diggelmann, M.; Fodor, S.P.A.; Gentalen, E.; Ngo, N. "The Efficiency of Light Directed Synthesis of DNA Arrays on Glass Substrates" *J. Am. Chem. Soc.* **1997**, *119*, 5081-5090. (e) Pease, A.C.; Solas, D.; Sullivan, E.J.; Cronin, M.T.; Holmes, C.P.; Fodor, S.P.A. “Light-generated Oligonucleotide Arrays for Rapid DNA Sequence Analysis”, *Proc. Nat. Acad. Sci. U.S.A.* **1994**, *91*, 5022-5026. (f) Fodor, S.P.A.; Read, J.L.; Pirrung, M.C.; Stryer, L.; Lu, A.T.; Solas, D. “Light-Directed, Spatially Addressable Parallel Chemical Synthesis”, *Science* **1991**, *251*, 767-773. (g) Amit, B.; Hazum, E.; Fridkin, M.; Patchornik, A. "Photolabile Protecting Group for the Phenolic Hydroxyl Function of Tyrosine", *Int. J. Peptide Protein Res.* **1977**, *9*, 91-96. (h) Lloyd-Williams, P.; Albericio, F.; Giralt, E. “Convergent Solid-Phase Peptide Synthesis”, *Tetrahedron* **1993**, *49*, 11065-11133.
26. Jia, J.; Sarker, M.; Steinmetz, M. G.; Shukla, R.; Rathore, R. *J. Org. Chem.* **2008**, *73*, 8867-8879.
27. (a) H. E. Zimmerman, Apparatus for quantitative and preparative photolysis. The Wisconsin black box, *Mol. Photochem.*, 1971, *3*, 281–292; (b) Nicolau, K.C.; *Angew. Chem. Int. Ed.* **2005**, *44*, 1378 – 1382.
28. <http://goldbook.iupac.org/O04286.html>

29. (a) *Fundamentals of Polymer Science*; (b) Fried J.R. "Polymer Science and Technology" (Pearson Prentice-Hall, 2nd edition 2003), p.27; (c) Flory, P.J. and Vrij, A. *J. Am. Chem. Soc.*; **1963**; 85(22) pp3548-3553.
30. (a) J. Heinze, M. Dietrich, J. Mortensen, *Makromol. Chem., Macromol. Symp.* **8**, 73 (1987); R. Schenk. H. Gregorius, K. Meerholz, J. Heinze, K. Mullen, *J. Am. Chem. Soc.* **113**, 2634 (1991); (b) J. Heinze, *Top. Curr. Chem.* **1990**, 152, 1.
31. (a) H.-H. Horhold, M. Helbig, *Makromol. Chem.* **1993**, 194, 1607 – 1618; *Material Science Forum* **1990**, 62 - 64, 411 – 417; *Macromol. Symp.*, **12**, 229 (1987); M. Helbig, H.-H. Horhold in "Electronic Properties of Polymers", (b) Springer Series in solid State Sciences, vol. **107**, H. Kuzmany, M. Mehring, S. Roth, Eds., Springer Verlag Berlin, Heidelberg, New York **1992**, pp. 321 - 325
32. (a) McMurry, J. E.; Felming, M. P. *J. Am. Chem. Soc.* **1974**, 96, 4708. (b) Mukaiyama, T.; Sato, T.; Hanna, J. *Chem. Lett.* **1973**, 1041.
33. (a) Ephritikhine, M. *Chem. Commun.* **1998**, 2549. (b) Furstner, A.; Bogdanovic, B. *Angew. Chem., Int. Ed. Engl.* **1996**, 35, 2442. (c) McMurry, J. E. *Chem. ReV.* **1989**, 89, 1513. (d) Lenoir, D. *Synthesis* **1989**, 883. (e) Kahn, B. E.; Rieke, R. D. *Chem. ReV.* **1988**, 88, 733.
34. (a) For the construction of 36-membered cyclic compounds, see Eguchi, T.; Terachi, T.; Kakinuma, K. *Chem. Commun.* **1994**, 137. (b) For 72-membered cyclic compounds, see Eguchi, T.; Ibaragi, K.; Kakinuma, K. *J. Org. Chem.* **1998**, 63, 2689.
35. Furstner, A.; Bogdanovic, B. *Angew. Chem., Int. Ed. Engl.* **1996**, 35, 2445.
36. (a) Reddy, S. M.; Duraisamy, M.; Walborsky, H. M. *J. Org. Chem.* **1986**, 51, 2361. (b) Paquette, L. A.; Yan, T.-H.; Wells, G. J. *J. Org. Chem.* **1984**, 49, 3610.
37. McMurry, J. E.; Krepski, L. R. *J. Org. Chem.* **1976**, 41, 3929.
38. Duan, X., Zeng, J., Lu, J., Zhang, Z.; *J. Org. Chem.* **2006**, 71, 9873 – 9876.
39. Buckles E., Robert; Matlack M., George, *Organic Syntheses*, **1951**, Vol. 31, 104.

Appendix I: NMR and MALDI SPECTRA

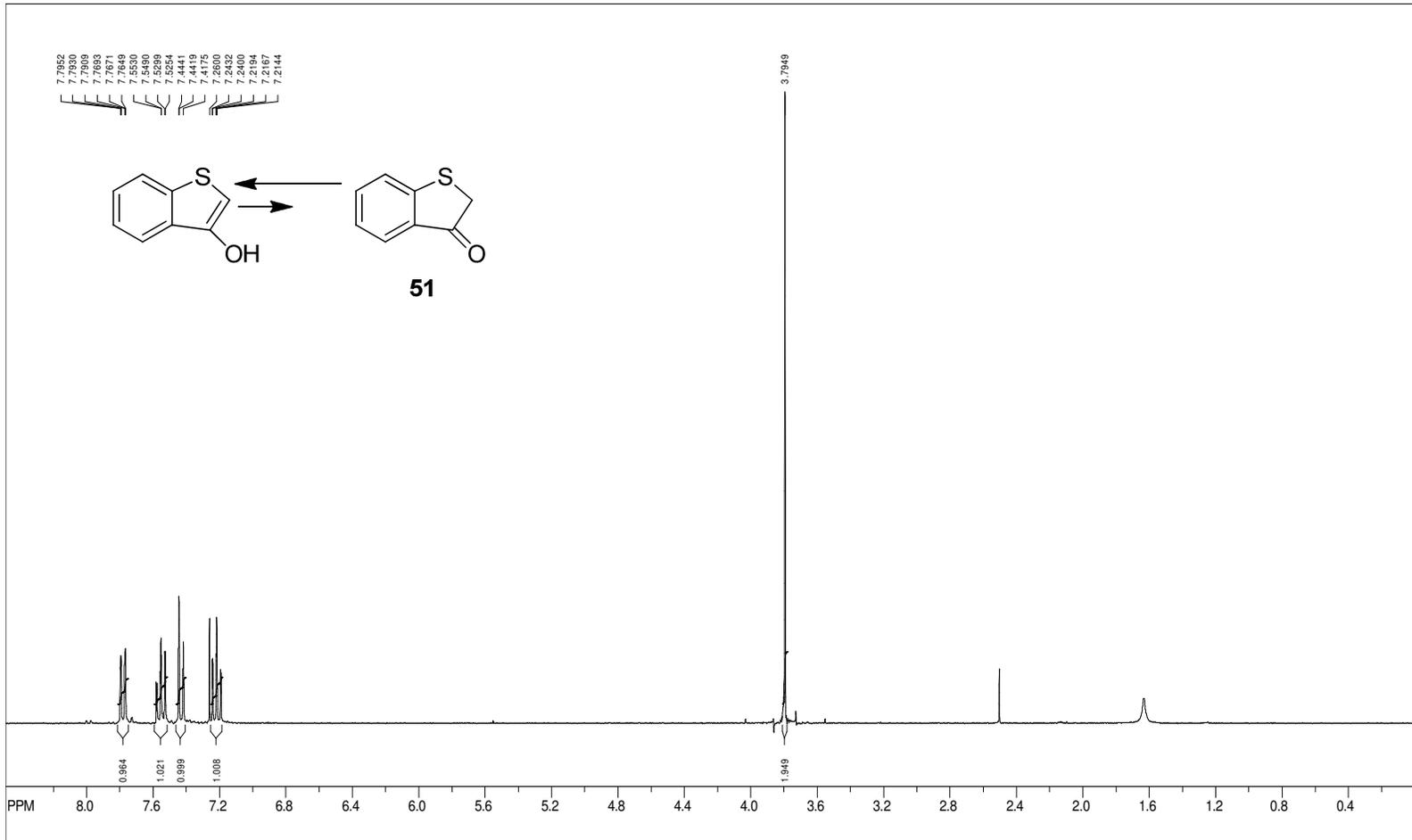
SpinWorks 3:



file: ...S\Dithiosalicylic acid\st1.fid\fid_block# 1 expt: "s2pul"
 transmitter freq.: 399.747950 MHz
 time domain size: 26264 points
 width: 6410.26 Hz = 16.0357 ppm = 0.244070 Hz/pt
 number of scans: 8

freq. of 0 ppm: 399.745551 MHz
 processed size: 65536 complex points
 LB: 0.000 GF: 0.0000
 Hz/cm: 143.845 ppm/cm: 0.35984

SpinWorks 2.5: STANDARD 1H OBSERVE



file: C:\Users\Pathore User\Desktop\Tas- Full Thesis-3-27\NMRs-MGS\Diethylsulfonic acid\2-solid1.fid\fid_block# 1 exp: "s2pu"

transmitter freq.: 300.133009 MHz

time domain size: 19192 points

width: 4903.07 Hz = 16.003151 ppm = 0.250264 Hz/pt

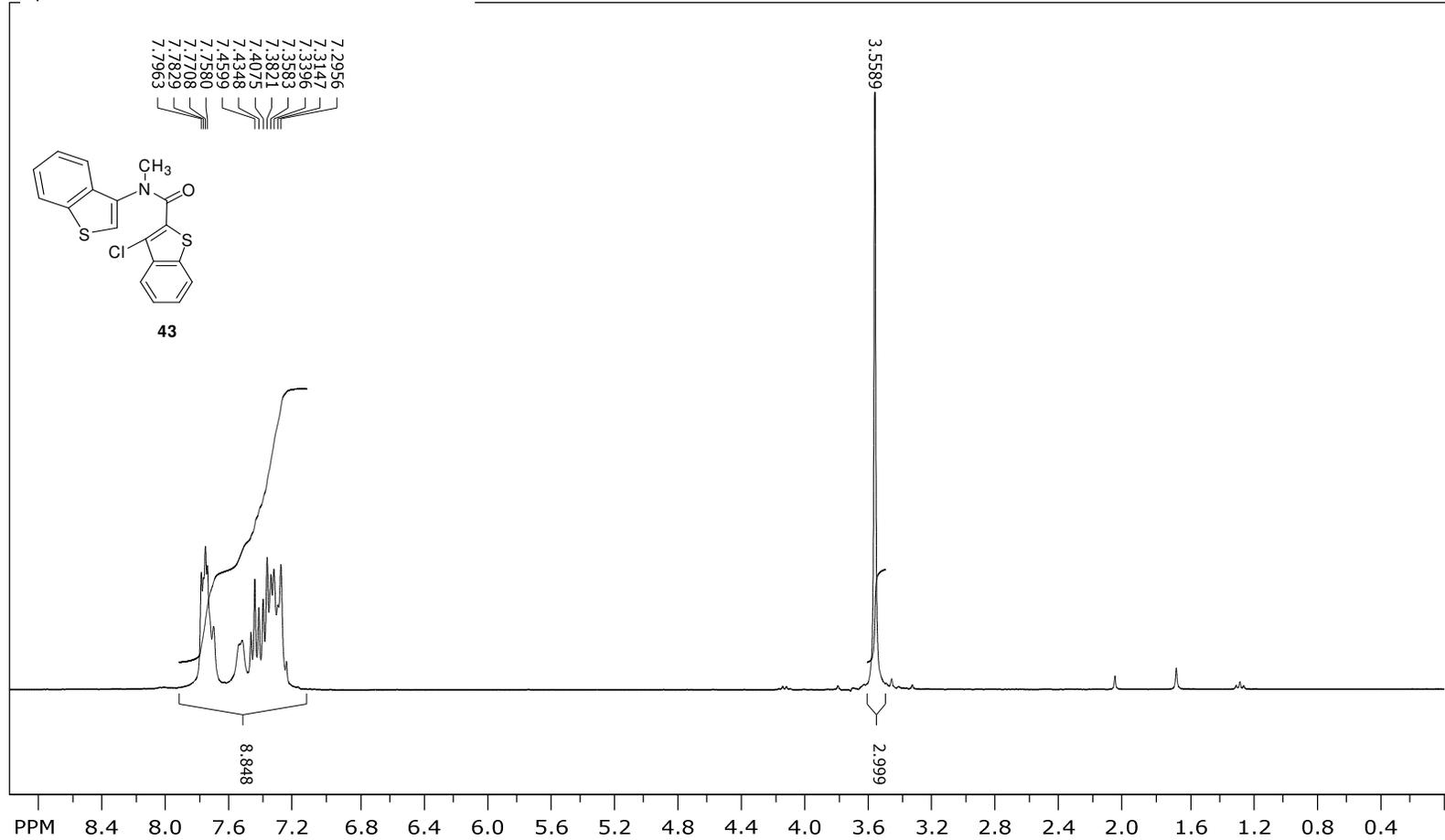
number of scans: 8

freq. of 0 ppm: 300.131205 MHz

processed size: 32768 complex points

LB: 0.000 GB: 0.0000

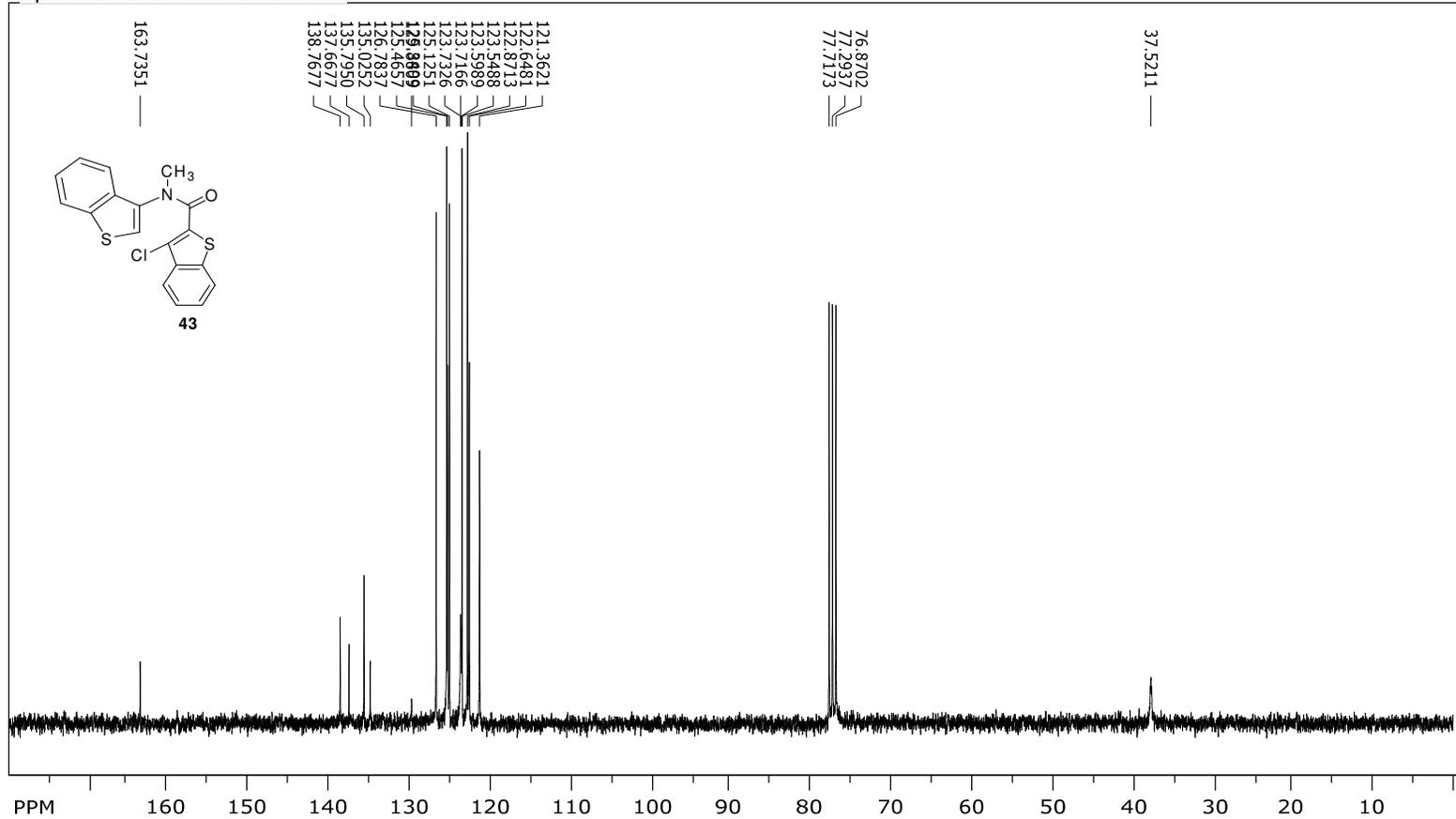
SpinWorks 3: STANDARD 1H OBSERVE



file: ...ng\Tas comp\dithioSM-Oct21.fid\fid_block# 1 expt: "s2pul"
 transmitter freq.: 300.133009 MHz
 time domain size: 19192 points
 width: 4803.07 Hz = 16.0032 ppm = 0.250264 Hz/pt
 number of scans: 8

freq. of 0 ppm: 300.131208 MHz
 processed size: 32768 complex points
 LB: 1.500 GF: 0.0000
 Hz/cm: 108.366 ppm/cm: 0.36106

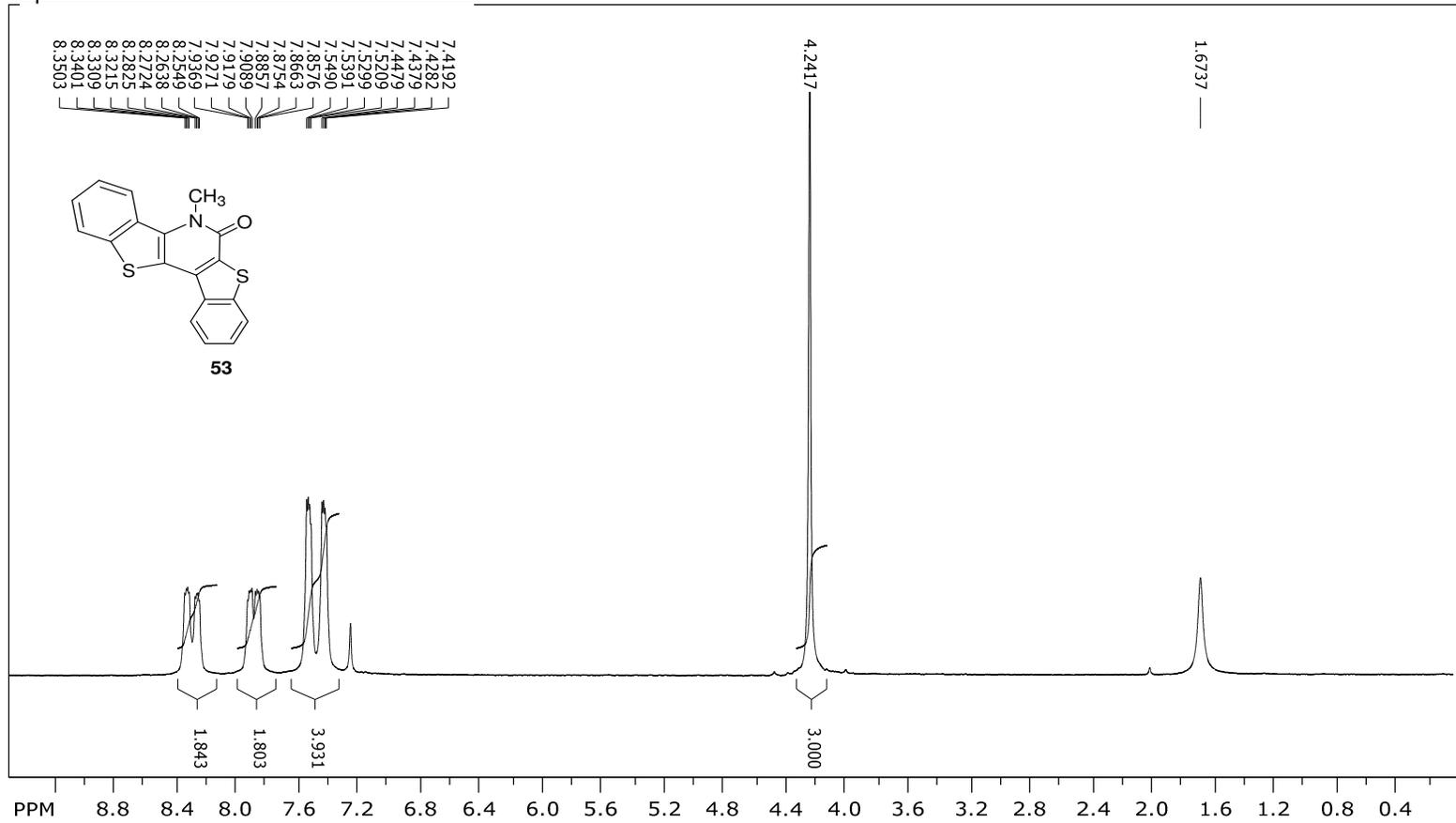
SpinWorks 3: 13C OBSERVE



file: ...as comp\dithioSM-C13-Oct22.fid\fid_block#1_expt:"s2pul"
 transmitter freq.: 75.476336 MHz
 time domain size: 68492 points
 width: 18867.92 Hz = 249.9846 ppm = 0.275476 Hz/pt
 number of scans: 576

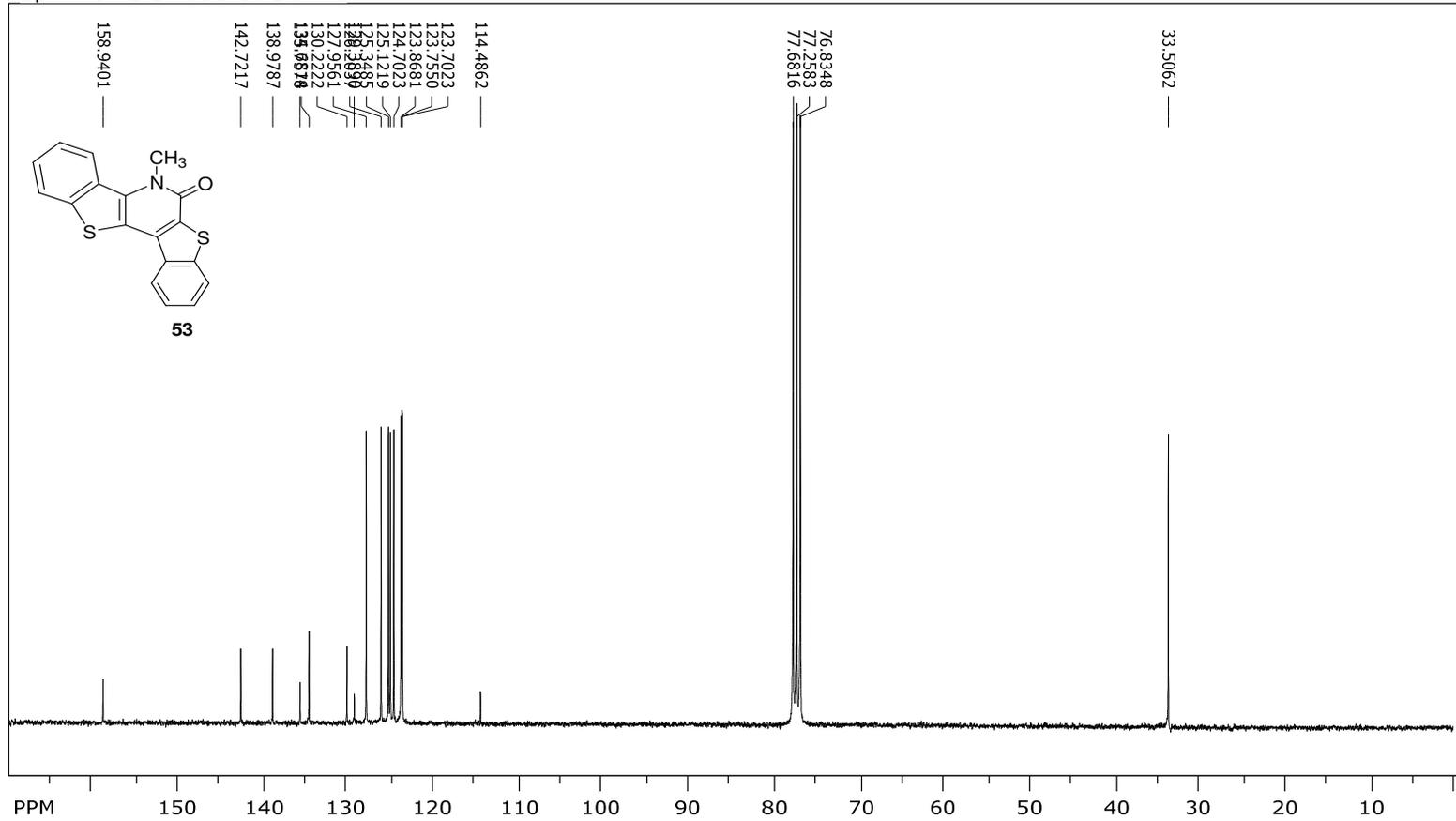
freq. of 0 ppm: 75.468034 MHz
 processed size: 131072 complex points
 LB: 1.000 GF: 0.0000
 Hz/cm: 544.414 ppm/cm: 7.21304

SpinWorks 3: STANDARD 1H OBSERVE



file: ...\\tas comp\dithioprod-Oct20.tid\fid_block# 1 expt: "s2pul"
 transmitter freq.: 300.133009 MHz
 time domain size: 19192 points
 width: 4803.07 Hz = 16.0032 ppm = 0.250264 Hz/pt
 number of scans: 8

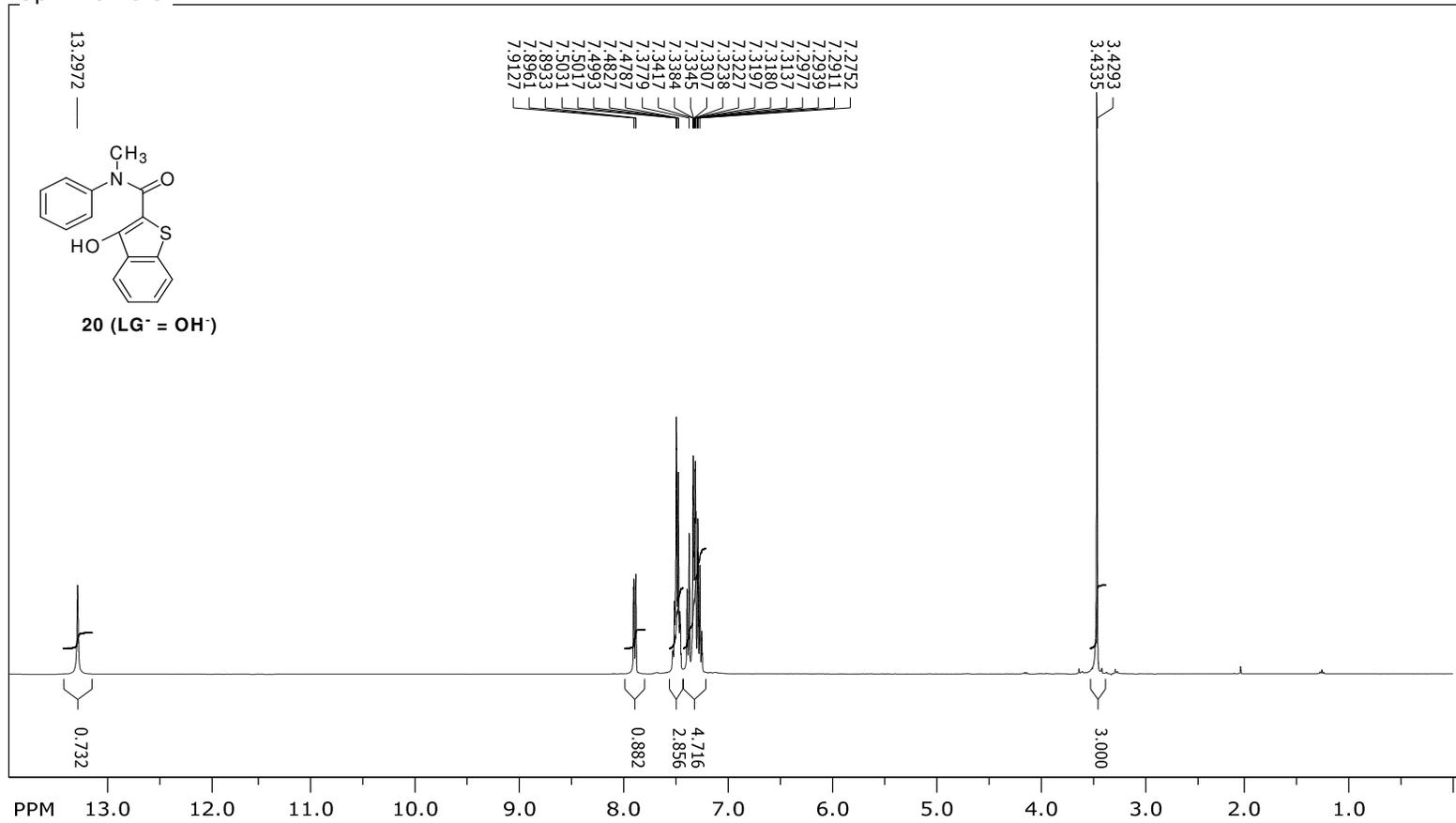
freq. of 0 ppm: 300.131208 MHz
 processed size: 32768 complex points
 LB: 1.500 GF: 0.0000
 Hz/cm: 113.979 ppm/cm: 0.37976

SpinWorks 3: ¹³C OBSERVE

file: ... comp\dithioprod-C13-Oct21.fid\fid_block# 1 expt: "szpul"
 transmitter freq.: 75.476336 MHz
 time domain size: 68492 points
 width: 18867.92 Hz = 249.9846 ppm = 0.275476 Hz/pt
 number of scans: 18000

freq. of 0 ppm: 75.468034 MHz
 processed size: 131072 complex points
 LB: 1.000 GF: 0.0000
 Hz/cm: 513.321 ppm/cm: 6.80108

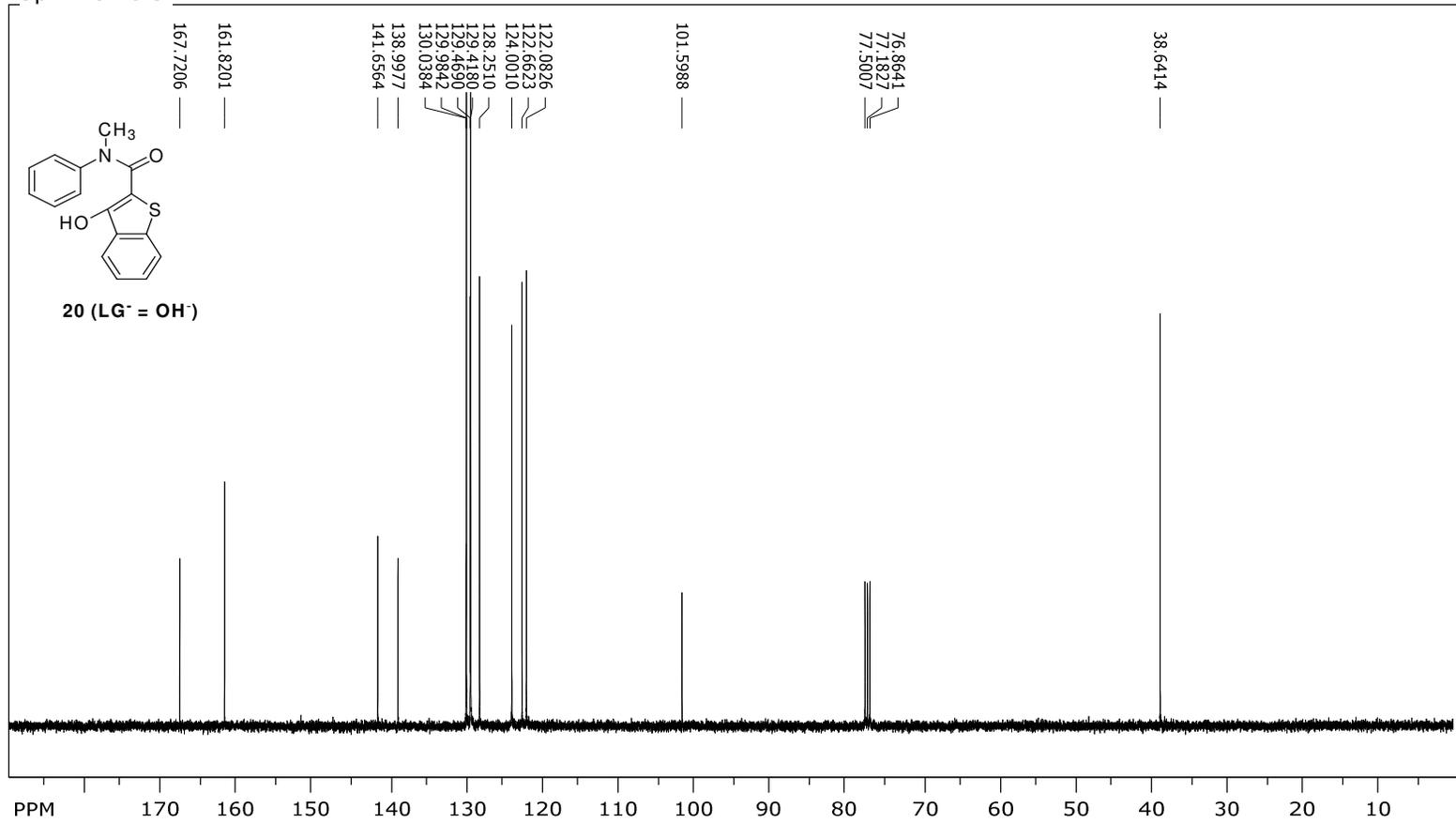
SpinWorks 3:



file: ...e LG-OH\OHLGarterrecrystal.fid\fid_block# 1_expt: "s2pul"
 transmitter freq.: 399.745875 MHz
 time domain size: 26264 points
 width: 6410.26 Hz = 16.0358 ppm = 0.244070 Hz/pt
 number of scans: 8

freq. of 0 ppm: 399.743477 MHz
 processed size: 65536 complex points
 LB: 0.000 GF: 0.0000
 Hz/cm: 223.375 ppm/cm: 0.55879

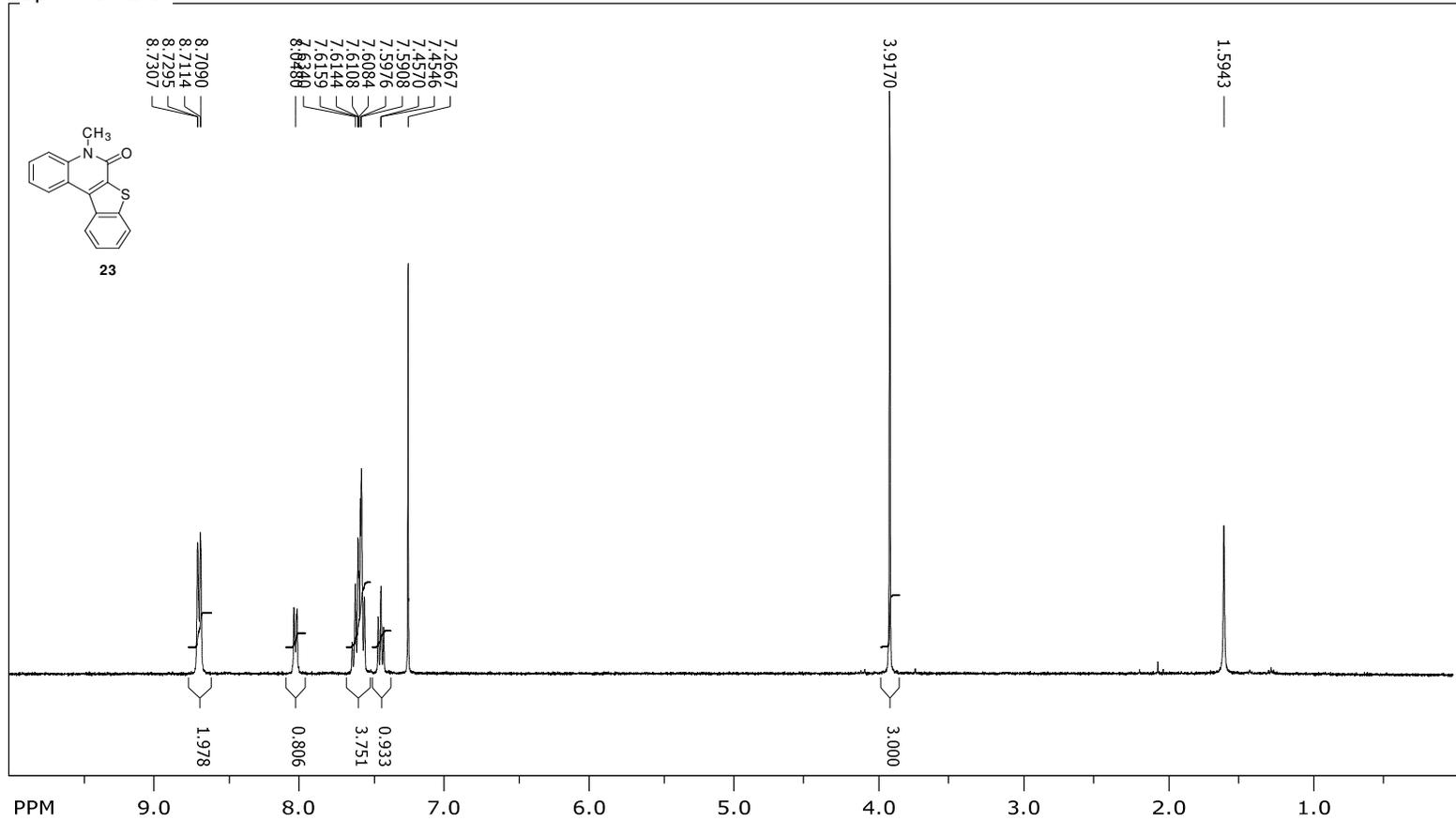
SpinWorks 3:



file: ...G-OH\OHLGC13afterrecrystal.fid\fid_block# 1 expt: "s2pul"
 transmitter freq.: 100.526131 MHz
 time domain size: 63750 points
 width: 24509.80 Hz = 243.8153 ppm = 0.384468 Hz/pt
 number of scans: 256

freq. of 0 ppm: 100.515577 MHz
 processed size: 65536 complex points
 LB: 0.500 GF: 0.0000
 Hz/cm: 764.486 ppm/cm: 7.60484

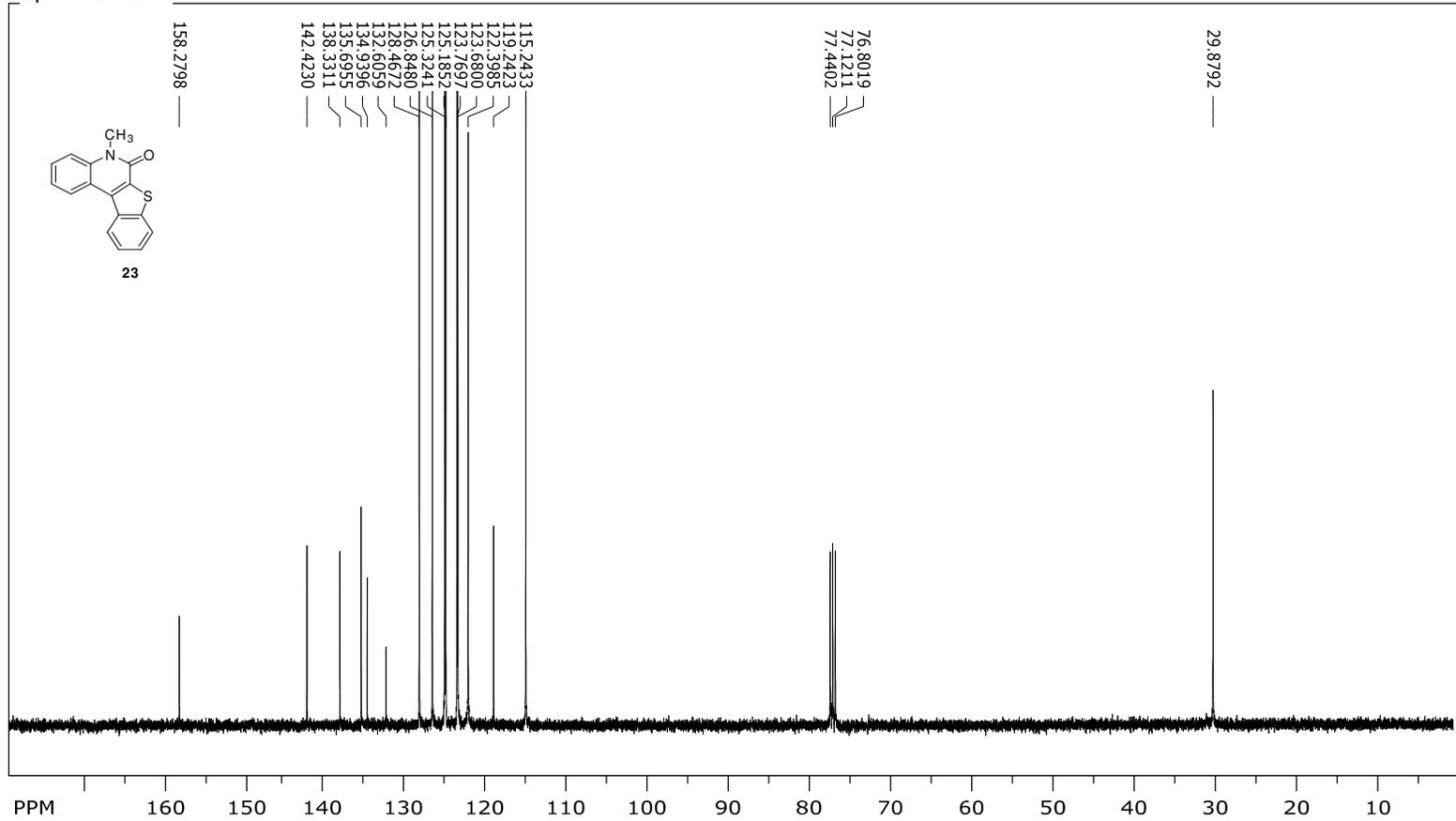
SpinWorks 3:



file: ...Aniline LG-Cl\hanovia30min.fid\fid_block# 1 expt: "s2pul"
 transmitter freq.: 399.745875 MHz
 time domain size: 26264 points
 width: 6410.26 Hz = 16.0358 ppm = 0.244070 Hz/pt
 number of scans: 8

freq. of 0 ppm: 399.743477 MHz
 processed size: 65536 complex points
 LB: 0.000 GF: 0.0000
 Hz/cm: 160.569 ppm/cm: 0.40168

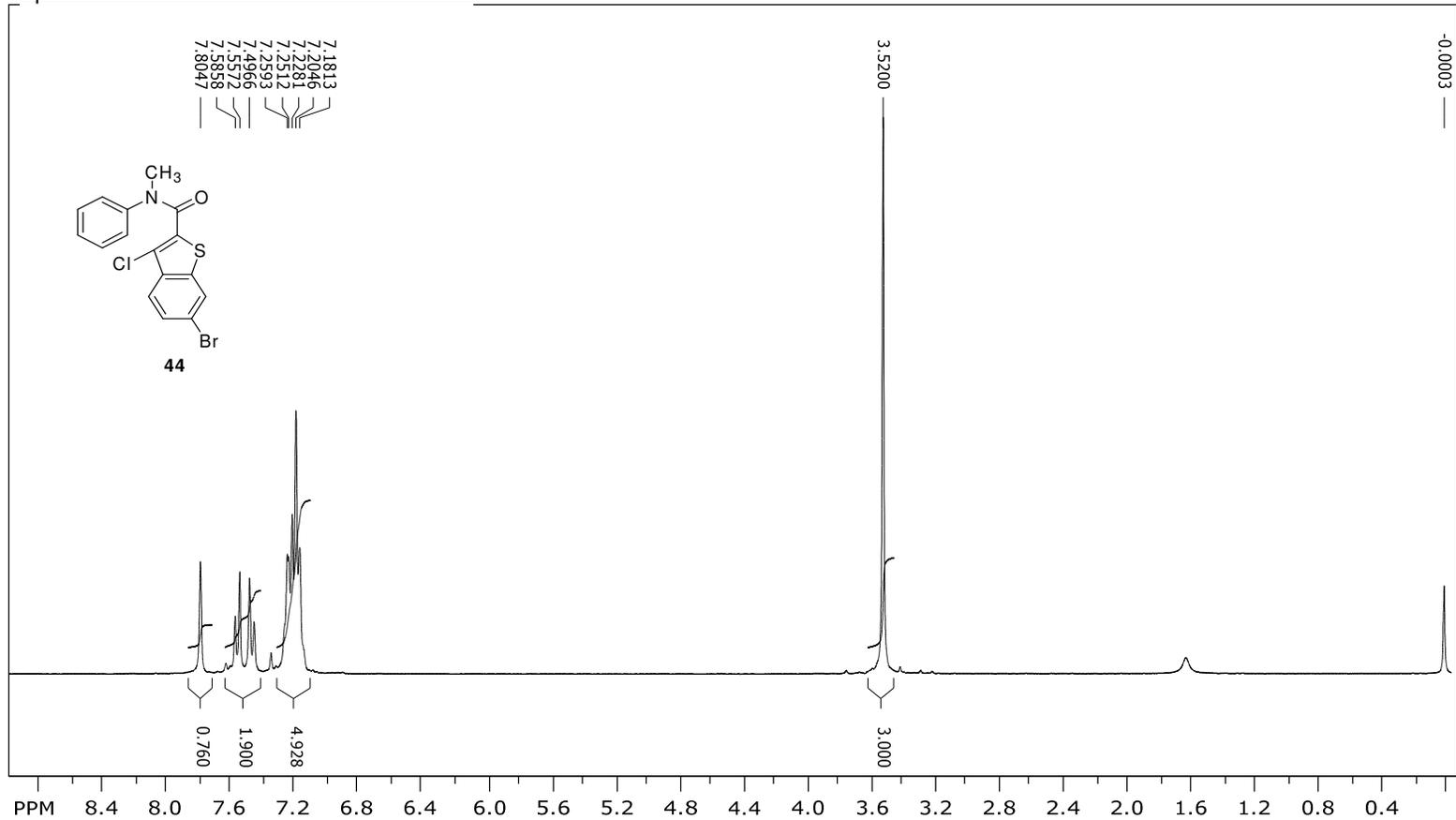
SpinWorks 3:



file: ...ne LG-Cl\cnmrphotocomppure.fid\fid_block# 1 expt: "s2pul"
 transmitter freq.: 100.526131 MHz
 time domain size: 63750 points
 width: 24509.80 Hz = 243.8153 ppm = 0.384468 Hz/pt
 number of scans: 800

freq. of 0 ppm: 100.515577 MHz
 processed size: 65536 complex points
 LB: 0.500 GF: 0.0000
 Hz/cm: 721.157 ppm/cm: 7.17383

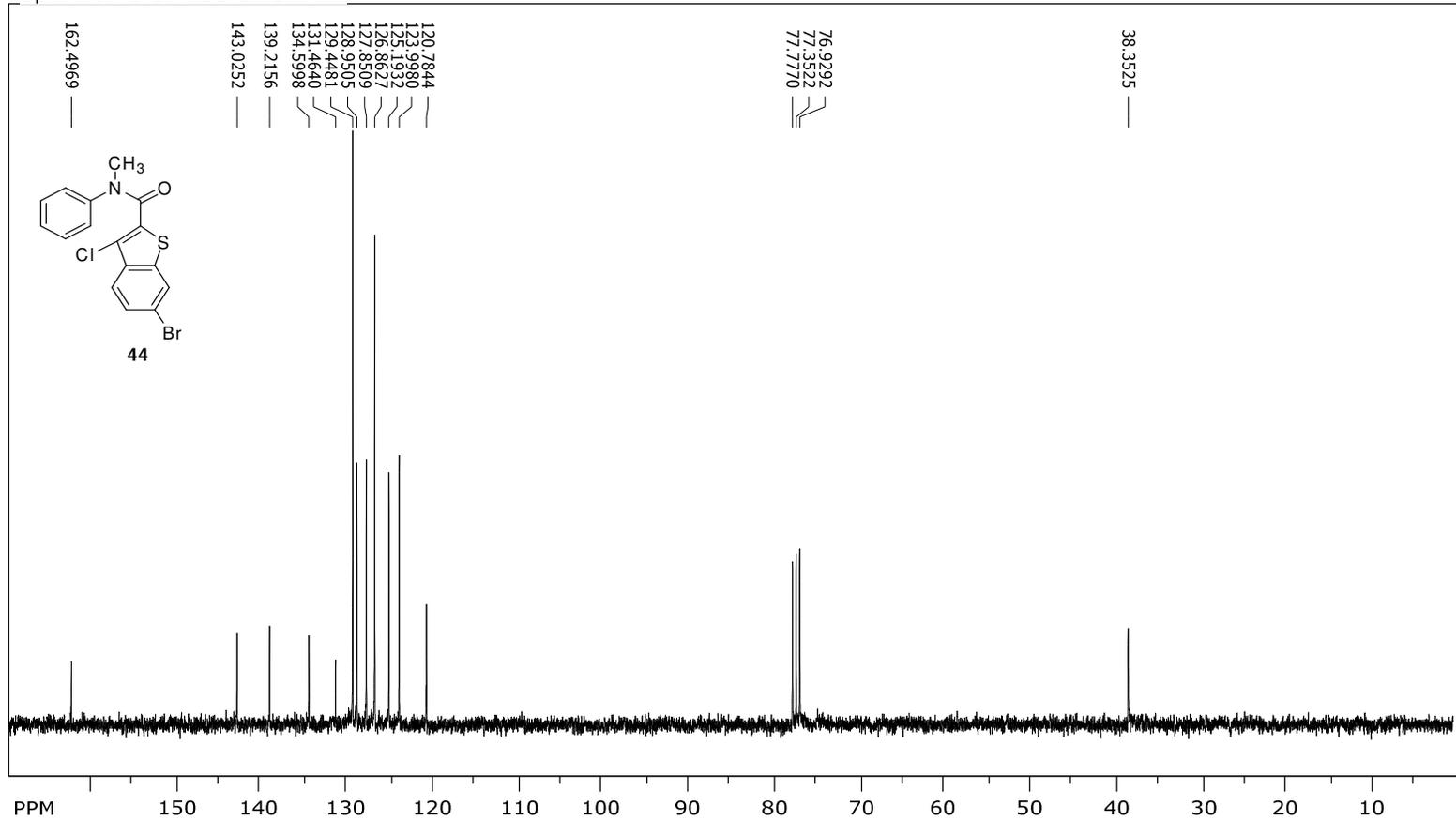
SpinWorks 3: STANDARD 1H OBSERVE



file: ...Ias comp\chotoSM-recrySep7.fid\fid_block# 1 expt: "s2pul"
 transmitter freq.: 300.133009 MHz
 time domain size: 19192 points
 width: 4803.07 Hz = 16.0032 ppm = 0.250264 Hz/pt
 number of scans: 8

freq. of 0 ppm: 300.131207 MHz
 processed size: 32768 complex points
 LB: 1.500 GF: 0.0000
 Hz/cm: 108.654 ppm/cm: 0.36202

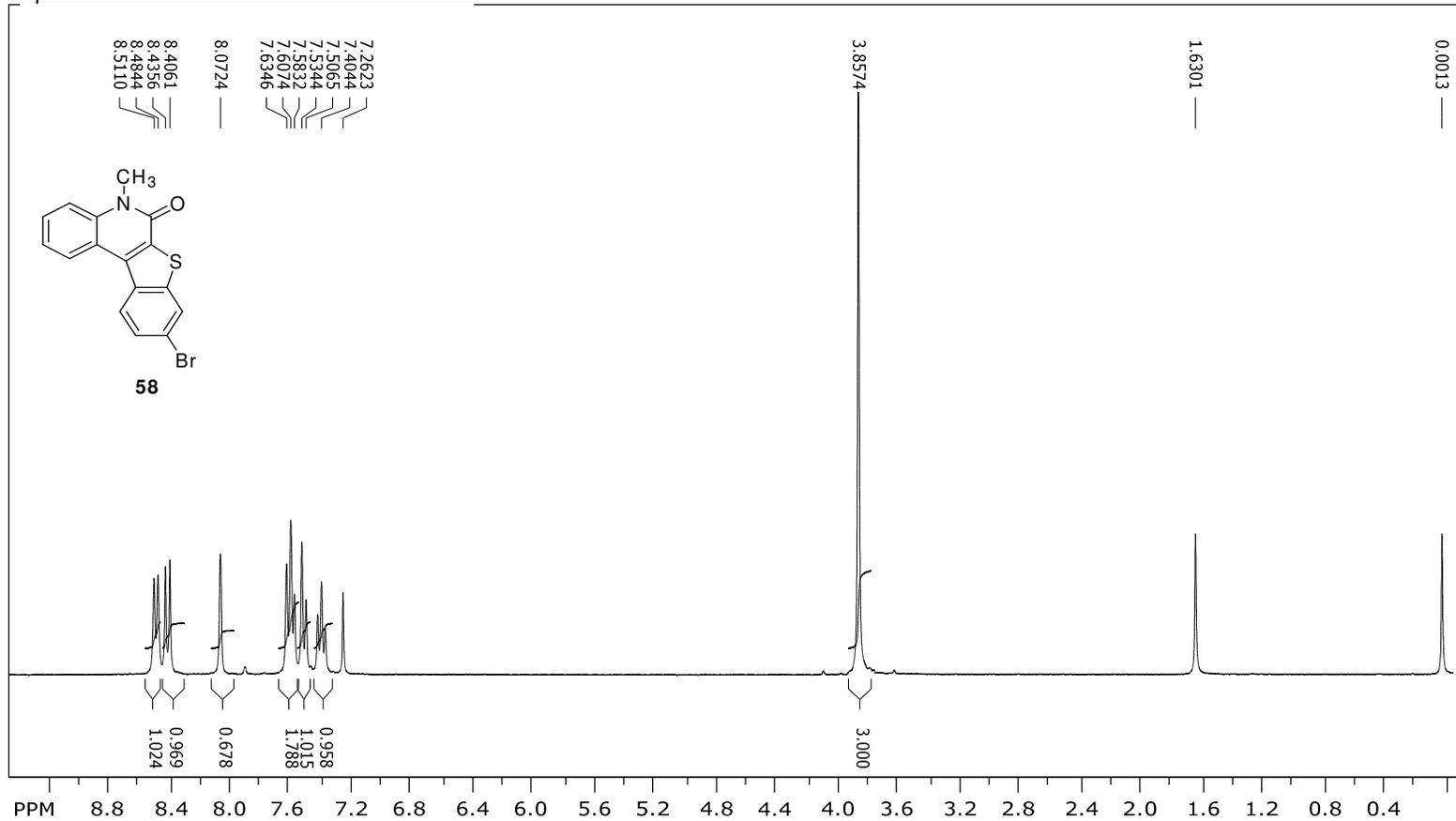
SpinWorks 3: 13C OBSERVE



file: ...eting\1as comp\chotoSM-C13.fid\fid_block# 1 exp: "s2pul"
 transmitter freq.: 75.476336 MHz
 time domain size: 68492 points
 width: 18867.92 Hz = 249.9846 ppm = 0.275476 Hz/pt
 number of scans: 64

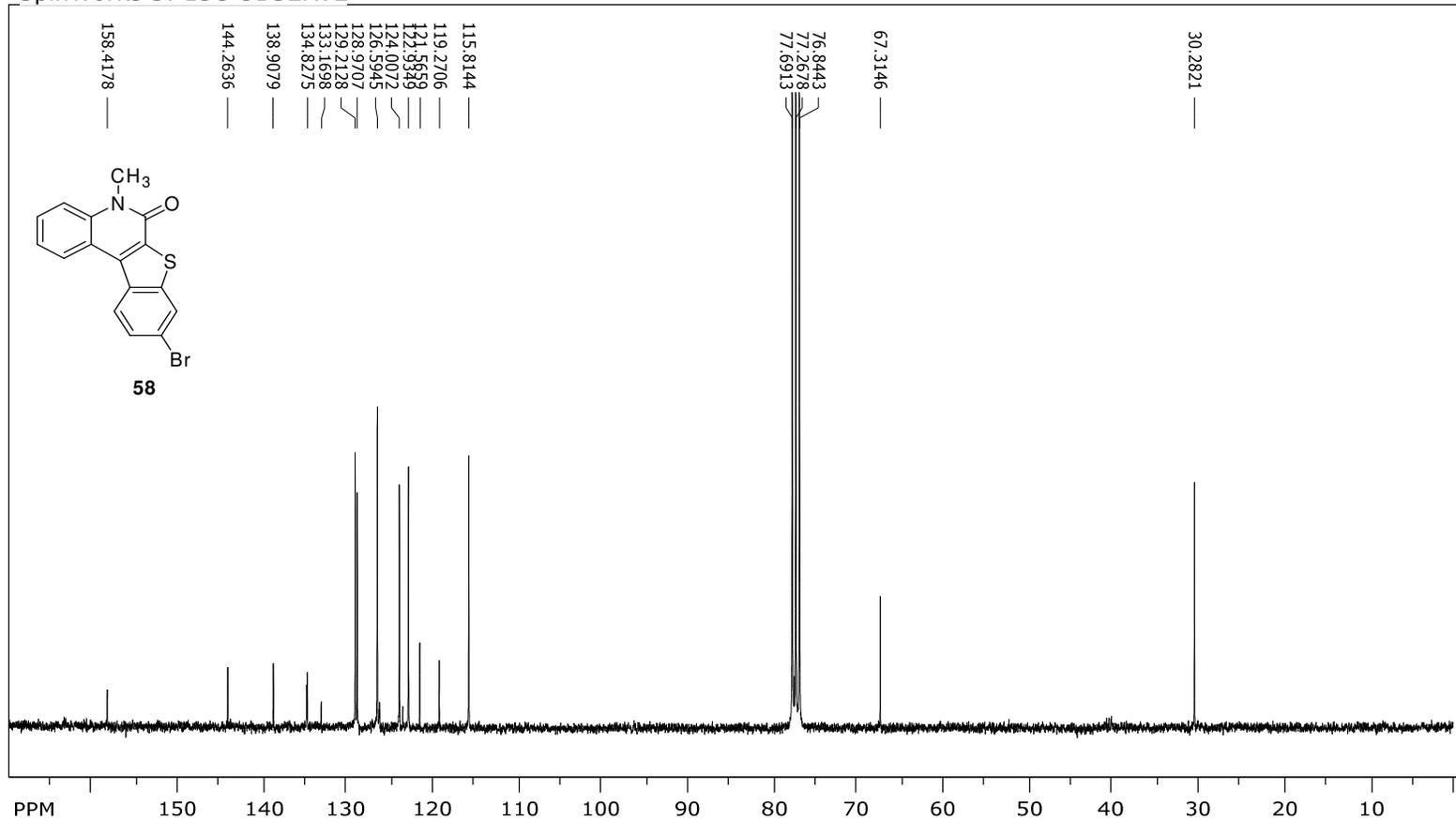
freq. of 0 ppm: 75.468034 MHz
 processed size: 131072 complex points
 LB: 1.000 GF: 0.0000
 Hz/cm: 512.190 ppm/cm: 6.78610

SpinWorks 3: STANDARD 1H OBSERVE



file: ... comp\chotoprod-recry-C6H6.fid\fid_block# 1 expt: "s2pur"
 transmitter freq.: 300.133009 MHz
 time domain size: 19192 points
 width: 4803.07 Hz = 16.0032 ppm = 0.250264 Hz/pt
 number of scans: 8

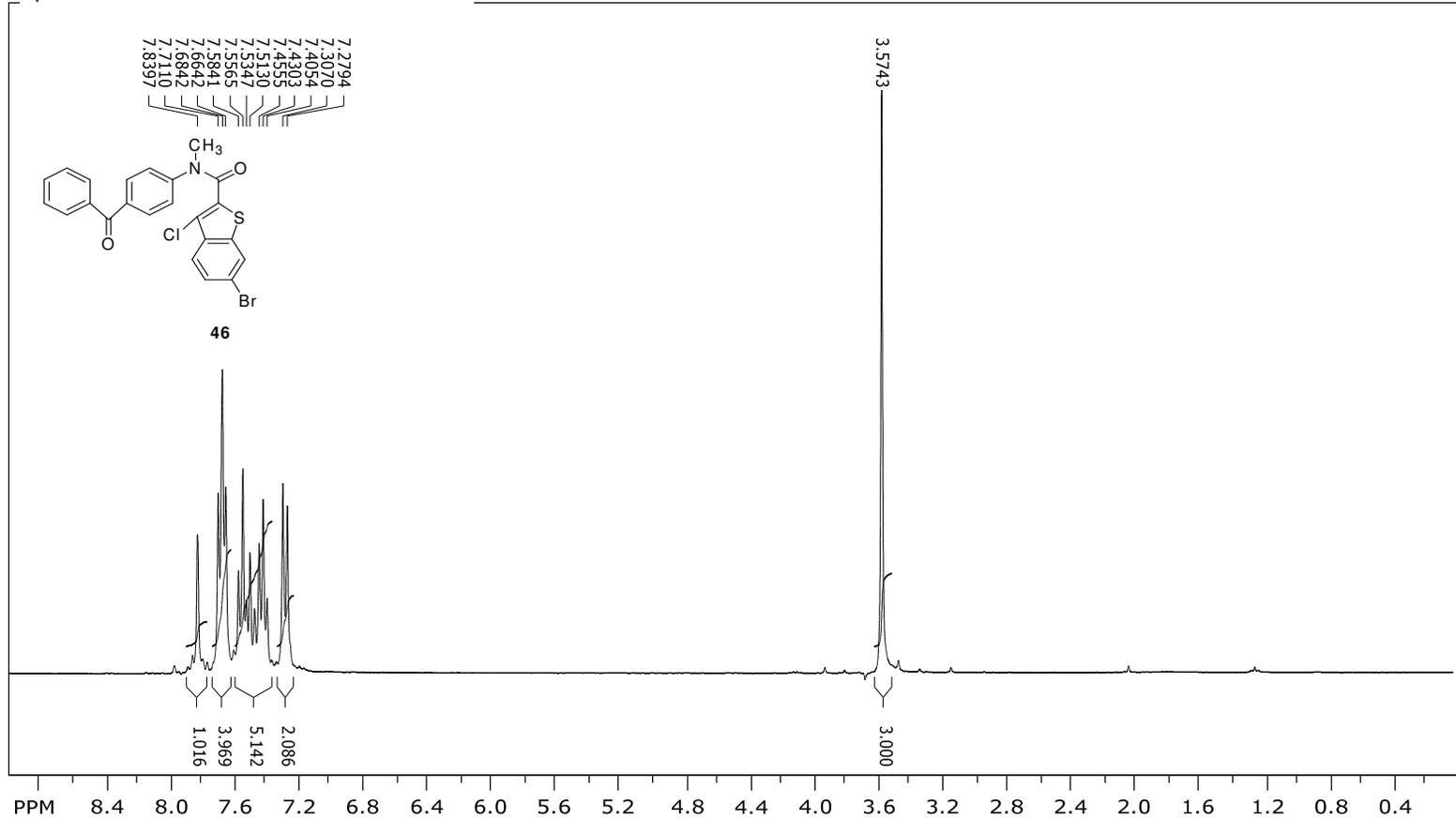
freq. of 0 ppm: 300.131208 MHz
 processed size: 32768 complex points
 LB: 1.500 GF: 0.0000
 Hz/cm: 114.554 ppm/cm: 0.38168

SpinWorks 3: ¹³C OBSERVE

file: ...s comp\chotoprod-C13-sep16.fid\fid_block# 1 exp: "s2pul"
 transmitter freq.: 75.476336 MHz
 time domain size: 68492 points
 width: 18867.92 Hz = 249.9846 ppm = 0.275476 Hz/pt
 number of scans: 16000

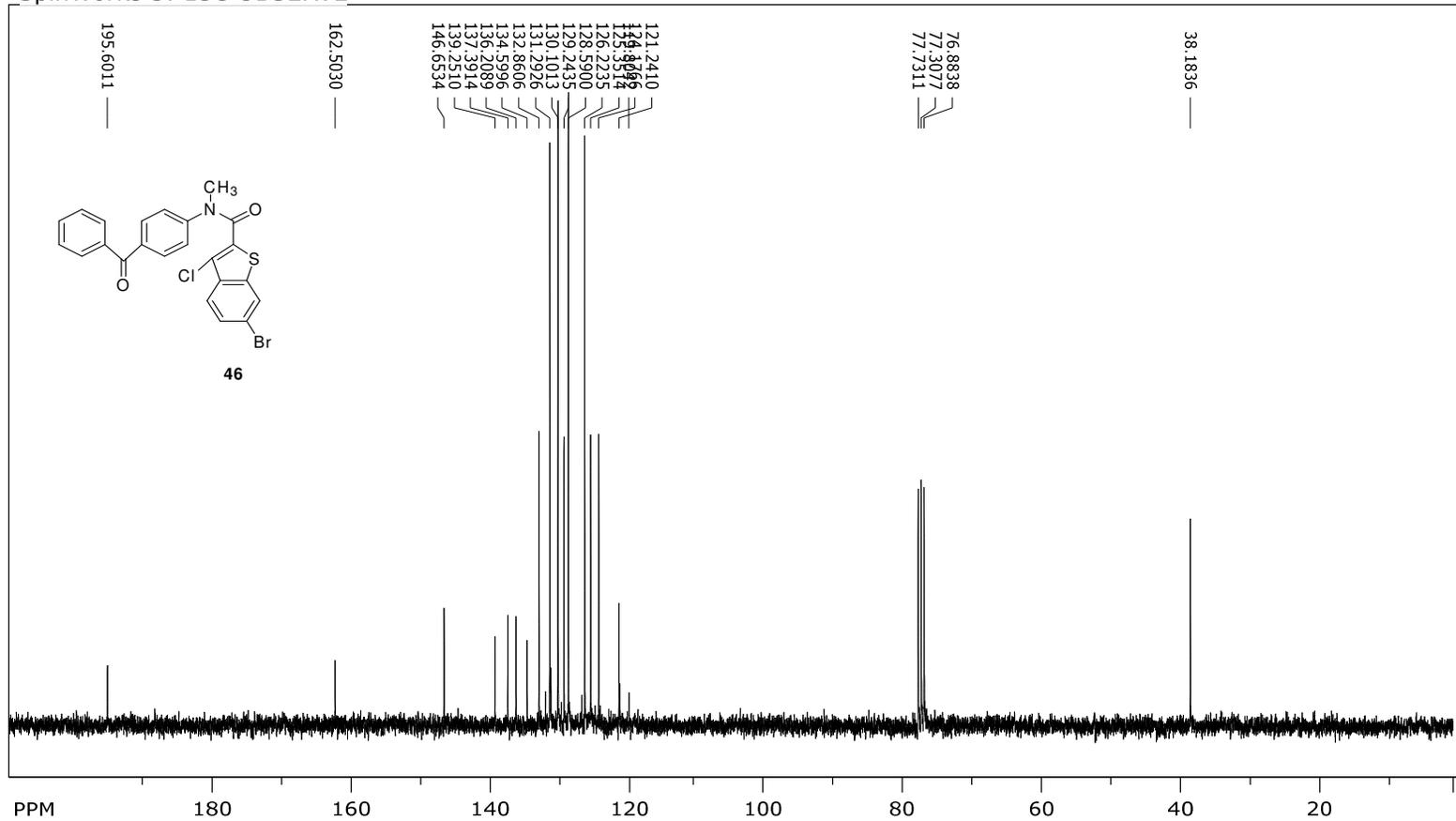
freq. of 0 ppm: 75.468034 MHz
 processed size: 131072 complex points
 LB: 1.000 GF: 0.0000
 Hz/cm: 513.886 ppm/cm: 6.80857

SpinWorks 3: STANDARD 1H OBSERVE



file: ...\\tas comp\amarborosM-Oct20.fid\fid_block# 1 exp: "s2pur"
 transmitter freq.: 300.133009 MHz
 time domain size: 19192 points
 width: 4803.07 Hz = 16.0032 ppm = 0.250264 Hz/pt
 number of scans: 8

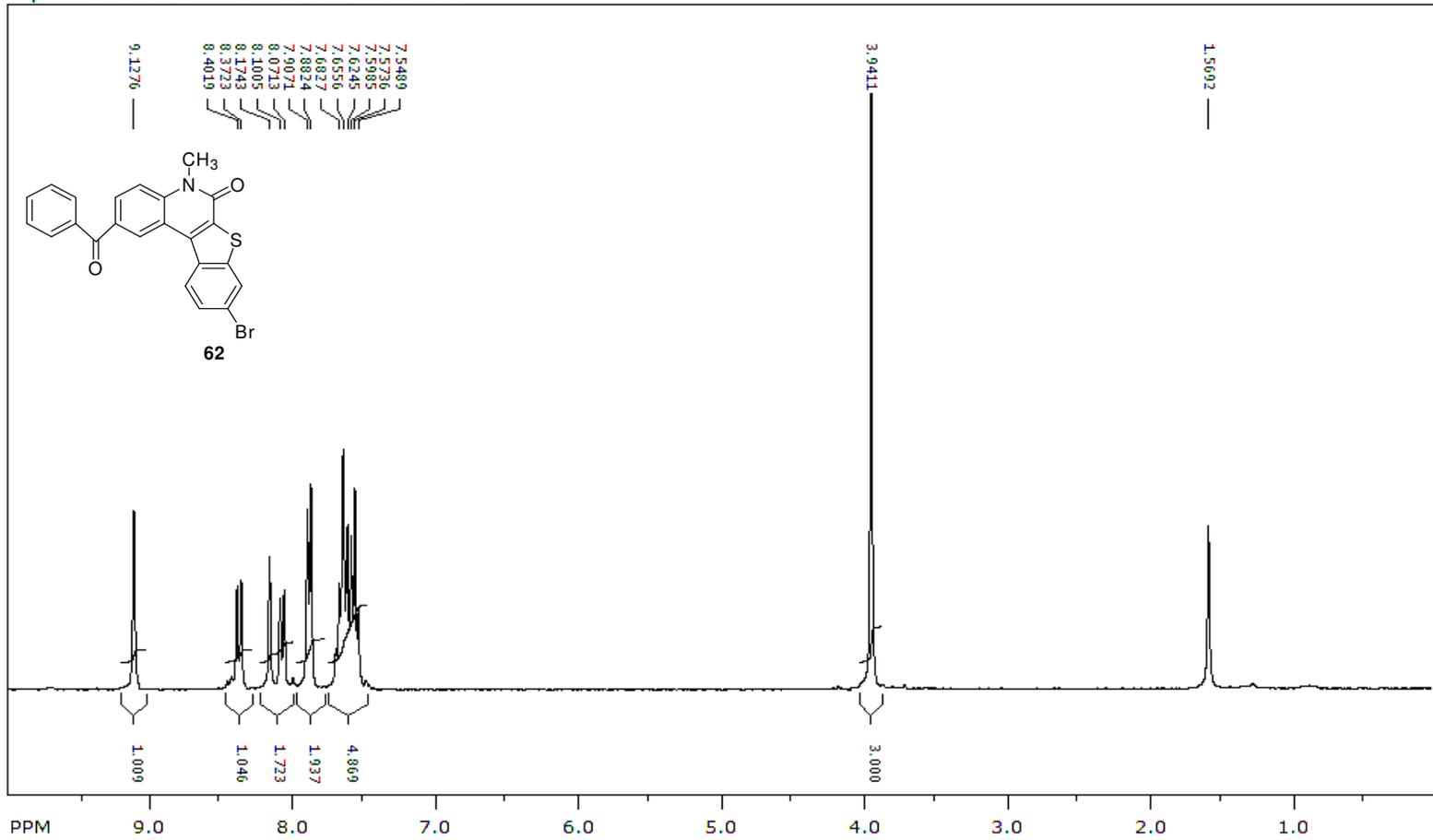
freq. of 0 ppm: 300.131208 MHz
 processed size: 32768 complex points
 LB: 1.500 GF: 0.0000
 Hz/cm: 108.078 ppm/cm: 0.36010

SpinWorks 3: ¹³C OBSERVE

file: ... comp\amarborosM-C13-Oct20.fid\fid_block# 1 expt: "s2pu1"
 transmitter freq.: 75.476336 MHz
 time domain size: 68492 points
 width: 18867.92 Hz = 249.9846 ppm = 0.275476 Hz/pt
 number of scans: 192

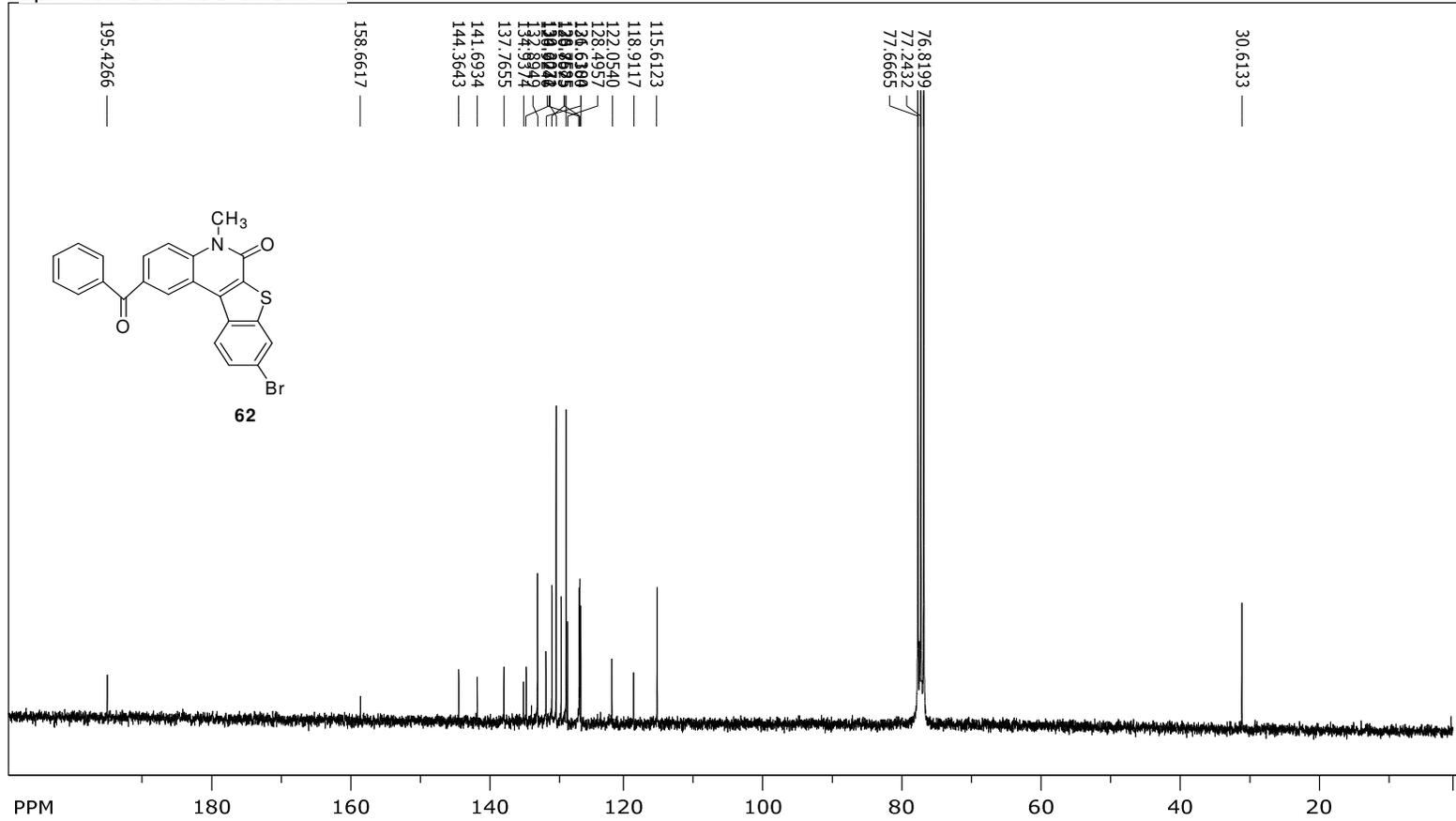
freq. of 0 ppm: 75.468034 MHz
 processed size: 131072 complex points
 LB: 1.000 GF: 0.0000
 Hz/cm: 633.736 ppm/cm: 8.39649

SpinWorks 3: STANDARD 1H OBSERVE



file: ...as comp\amarboroprod-Oct20.fid\fid_block= 1 expt: "s2pul"
 transmitter freq.: 300.133009 MHz
 time domain size: 19192 points
 width: 4803.07 Hz = 16.0032 ppm = 0.250264 Hz/pt
 number of scans: 8

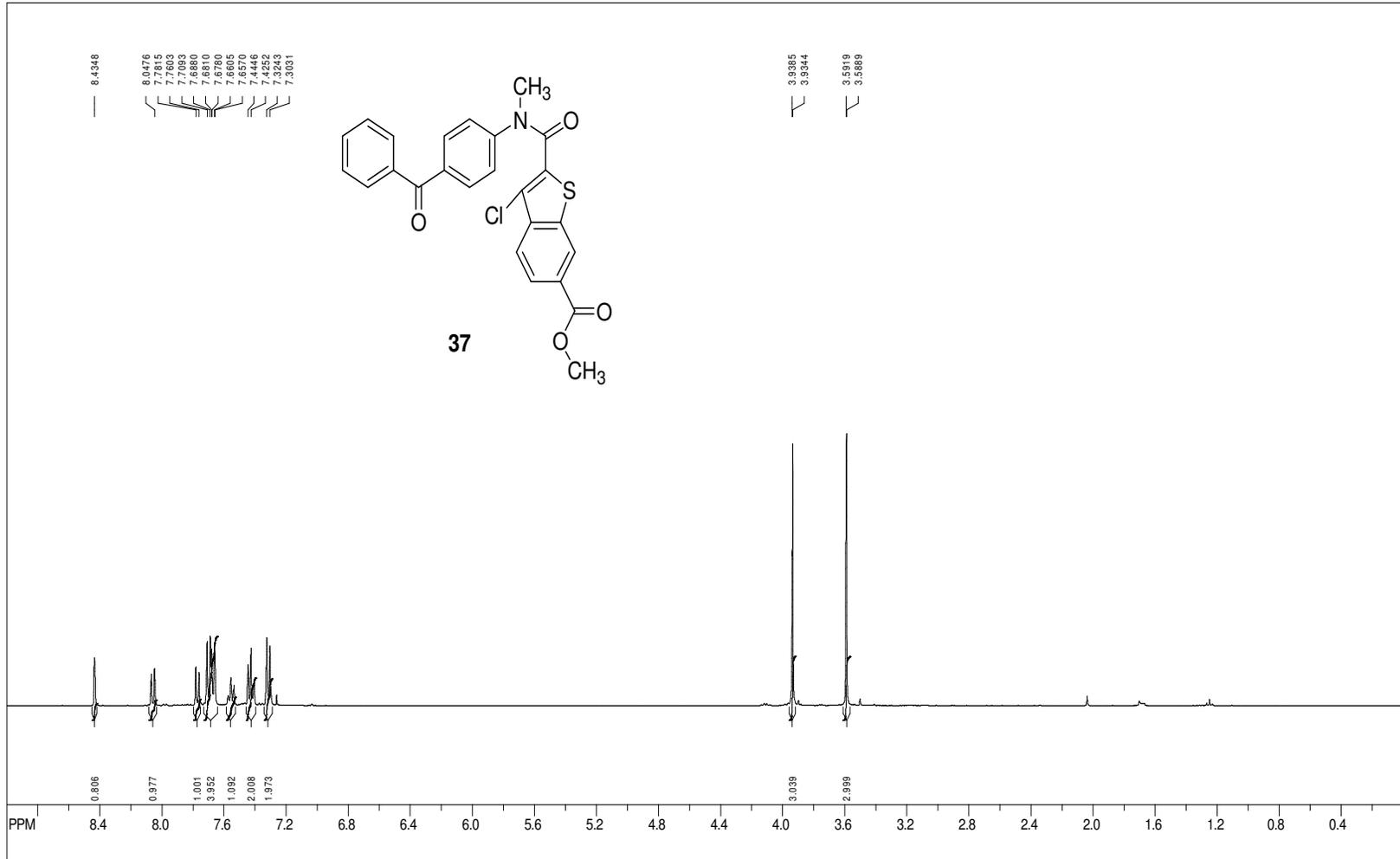
freq. of 0 ppm: 300.131208 MHz
 processed size: 32768 complex points
 LB: 1.500 GF: 0.0000
 Hz/cm: 120.311 ppm/cm: 0.40086

SpinWorks 3: ¹³C OBSERVE

file: ...omp\amarboroprod-C13-Oct20.fid\fid_block# 1 expt: "s2pur"
 transmitter freq.: 75.476336 MHz
 time domain size: 68492 points
 width: 18867.92 Hz = 249.9846 ppm = 0.275476 Hz/pt
 number of scans: 17000

freq. of 0 ppm: 75.468034 MHz
 processed size: 131072 complex points
 LB: 1.000 GF: 0.0000
 Hz/cm: 633.171 ppm/cm: 8.38900

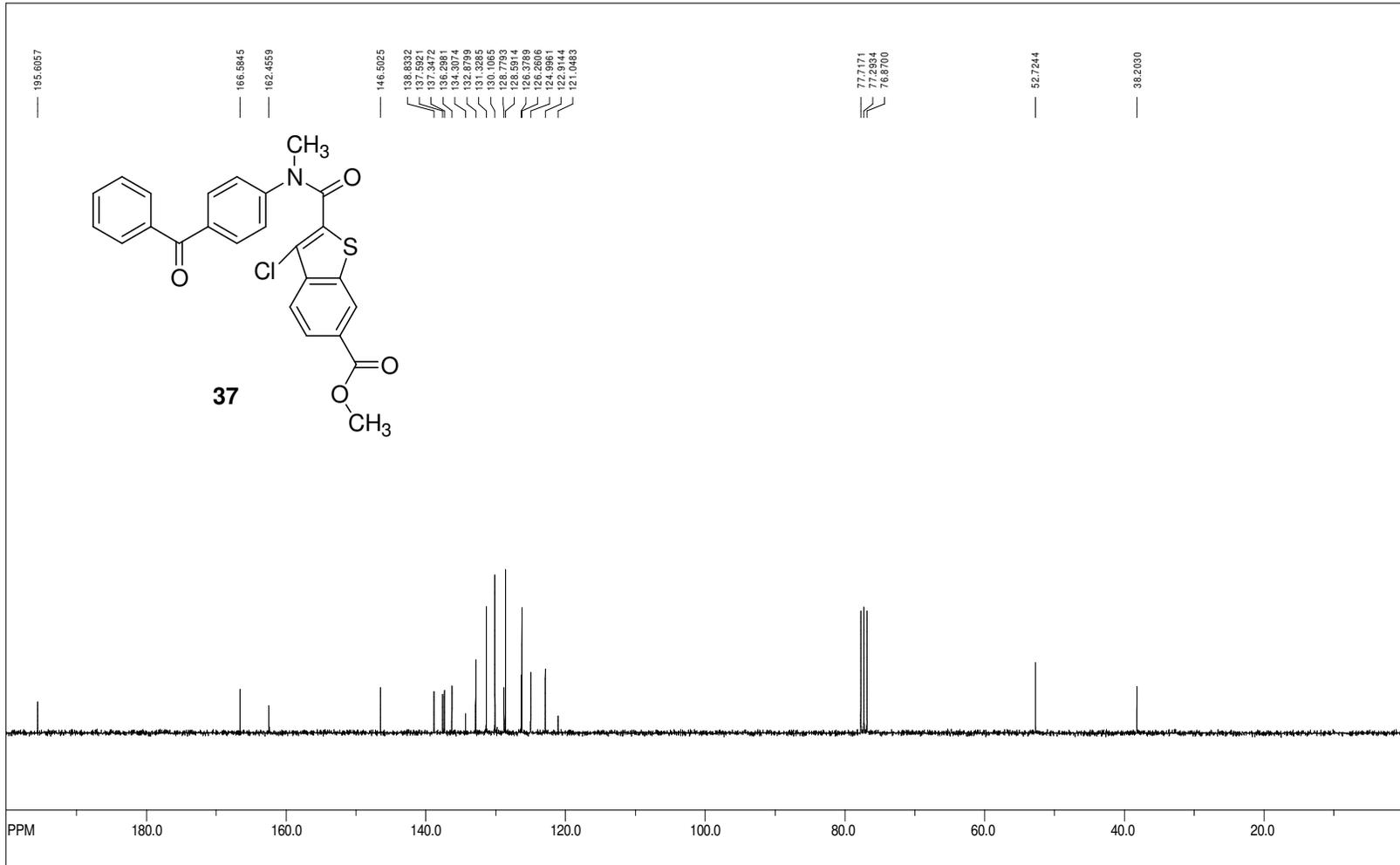
SpinWorks 2.5:



file: C:\Users\Paijore User\Desktop\Tasruva NMR\MGSIformylbenzacid-s4-ester-s4-ester-photoreactant-apr27.fid fid block# 1 exp: "s2pur"
 transmitter freq.: 399.745675 MHz
 time domain size: 26264 points
 width: 6410.26 Hz = 16.035829 ppm = 0.244070 Hz/pt
 number of scans: 8

freq. of 0 ppm: 399.743477 MHz
 processed size: 65536 complex points
 LB: 0.200 GB: 0.0000

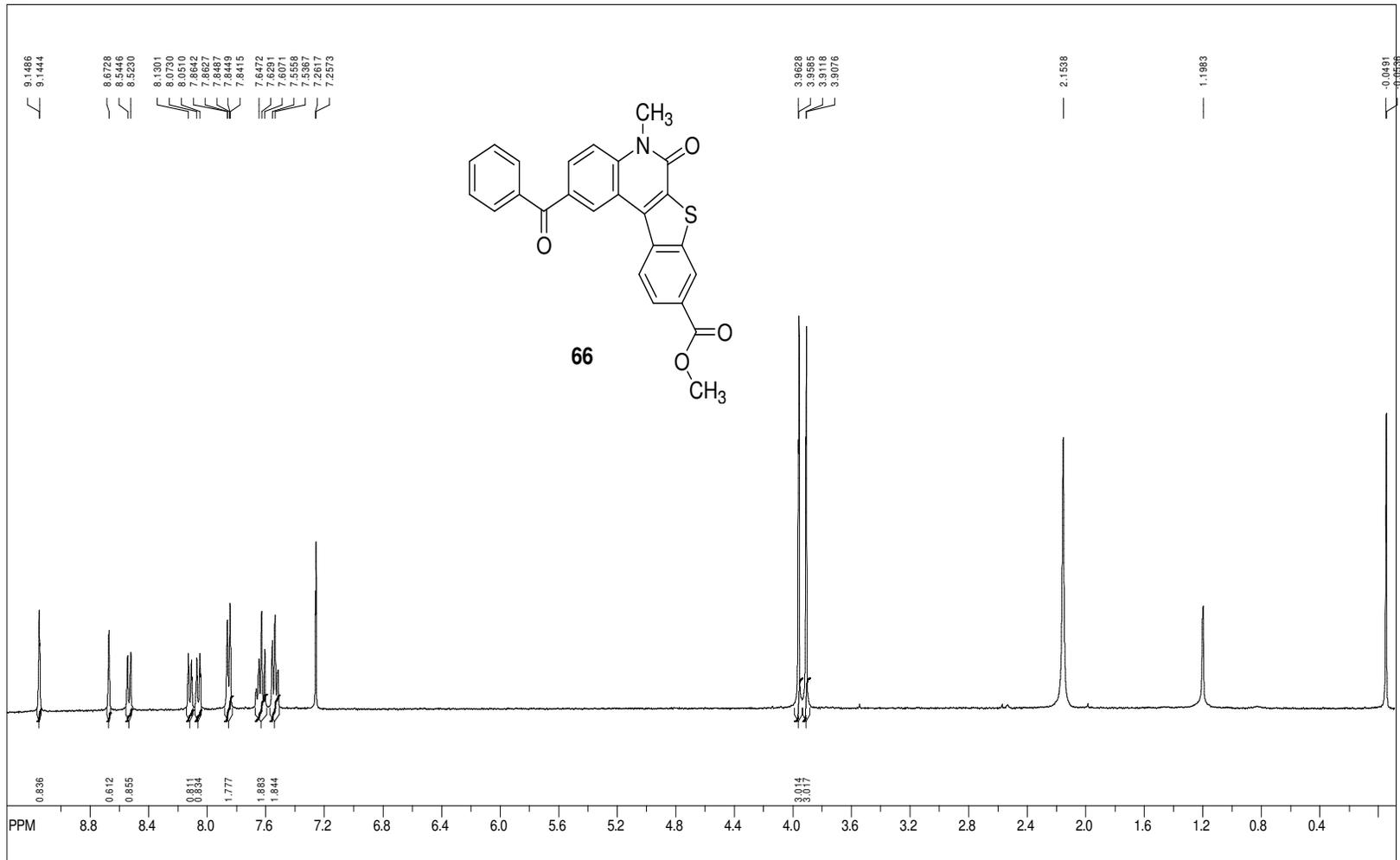
SpinWorks 2.5: 13C OBSERVE



file: C:\Users\Pathone User\Desktop\Tasnuva NMRs\MGS\lormylbenzacid\st4-ester\st4-ester-photoreactant-apr28-C13.fid fid block# 1 exp: "s2pul"
 transmitter freq.: 75.476336 MHz
 time domain size: 68492 points
 width: 18867.92 Hz = 249.984639 ppm = 0.275476 Hz/pt
 number of scans: 768

freq. of 0 ppm: 75.468034 MHz
 processed size: 131072 complex points
 LB: 0.200 GB: 0.0000

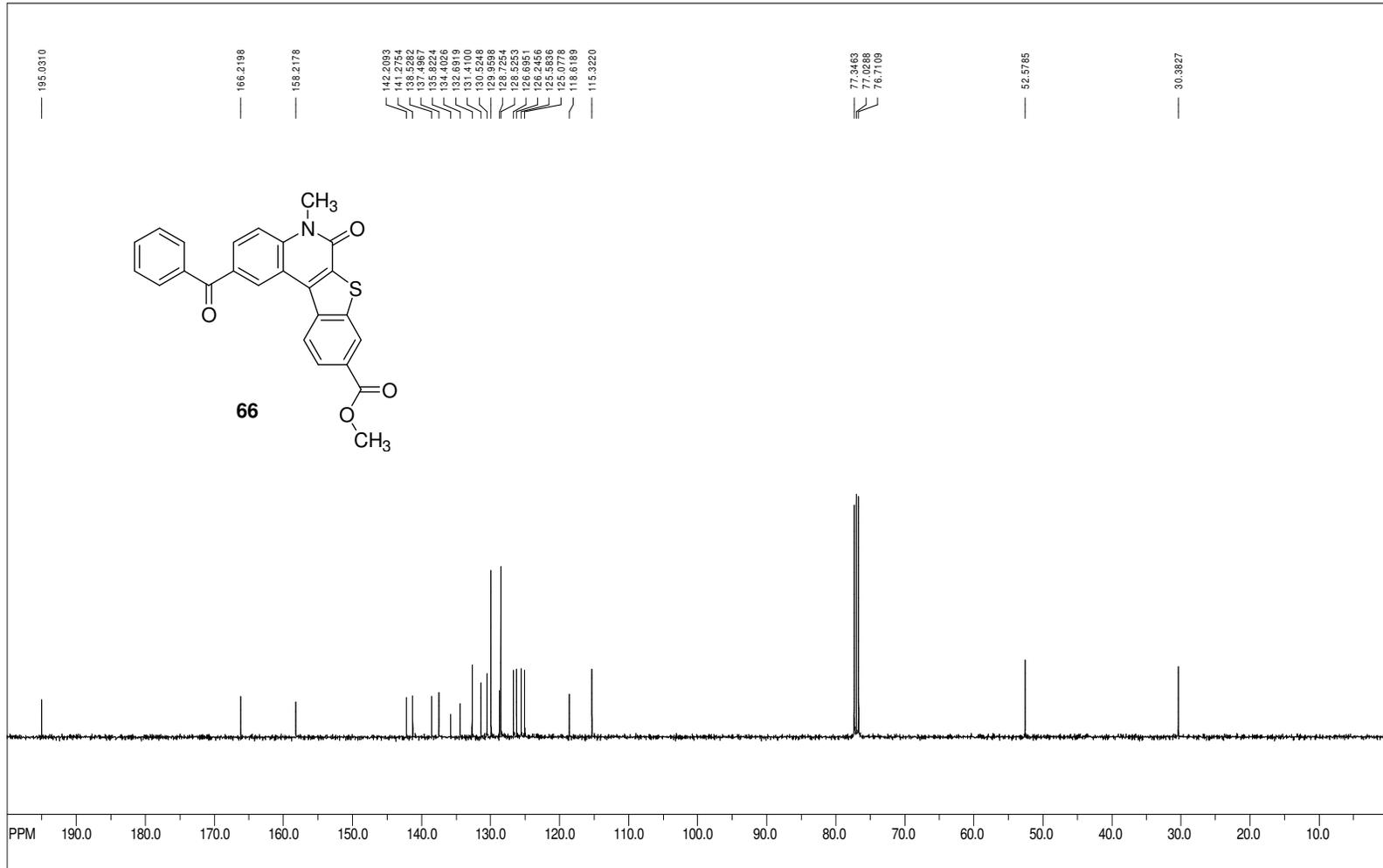
SpinWorks 2.5:



file: C:\Users\Pathore User\Desktop\Tasruva NMR\MCS\formylbenzacid-s4-ester\si4-ester-hanophprod-dec23-odd3.fid\fid_block# 1 exp: "s2pu"
 transmitter freq.: 399.745675 MHz
 time domain size: 28264 points
 width: 6410.26 Hz = 16.035829 ppm = 0.244070 Hz/pt
 number of scans: 8

freq. of 0 ppm: 399.745191 MHz
 processed size: 65536 complex points
 LB: 0.200 GB: 0.0000

SpinWorks 2.5:



File: C:\Users\Rathore User\Desktop\Tasruva NMR\6-MGS\Imp. NMR\6-MGS-ester-photprod-C13-may3.fid\fid_block#1.expt:"s2pu"

transmitter freq: 100.526131 MHz

time domain size: 63750 points

width: 24509.80 Hz = 243.815251 ppm = 0.384468 Hz/pt

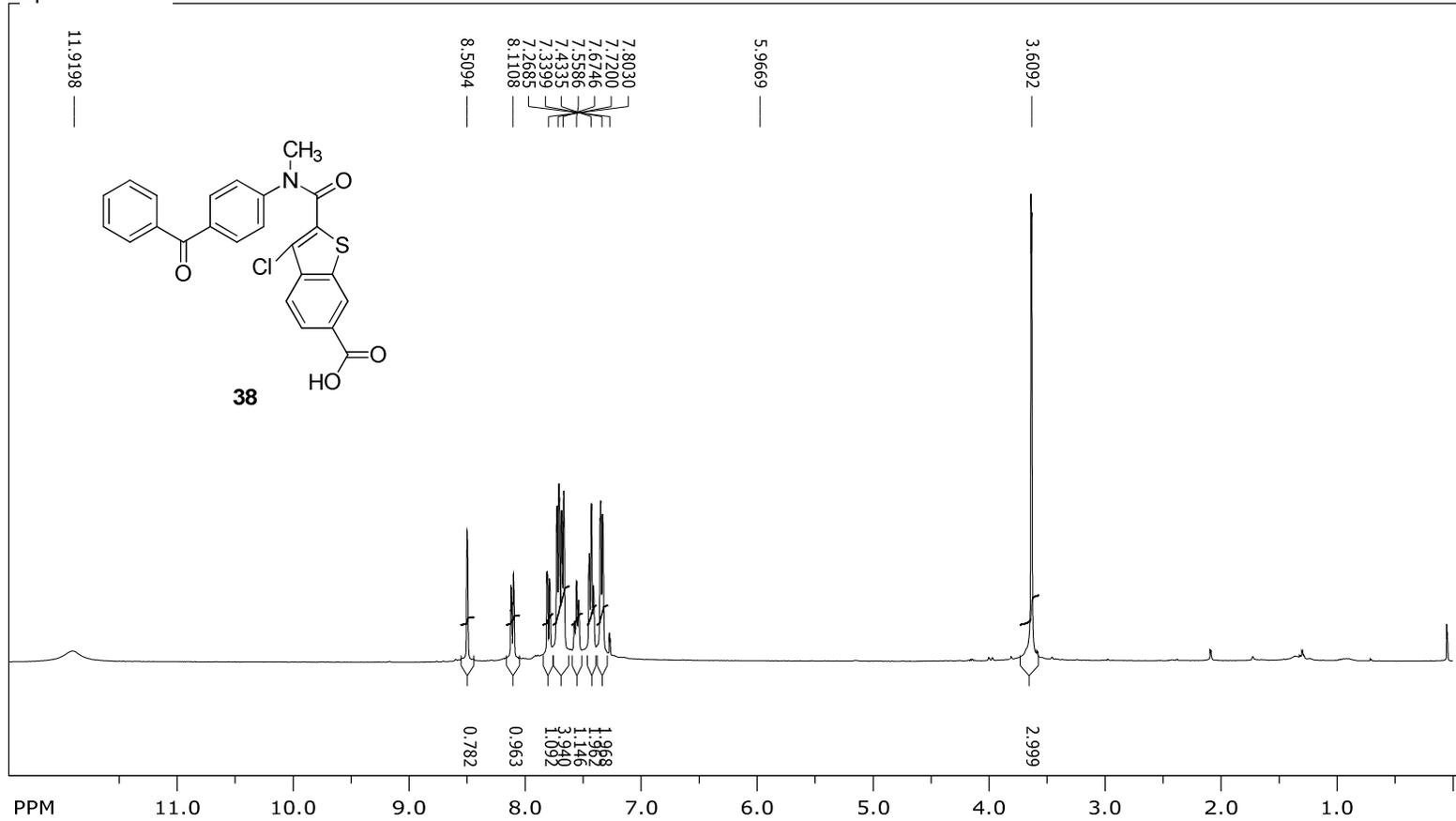
number of scans: 16000

freq of 0 ppm: 100.515577 MHz

processed size: 65536 complex points

LB: 0.200 GB: 0.0000

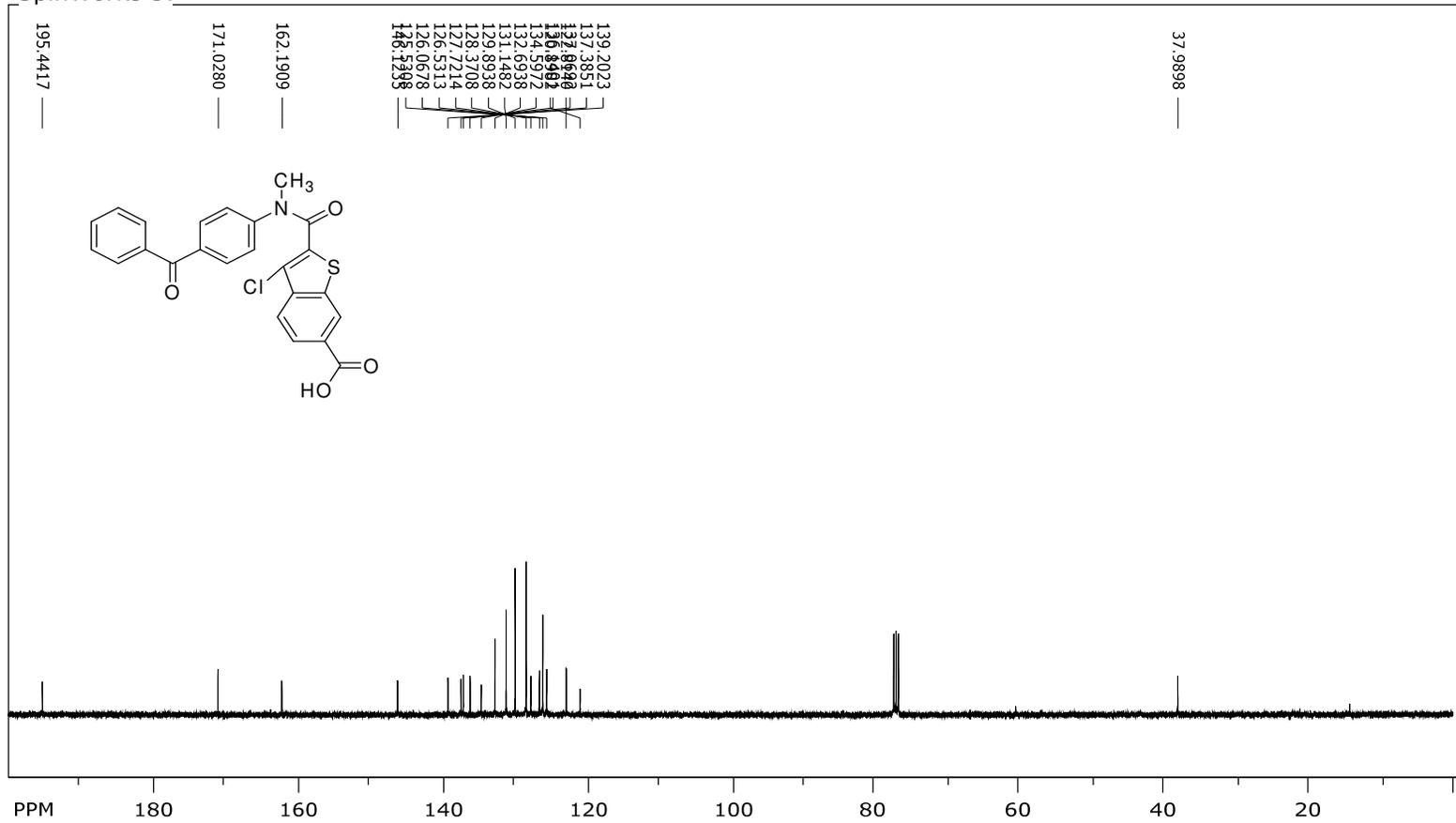
SpinWorks 3:



file: ...1\NMR5\st5-ester-col3-feb2.fid\fid_block# 1 expt: "s2pul"
 transmitter freq.: 399.745875 MHz
 time domain size: 26264 points
 width: 6410.26 Hz = 16.0358 ppm = 0.244070 Hz/pt
 number of scans: 8

freq. of 0 ppm: 399.743472 MHz
 processed size: 65536 complex points
 LB: 0.000 GF: 0.0000
 Hz/cm: 200.436 ppm/cm: 0.50141

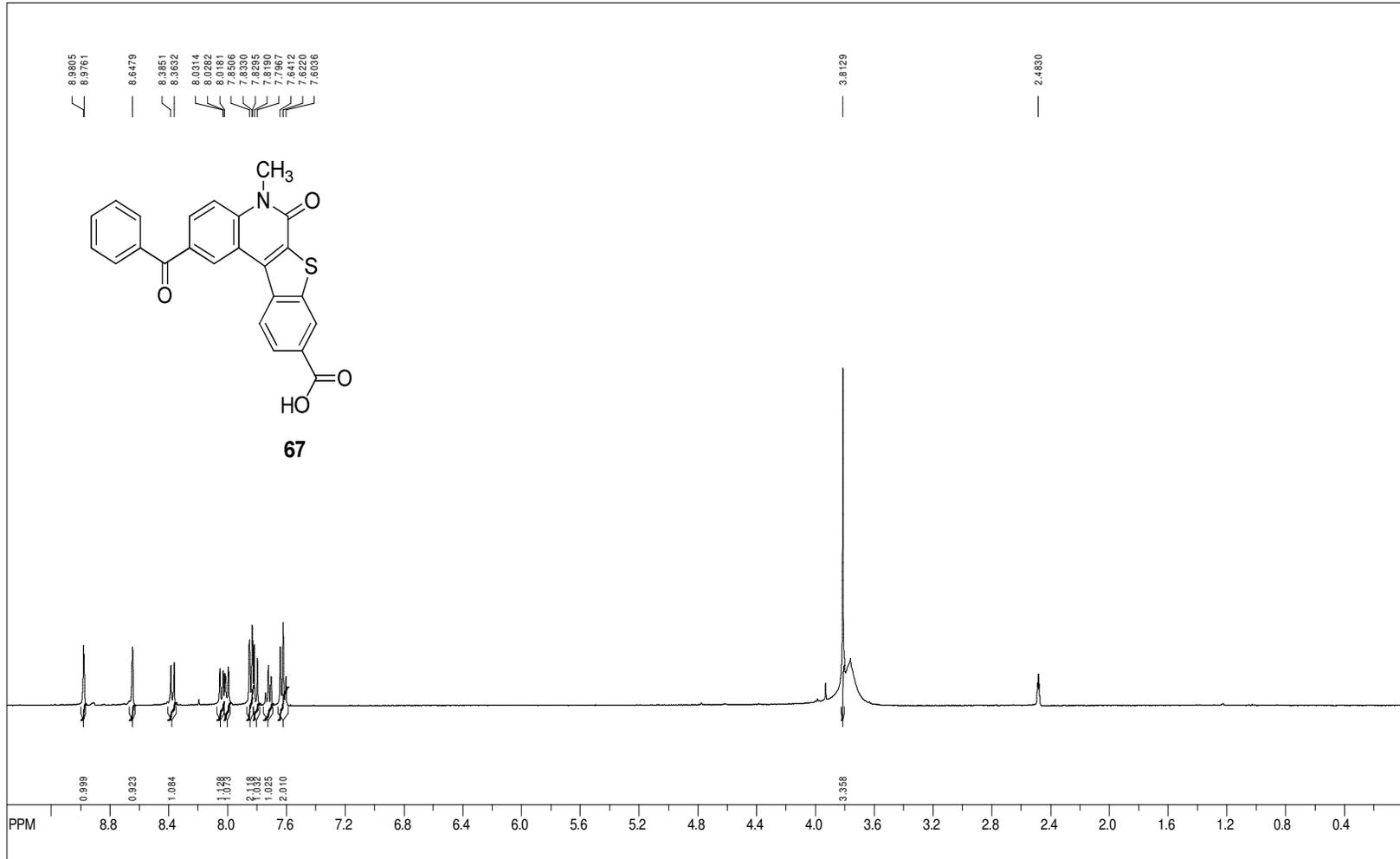
SpinWorks 3:



file: ...st5-ester-col3sol-feb1-c13.fid\fid_block# 1 expt: "szpul"
 transmitter freq.: 100.526131 MHz
 time domain size: 63750 points
 width: 24509.80 Hz = 243.8153 ppm = 0.384468 Hz/pt
 number of scans: 512

freq. of 0 ppm: 100.515577 MHz
 processed size: 65536 complex points
 LB: 0.000 GF: 0.0000
 Hz/cm: 804.929 ppm/cm: 8.00716

SpinWorks 2.5:



file: E:\Taruva NMR-MGS for mylbenzazidst5-ester-finalst5-ester-hanoprod90c-fet2.fid\fid block# 1 exp: "s2pu"

transmitter freq.: 399.747774 MHz

time domain size: 26264 points

width: 6410.26 Hz = 16.035753 ppm = 0.244070 Hz/pt

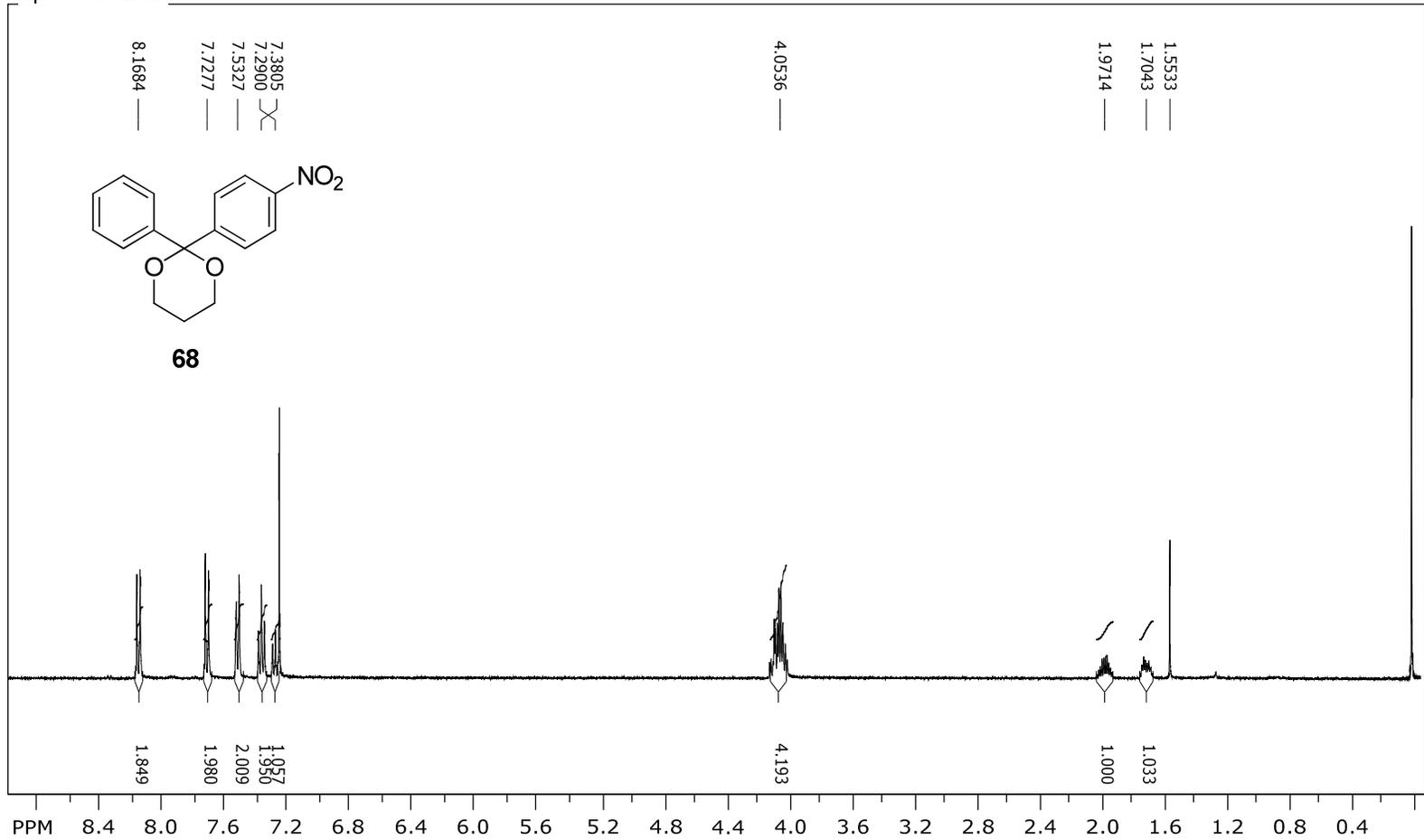
number of scans: 8

freq. of 0 ppm: 399.745375 MHz

processed size: 65536 complex points

LB: 0.200 GB: 0.0000

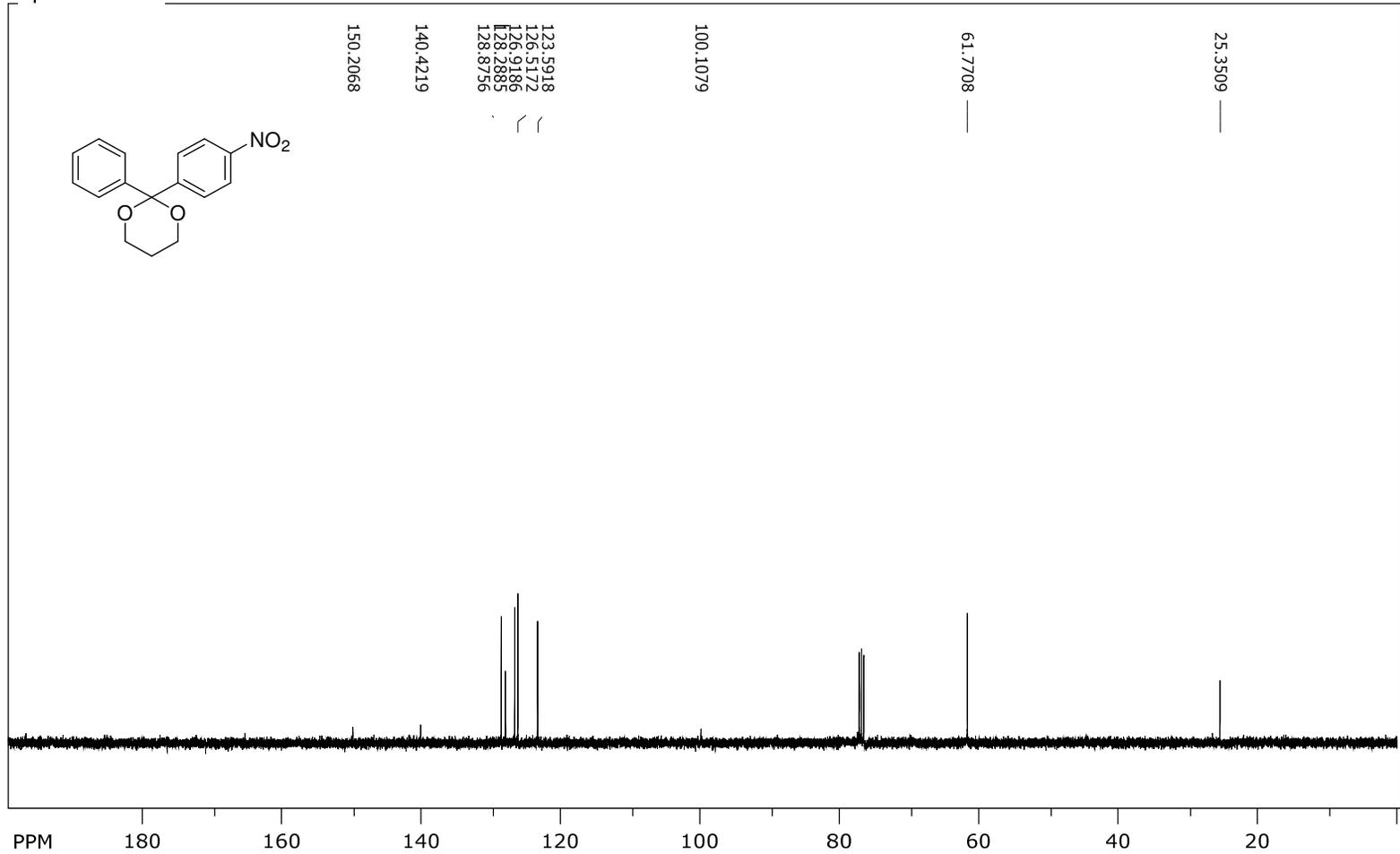
SpinWorks 3:



file: ...etalfrnitro5thT-col6-apr27.fid\fid block# 1 expt: "s2pul"
 transmitter freq.: 399.745875 MHz
 time domain size: 26264 points
 width: 6410.26 Hz = 16.0358 ppm = 0.244070 Hz/pt
 number of scans: 8

freq. of 0 ppm: 399.743474 MHz
 processed size: 65536 complex points
 LB: 0.000 GF: 0.0000
 Hz/cm: 144.874 ppm/cm: 0.36241

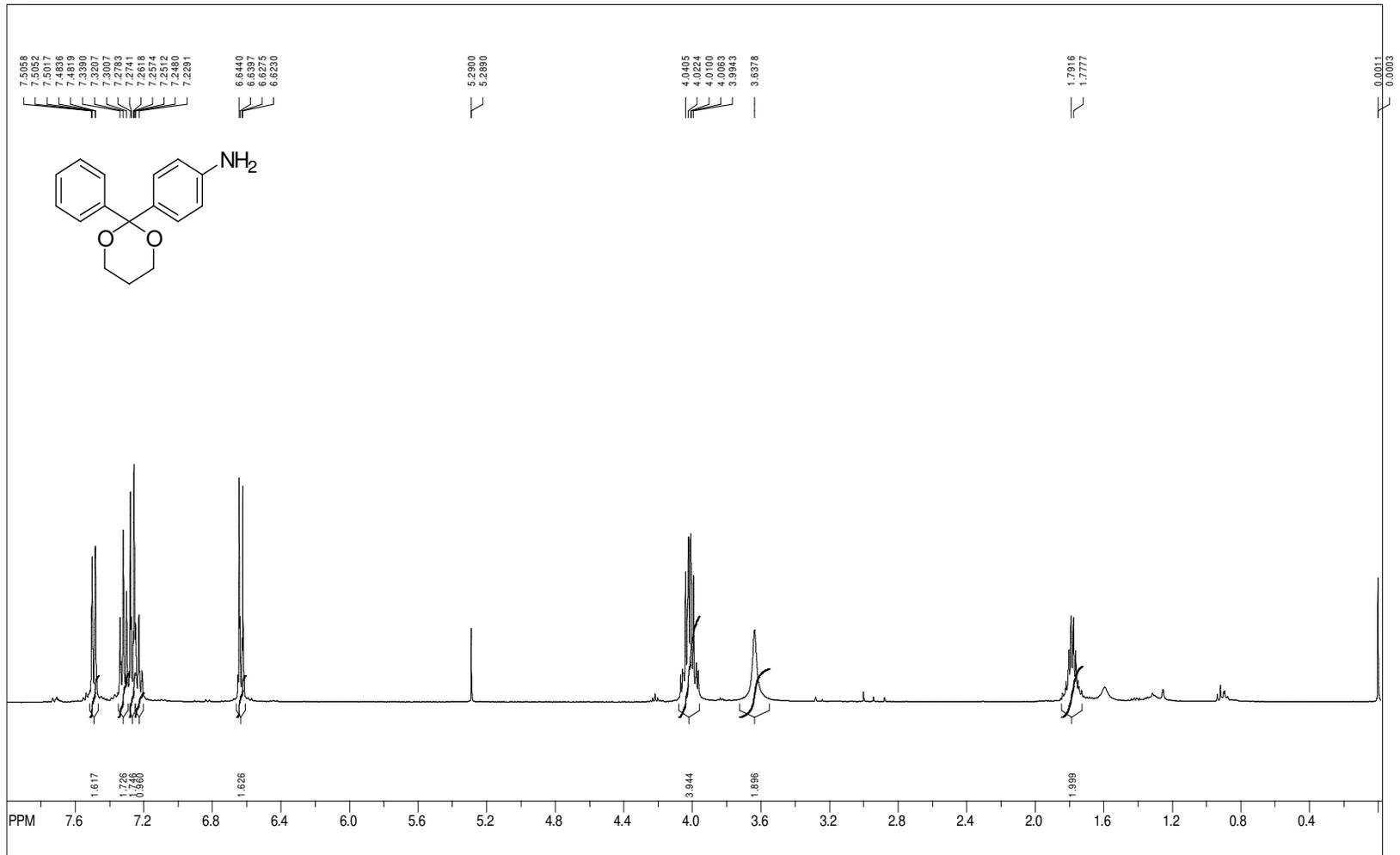
SpinWorks 3:



file: ...fnitro5th1-col6-apr30-c13.fid\fid_block# 1 expt: "s2pul"
 transmitter freq.: 100.526131 MHz
 time domain size: 63750 points
 width: 24509.80 Hz = 243.8153 ppm = 0.384468 Hz/pt
 number of scans: 256

freq. of 0 ppm: 100.515577 MHz
 processed size: 65536 complex points
 LB: 0.000 GF: 0.0000
 Hz/cm: 804.142 ppm/cm: 7.99933

SpinWorks 2.5:



file: C:\Users\Pathore User\Desktop\Tasnuva NMRs\MGS\formylbenzamidacetalmiro-s2-jun19.fid\fid_block# 1 exp: "s2pu"

transmitter freq.: 399.745675 MHz

time domain size: 28264 points

width: 6410.26 Hz = 16.036829 ppm = 0.244070 Hz/pt

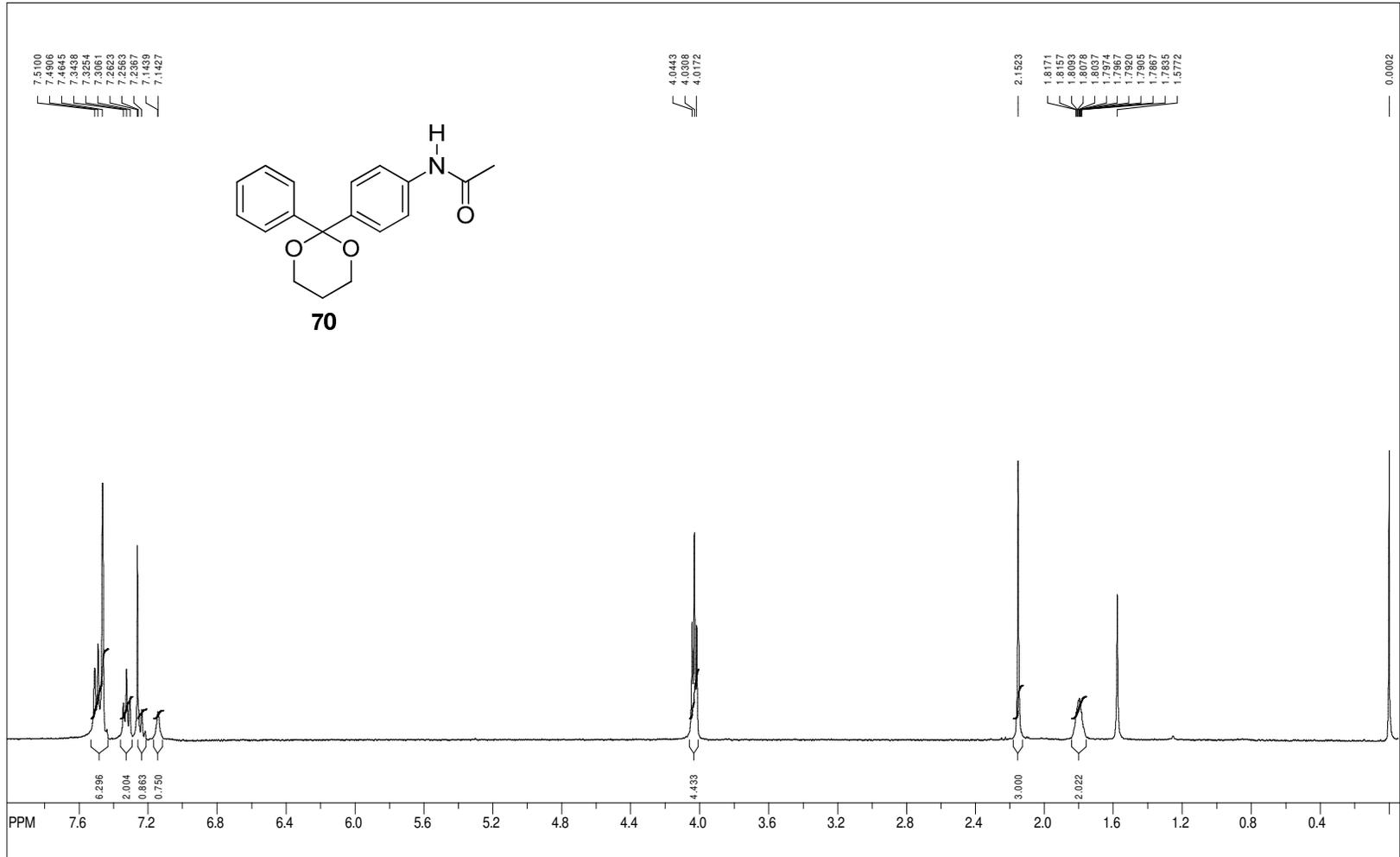
number of scans: 8

freq. of 0 ppm: 399.743478 MHz

processed size: 65536 complex points

LB: 0.000 GB: 0.0000

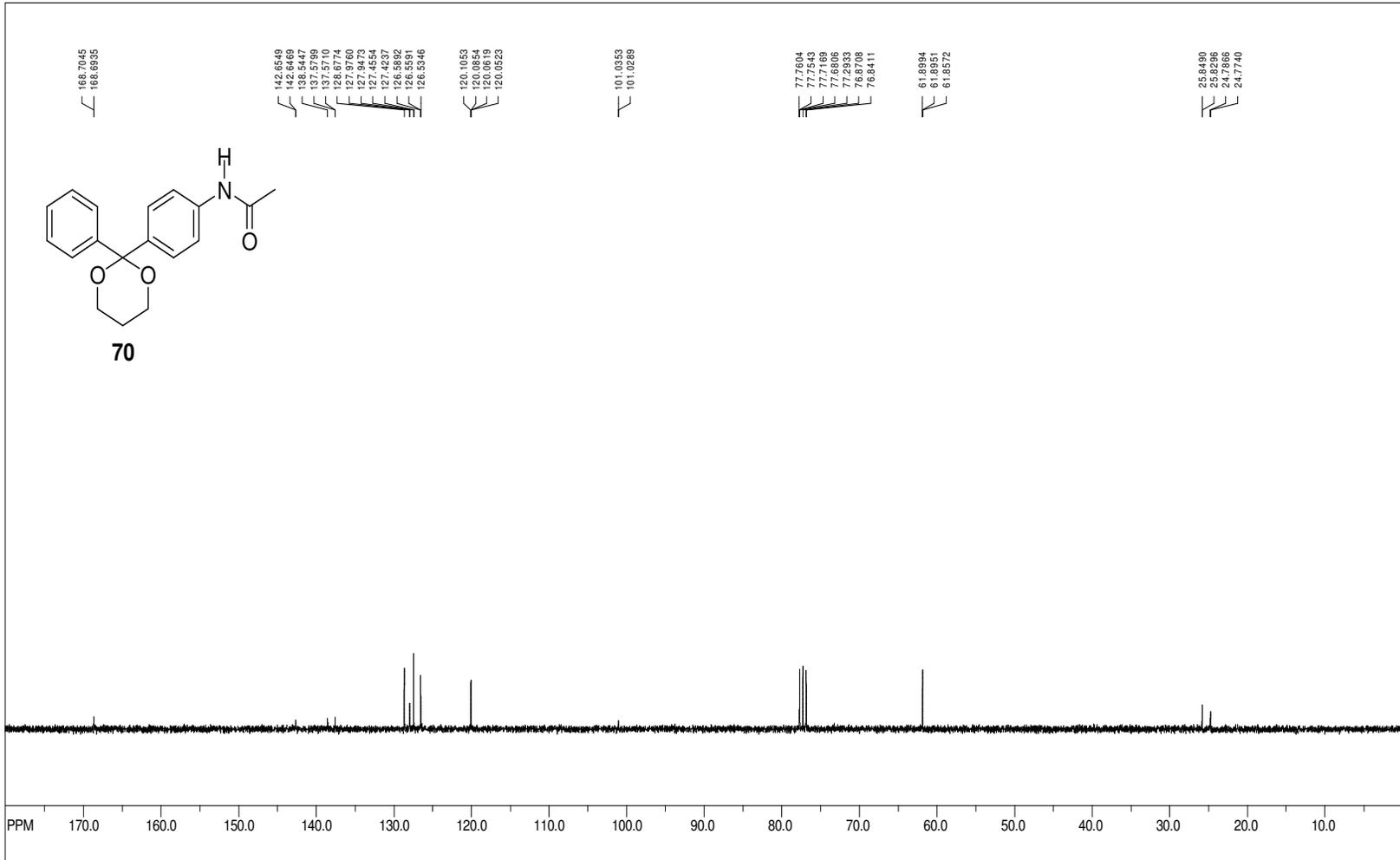
SpinWorks 2.5:



file: C:\Users\Paijore User\Desktop\Tasruva NMR\MGSI\formybenzacid\acetalimiro-s3-jun19\fid\fid_block# 1 exp: "s2pur"
 transmitter freq.: 399.743475 MHz
 time domain size: 26264 points
 width: 6410.26 Hz = 16.035829 ppm = 0.244070 Hz/pt
 number of scans: 8

freq. of 0 ppm: 399.743475 MHz
 processed size: 65536 complex points
 LB: 0.000 GB: 0.0000

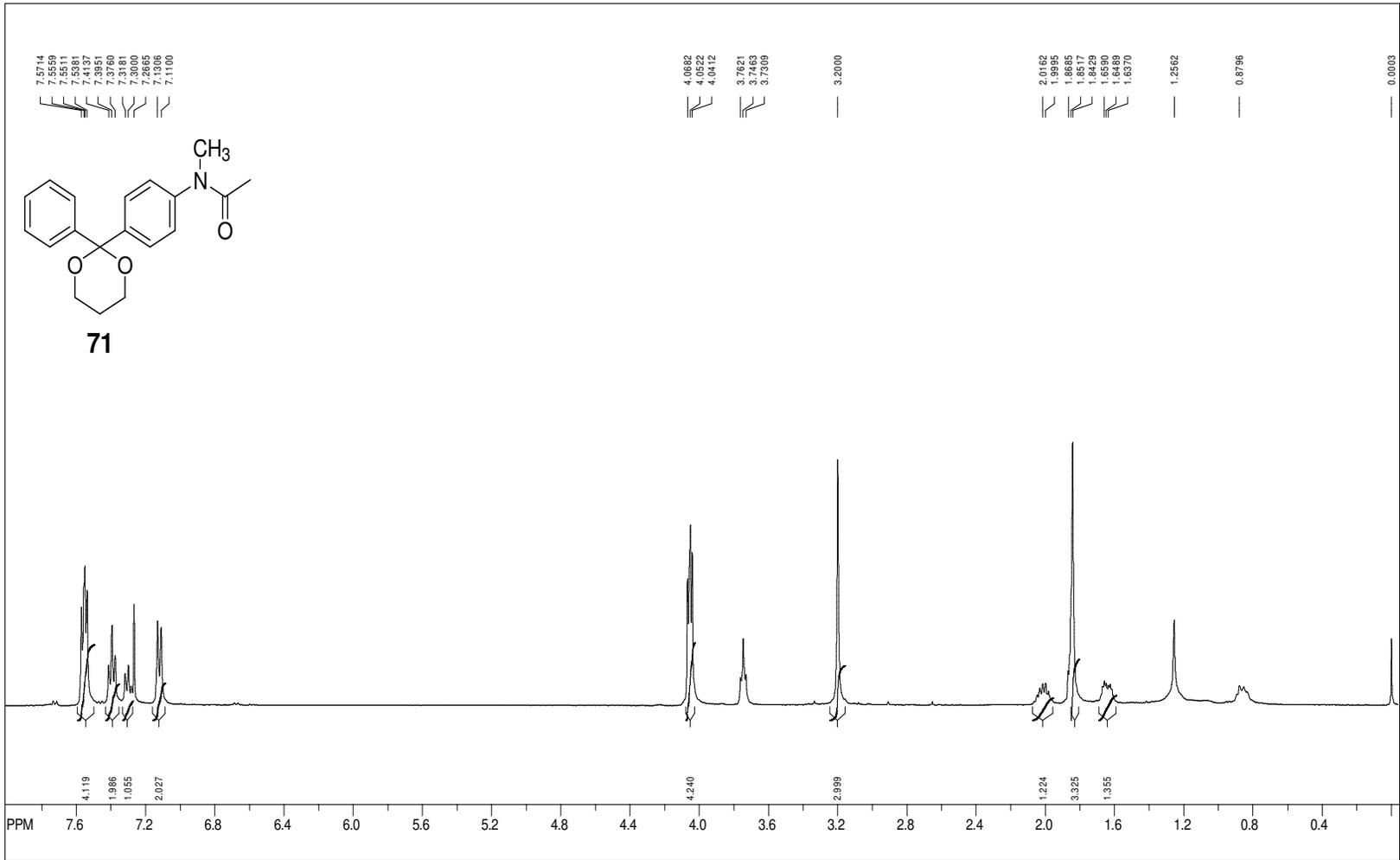
SpinWorks 2.5: 13C OBSERVE



file: C:\Users\Pattore User\Desktop\Tasruva NMR\MGSI\formybenzacid\acetalimiro-s0c13-jun25.fid\fid_block#1 expt.'s2pul'
 transmitter freq.: 75.476336 MHz
 time domain size: 68492 points
 width: 18867.92 Hz = 249.984639 ppm = 0.275476 Hz/pt
 number of scans: 256

freq. of 0 ppm: 75.468034 MHz
 processed size: 131072 complex points
 LB: 0.200 GB: 0.0000

SpinWorks 2.5:



file: C:\Users\Pattore User\Desktop\Tasruva NMRs\MGS\formylbenzacid\acetalnitro-st4-jun27-2nd.fid\fid block# 1 exp: "s2pu"

transmitter freq.: 399.745875 MHz

time domain size: 28264 points

width: 6410.26 Hz = 16.035829 ppm = 0.244070 Hz/pt

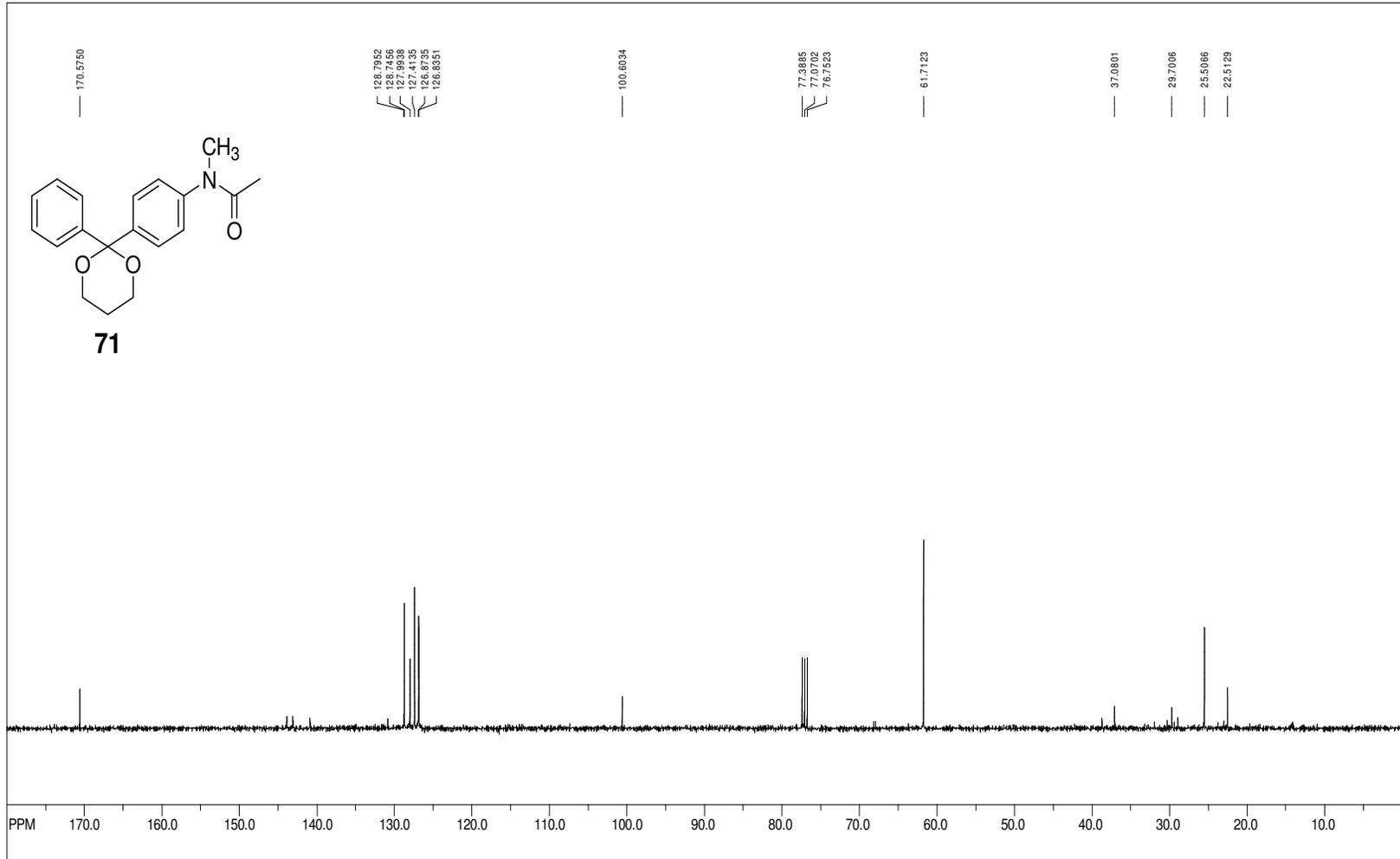
number of scans: 8

freq. of 0 ppm: 399.743473 MHz

processed size: 65536 complex points

LB: 0.200 GB: 0.0000

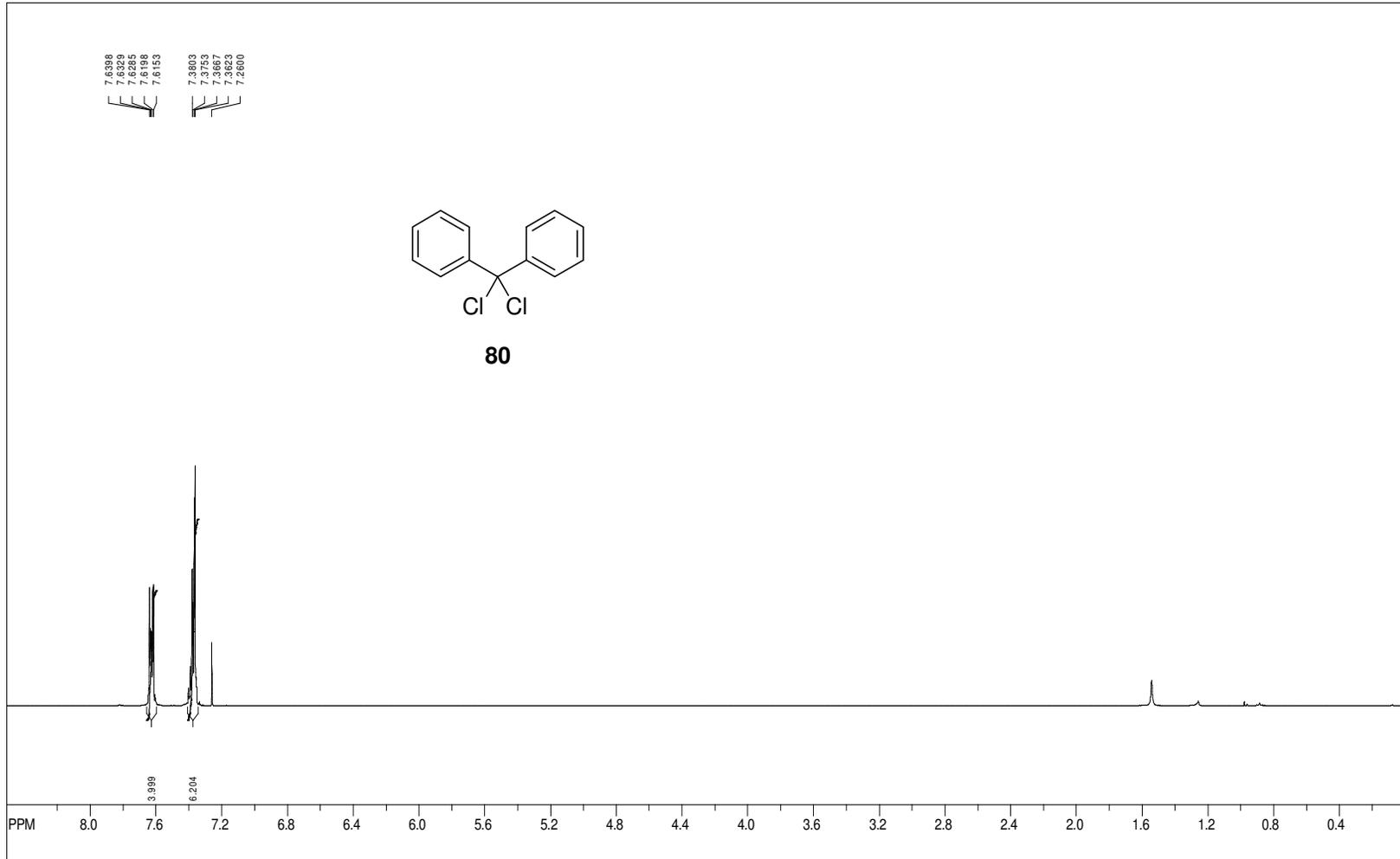
SpinWorks 2.5:



file: C:\Users\Pathore User\Desktop\Tasruva NMRs\MGS\formylbenzamid\acetalnitro-s4c13-jun28.fid\fid block# 1 expt. "s2pu"
 transmitter freq.: 100.526131 MHz
 time domain size: 63750 points
 width: 24509.80 Hz = 243.815251 ppm = 0.384468 Hz/pt
 number of scans: 256

freq. of 0 ppm: 100.515577 MHz
 processed size: 65536 complex points
 LB: 0.200 GB: 0.0000

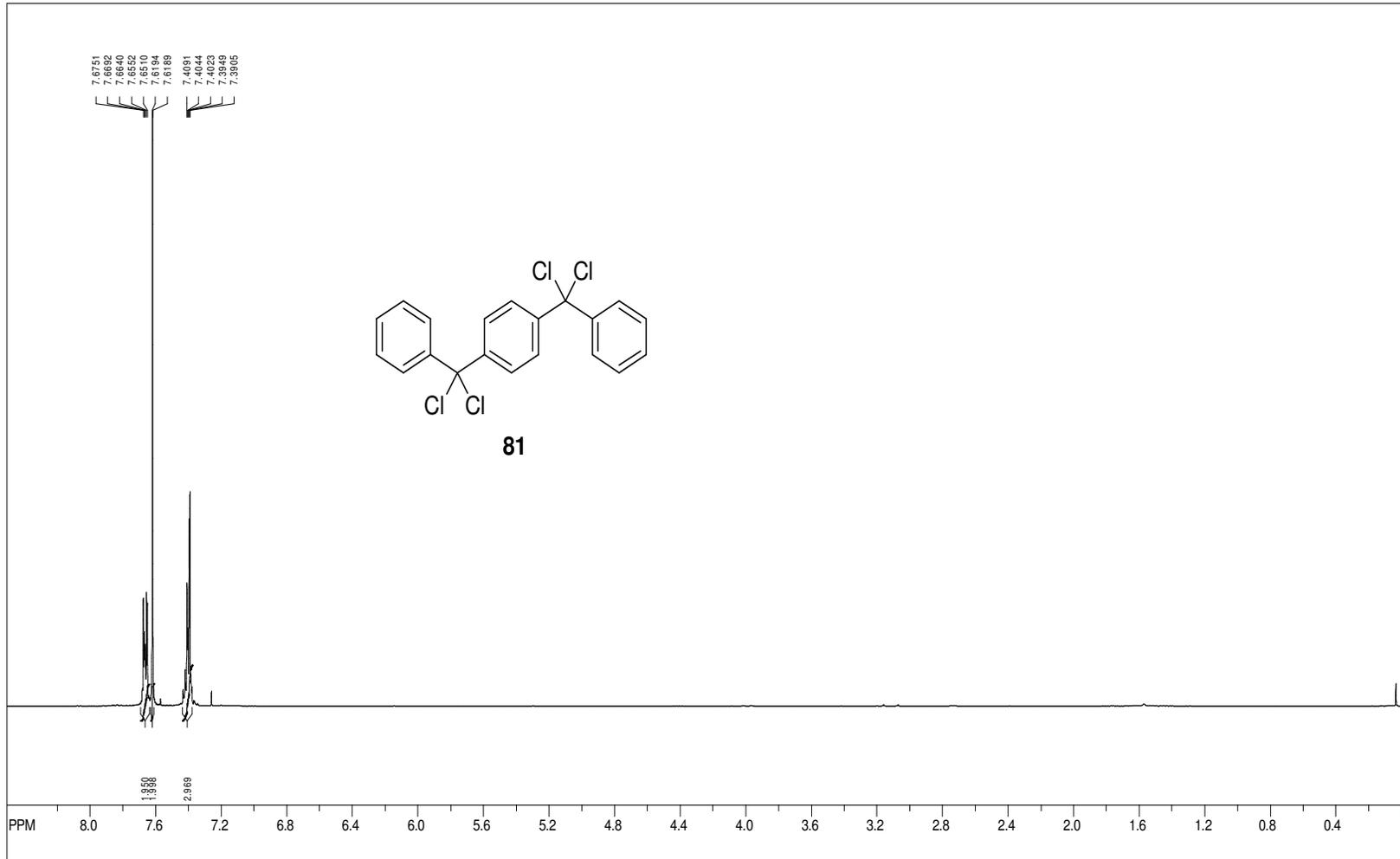
SpinWorks 2.5:



file: C:\Users\Pathore User\Desktop\Tasruva NMR\Run3\F3Altst1\F3altst1T4-sep8.fid\fid_block# 1 exp: "squr"
transmitter freq.: 399.745675 MHz
time domain size: 26264 points
width: 6410.26 Hz = 16.035829 ppm = 0.244070 Hz/pt
number of scans: 8

freq. of 0 ppm: 399.743476 MHz
processed size: 65536 complex points
LB: 0.200 GB: 0.0000

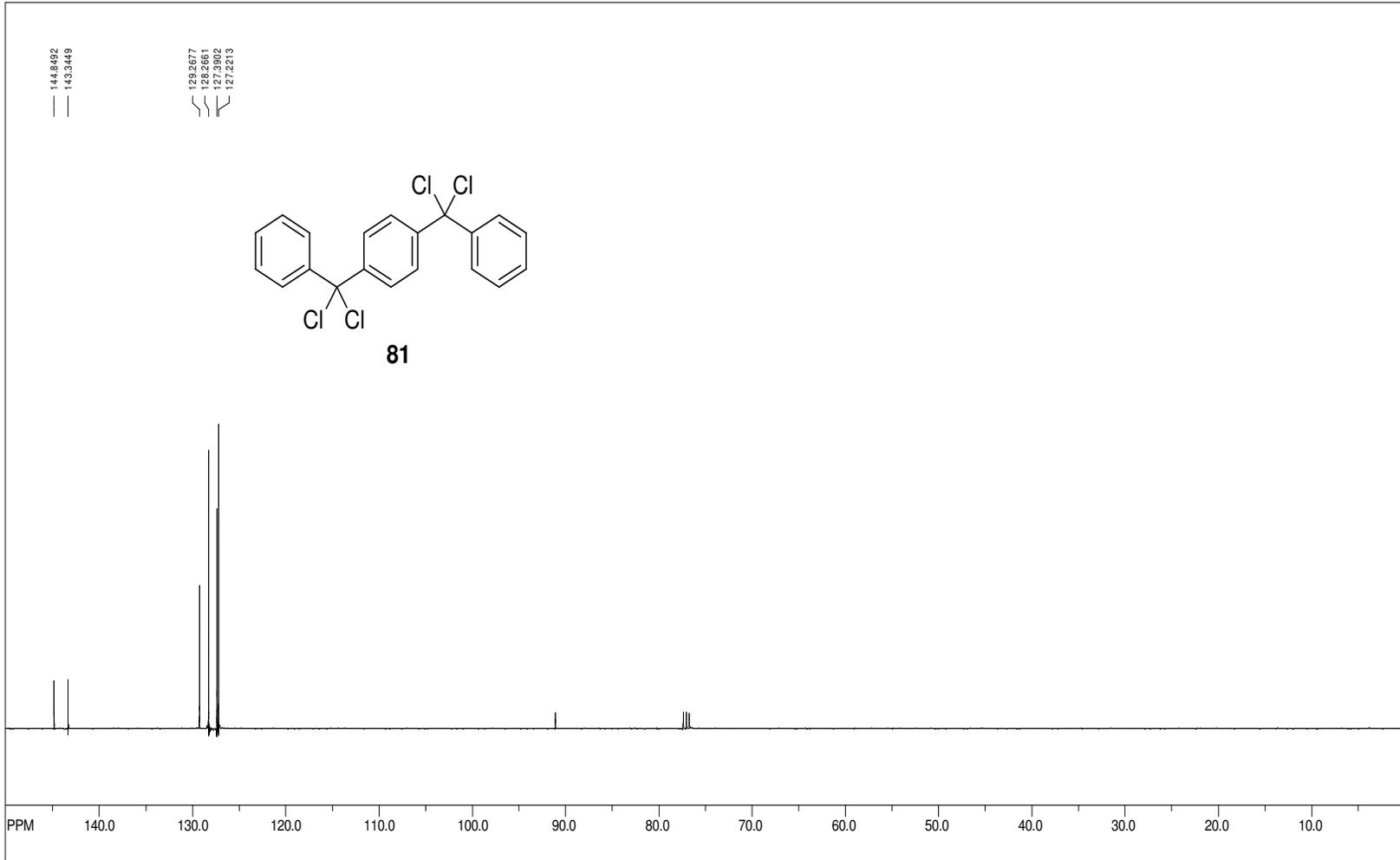
SpinWorks 2.5:



file: C:\Users\Pathore User\Desktop\Tasnuva NMR\Fn3\F3A1st3\F3alts3-mar13.fid\fid_block# 1 expt: "sqpu"
transmitter freq.: 399.745875 MHz
time domain size: 26264 points
width: 6410.26 Hz = 16.035829 ppm = 0.244070 Hz/pt
number of scans: 8

freq. of 0 ppm: 399.743477 MHz
processed size: 65536 complex points
LB: 0.200 GB: 0.0000

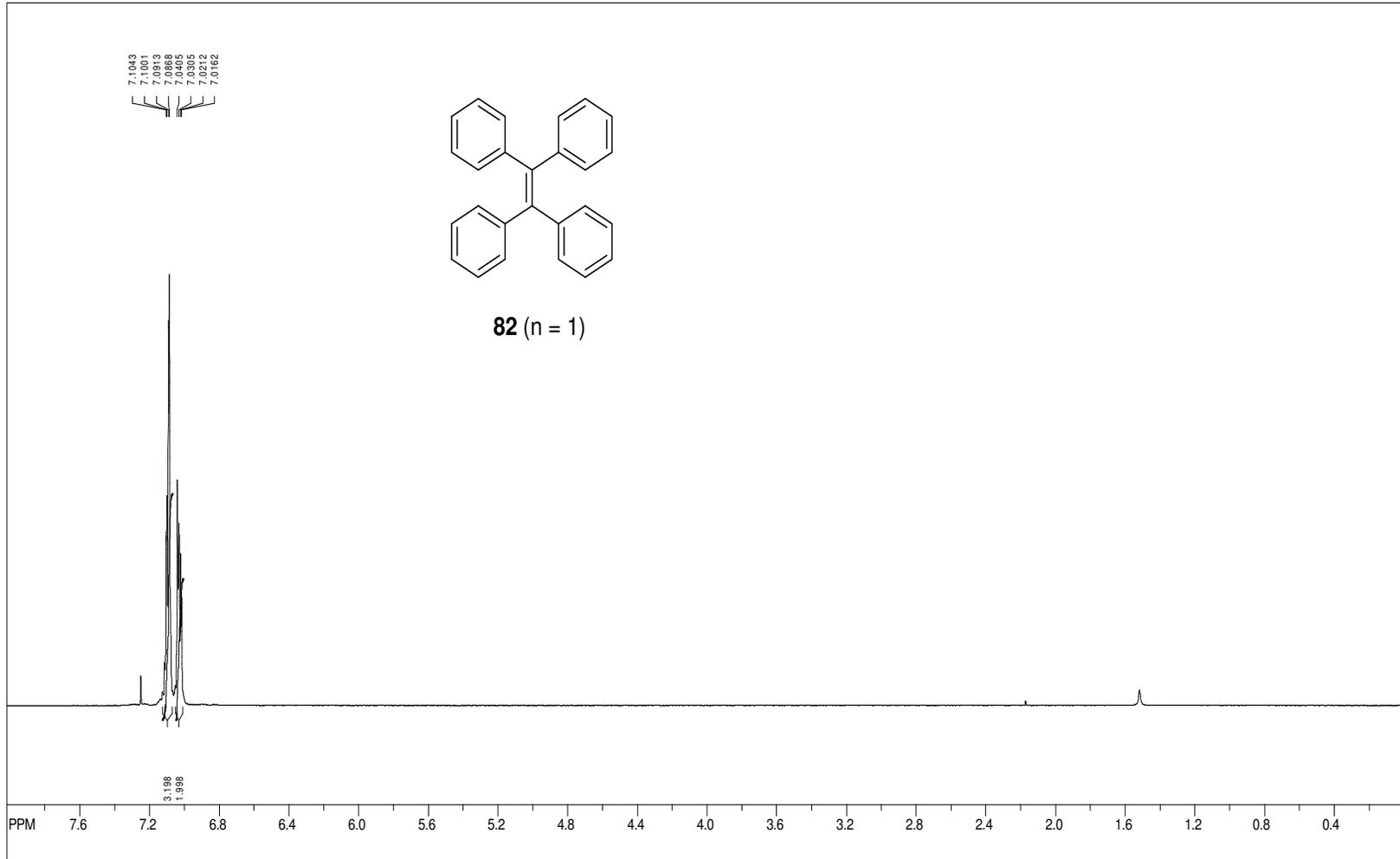
SpinWorks 2.5:



file: C:\Users\Rathore User\Desktop\Tasnuva NMR\Fw3\F3\Ats3\F3\alts3-mar13-C13.fid block# 1 exp: "s2pul"
transmitter freq.: 100.526131 MHz
time domain size: 63750 points
width: 24509.80 Hz = 243.815251 ppm = 0.384468 Hz/pt
number of scans: 256

freq. of 0 ppm: 100.515577 MHz
processed size: 65536 complex points
LB: 0.200 GB: 0.0000

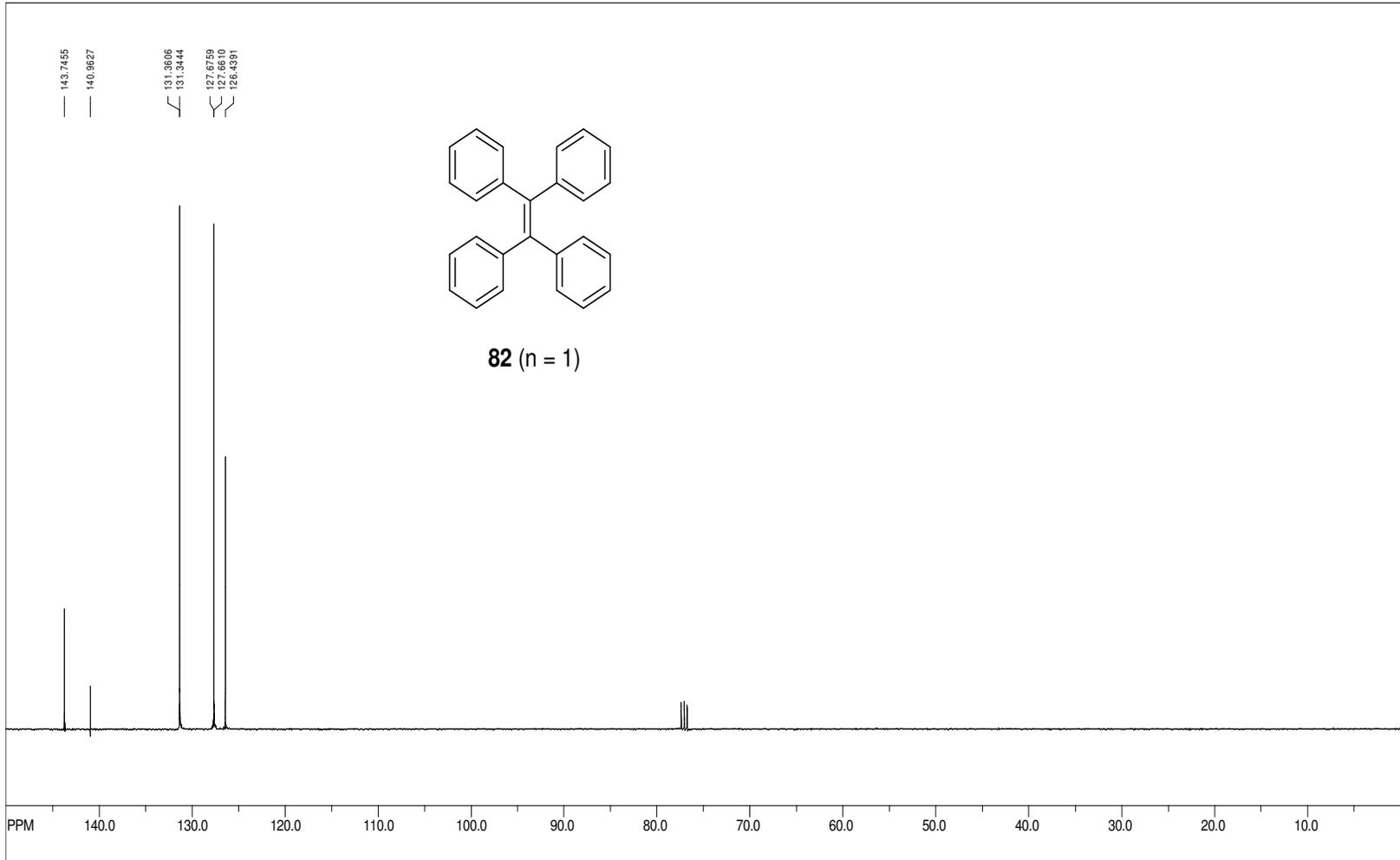
SpinWorks 2.5:



file: C:\Users\Pathore User\Desktop\Tasruva NMR\Run3\F3P1-sep24.fid\fid block# 1 exp1: "s2pu1"
transmitter freq.: 399.743675 MHz
time domain size: 26264 points
width: 6410.26 Hz = 16.035829 ppm = 0.244070 Hz/pt
number of scans: 8

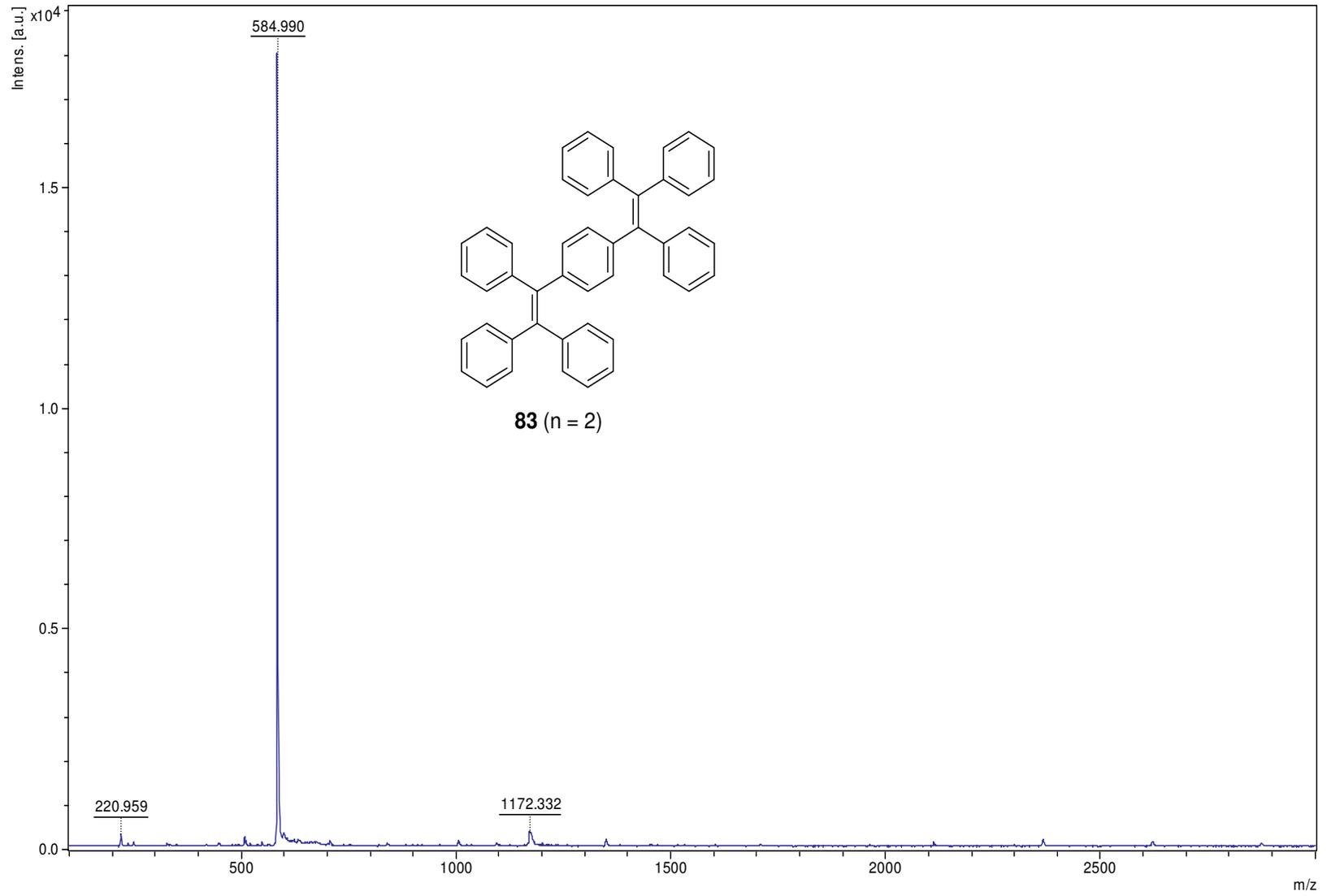
freq. of 0 ppm: 399.743480 MHz
processed size: 65536 complex points
LB: 0.000 GB: 0.0000

SpinWorks 2.5:

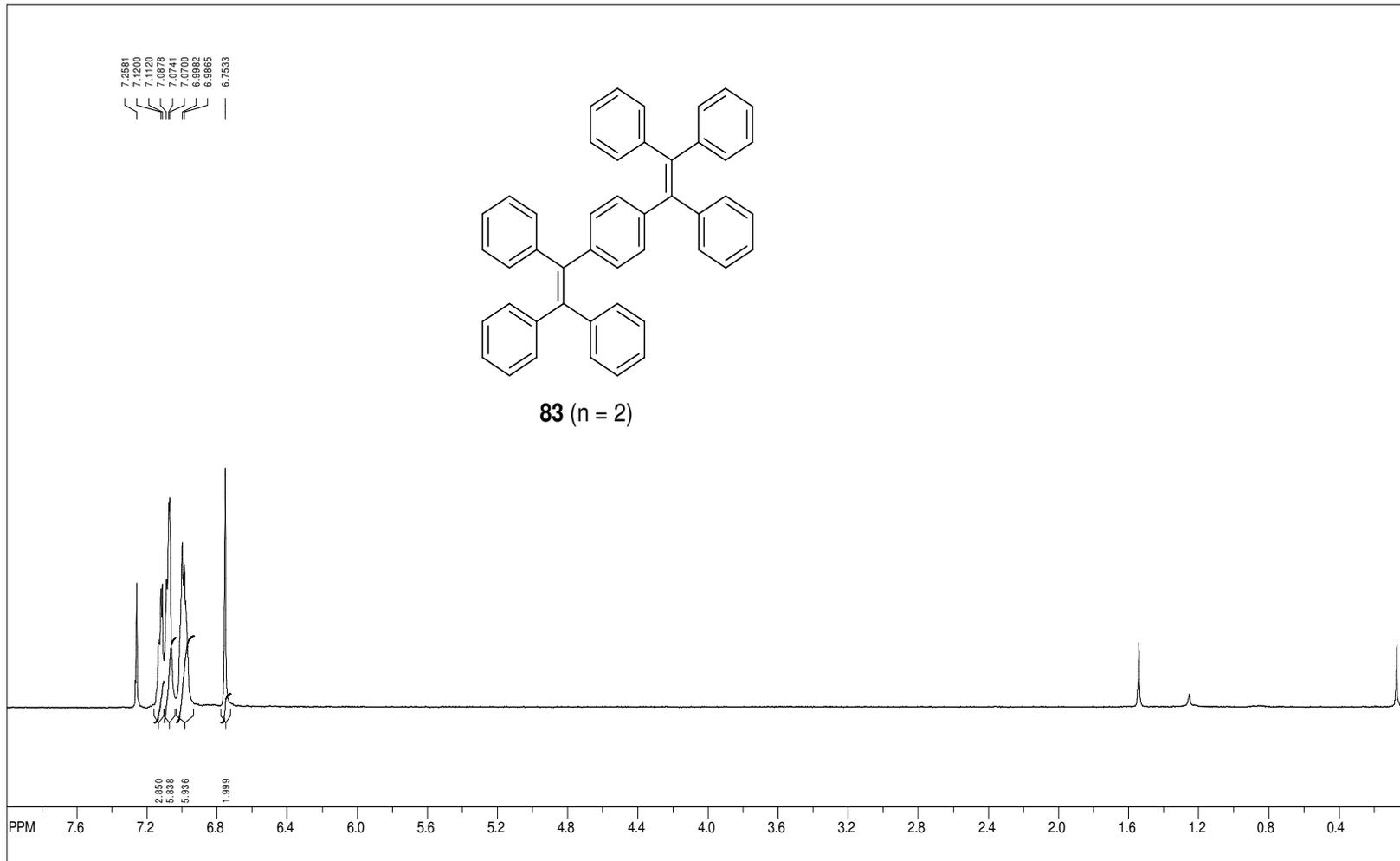


file: C:\Users\Pethore User\Desktop\Tasruva NMR\Prn3\F3alts4-P1-feb28-C13.fid\fid_block# 1 exp: "s2pul"
transmitter freq.: 100.526131 MHz
time domain size: 63750 points
width: 24509.80 Hz = 243.815251 ppm = 0.384468 Hz/pt
number of scans: 256

freq. of 0 ppm: 100.515577 MHz
processed size: 65536 complex points
LB: 0.200 GB: 0.0000

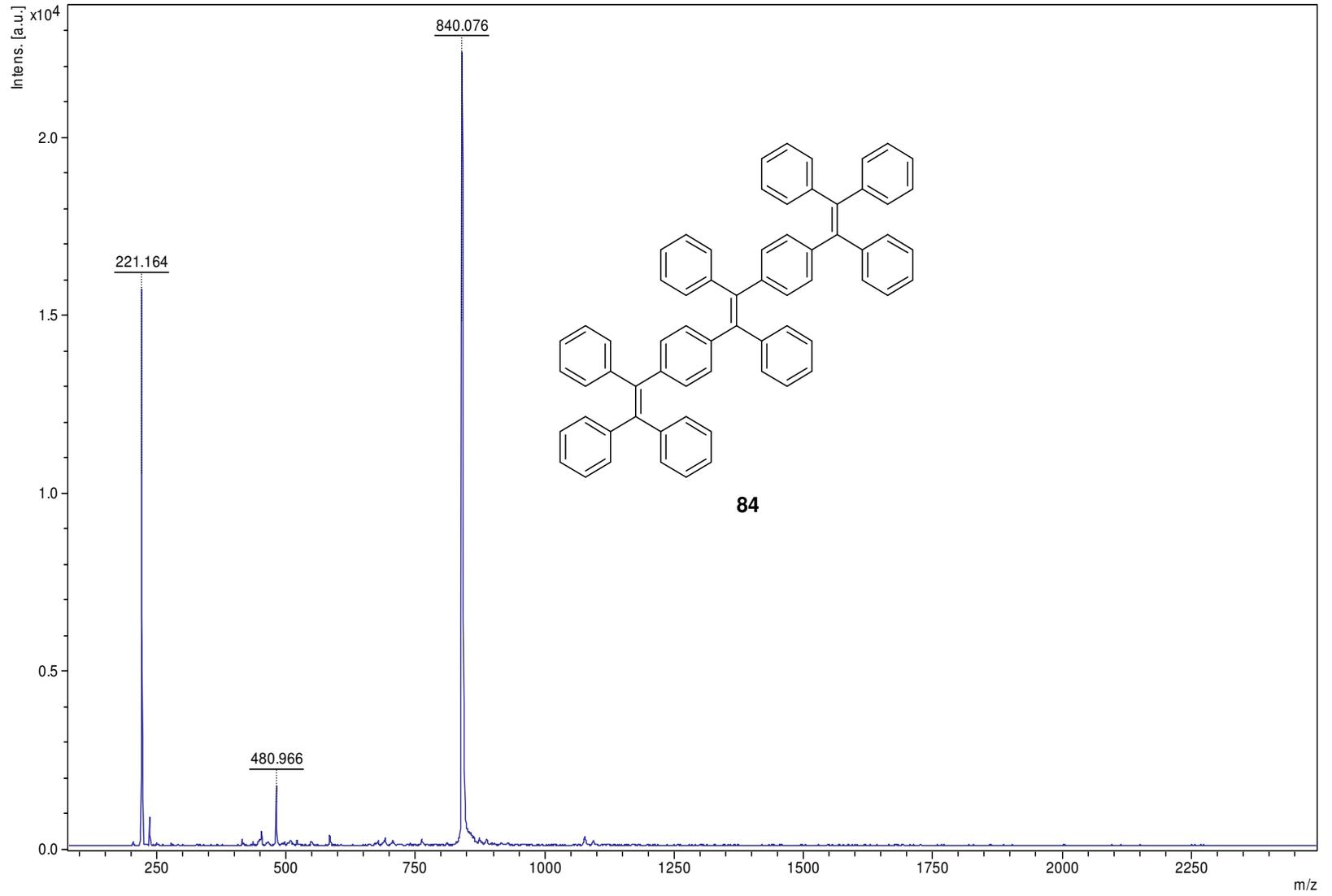


SpinWorks 2.5: STANDARD 1H OBSERVE

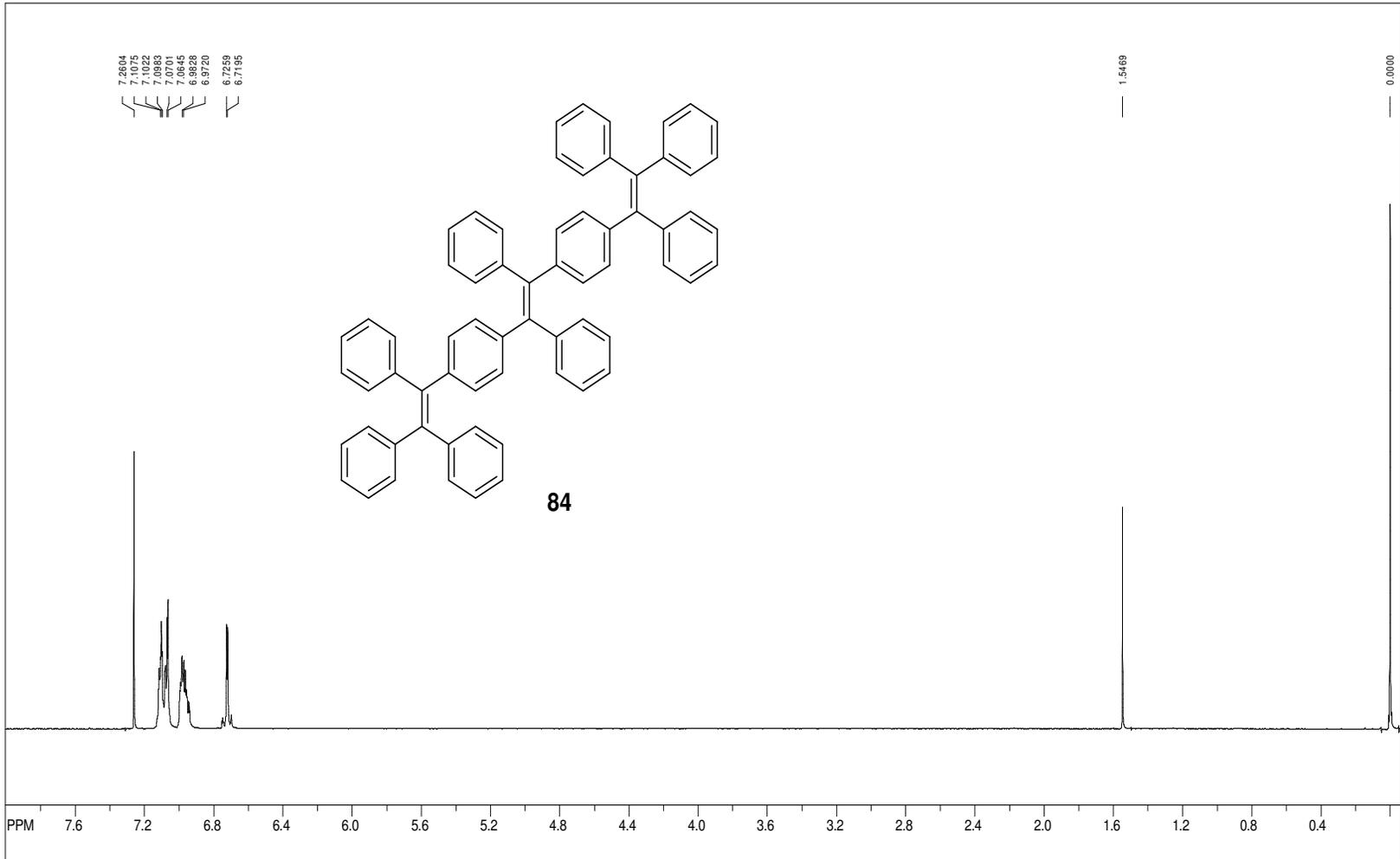


file: C:\Users\Pathore User\Desktop\Tasnuva NMR\Fn3\F3ats4-P2-feb28.fid\fid_block#1 expt "s2pu"
transmitter freq.: 300.133009 MHz
time domain size: 19192 points
width: 4803.07 Hz = 16.003151 ppm = 0.250264 Hz/pt
number of scans: 8

freq. of 0 ppm: 300.131208 MHz
processed size: 32768 complex points
LB: 0.200 GB: 0.0000



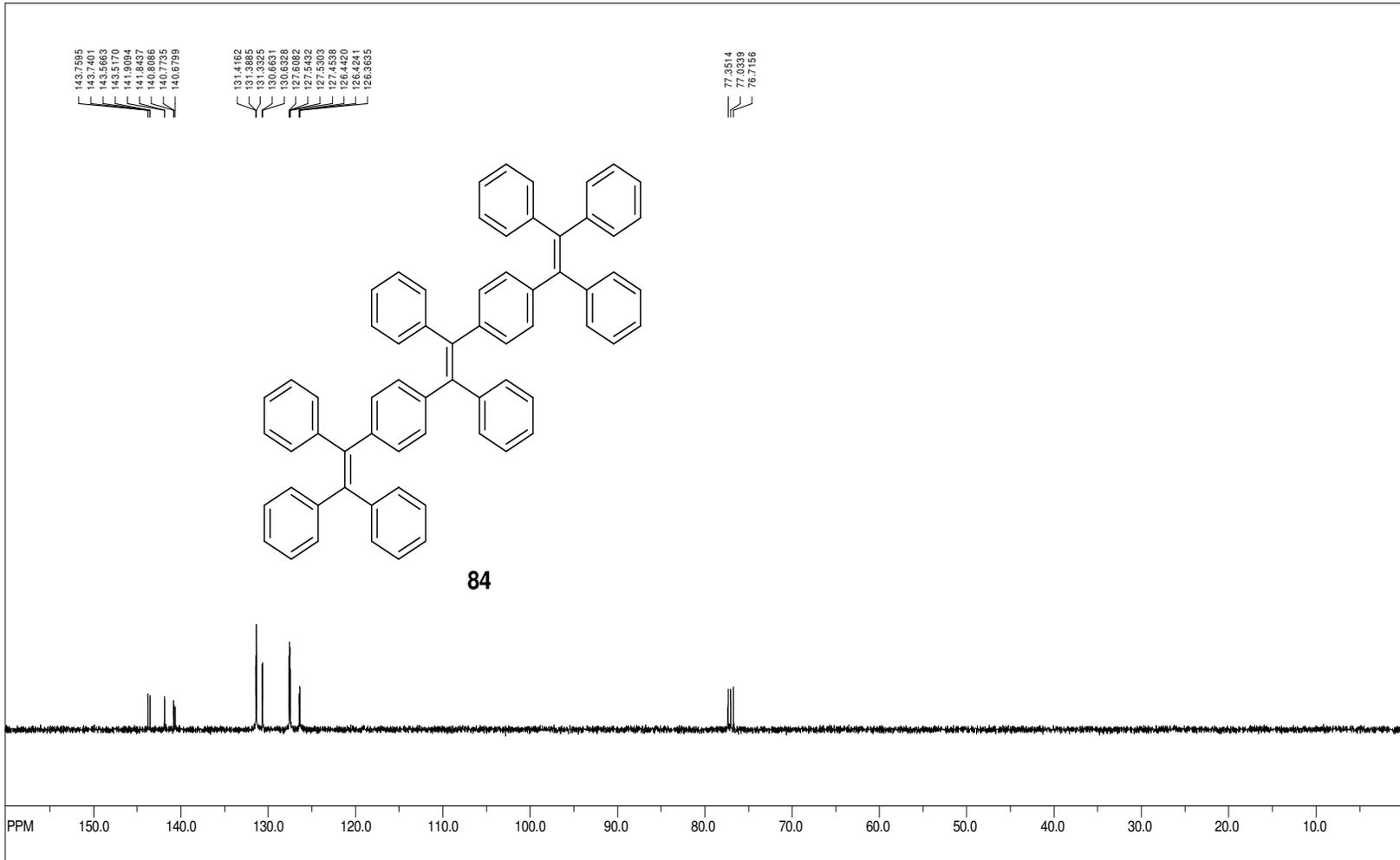
SpinWorks 2.5:



file: C:\Users\Pathore User\Desktop\Tasnuva NMR\Run3\F3Ats\F3Ats4-fr2prev-pres-2s01-dec3-fidfid_block#1 expt: "s2pul"
 transmitter freq.: 399.745875 MHz
 time domain size: 26264 points
 width: 6410.26 Hz = 16.035829 ppm = 0.244070 Hz/pt
 number of scans: 8

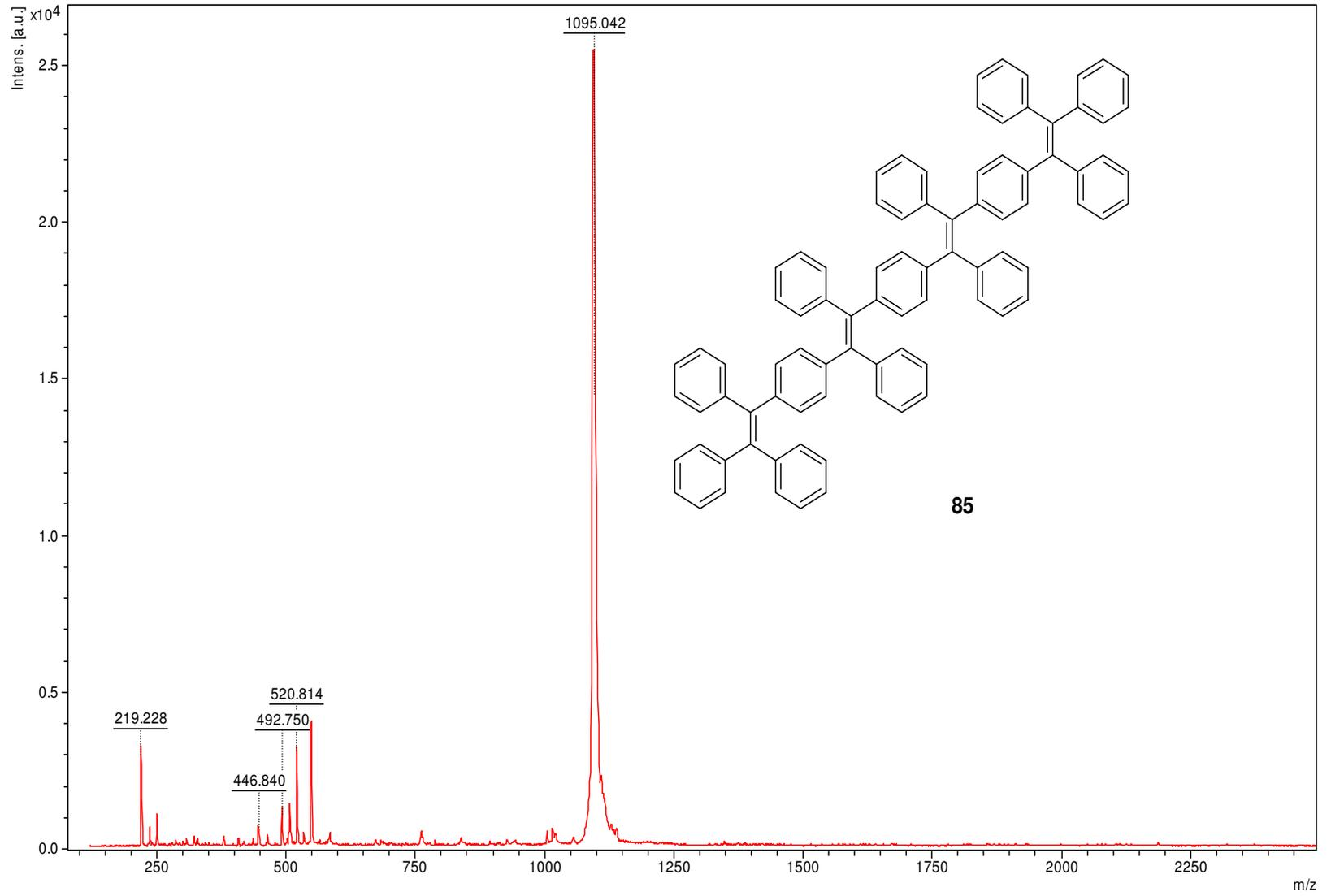
freq. of 0 ppm: 399.743476 MHz
 processed size: 65536 complex points
 LB: 0.000 GB: 0.0000

SpinWorks 2.5: STANDARD 1H OBSERVE - profile

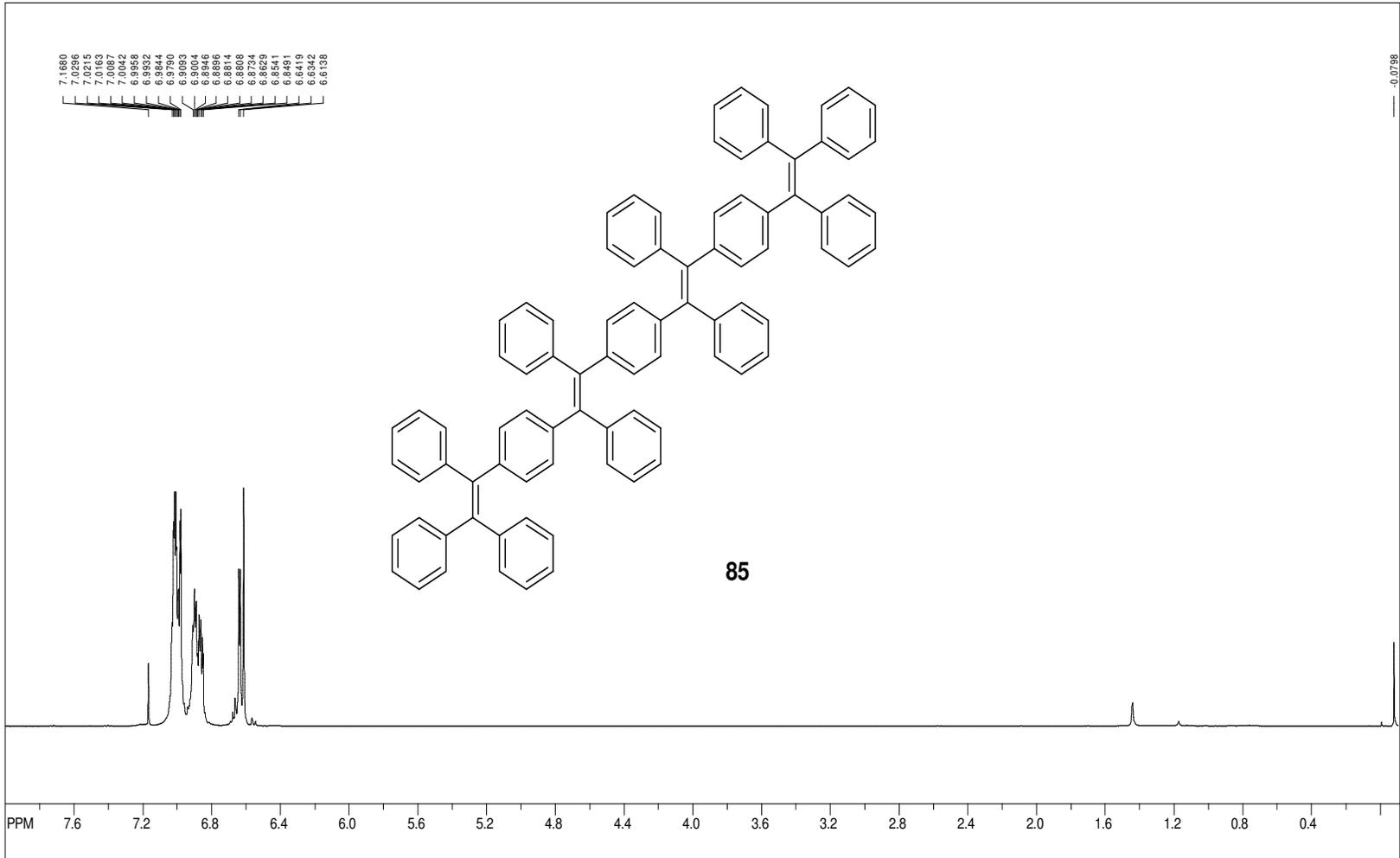


file: C:\Users\Pethore User\Desktop\Tasruva NMR\Fn3\F3Altst4\F3altst4-f2prev-pres-2sc11-dec31-c13.fid\fid_block#1 exp: "s2pu1"
transmitter freq.: 100.526131 MHz
time domain size: 63750 points
width: 24509.80 Hz = 243.815251 ppm = 0.384468 Hz/pt
number of scans: 256

freq. of 0 ppm: 100.515577 MHz
processed size: 65536 complex points
LB: 0.000 GB: 0.0000



SpinWorks 2.5:



file: C:\Users\Paijore User\Desktop\Tasruva NMR\Run3\F0Alt4\F0Alt4-fr2prev-pres-6s03-dec31.fid\fid block# 1 expt. "s2pu"

transmitter freq.: 399.745675 MHz

time domain size: 26264 points

width: 6410.26 Hz = 16.035829 ppm = 0.244070 Hz/pt

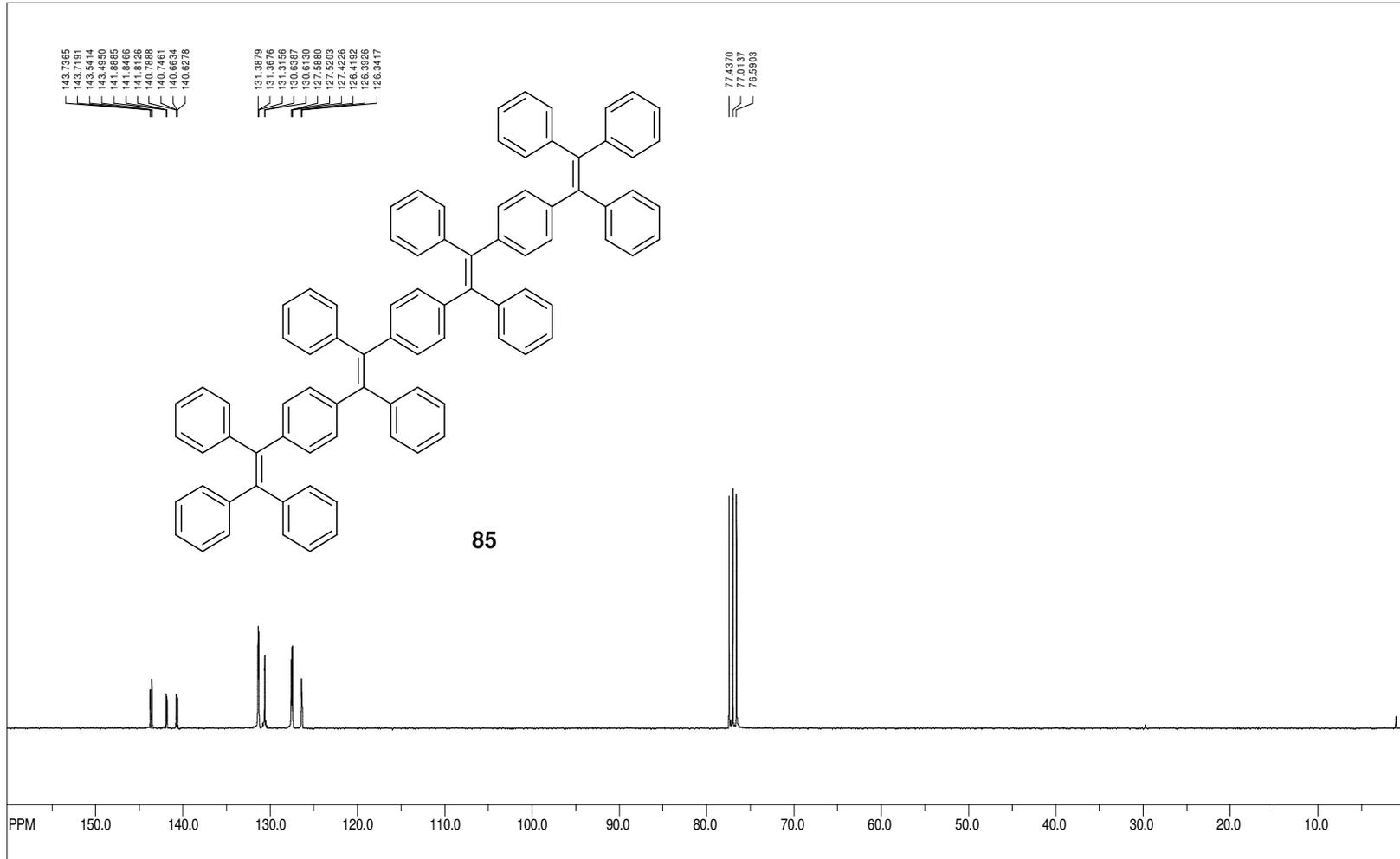
number of scans: 8

freq. of 0 ppm: 399.743513 MHz

processed size: 65536 complex points

LB: 0.000 GB: 0.0000

SpinWorks 2.5: 13C OBSERVE



file: C:\Users\Pathore User\Desktop\Tasnuva NMR\Run3\F3Altst4\F3altst4-fr2prev-pres-6sol1-jan2-c13.fid fid block# 1 exp: "s2pu"

transmitter freq.: 75.476336 MHz

time domain size: 68492 points

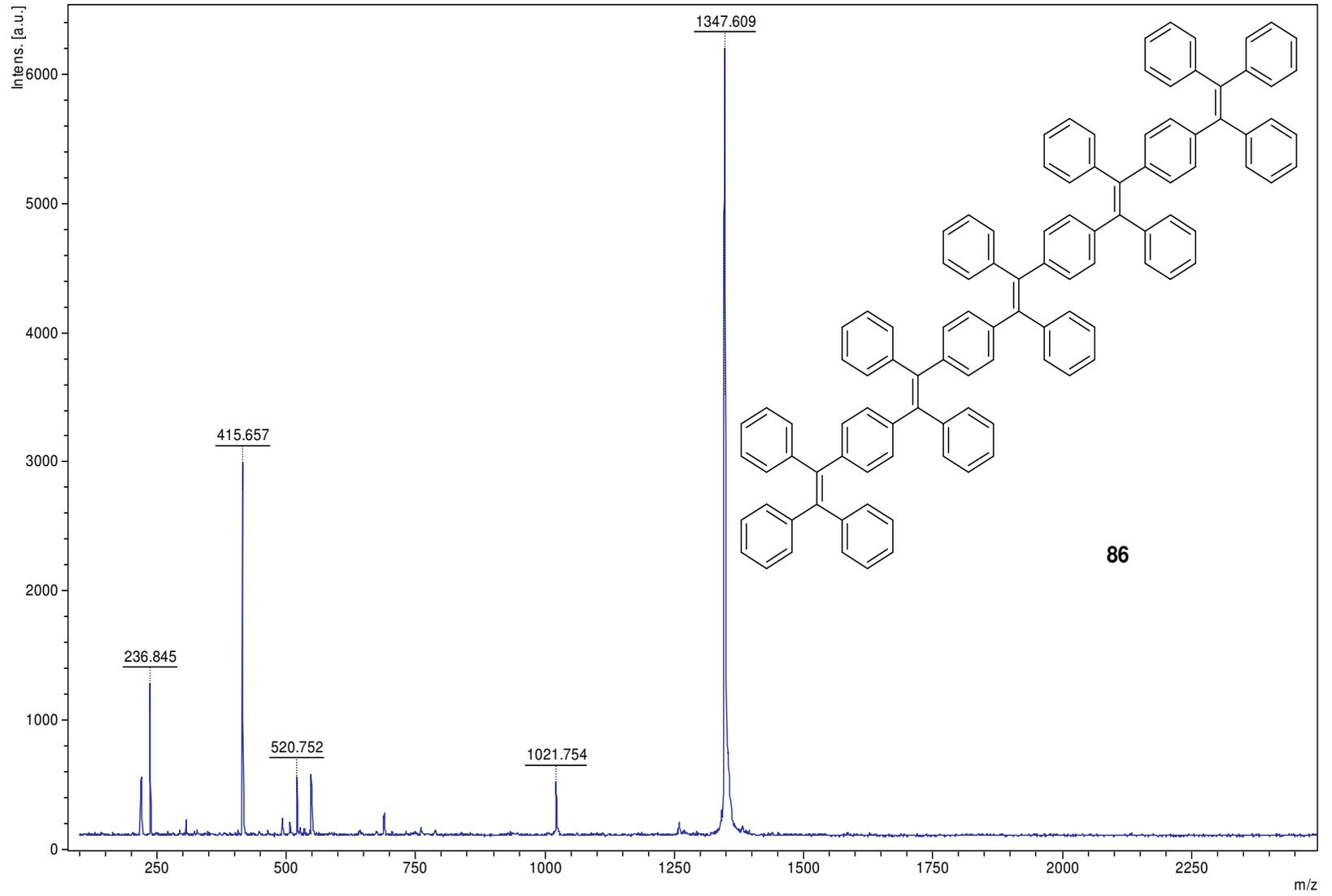
width: 18867.92 Hz = 249.984639 ppm = 0.275476 Hz/pt

number of scans: 12400

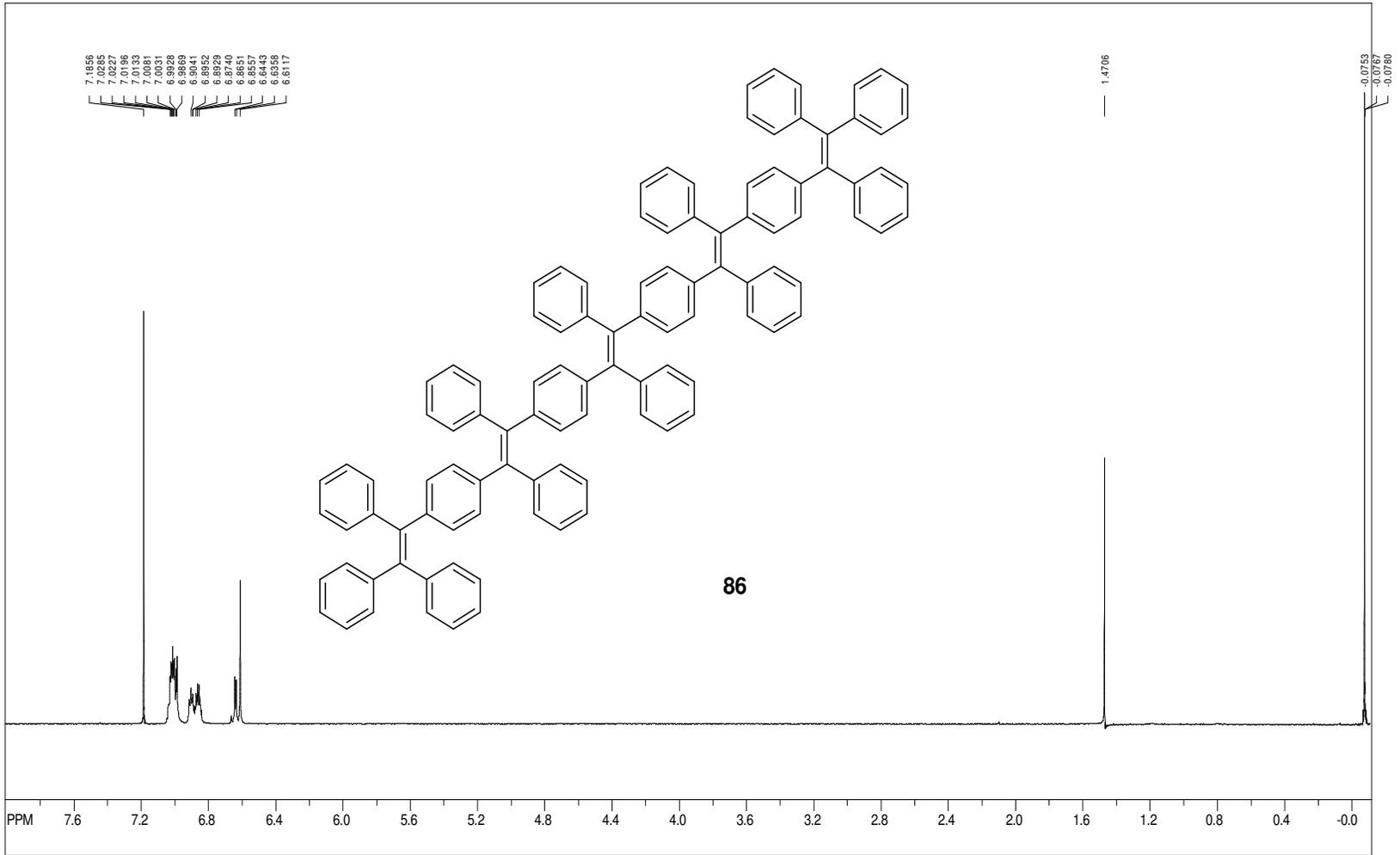
freq. of 0 ppm: 75.468053 MHz

processed size: 131072 complex points

LB: 0.000 GB: 0.0000



SpinWorks 2.5:



file: C:\Users\Pathore User\Desktop\Tasnuva NMR\Raw3\F3A1st4\F3A1st4-fr3pres-7\yelsol-nov27-fid.fid block# 1 exp: "s2pu"

transmitter freq.: 399.745675 MHz

time domain size: 26264 points

width: 6410.26 Hz = 16.035829 ppm = 0.244070 Hz/pt

number of scans: 8

freq. of 0 ppm: 399.743506 MHz

processed size: 65536 complex points

LB: 0.000 GB: 0.0000

